17BEBME601 BIOMEDICAL IMAGE PROCESSING 3 0 0 2 100

OBJECTIVE

- To expose the students to the fundamentals of medical image acquisition, processing and storage.

INTENDED OUTCOMES

- To study the image fundamentals and mathematical transforms necessary for image processing. To study the image enhancement techniques
- To study image restoration procedures.
- To study the image compression procedures.

UNIT I DIGITAL IMAGE FUNDAMENTAL (9)

Elements of digital image processing systems, Elements of Visual perception, Image sampling and quantization, – Some Basic relationships between pixels, Matrix and Singular Value representation of discrete images.

UNIT II IMAGE TRANSFORMS (9)

2D DFT, Cosine, Sine Hadamard, Haar, Slant, KL transform and their properties.

UNIT III IMAGE ENHANCEMENT (9)

Histogram – Modification and specification techniques, Enhancement by point processing Image smoothening, Image sharpening, generation of spatial masks from frequency domain specification, Homomorphic filtering, and color image processing.

UNIT IV IMAGE RESTORATIONAND RECONSTRUCTION OF MEDICAL IMAGES (9)

Image degradation models, Unconstrained and Constrained restoration, inverse filtering, Least mean square filter, Image reconstruction from projections – Radon transforms, Filter back projection algorithm, Fourier reconstruction of MRI Images.

UNIT V MEDICAL IMAGE COMPRESSION TECHNIQUES (9)

Run length, Huffman coding, arithmetic coding, Pixel coding, transform coding, JPEG Standard, predictive techniques, Application of image processing techniques in thermography, SPECT, PET images.

Total : 45

TEXT BOOKS

S.NO.	Author(s) Name	Title of the book	Publisher	Year of publication
1	Rafael C., Gonzalez and Richard E. Woods	Digital Image Processing	Pearson Education Asia	2001
2	Anil K. Jain	Fundamentals of Digital Image Processing	Prentice Hall of India	1997

REFERENCE BOOKS

S.NO.	Author(s) Name	Title of the book	Publisher	Year of publication
1	William K. Pratt	Digital Image Processing	John Wiley	1987

KARPAGAM ACADEMY OF HIGHER EDUCATION
(Deemed to be University Established Under Section 3 of UGC Act 1956)
Pollachi Main Road, Eachanari Post,
Coimbatore – 641 021
FACULTY OF ENGINEERING
DEPARTMENT OF BIOMEDICAL ENGINEERING

LECTURE PLAN

NAME OF THE STAFF : DR. KAMALRAJ SUBRAMANIAM
DESIGNATION : ASSOCIATE PROFESSOR
CLASS : B.E-III YEAR BME
SUBJECT : BIOMEDICAL IMAGE PROCESSING
SUBJECT CODE : 17BEBME601

S.No	TOPICS TO BE COVERED	TIME DURATION	SUPPORTING MATERIALS	TEACHING AIDS
UNIT-I FUNDAMENTALS OF IMAGE PROCESSING				
1.	Introduction	01	T1 - 1-3	PPT
2.	Application in various fields	01	T1 - 7-24	PPT
3.	Elements and key stages of Digital Image Processing	01	T1 - 25-30	PPT
4.	Elements of visual perception – Image sampling and quantization	01	T1 - 36-38	PPT
5.	Basic relationship between pixels and neighborhood	01	T1 - 68	PPT
6.	Relation between Adjacent and Connectivity	01	T1 - 69	PPT
7.	Relation between Region and Boundary	01	T1 - 70	PPT
8.	Matrix	01	T1 - 568	PPT
9.	Singular Value representation and Discrete Images	01	T1 - 569 - 570	PPT
Introduction	**01**			
Total Lecture Hours	**08**			
Total Hours	**09**			

UNIT-II IMAGE TRANSFORM				
10	1D Discrete Fourier Transform 2D Discrete Fourier Transform	01	T1 – 148 - 149	PPT
11	Cosine Transform	01	T2 – 150 – 151	PPT
12	Properties of Cosine Transform	01	T1 – 152 - 154	PPT
13	Sine Transform	01	T2 – 175 - 203	PPT
14	Haar Transform	01	T1 – 156 - 157	PPT
15	Walsh Hadamard Transform	01	T1 – 568 - 569	PPT
16	Slant Transform	01	T2 - 161	PPT
17	KL Transform	01	T3 – 34 - 92	PPT
18	KL Transform	01	T2 – 137 - 165	PPT
Total Lecture Hours		**09**		
Total Hours		**09**		

UNIT-III IMAGE ENHANCEMENT				
19	Histogram Modification	01	T1 – 120 – 127	PPT
20	Histogram Specification techniques	01	T1 – 128 – 139	PPT
21	Enhancement of Point processing techniques	01	T1 – 106 - 107	PPT
22	Image Sharpening	01	T1 - 157	PPT
23	Image Smoothening and Non – Linear filter	01	T1 - 152 - 157	PPT
24	Generation of Spatial Masks Frequency Domain Specification	01	T1 - 332 - 336	PPT
25	Homomorphic Filtering	01	T1 - 289 - 290	PPT
26	Color Image Processing	01	T1 – 390 - 410	PPT
Total Lecture Hours		**09**		
Total Hours		**09**		

UNIT-IV IMAGE RESTORATION AND RECONSTRUCTION OF MEDICAL IMAGES				
27	Image degradation models	01	https://prezi.com/l-e4nfgnkb9j/a-model-of-the-image-degradation-restoration-process/	PPT
28	Constrained and Unconstrained Vector	01	T1 – 290 - 297	PPT
29	Inverse Filtering	01	T1 – 351 - 352	PPT
30	Least Mean Square Filtering	01	T1 – 887	PPT

31	Image Reconstruction from projections	01	T1 – 362 - 381	PPT
32	Radon Transform	01	T1 - 368 - 373	PPT
33	Filter Bak Projection	01	T1 - 446 - 451	PPT
34	3D Tomography	01	https://en.wikipedia.org/wiki/Tomography	PPT
35	Fourier Reconstruction of MRI Images	01	T2 - 542	PPT
Total Lecture Hours		**09**		
Total Hours		**09**		

UNIT-V	**MEDICAL IMAGE COMPRESSION TECHNIQUES**			
36	Run Length Coding	01	T1 – 553	PPT
37	Huffman Coding	01	T1 - 542	PPT
38	Arithmetic Coding	01	T1 - 548	PPT
39	Pixel Coding	01	T1 - 479	PPT
40	Transform Coding	01	T2 - 477 - 504	PPT
41	JPEG Standard	01	T1 – 507 - 603	PPT
42	Predictive Standard	01	T1 – 577 - 603	PPT
43	Application of Image Processing techniques in thermography	01	https://www.ndt.net/article/aero2012/papers/we2a1.pdf	PPT
44	SPECT	01	https://mayfieldclinic.com/pe-spect.htm	PPT
45	PET Images	01	https://www.healthline.com/health/pet-scan	PPT
Total Lecture Hours		**09**		
Total Hours		**09**		

Total No of Hours for Introduction: 01 Hrs

Total No of Lecture Hours Planned: 44 Hrs

Total No of Hours Planned : 45 Hours

TEXT BOOK:

S.NO.	Author(s) Name	Title of the book	Publisher	Year of publication
1	Rafael Gonzalez, Richard E Woods	Digital Image Processing	2nd Edition, Parson	2003

REFERENCES:

S.NO.	Author(s) Name	Title of the book	Publisher	Year of publication
1	R. William K Prati	Digital Image Processing	John Wilsey	2013
2	Jain A.K	Fundamentals of Digital Image Processing	-	2002

STAFF IN-CHARGE **HOD/BME**

DIGITAL IMAGE FUNDAMENTAL

Dr Kamalraj Subramaniam

Associate Professor

Department of Biomedical Engg

FOE

Karpagam Academy of Higher Education

Digital Image Processing

- It is a processing of digital image by means of digital computer.
- It can be done through computer algorithms, in order to get enhanced image either to extract some useful information.

What is an Image?

- An image is a two-dimensional array which are specifically arranged in rows and columns.

$$f(x,y) = \begin{bmatrix} f(0,0) & f(0,1) & f(0,2) & \cdots & f(0,N-1) \\ f(1,0) & f(1,1) & f(1,2) & \cdots & f(1,N-1) \\ \vdots & \vdots & \vdots & & \vdots \\ f(M-1,0) & f(M-1,1) & f(M-1,2) & \cdots & f(M-1,N-1) \end{bmatrix}$$

- In other words, it is a two-dimensional function ie). **F(x,y)**, where x and y are spatial coordinates, and **F** is the amplitude at any pair of coordinates (x,y).

Fundamental types of Image:

Binary Image:

- The name itself we can suggest, it contain only two pixel elements i.e 0 & 1,where **0 refers to black and 1 refers to white**. It is also known as Monochrome.

Black and White Image:

- The image which consist of **only black and white color** is called black and white image.

8 bit Color Format:

- It is the most popular image format which has 256 different shades of colors in it and commonly known as Grayscale Image. In this format, 0 stands for Black, and 255 stands for white, and 127 stands for gray.

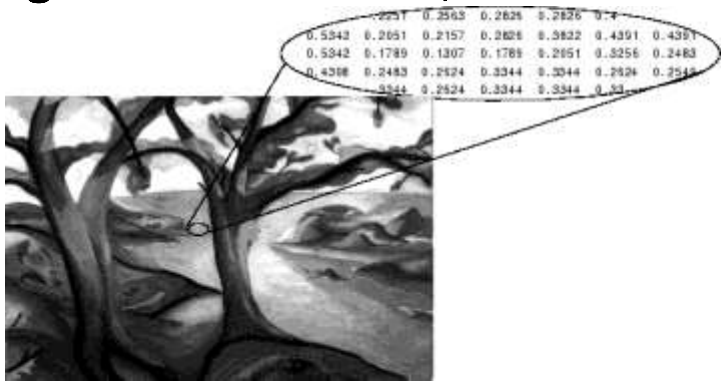

16 bit Color Format:

- It is a color image format which has 65,536 different colors in it. It also known as High Color Format. In this format the distribution of color is not as same as Grayscale image.
- A 16 bit format is actually divided into three further formats which are Red, Green and Blue. That famous RGB format.

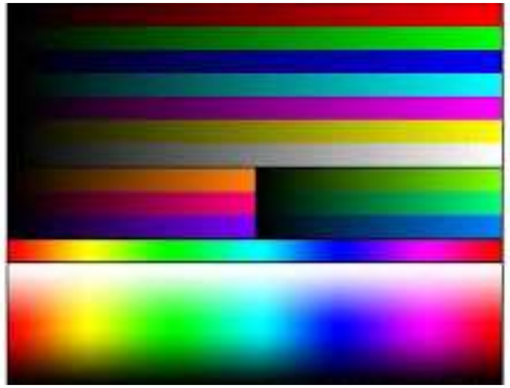

What is Digital Image?

- When x,y and **F** are finite, we call it as **digital image**.
- It is composed of a finite number of elements and each elements have a particular value at a particular location. These elements are referred as ***picture elements, image elements, and pixels*.**

A Pixel is most widely used to denote the elements of a Digital Image.

Elements of Image Processing

- The basic operations performed in a digital **image processing** systems includes

✓ **Acquisition**

✓ **Storage**

✓ **Processing**

✓ **Communication**

✓ **Display.**

Elements of Visual perception

- ✓Structure of the human eye
- ✓Image formation in the human eye
- ✓Brightness adaptation and discrimination
- ✓Match bands

Structure of Human Eye

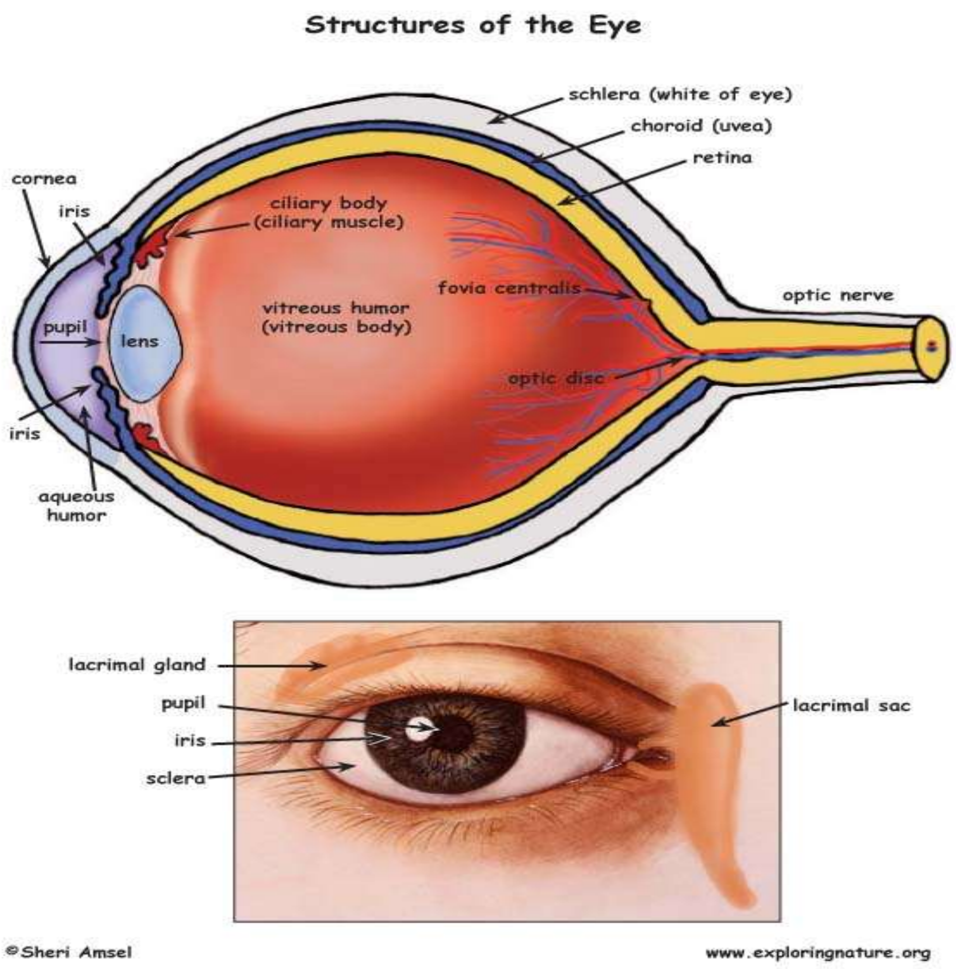

- The eye is nearly spherical in form with an average diameter of approximately 20 mm.
- It is enclosed by three membranes; the *cornea and sclera* outer cover, the *choroid*, and the *retina*.
- The cornea is a tough, transparent tissue that covers the anterior or front surface of the eye. The sclera is continuous with the cornea.

Human Vision

- The cornea and sclera outer cover
- The choroid

✓ **Ciliary body**

✓ **Iris diaphragm**

✓ **Lens**

- The retina (two kinds of receptors)

  The choroid lies the retina, the innermost membrane of the eye where the light entering the eye is sensed by the receptor cells. The retina has 2 types of photoreceptor cells – rods and cones. These receptor cells respond to light in the 330 to 730 nm wavelength range.

- Cones vision (photopic/bright-light vision) : centered at fovea, highly - **Sensitive to color**
- Rods (scotopic/dim-light vision) : general view - **Blind spot**

Cones and Rods

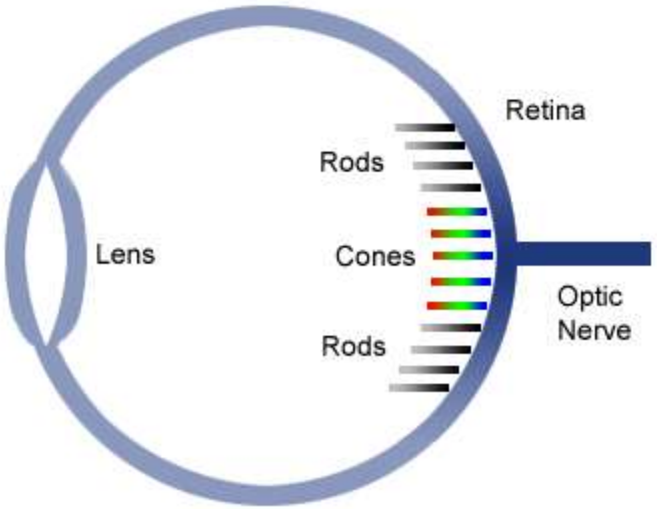

Rods	Cones
Outer segment is rod-shaped	Outer segment is cone-shaped
More numerous than cones	Few in number than rods
Distributed more or less even over the retina	More concentrated in & around yellow spot
None found at the yellow spot	Most numerous at yellow spot
Give poor visual acuity because many rods share a single neuron to brain	Give good visual acuity because each cone has its own neurone connected to the brain
Sensitive to low light intensity; therefore for night vision	Sensitive to high light intensity, therefore for day vision
Not sensitive to colour vision	Sensitive for colour vision
Contain rhodopsin in one form	Contain iodopsin in 3 forms

Distribution of Rods and Cones

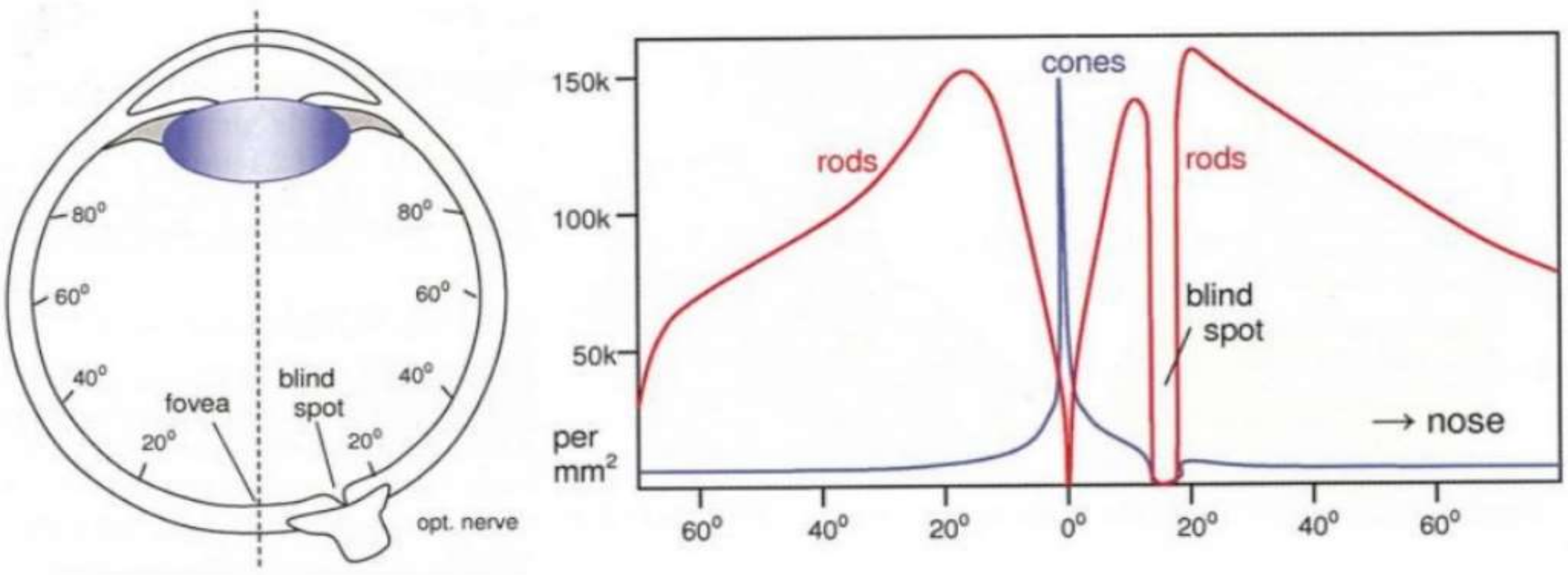

- Highest density of cones around fovea
- Blind spot at Optic Nerve exit point

Sensitivity and Color perception of Rods and Cones

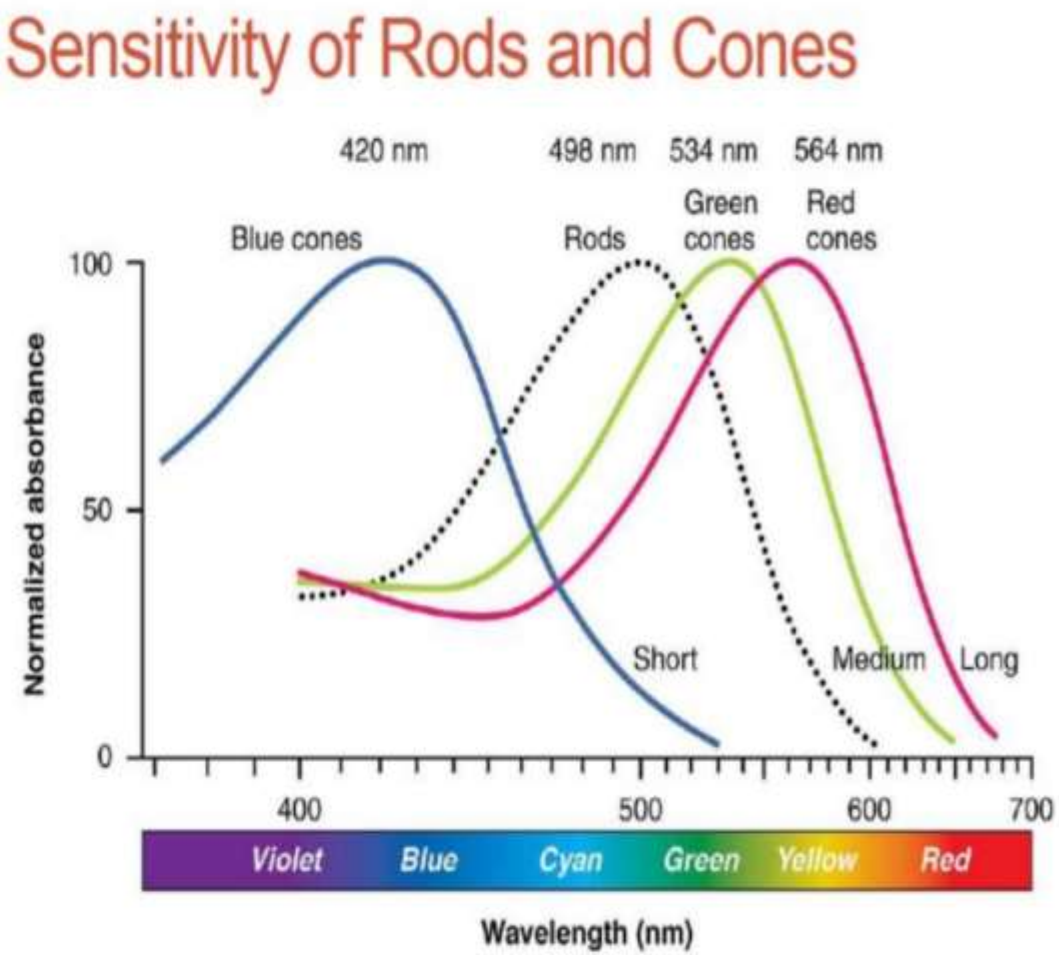

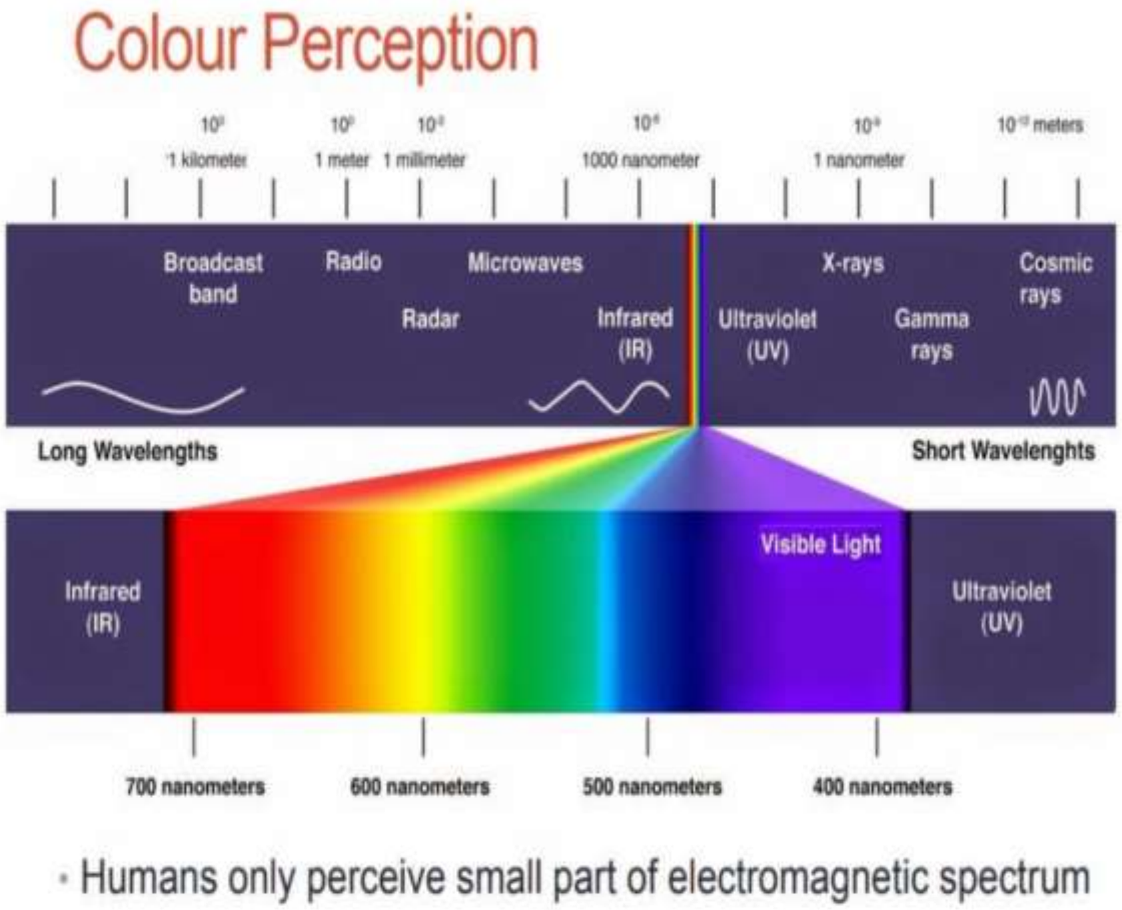

Image formation in the Human Eye

- Flexible lens:

  The principle difference from an ordinary optical lens.

- Controlled by the tension in the fibers of the ciliary body

✓ **To focus on distant objects – flattened**

✓ **To focus on objects near eye – thicker**

✓ **Near-sighted and far-sighted**

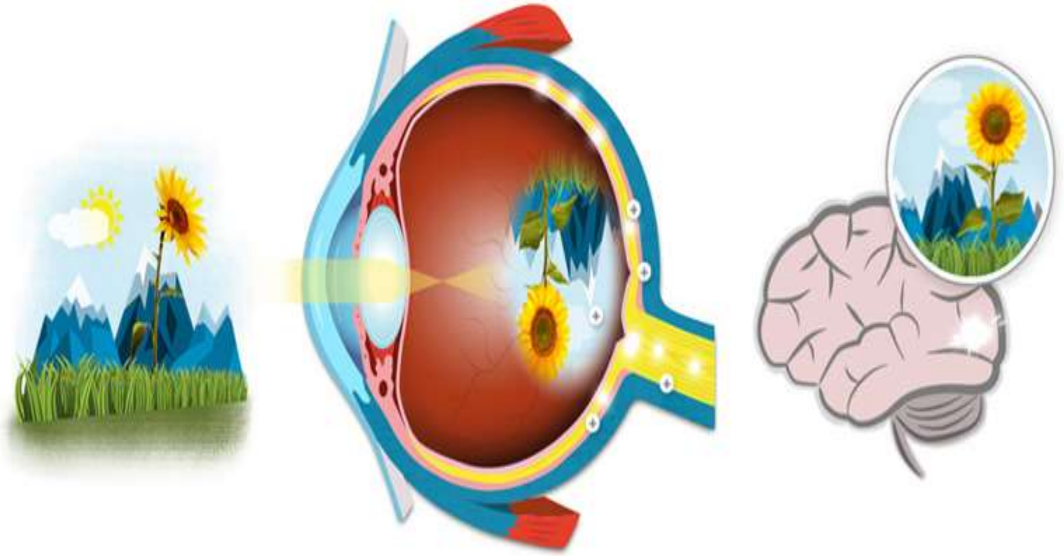

An interactive guide to the human eye and how it works.

From the moment light enters the eye to the interpretation of an image in the brain.

Brightness and Adaptation of Human Eye

Brightness Adaptation of Human Eye

The **brightness adaptation** is a phenomenon which describes the ability of the human eye in simultaneously discriminating distinct intensity levels.

The **brightness adaptation level** is the current sensitivity level of the visual system for any given set of conditions.

The **simultaneous contrast** is a phenomenon which describes that the perceived brightness of a region in an image is not a simple function of its intensity rather it depends on the intensities of neighboring regions.

Brightness Adaptation and Discrimination

Brightness Adaptation

- Dynamic range of human visual system:

  10-6~104 mL (millilambert)

- It can not accomplish this range simultaneously
- The current sensitivity level of the visual system is called brightness adaptation level

FIGURE 2.4 Range of subjective brightness sensations showing a particular adaptation level.

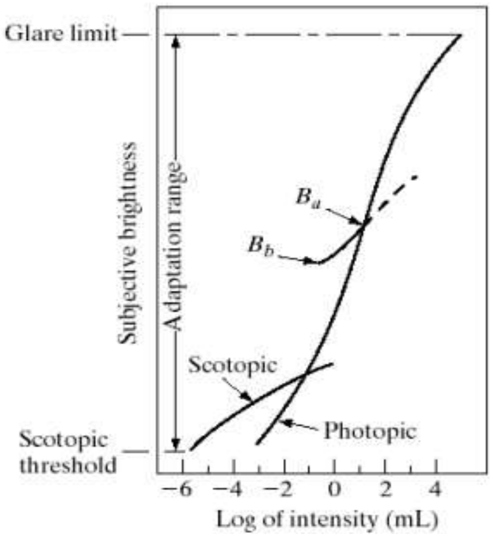

Brightness Discrimination

- Weber ratio (the experiment) :

  I: the background illumination

  I_c: the increment of illumination

- Small Weber ratio indicates good discrimination
- Larger Weber ratio indicates poor discrimination

FIGURE 2.6 Typical Weber ratio as a function of intensity.

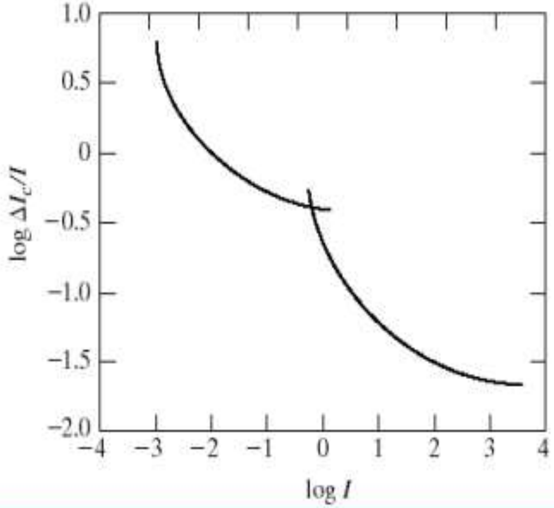

Mach band Effect

What is **Mach band effect**

- **Mach bands** is an optical illusion named after the physicist ***Ernst Mach in 1865***. It exaggerates the contrast between edges of the slightly differing shades of gray, as soon as they contact one another, by triggering edge-detection in the human visual system.

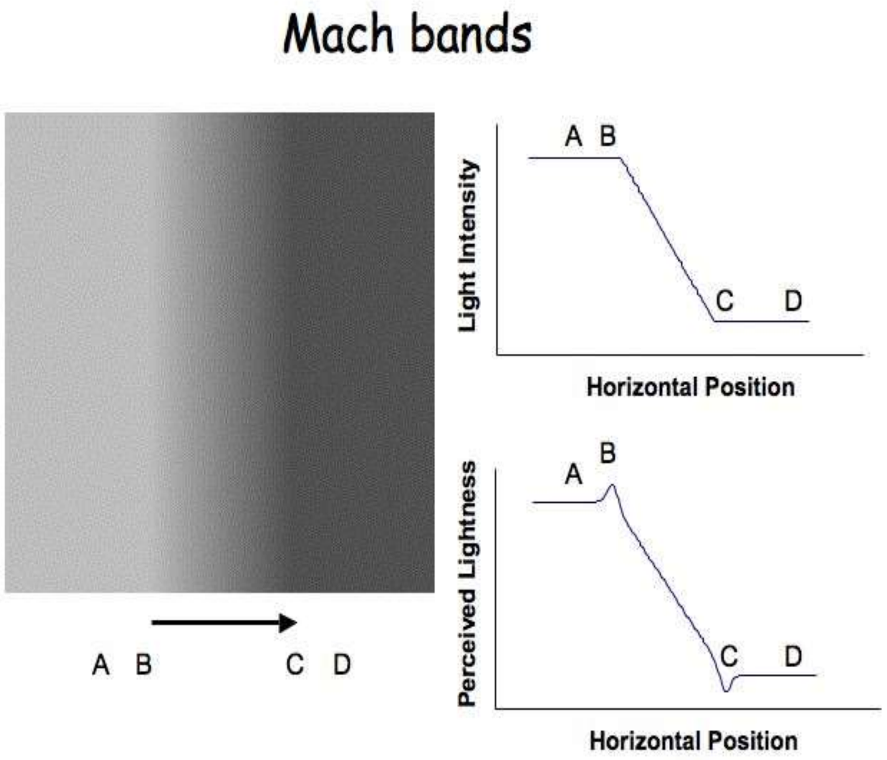

Simultaneous Contrast

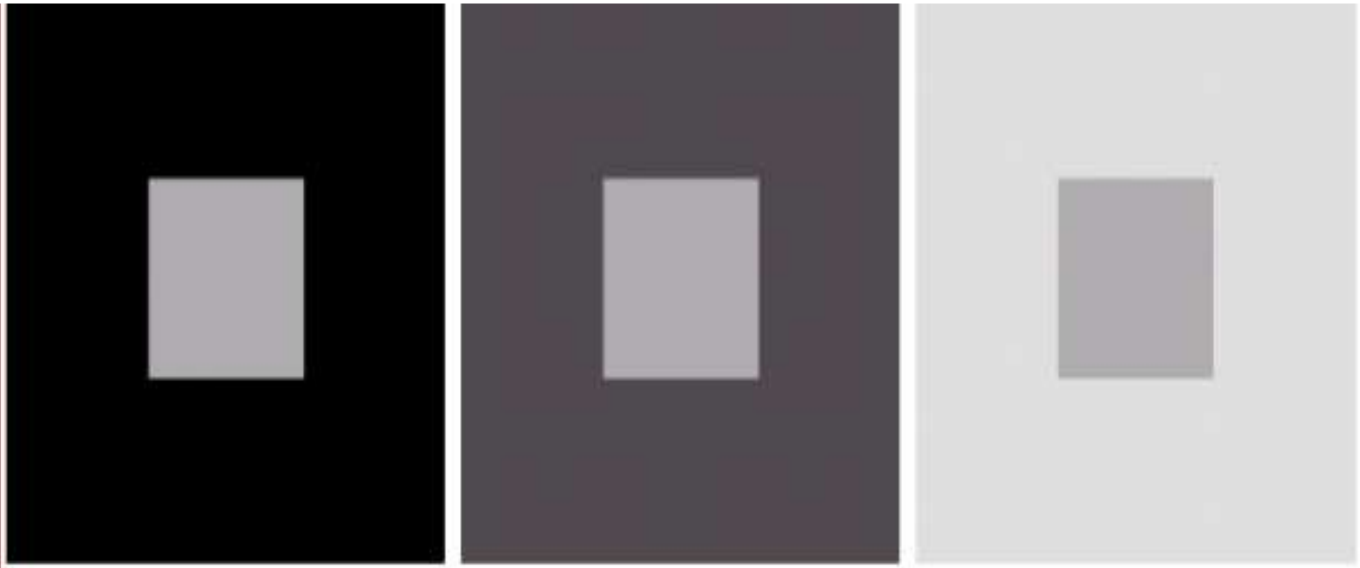

a b c

FIGURE 2.8 Examples of simultaneous contrast. All the inner squares have the same intensity, but they appear progressively darker as the background becomes lighter.

Optical Illusion

- An optical illusion also called a **visual illusion** is an illusion caused by the visual system and characterized by a visual percept that possibly appears to differ from reality.

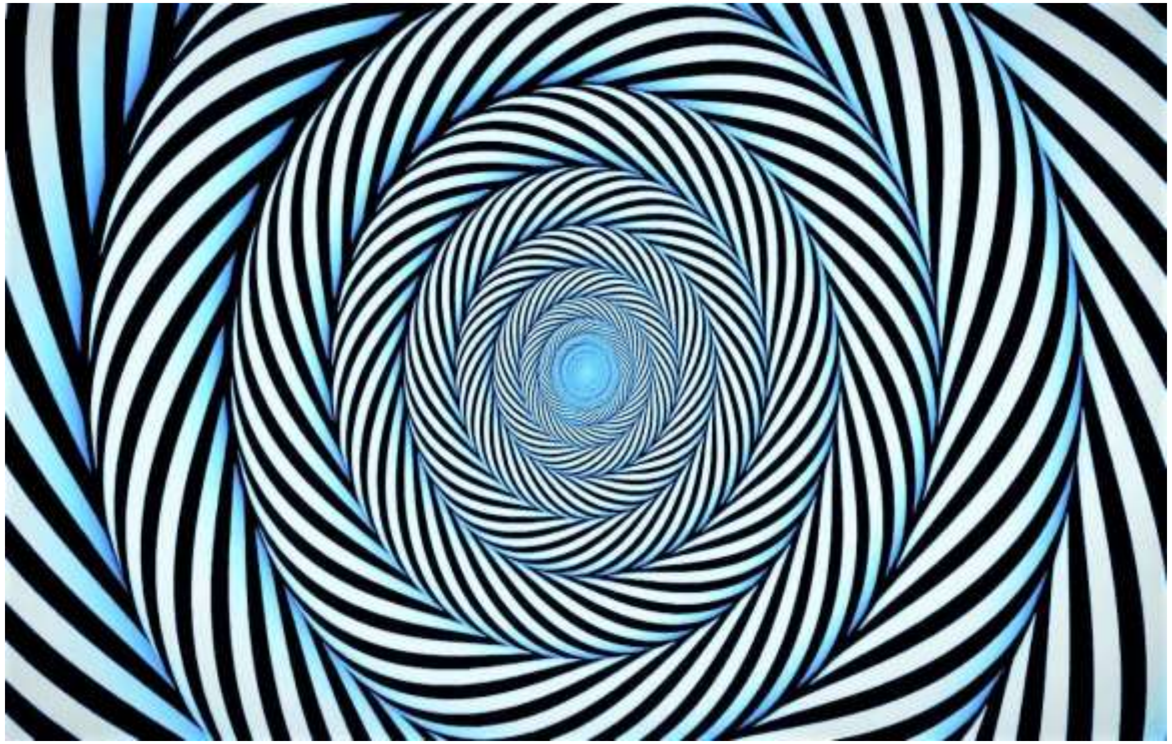

Hue, Saturation and Brightness

Color Model

- **HSB color** - Hue, Saturation, Brightness, the basic colors are created based on the amount of light (brightness) and the intensity of the color (saturation). Used in optical reproduction.
  - **Hue** - Hue is defined as the variation of the **tint** or **shade** of a color.
  - **Saturation -** The amount of a primary color applied on any specific area.
  - **Brightness** - The amount of light that a color allows to pass through, also called luminosity.

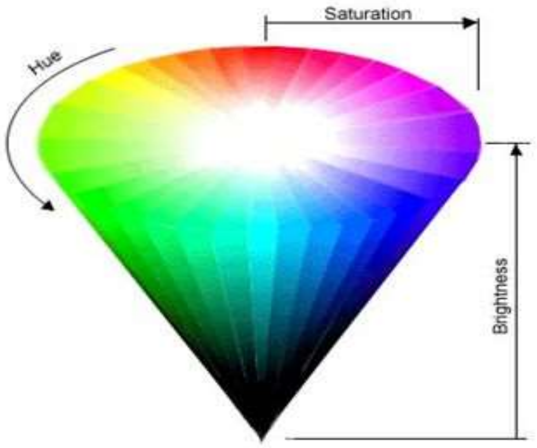

Image Sampling and Quantization

Image sampling and quantization

continuous image (in real life) → digital (computer)

To do this we use Two processes:
sampling and **quantization**.

Remember that:

the image is a function f(x,y),

□□ x and y are coordinates
□□ F: intensity value (Amplitude)

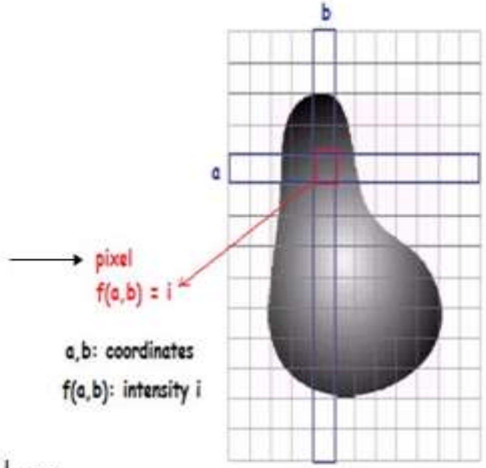

Sampling: digitizing the coordinate values
Quantization: digitizing the amplitude values
Thus, when x, y and f are all finite, discrete quantities, we call the image a digital image.

SAMPLING AND QUANTIZATION

- Quantization: limit of intensity resolution
- Sampling: Limit of spatial and temp resolution
  - Uniform and non-uniform

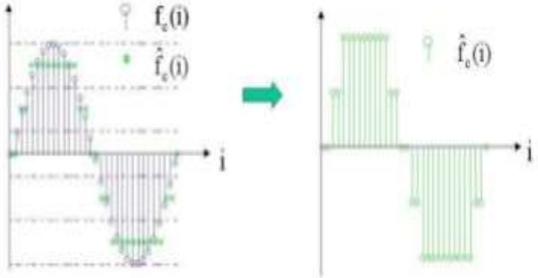

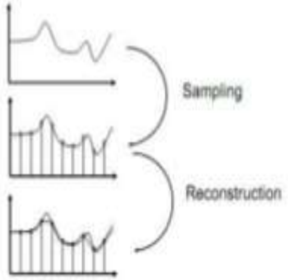

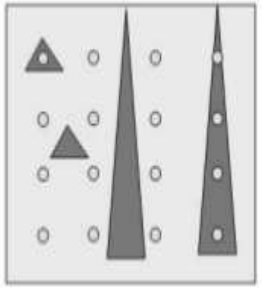

Basic relationships between Pixels, Matrix and Singular value for discrete images

Pixels:

- Pixels is the smallest element of an image, where each pixel correspond to any one value.

Matrix:

- In image processing, the matrix is said to be a kernel, convolution matrix, or mask is a small matrix. It is used for blurring, sharpening, edge detection of images.

Singular Value:

- It represent the image with a smaller set of values. It defines useful features of original image with less storage capacity in order to achieve the image compression process.

Relationship between pixels

Neighbors pixels:

- A pixel *p* at coordinates (*x*,*y*) has four *horizontal* and *vertical* neighbors whose coordinates are given by:

  (x+1,y), (x-1, y), (x, y+1), (x,y-1)

	(x, y-1)	
(x-1, y)	*P (x,y)*	(x+1, y)
	(x, y+1)	

This set of pixels, called the 4-*neighbors* or *p*, is denoted by $N_4(p)$. Each pixel is one unit distance from (x,y) and some of the neighbors of p lie outside the digital image if (x,y) is on the border of the image.

- The four *diagonal* neighbors of *p* have coordinates:

  (x+1, y+1), (x+1, y-1), (x-1, y+1), (x-1, y-1)

(x-1, y+1)		(x+1, y-1)
	P (x,y)	
(x-1, y-1)		(x+1, y+1)

and are denoted by $N_D(p)$.

These points, together with the 4-neighbors, are called the 8-neighbors of p, denoted by $N_8(p)$.

(x-1, y+1)	(x, y-1)	(x+1, y-1)
(x-1, y)	*P (x,y)*	(x+1, y)
(x-1, y-1)	(x, y+1)	(x+1, y+1)

As before, some of the points in $N_D(p)$ and $N_8(p)$ fall outside the image if (x,y) is on the border of the image.

Adjacency and Connectivity

- Let V: a set of intensity values used to define adjacency and connectivity.
- In a binary image, $V = \{1\}$, if we are referring to adjacency of pixels with value 1.
- In a gray-scale image, the idea is the same, but V typically contains more elements, for example, $V = \{180, 181, 182, \ldots, 200\}$
- If the possible intensity values 0 – 255, V set can be any subset of these 256 values.

Types of Adjacency

1. **4-adjacency:** Two pixels *p* and *q* with values from *V* are 4-adjacent if *q* is in the set $N_4(p)$.
2. **8-adjacency:** Two pixels *p* and *q* with values from *V* are 8-adjacent if *q* is in the set $N_8(p)$.
3. **m-adjacency =(mixed)**

   Two pixels *p* and *q* with values from *V* are m-adjacent if :

   - *q* is in $N_4(p)$ or
   - *q* is in $N_D(p)$ and the set $N_4(p) \cap N_4(q)$ has no pixel whose values are from V (no intersection)

A Digital Path

- A digital path (or curve) from pixel *p* with coordinate (x,y) to pixel *q* with coordinate (s,t) is a sequence of distinct pixels with coordinates (x_0,y_0), (x_1,y_1), …, (x_n, y_n) where $(x_0,y_0) = (x,y)$ and $(x_n, y_n) = (s,t)$ and pixels (x_i, y_i) and (x_{i-1}, y_{i-1}) are adjacent for $1 \le i \le n$
- n is the length of the path
- If $(x_0,y_0) = (x_n, y_n)$, the path is closed.
- We can specify 4-, 8- or m-paths depending on the type of adjacency specified.
- Return to the previous example:

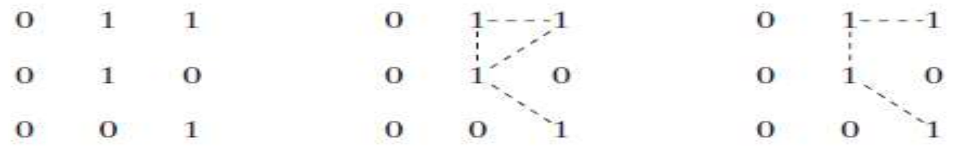

a b c

FIGURE 2.26 (a) Arrangement of pixels; (b) pixels that are 8-adjacent (shown dashed) to the center pixel; (c) *m*-adjacency.

In figure (b) the paths between the top right and bottom right pixels are 8-paths. And the path between the same 2 pixels in figure (c) is m-path

Connectivity:

- Let S represent a subset of pixels in an image, two pixels p and q are said to be connected in S if there exists a path between them consisting entirely of pixels in S.
- For any pixel p in S, the set of pixels that are connected to it in S is called a *connected component* of S. If it only has one connected component, then set S is called a *connected set*.

Region and Boundary:

Region

- Let R be a subset of pixels in an image, we call R a region of the image if R is a connected set.

Boundary

- The *boundary* (also called *border* or *contour*) of a region R is the set of pixels in the region that have one or more neighbors that are not in R.

Distance Measures

- It is defined as the shortest m-path between the points.
- In this case, the distance between two pixels will depend on the values of the pixels along the path, as well as the values of their neighbors.
- For pixels p, q and z, with coordinates (x,y), (s,t) and (v,w), respectively, D is a distance function if:

  (a) $D(p,q) \geq 0$ ($D(p,q) = 0$ iff $p = q$),

  (b) $D(p,q) = D(q, p)$, and

  (c) $D(p,z) \leq D(p,q) + D(q,z)$.

- The *Euclidean Distance* between p and q is defined as:

$$D_e(p,q) = [(x - s)^2 + (y - t)^2]^{1/2}$$

Pixels having a distance less than or equal to some value r from (x,y) are the points contained in a disk of radius r centered at (x,y)

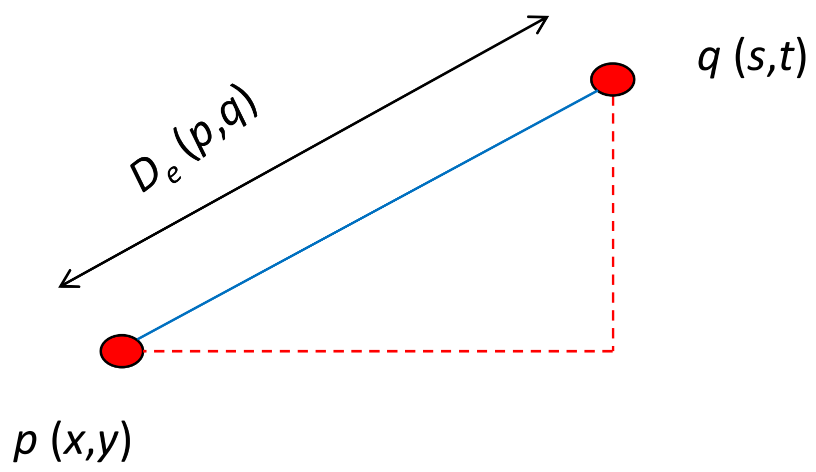

- The D_4 *distance* (also called *city-block distance*) between *p* and *q* is defined as:

  $D_4(p,q) = | x - s | + | y - t |$

Pixels having a D_4 distance from (x,y), less than or equal to some value r form a Diamond centered at (x,y)

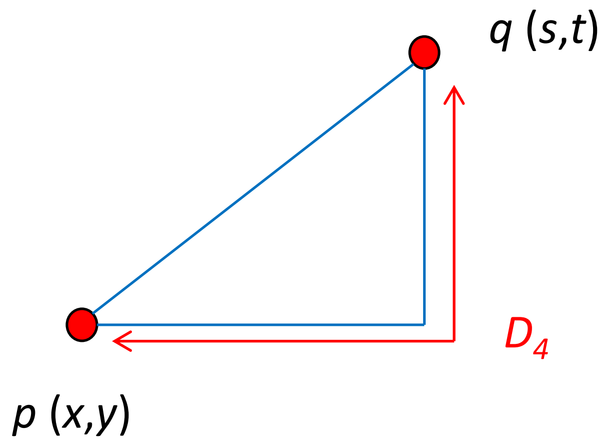

Example:

The pixels with distance $D_4 \leq 2$ from (x,y) form the following contours of constant distance.

The pixels with $D_4 = 1$ are

the 4-neighbors of (x,y)

		2		
	2	1	2	
2	1	0	1	2
	2	1	2	
		2		

The D_8 *distance* (also called *chessboard distance*) between *p* and *q* is defined as:

$$D_8(p,q) = \max(|x - s|, |y - t|)$$

Pixels having a D_8 distance from (x,y), less than or equal to some value r form a square Centered at (x,y)

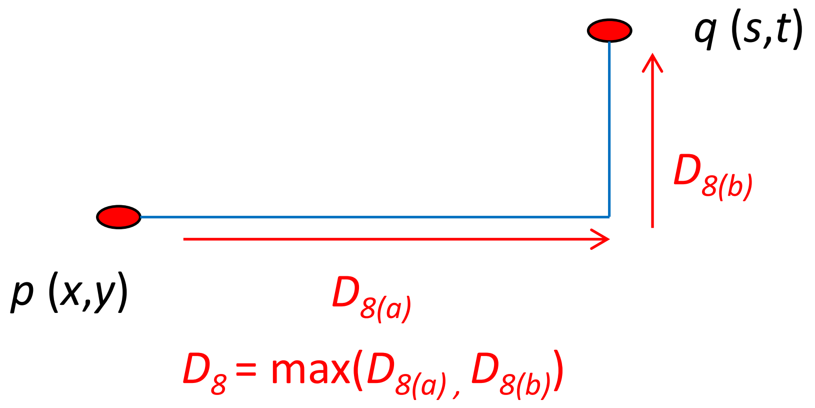

- Cont. Example:

  Now, to compute the D_m between points p and p_4

  Here we have 4 cases:

Case1: If p_1 =0 and p_3 = 0

The length of the shortest m-path

(the D_m *distance) is 2 (p,* p_2*,* p_4*)*

	0	1
0	1	
1		

Case2: If p_1 =1 and p_3 = 0

now, p_1 *and p will no longer be adjacent (see m-adjacency definition)*

then, the length of the shortest path will be 3 (p, p_1, p_2, p_4)

	0	1
1	1	
1		

Case3: If p_1 =0 and p_3 = 1

The same applies here, and the shortest –m-path will be 3 (p, p_2, p_3, p_4)

	1	1
0	1	
1		

Case4: If p_1 =1 and p_3 = 1

The length of the shortest m-path will be 4 (p, p_1 , p_2, p_3, p_4)

	1	1
1	1	
1		

Singular Value Decomposition

- If ***m=n,*** then:

$$A = UDV^T$$

- *U* is ***n x n*** and orthonormal ($U^TU=UU^T=I$)
- *D* is ***n x n*** and diagonal

$$D = diag(\sigma_1, \sigma_2, \ldots, \sigma_n)$$

- *V* is ***n x n*** and orthonormal

- The columns of U are eigenvectors of AA^T
- The columns of V are eigenvectors of A^TA

$$AA^T = UDV^TVDU^T = UD^2U^T$$

- If λ_i is an eigenvalue of A^TA (or AA^T), then $\lambda_i = \sigma_i^2$

$$A^TA = VDU^TUDV^T = VD^2V^T$$

SVD Example

$$A = \begin{bmatrix} 0.9501 & 0.8913 & 0.8214 & 0.9218 \\ 0.2311 & 0.7621 & 0.4447 & 0.7382 \\ 0.6068 & 0.4565 & 0.6154 & 0.1763 \\ 0.4860 & 0.0185 & 0.7919 & 0.4057 \end{bmatrix} \qquad A = \sum_{i=1}^{n} \sigma_i u_i v_i^T$$

$U = (u_1\ u_2\ .\ .\ .\ u_n)$

$V = (v_1\ v_2\ .\ .\ .\ v_n)$

$$U = \begin{bmatrix} 0.7301 & 0.1242 & 0.1899 & -0.6445 \\ 0.4413 & 0.6334 & -0.3788 & 0.5104 \\ 0.3809 & -0.3254 & 0.6577 & 0.5626 \\ 0.3564 & -0.6910 & -0.6229 & 0.0871 \end{bmatrix}$$

$$V = \begin{bmatrix} 0.4903 & -0.4004 & 0.5191 & -0.5743 \\ 0.4770 & 0.6433 & 0.4642 & 0.3783 \\ 0.5362 & -0.5417 & -0.2770 & 0.5850 \\ 0.4945 & 0.3638 & -0.6620 & -0.4299 \end{bmatrix}$$

$$D = \begin{bmatrix} 2.4479 & 0 & 0 & 0 \\ 0 & 0.6716 & 0 & 0 \\ 0 & 0 & 0.3646 & 0 \\ 0 & 0 & 0 & 0.1927 \end{bmatrix}$$

Another Example

$$A = \begin{bmatrix} 1 & 2 & 1 \\ 2 & 3 & 2 \\ 1 & 2 & 1 \end{bmatrix},$$

The eigenvalues of AA^T , A^TA are:

$$\begin{bmatrix} \lambda_1 \\ \lambda_2 \\ \lambda_3 \end{bmatrix} = \begin{bmatrix} 28.86 \\ 0.14 \\ 0 \end{bmatrix}$$

The eigenvectors of AA^T , A^TA are:

$$u_1 = v_1 = \begin{bmatrix} 0.454 \\ 0.766 \\ 0.454 \end{bmatrix}, u_2 = v_2 = \begin{bmatrix} 0.542 \\ -0.643 \\ 0.542 \end{bmatrix}, u_3 = v_3 = \begin{bmatrix} -0.707 \\ 0 \\ -0.707 \end{bmatrix}$$

Properties of SVD

- A square ($n \times n$) matrix A is singular iff at least one of its singular values $\sigma_1, \ldots, \sigma_n$ is zero.
- The rank of matrix *A* is equal to the number of nonzero singular values σ_i


Thank You

PET
(Positron Emission Tomography)

BY:
Prikshit Kumar
2011CS1029

Contents

- Introduction
- How does it work?
- Applications
- Where it is used in Neurolinguistics?
- Summary

- Positron Emission Tomography (PET) is a nuclear imaging technique that produces a 3-D image of functional processes in the body by detecting the radiation emitted by photons .
- The system detects pairs of gamma rays emitted indirectly by positron emitting radionuclide (tracer), which was previously injected in body on a biologically active molecule,
- 3-D images of tracer concentration within the body are then constructed by computer analysis.

A PET facility

Scanner

Working

- Injection of Short lived Radioactive Isotope in body.

most commonly used is FDG (fluoro-2-deoxyglucose).

- Wait till tracer gets accumulated in tissues of interests.
- Subject is placed in the imaging scanner
- Tissue concentration is recorded with time.
- As isotope decays in body, it releases a positron in body. On interaction with an electron, it produces a pair of photons.

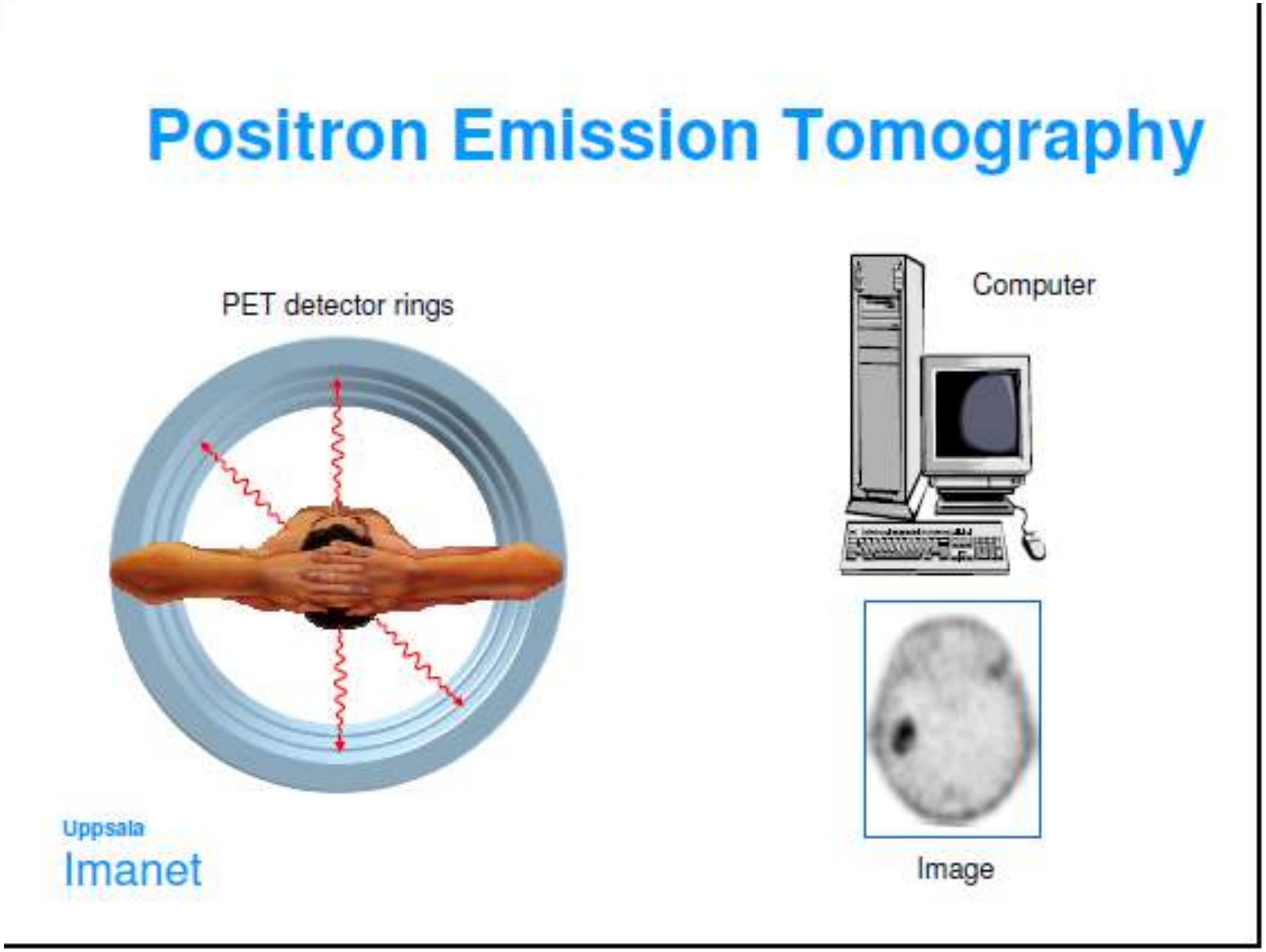

PET scanner detect these photons and with the help of a computer creates pictures offering details on both the structure and function of organs and tissues in your body.

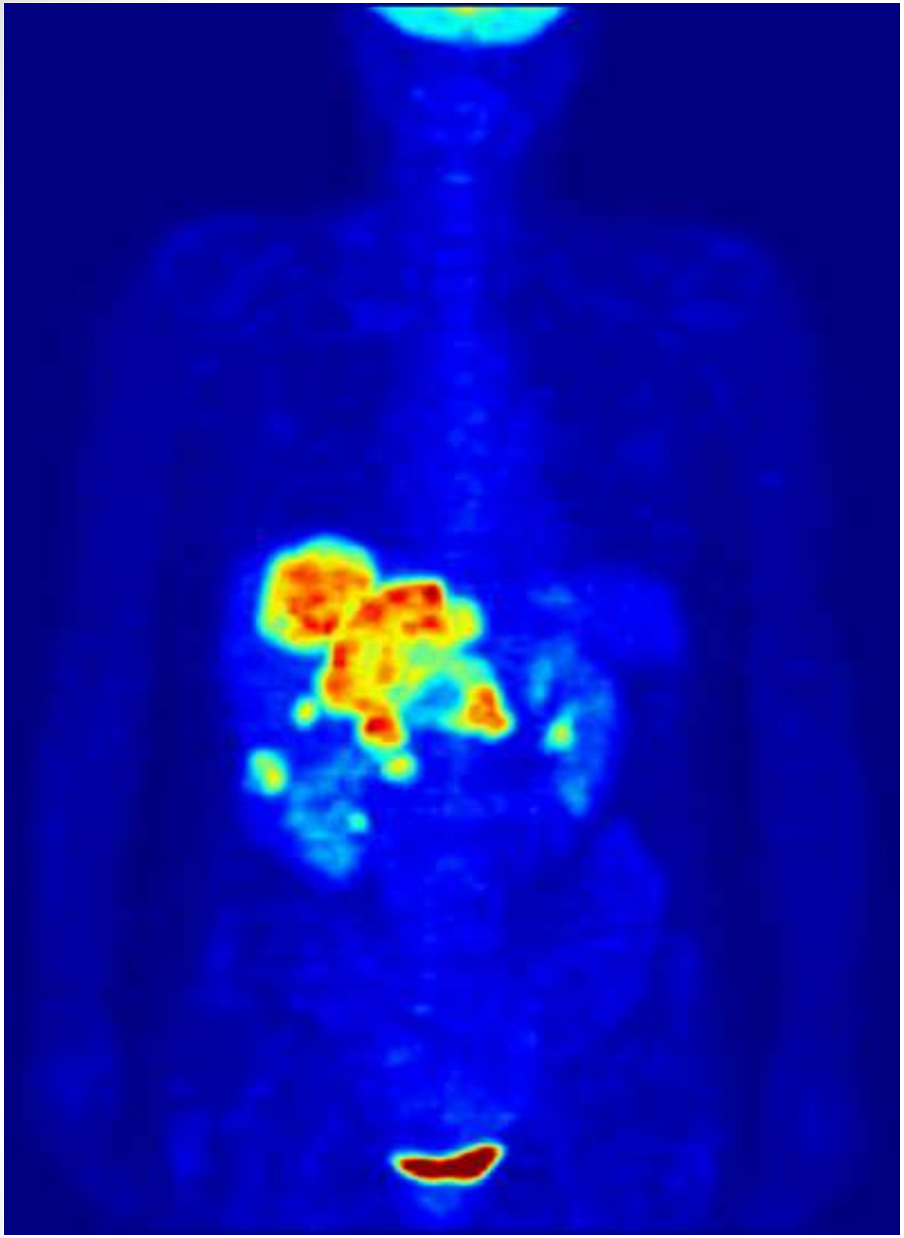

A whole body Pet scan using FDG.

Applications of PET

- PET is used in following areas.
- **Neuroimaging**
- **Clinical oncology** (medical imaging of tumors).
- **Musculo-skeletal imaging**
- **Cardiology**
- **Pharmacology**
- **Neuropsychology**

Neuroimaging

- The greatest benefit of PET is that it can show blood and oxygen flow and glucose metabolism to different tissues of working brain. These measurements help in understanding amount of brain activity and allow us to know more about how brain works.
- PET is superior to all other imaging techniques because of its resolution and speed of completion.

BRAIN PET SCANS DURING LINGUISTICS ACTIVITIES

By analyzing the BRAIN PET scans , we can find out that the person has difficulty in which areas.

For e.g.

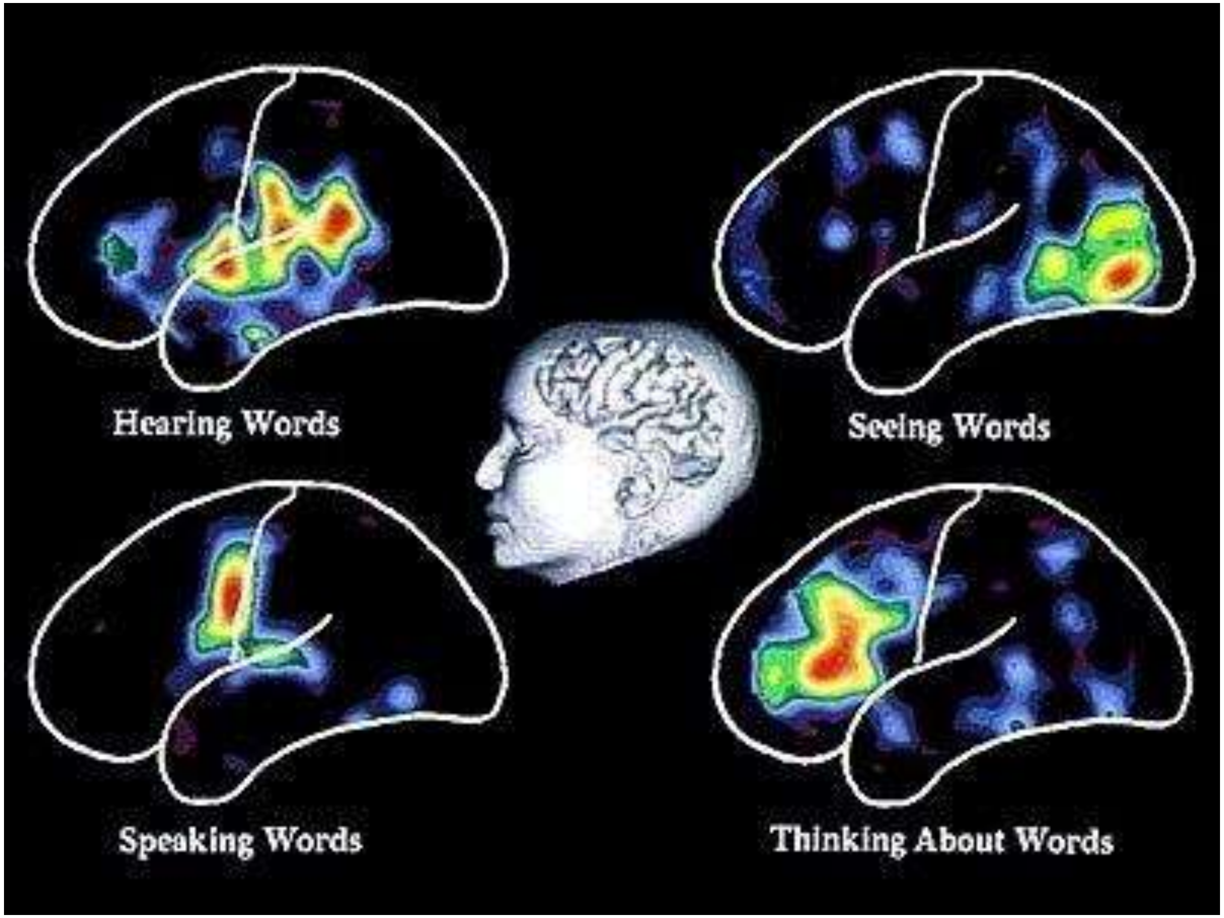

Brain PET scans of different Addicts

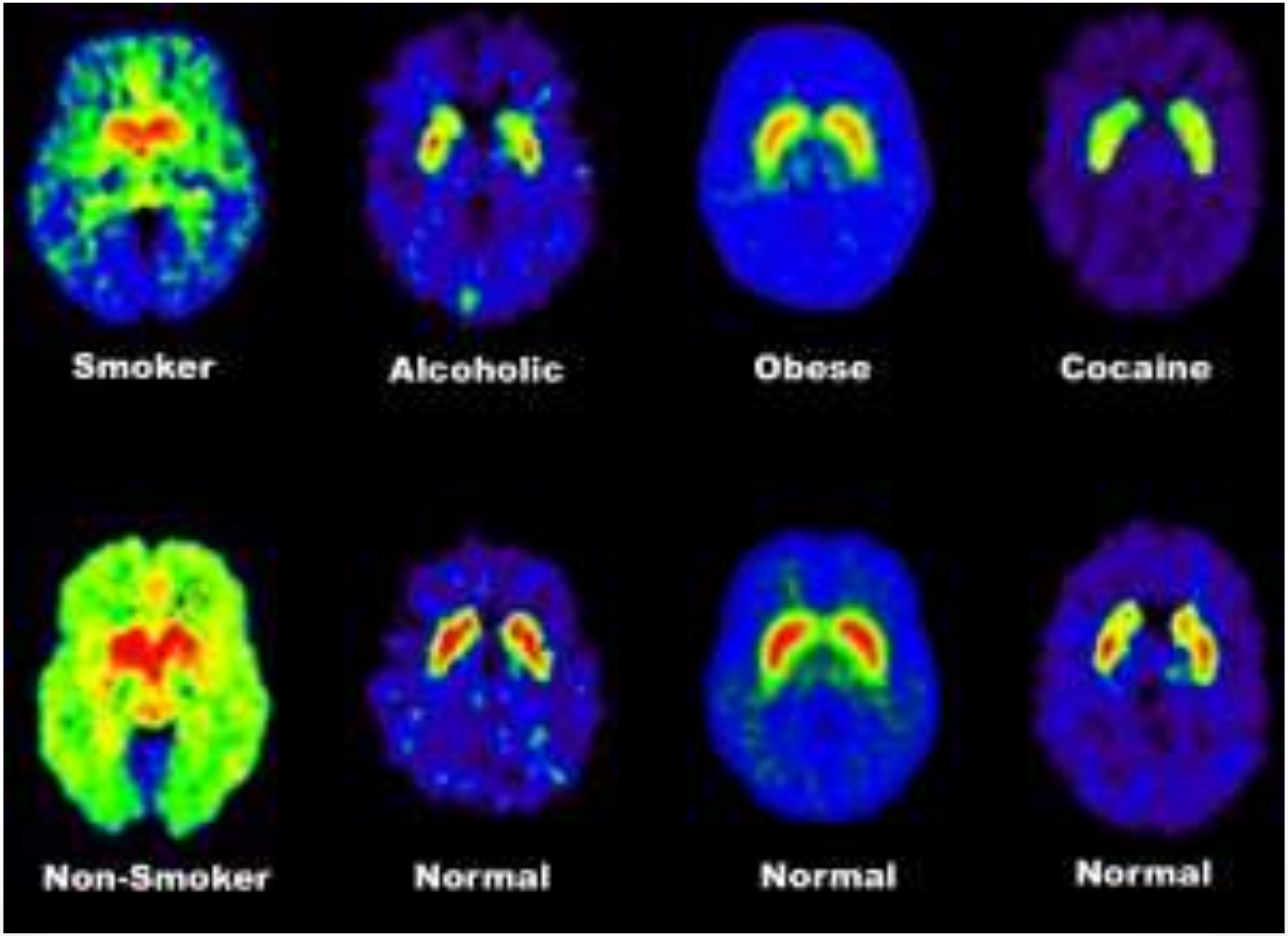

Brain Diseases and PET

- PET scanning is also used for diagnosis of brain diseases most notably because all the brain diseases like tumors, strokes and neuron damaging diseases which cause Dementia (like Alzheimer's disease) all cause great change in brain metabolism which causes easily detectable changes in PET scans.
- PET scan is most commonly used in case of certain dementias like(***Alzheimer's Disease*** and ***Pick's Disease***) where the early damage is not detected by using CT and MRI scans.

Brain PET scans of Other Diseases

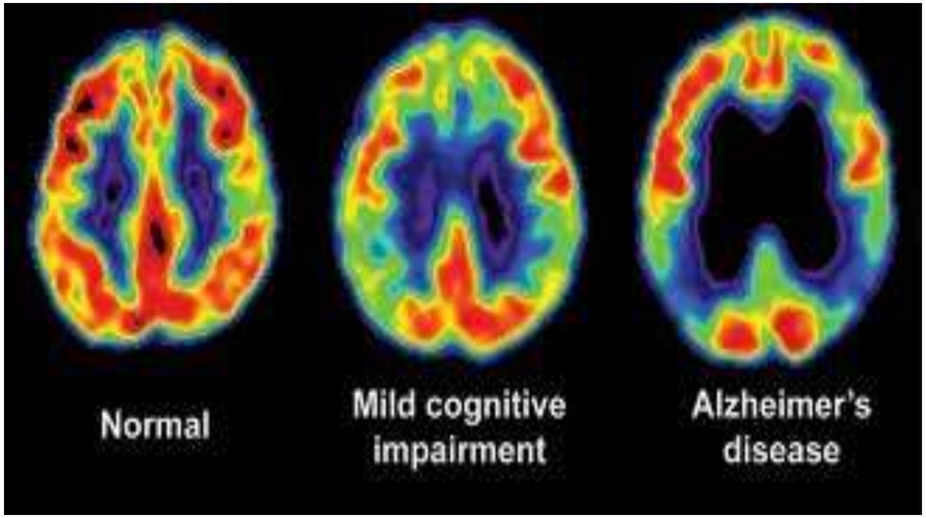

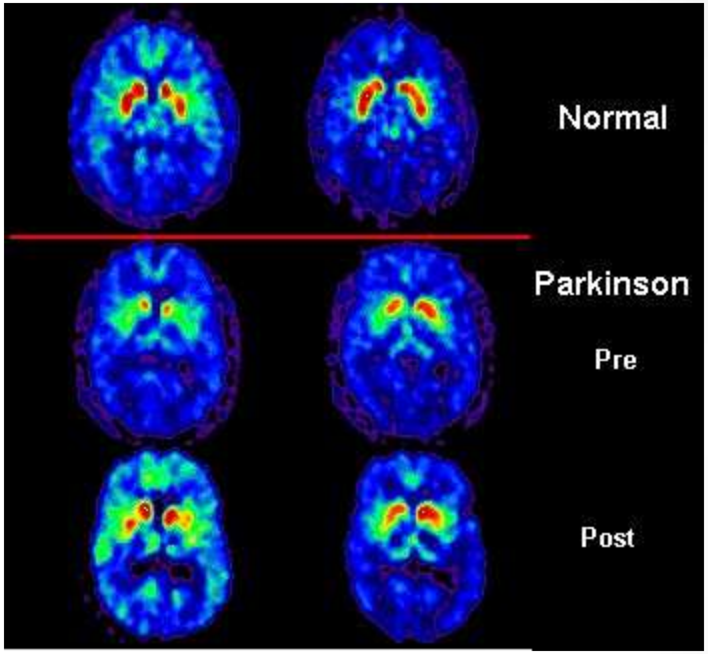

Pick's Disease

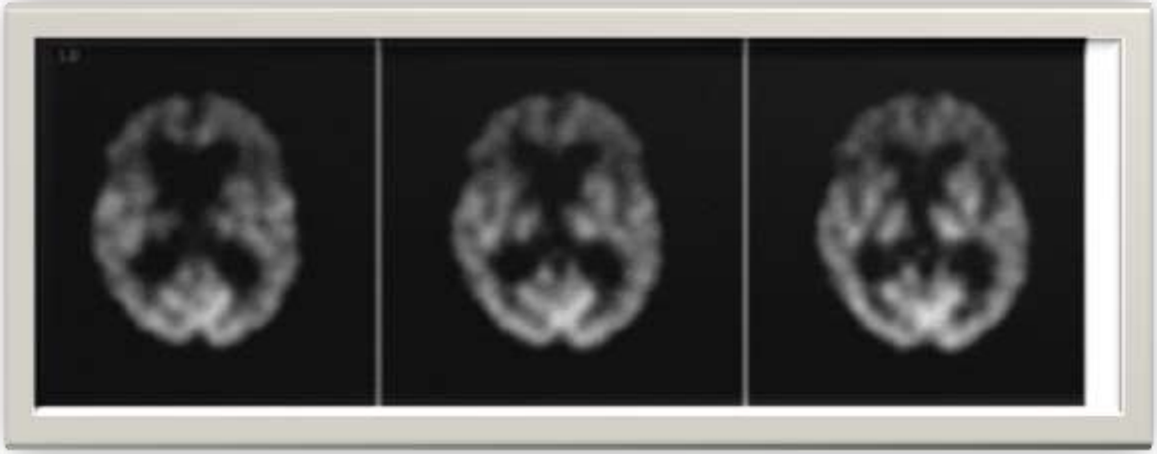

PET scan of patient with Pick's Disease showing Decreased Metabolism in frontal lobe. (Activity is represented in black)

Neuropsychology

- PET is used in neuropsychology to examine links between specific psychological processes or disorders and brain activity.

  - Psychiatry:

- To cure mental disorders, patients are given some drugs that selectively bind to Neuroreceptors of interest. To check the states of these receptors , we need to use to PET SCANS.

Oncology

- Most widely used Application of PET
- Tracer used is FDG-18.
- Highly accurate as tumor cells consume lot of glucose.
- And Tracer is a glucose analog.

- Also, tracer is bound in tumor cell once it got there until it decays.

- Thereby, giving more accurate results.

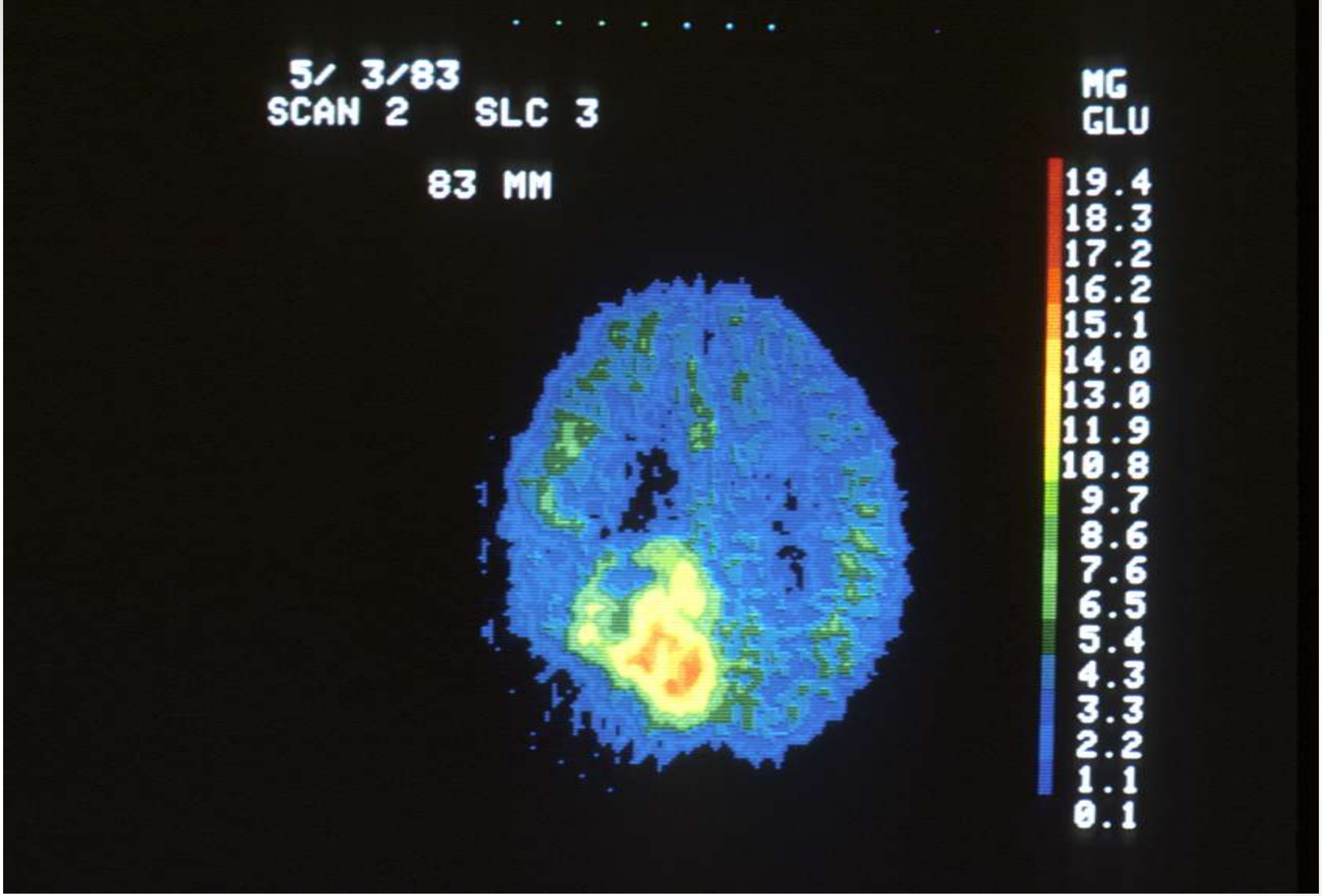

PET SCAN of Brain Tumor

White shows the areas of high Metabolic Activity

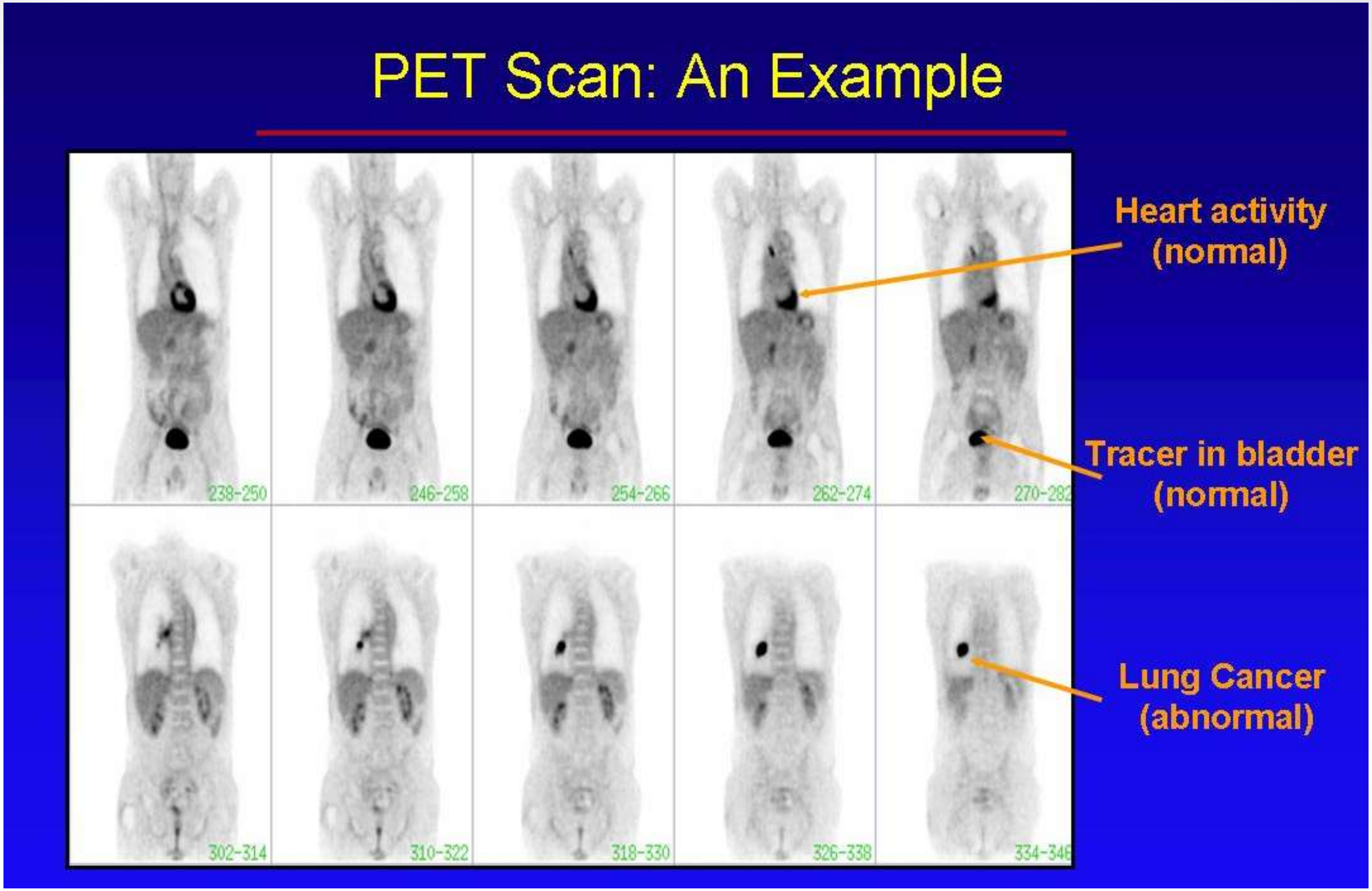

PET Scan Showing Lung Cancer

Musculo –Skeletal Imagaing

- One of the main advantage using PET is that it can also provide muscle activation data about deeper lying muscles as compared to other muscle studying techniques.

  But…

- there is an disadvantage also as provides no timing information about muscle activation because it has to be measured after the exercise is complete.

Cardiology and Pharmacology

- In Cardiology, PET helps us to detect patients at the risk of stroke.
- In pre-clinical trials, it is possible to radiolabel a new drug and test it on animals. The drug accumulates in tissues of interest and hence, providing information about the effectiveness of drug.

Summary

- PET scan is very good imaging technique used in both medical oncology and brain imaging.
- This scan is most effective due to its lesser time of completion and better resolution and also less exposing to radioactivity than CT scan, high accuracy in detecting brain diseases (at very early stage too)and prediction of various strokes.
- But its high cost is a major drawback.
- In future, if we are able to reduce its cost, than this technique can of great use to us.

References

- [[PET]] Wikipedia.com
- Science Direct
- Google
- House.Wikia
- Medicalnewstoday.com

Thank You

IMAGE ENHANCEMENT

Dr Kamalraj Subramaniam
Associate Professor
Department of Biomedical Engg
FOE
Karpagam Academy of Higher Education

OUTLINE

- Introduction
- Image enhancement methods:

  Spatial-Frequency domain

  Point operations

  Histogram

  Spatial Transform
- False color and pseudocoloring
- Color image enhancement

INTRODUCTION

•**Image enhancement** is the process of adjusting digital **images** which the results are more suitable for display or further **image** analysis.

•For example, you can remove noise, sharpen, or brighten an **image**, making it easier to identify key features.

Cont.

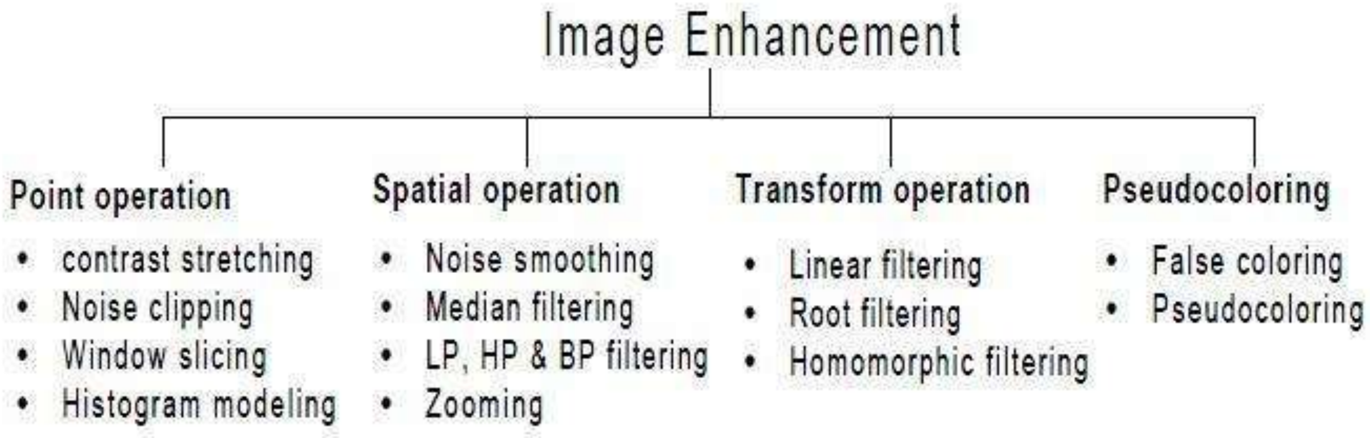

- Image enhancement methods can be based on either spatial or frequency domain techniques.

Spatial-Frequency domain enhancement methods

Spatial domain enhancement methods:

- Spatial domain techniques are performed to the image plane itself and they are based on direct manipulation of pixels in an image.
- The operation can be formulated as $g(x,y) = T[f(x,y)]$,

  where g is the output, f is the input image and T is an operation on *f defined over some* neighborhood of (x,y).
- According to the operations on the image pixels, it can be further divided into 2 categories: *Point operations and spatial operations*.

Frequency domain enhancement methods:

- These methods enhance an image *f(x,y) by* convoluting the image with a linear, position invariant operator.
- The 2D convolution is performed in frequency domain with DFT. Spatial domain: $g(x,y)=f(x,y)*h(x,y)$

  Frequency domain: $G(w1,w2)=F(w1,w2)H(w1,w2)$

Point operations

-Zero-memory operations where a given gray level u∈[0,L] is mapped into a gray level v∈[0,L] according to a transformation.

v(m,n)=*f(u(m,n))*

$$v(m,n) = f\big(u(m,n)\big), \forall m = 0,1,\ldots,M-1; n = 0,1,\ldots,N-1;$$

$$f : \{0,1,\ldots,L_{Max}\} \rightarrow \{0,1,\ldots,L_{Max}\}$$

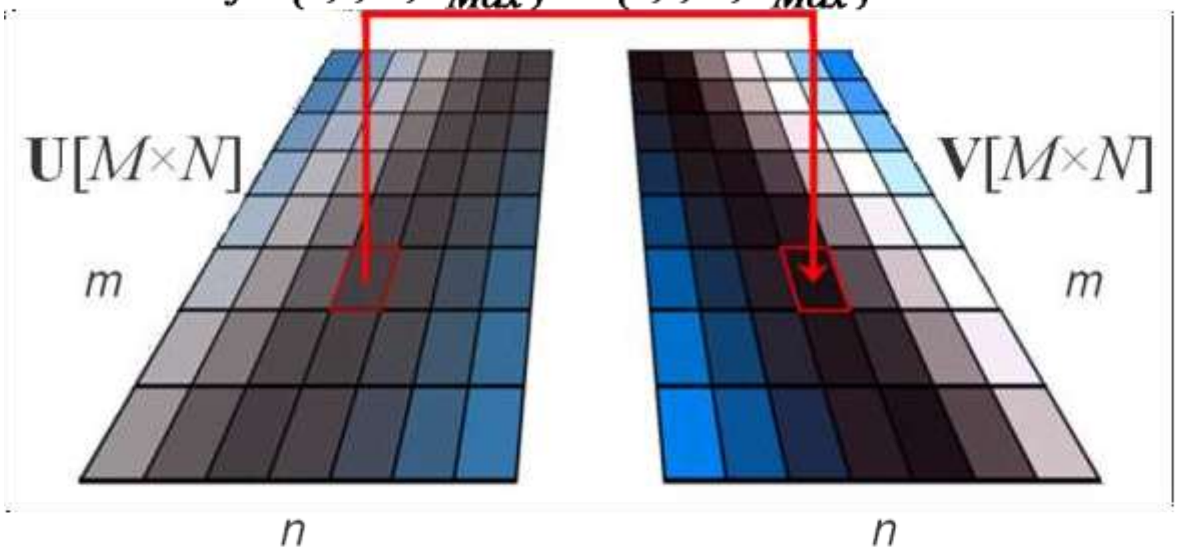

1-contrast stretching

- The idea behind contrast stretching is to increase the dynamic range of the gray levels in the image being processed.

- Low contrast images occur often due to :

  -poor or nonuniform lightning conditions

  -small dynamic range of imaging sensors

- $$v = \begin{cases} \alpha u, & 0 \le u < a \\ \beta(u-a) + v_a, & a \le u < b \\ \gamma(u-b) + v_b, & b \le u < L \end{cases}$$

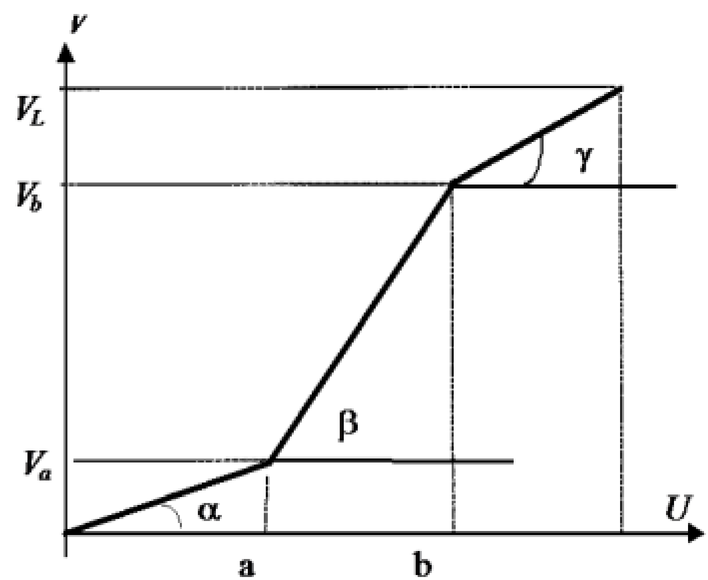

-For dark region stretch α>1 ,a=L/3

-For mid region stretch β>1 ,b=2/3L

-For bright region stretch γ>1

Example 1

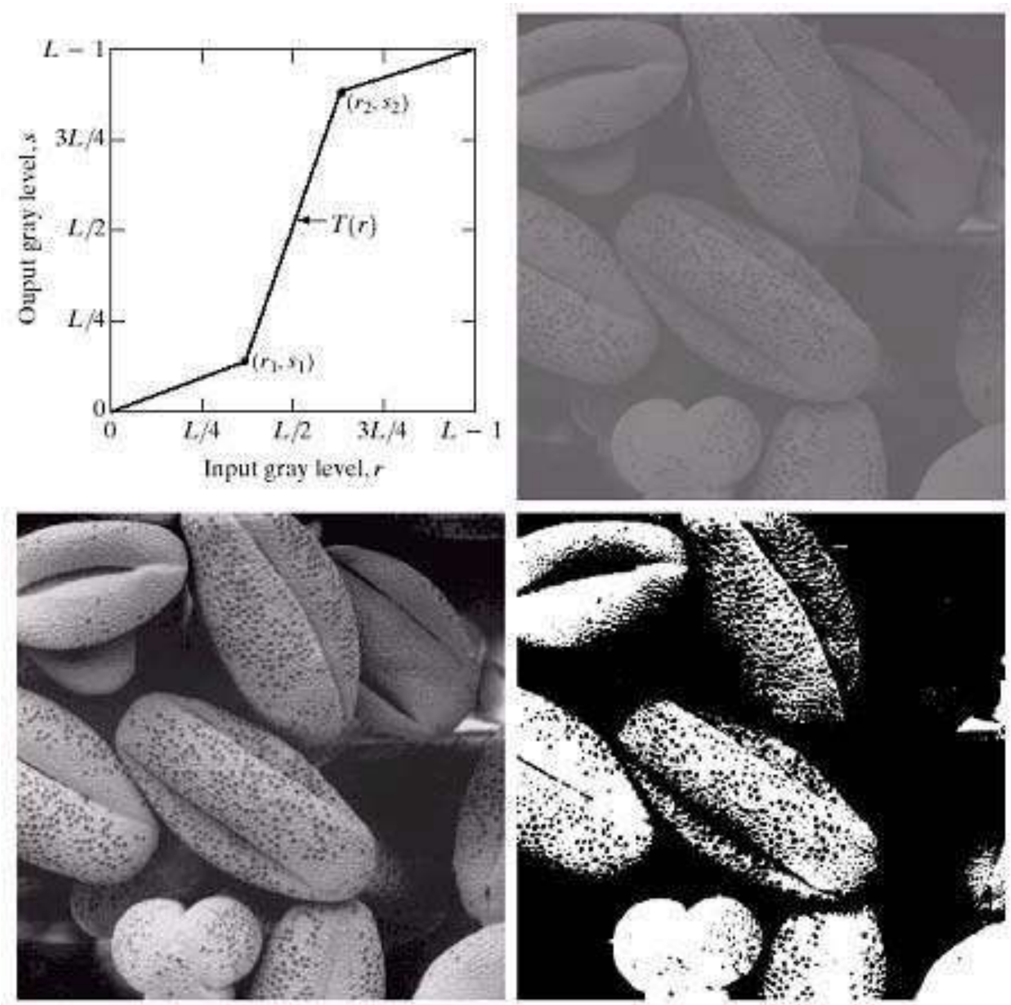

- (b) a low-contrast image : results from poor illumination, lack of dynamic range in the imaging sensor, or even wrong setting of a lens aperture of image acquisition

- (c) result of contrast stretching : (r1,s1) = (rmin,0) and (r2,s2) = (rmax,L-1)

- (d)result of thresholding

2-Clipping and Thresholding

- Expressed as :

Noise clipping and thresholding

$$f(u) = \begin{cases} 0, & 0 \le u < a \\ \alpha u, & a \le u \le b \\ L, & u \ge b \end{cases}$$

Useful for binary or other images that have bimodal distribution of gray levels. The a and b define the valley between the peaks of the histogram. For $a = b = t$, this is called *thresholding*.

- **<u>Clipping:</u>**

-Special case of contrast stretching ,where α= γ=0

-Useful for noise reduction when the input signal is known to lie in the range [a,b].

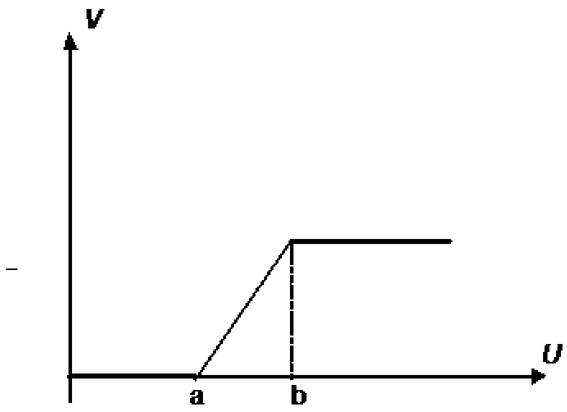

Cont.

- **Thresholding:**

- is a special case of case of clipping where a=b=t and the output comes binary.

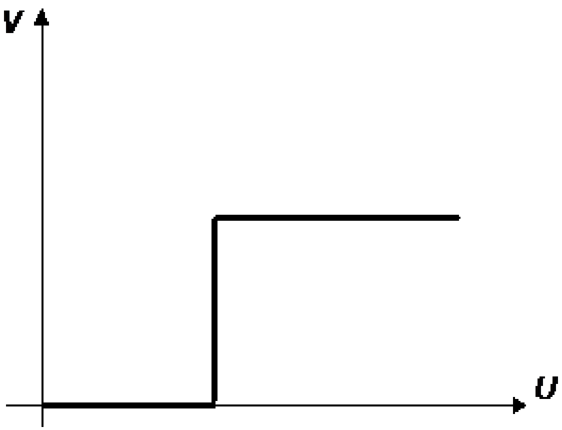

Example 1

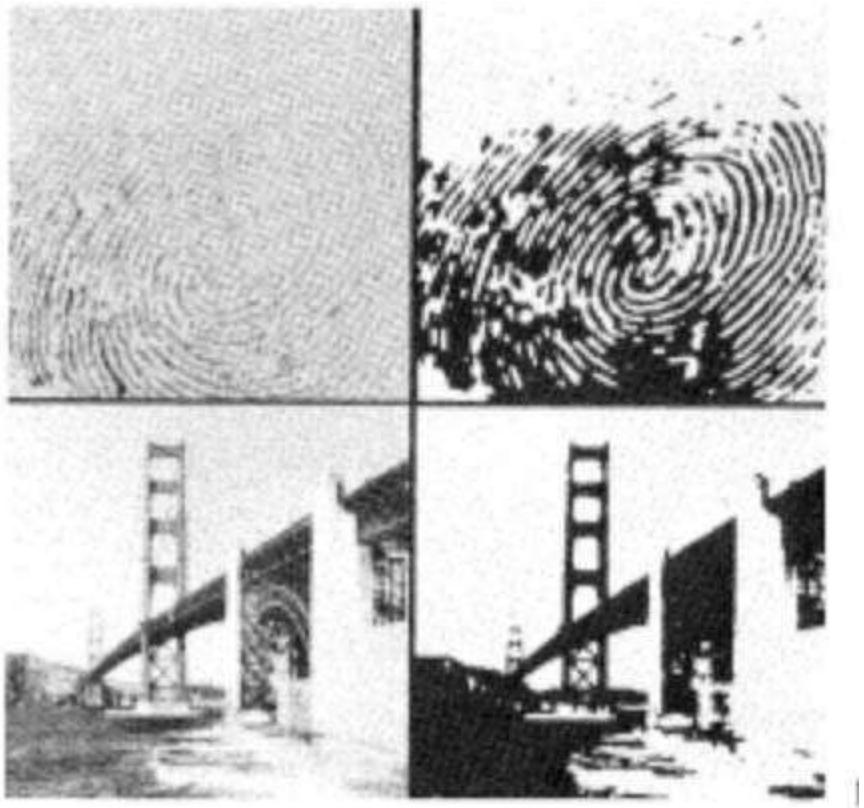

Clipping and

Example2

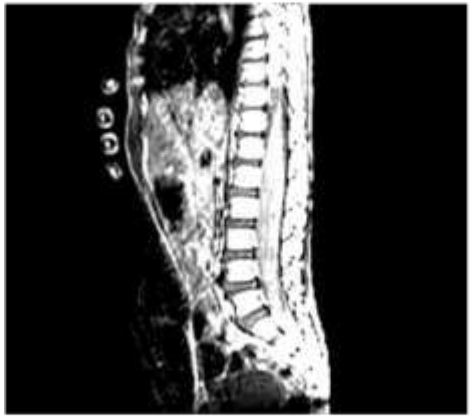

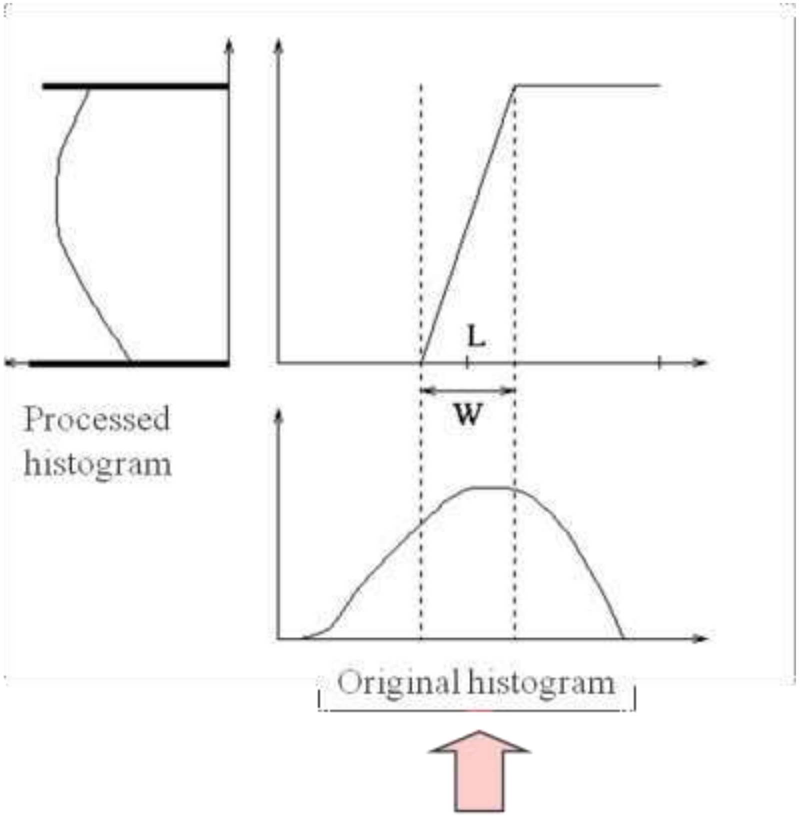

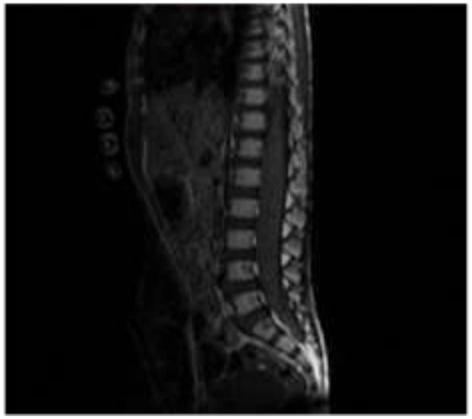

3-Digital negative

- Negative image can be obtained by reverse scaling of the gray levels according to the transformation

$$v=L-u$$

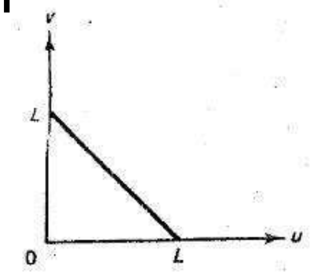

- Useful in the display of medical images.
- Example:

4-intensity level slicing

- Permit segmentation of certain gray level regions from the rest of the image.

$$v = \begin{cases} L, & a \le u \le b \\ 0, & otherwise \end{cases} \qquad v = \begin{cases} L, & a \le u \le b \\ u, & otherwise \end{cases}$$

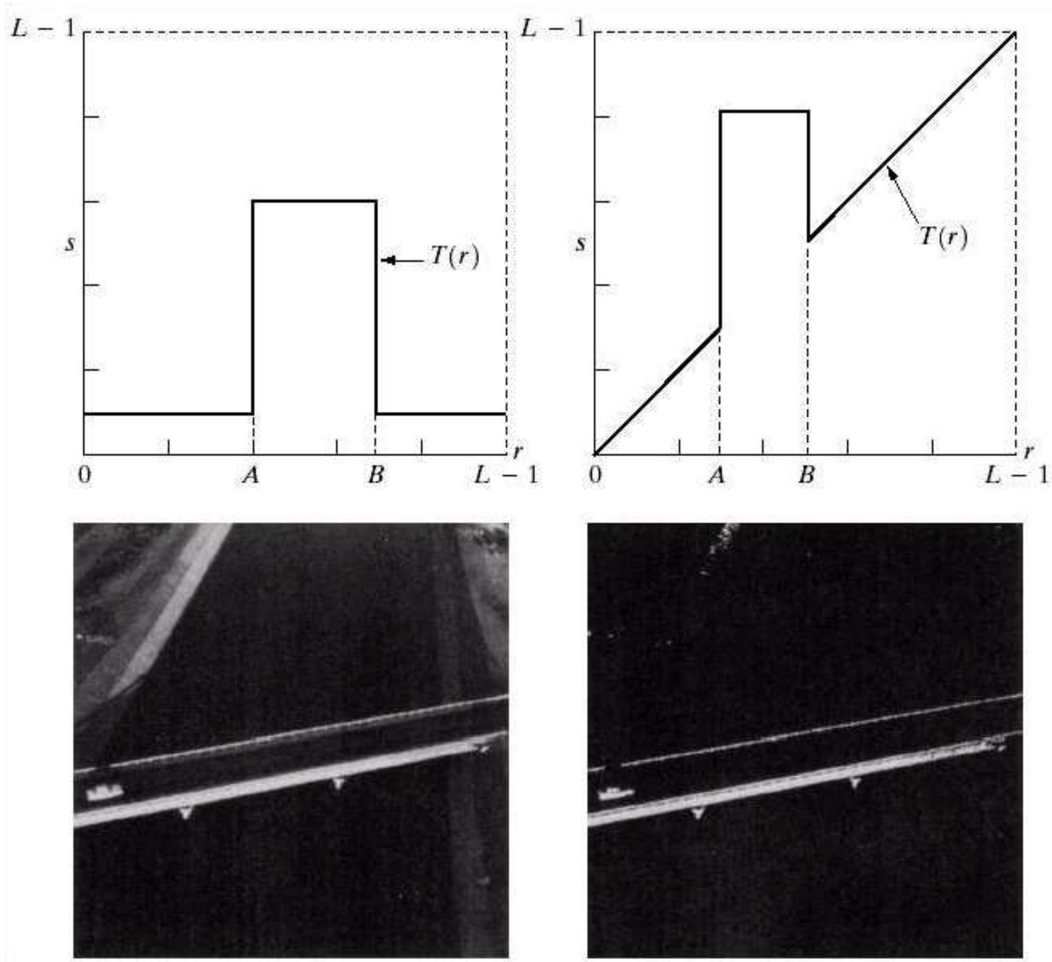

a b
c d

FIGURE 3.11 (a) This transformation highlights range [A, B] of gray levels and reduces all others to a constant level. (b) This transformation highlights range [A, B] but preserves all other levels. (c) An image. (d) Result of using the transformation in (a).

5-Bit extraction

•This transformation is useful In determining the number of Visually significant bits in an Image.

•Suppose each pixel is represented by 8 bits it is desired

To extract the *n*th most significant bit

And display it .

- Higher-order bits contain the majority of the visually significant

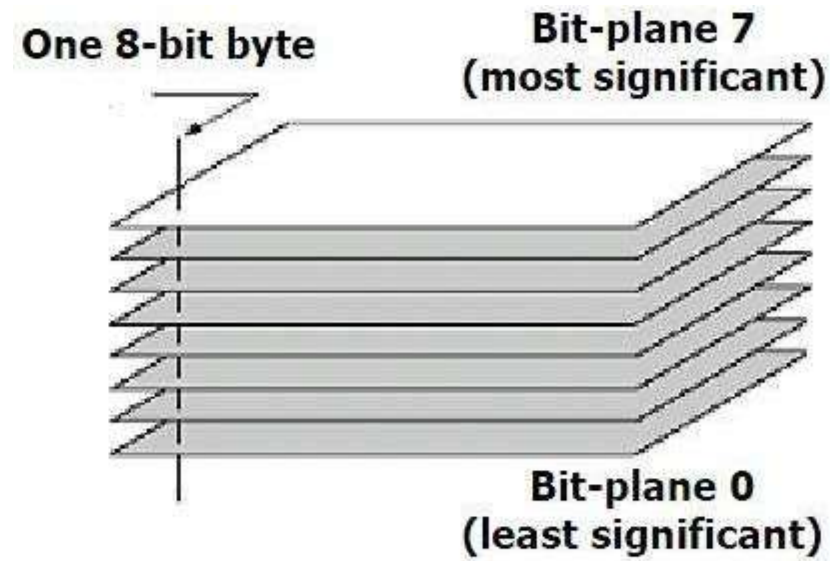

Example

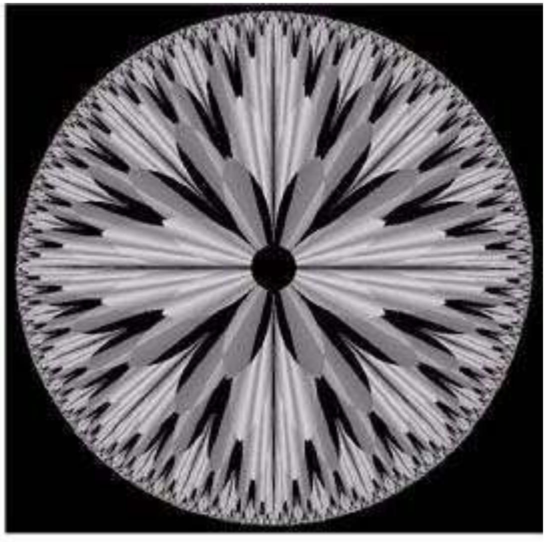

8-bit fractal image

- The (binary) image for bit-plane 7 can be obtained by processing the input image with a thresholding gray-level transformation.

 -Map all levels between 0 and 127 to 0

 -Map all levels between 129 and 255 to 255

Cont.

8-bit plane image

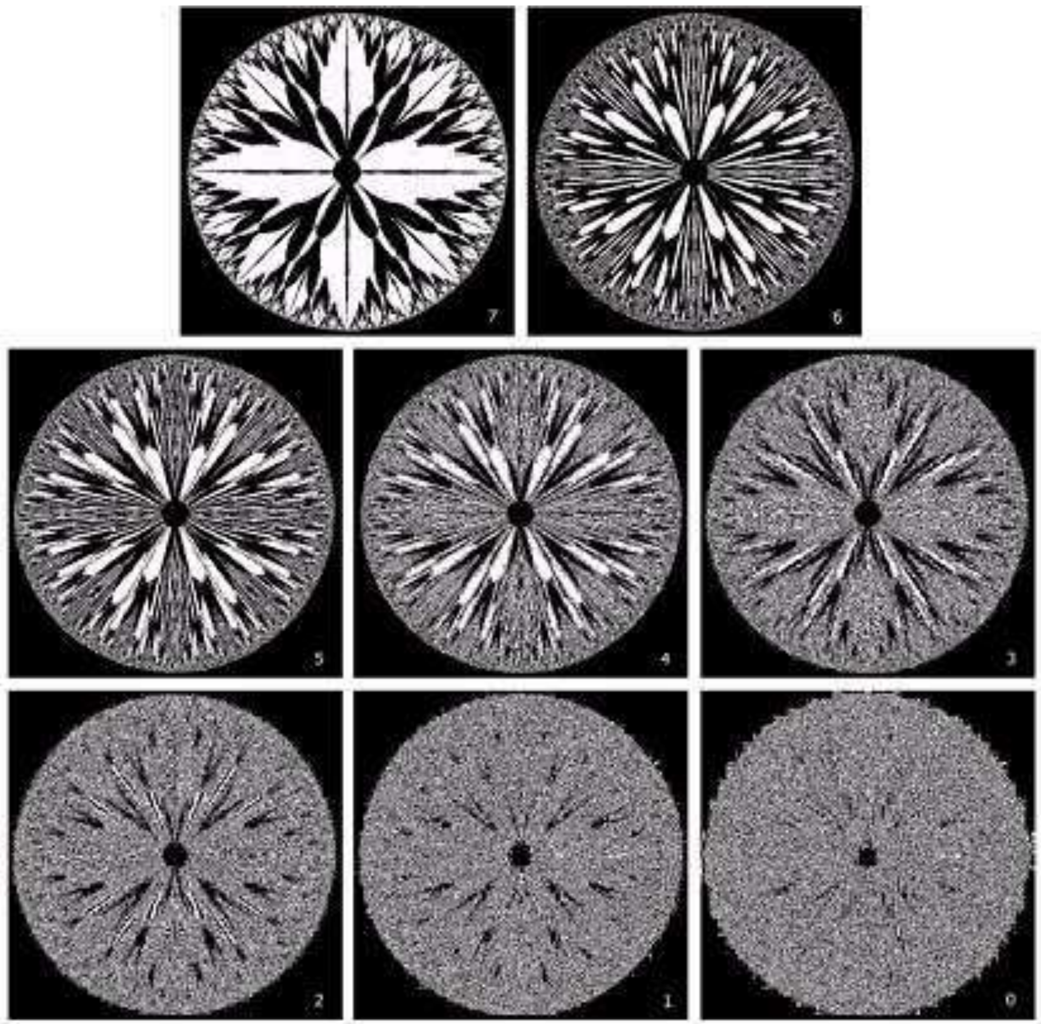

Bit-plane 7	Bit-plane 6	
Bit-plane 5	Bit-plane 4	Bit-plane 3
Bit-plane 2	Bit-plane 1	Bit-plane 0

6-Range compression

- Sometimes the dynamic range of a processed image far exceeds the capability of the display device, in which case only the brightest parts of the images are visible on the display screen.

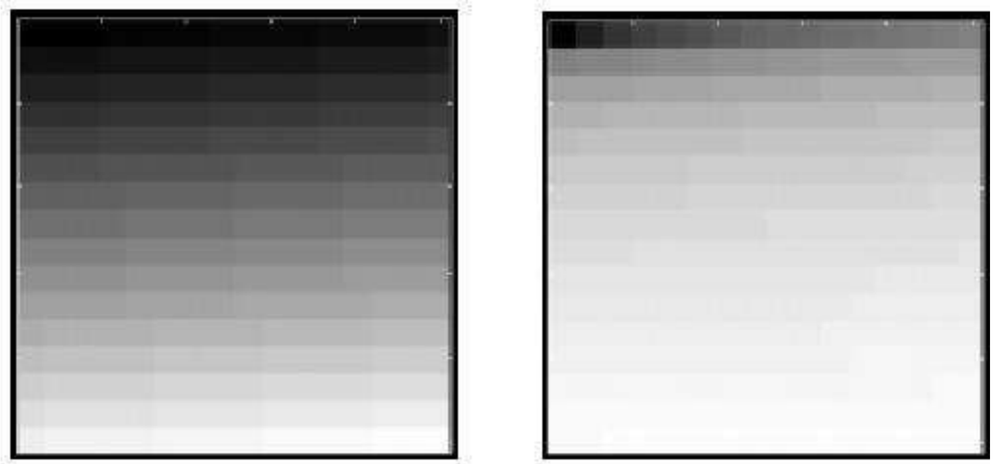

Original Processed output

- An effective way to compress the dynamic range of pixel values is to perform the following intensity transformation function:

$$s = c \log(1+|u|)$$

where c is a scaling constant, and the logarithm function performs the desired compression.

7-Image subtraction and change detection

- In many imaging applications it is desired to compare two complicated or busy images .
- A simple ,but powerful method is to align the two images and subtract them .The difference image is then enhanced .
- Applications such as imaging of the blood vessils and arteries in a body , security monitoring systems .
- Exampl e:

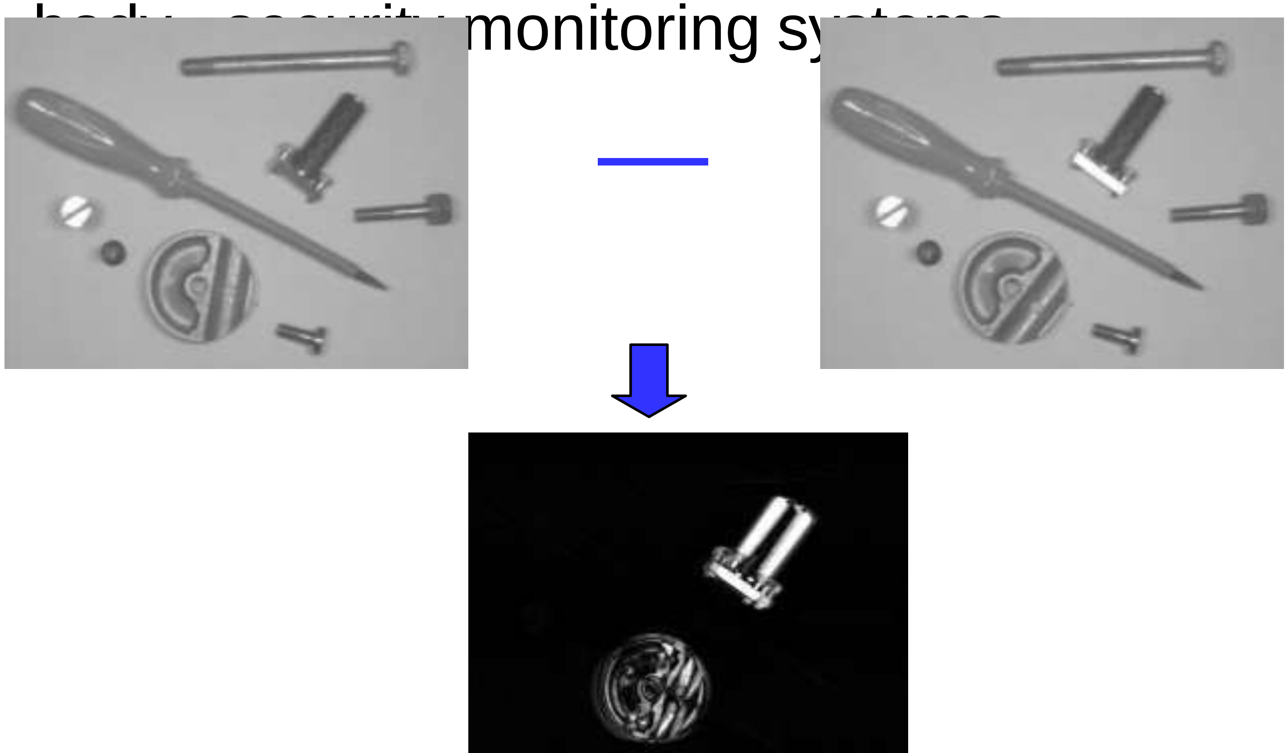

Histogram modeling

Histogram modeling techniques modify an image so that it's histogram has a desired shape . This is useful in stretching the low contrast levels with narrow histograms .

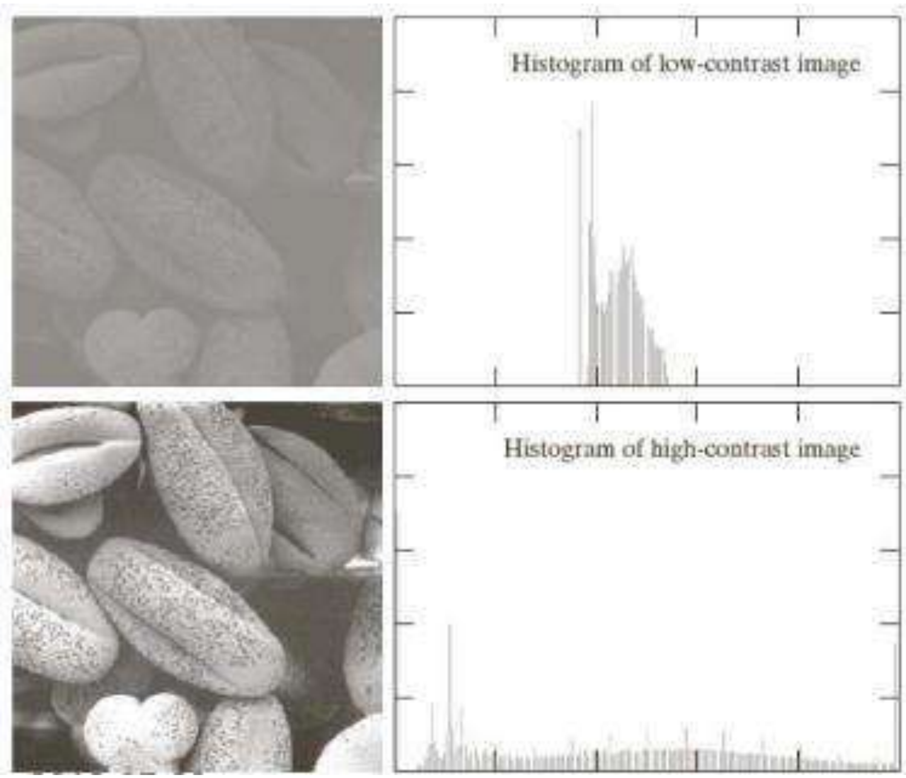

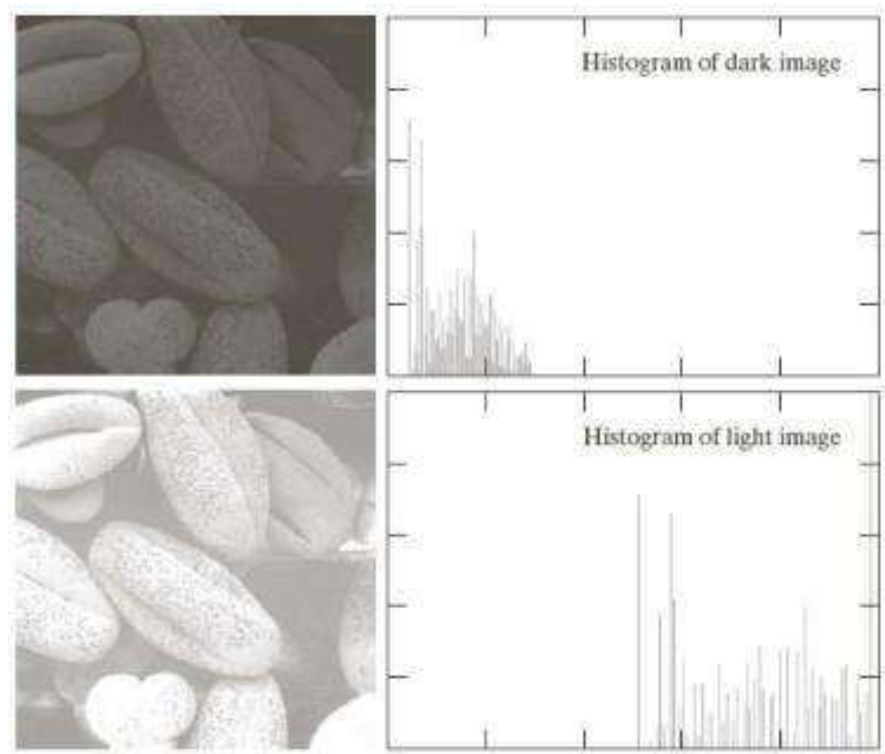

It is possible to develop a transformation function that can automatically achieve this effect ,based on histogram of input image .

Histogram modeling Cont.

Image

Histogram

- Assume we have image with n_k pixels with intensity r_k, $k = 0,1,\ldots,L-1$
- We define the image histogram as $h(r_k) = n_k$, and we define the normalized histogram as:

$$p(r_k) = h(r_k) / (M \cdot N)$$

- The normalized histogram is an estimate of the probability of occurrence of intensity level r_k in an image
- The normalized histogram sums to 1

1-Histogram equalization

- The objective is to map an input image to an output image such that its histogram is uniform after the mapping.
- Let *r* represent the gray levels in the image to be enhanced and s is the enhanced output with a transformation of the form *s*=***T(r).***
- A

1. $\mathbf{T}(r)$ is single-valued and monotonically increasing in the interval [0,1], which preserves the order from black to white in the gray scale.
2. $0 \le T(r) \le 1$ for $0 \le r \le 1$, which guarantees the mapping is consistent with the allowed range of pixel values.

- Possible for multiple values of ***r*** to map to a single value of ***s.***

Histogram Equalization cont.

Example 1:

Suppose that a 3-bit image (L=8) of size 64 × 64 pixels (MN = 4096) has the intensity distribution shown in following table.
Get the histogram equalization transformation function and give the $p_s(s_k)$ for each s_k.

r_k	n_k	$p_r(r_k) = n_k/MN$
$r_0 = 0$	790	0.19
$r_1 = 1$	1023	0.25
$r_2 = 2$	850	0.21
$r_3 = 3$	656	0.16
$r_4 = 4$	329	0.08
$r_5 = 5$	245	0.06
$r_6 = 6$	122	0.03
$r_7 = 7$	81	0.02

Solution

r_k	n_k	$p_r(r_k) = n_k/MN$
$r_0 = 0$	790	0.19
$r_1 = 1$	1023	0.25
$r_2 = 2$	850	0.21
$r_3 = 3$	656	0.16
$r_4 = 4$	329	0.08
$r_5 = 5$	245	0.06
$r_6 = 6$	122	0.03
$r_7 = 7$	81	0.02

$$\boxed{s_k = \frac{L-1}{MN}\sum_{j=0}^{k} n_j}$$

$$s_0 = T(r_0) = 7\sum_{j=0}^{0} p_r(r_j) = 7 \times 0.19 = 1.33 \quad \rightarrow 1$$

$$s_1 = T(r_1) = 7\sum_{j=0}^{1} p_r(r_j) = 7 \times (0.19 + 0.25) = 3.08 \quad \rightarrow 3$$

$$s_2 = 4.55 \quad \rightarrow 5 \qquad s_3 = 5.67 \quad \rightarrow 6$$

$$s_4 = 6.23 \quad \rightarrow 6 \qquad s_5 = 6.65 \quad \rightarrow 7$$

$$s_6 = 6.86 \quad \rightarrow 7 \qquad s_7 = 7.00 \quad \rightarrow 7$$

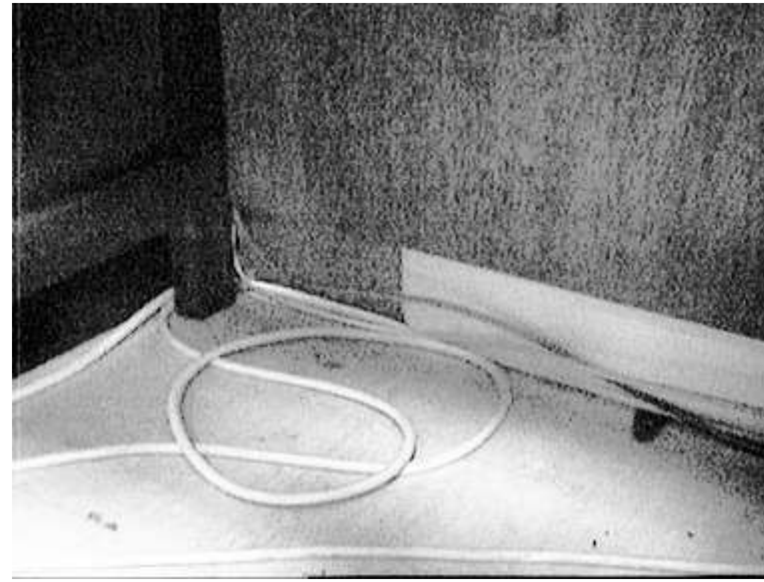

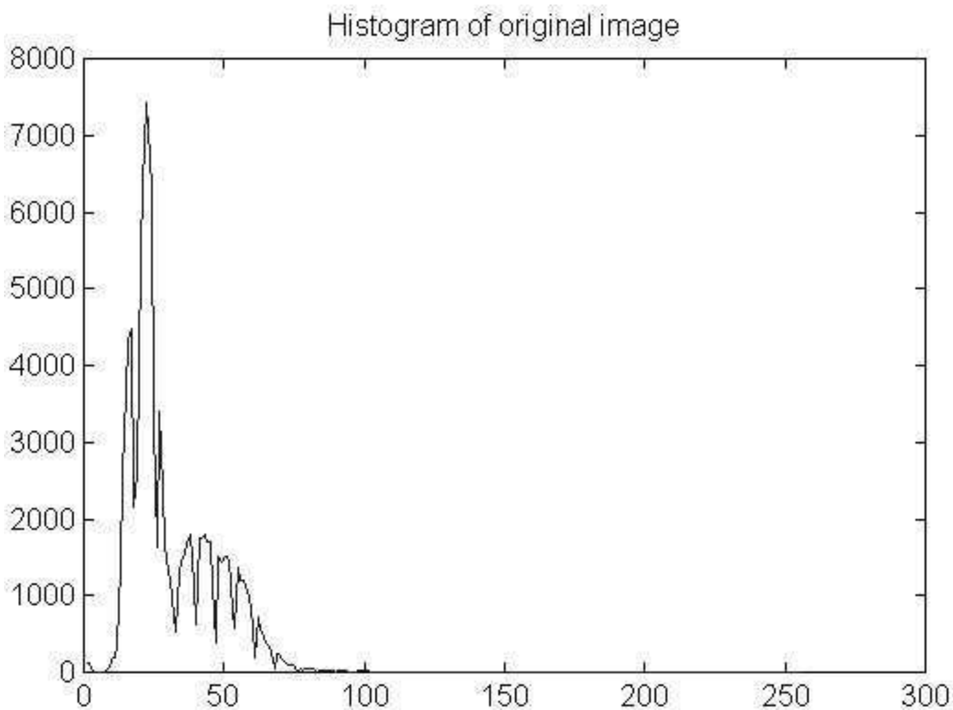
Histogram of original image
0
1000
2000
3000
4000
5000
6000
7000
8000
0
50
100
150
200
250
300

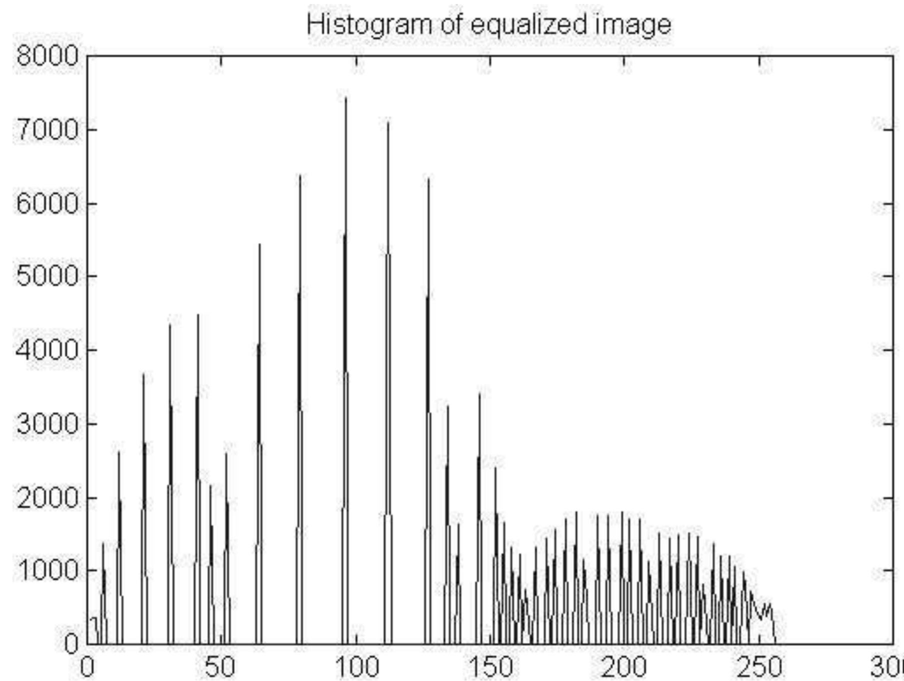
Histogram of equalized image
0
1000
2000
3000
4000
5000
6000
7000
8000
0
50
100
150
200
250
300

Histogram specification

- Histogram equalization only generates an approximation to a uniform histogram.
- With Histogram Specification, we can specify the shape of the histogram that we wish the output image to have.
- It doesn't have to be a uniform histogram.
- The principal difficulty in applying the histogram specification method to image enhancement lies in being able to construct a meaningful histogram.

Histogram specification cont.

- histogram equalization gives:

$$s_k = T(r_k) = (L-1)\sum_{j=0}^{k} p_r(r_j)$$

$$= \frac{(L-1)}{MN}\sum_{j=0}^{k} n_j \qquad 0 \le k \le L-1 \quad (5)$$

- given the value of s_k, we can solve for z_q as:

$$G(z_q) = (L-1)\sum_{i=0}^{q} p_z(z_i) \qquad (6)$$

- for a value of q, so that:

$$G(z_q) = s_k \qquad (7)$$

- we can find z_q as:

$$z_q = G^{-1}(s_k) \qquad (8)$$

- this is the mapping from s to z

Histogram specification cont.

Procedure

:

1. compute histogram, $p_r(r)$, of image; find histogram equalization transformation:

$$s_k = T(r_k) = \frac{(L-1)}{M \cdot N}\sum_{j=0}^{k} n_j \quad 0 \le k \le L-1$$

round all values of s_k to nearest integer in $[0, L-1]$

2. compute all values of transformation G

$$G(z_q) = (L-1)\sum_{i=0}^{q} p_z(z_i)$$

for $q = 0, 1, \ldots, L-1$ where $p_z(z_i)$ are values of specified histogram; round values of G to integers in range $[0, L-1]$; store values of G in table

3. for every value of s_k, $0 \le k \le L-1$, use stored values of G to find corresponding value of z_q so that $G(z_q)$ is closest to s_k, and store these mappings from s to z. For multiple z_q matches to s_k, choose smallest z_q.

4. form histogram matched image by first histogram equalizing input image and then mapping every equalized pixel value, s_k, to the corresponding value, z_q, using the mappings in Step 3.

Example

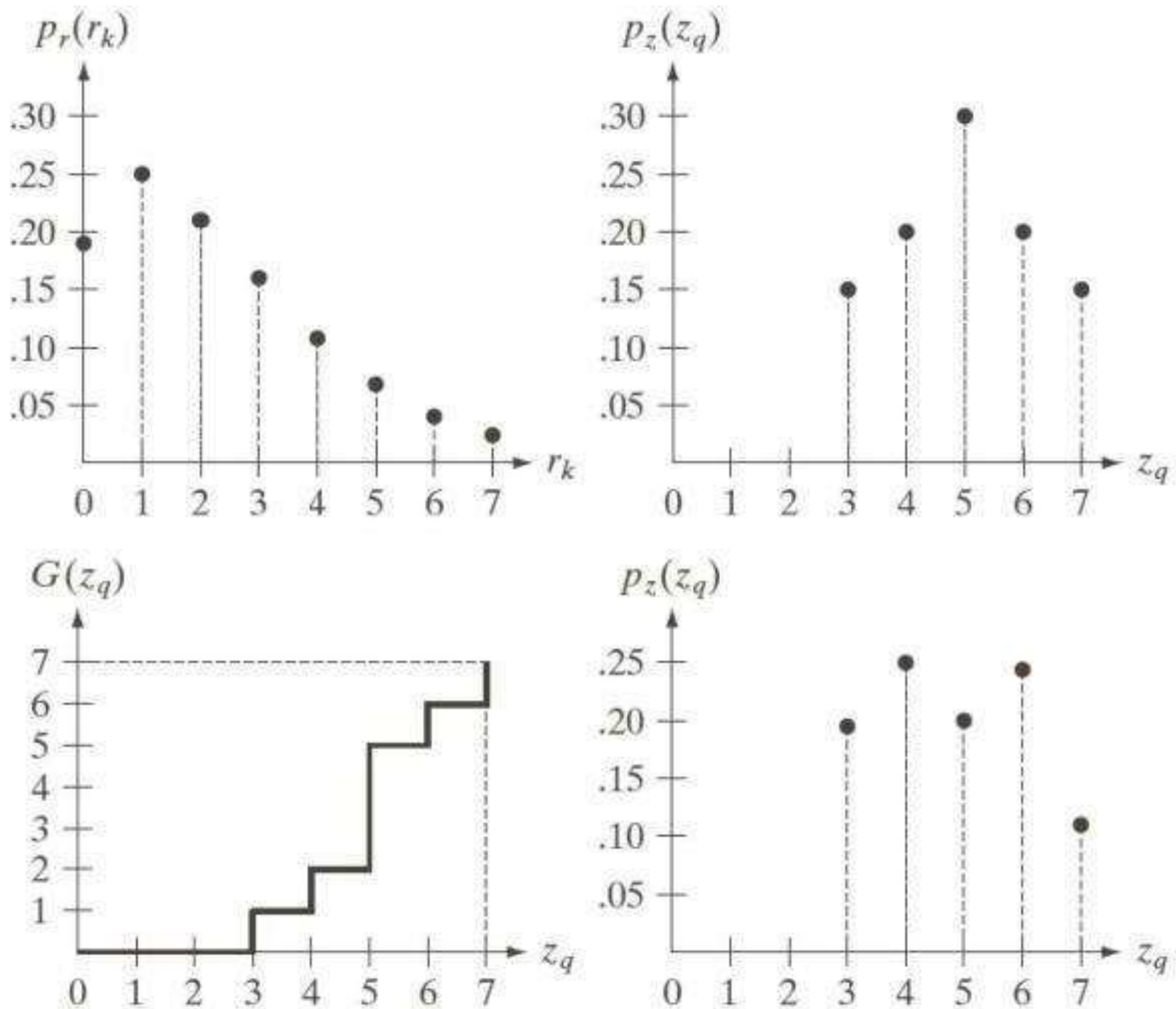

a	b
c	d

FIGURE 3.22
(a) Histogram of a 3-bit image. (b) Specified histogram.
(c) Transformation function obtained from the specified histogram.
(d) Result of performing histogram specification. Compare (b) and (d).

Spatial operations

- Operations performed on local neighborhoods of input pixels

- Image is convolved with [FIR] finite impulse response filter called
spatial mask .

- Techniques such as :
  - Noise smoothing
  - Median filtering
  - LP,HP &PB filtering
  - Zooming

Spatial averaging and spatial low-pass filtering

- Each pixel is replaced by a weighted average of it's neighborhood pixels that is,

$$v(m,n) = \sum \sum_{(k,l)\in W} a(k,l)y(m-k,n-l)$$

  -*y(m,n)* and *v(m,n)* are the input and output images ,respectively.

  -*W* is suitably chosen window .

  -*a(k,l)* are the filter weights .

- A common class of spatial averaging filters has all equal weights,

$$v(m,n) = \frac{1}{N}\sum \sum_{(k,l)\in W} y(m-k,n-l)$$

- Used for Noise smoothing , low-pass filtering and subsampling of images.

Example

Figure 7.18 Spatial averaging filters for smoothing images containing Gaussian noise.

directional smoothing

- To protect edges from blurring while smoothing.

- spatial averages are calculated in several directions , and the direction giving the smallest changes before and after filtering is selected.

$$v(m,n:\theta) = \frac{1}{N_\theta} \sum_{(k,l)\in W_\theta} \sum y(m-k, n-l)$$

- The direction (θ) is found such th $|y(m,n) - v(m,n:\theta^*)|$ is minimum

- Then $v(m,n) = v(m,n:\theta^*)$ gives the desired result.

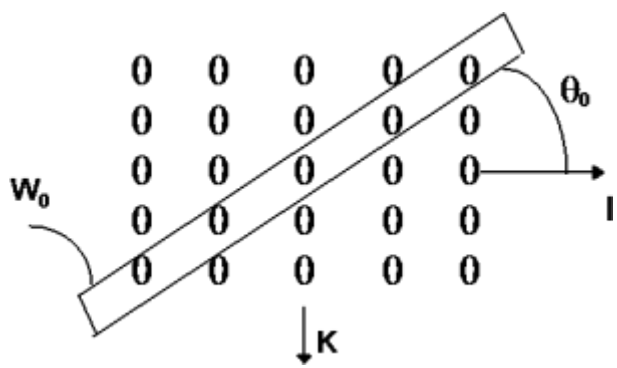

Median filtering

- Input pixel is replaced by the median of the pixels contained in a window around a pixel

$$v(m, n) = \text{median}\ \{y(m-k, n-l), (k, l) \in W\}$$

- The algorithm requires arranging the pixels in an increasing or decreasing order and picking the middle value.
- For Odd window size is commonly used [3*3-5*5-7*7]
- For even window size the average of two middle values is taken.

- Median filter properties:

1- Non-linear filter

2 Performes very well on images containing binary noise , poorly when the noise is gaussian.

$$\text{median}\{x(m) + y(m)\} \neq \text{median}\{x(m)\} + \text{median}\{y(m)\}$$

3 performance is poor in case that the number of noise pixels in the window is greater than or half the number of pixels in the window.

Example:

(a) Image with binary noise

(b) 3 × 3 median filtered

(c) Image with Gaussian noise

(d) 3 × 3 median filtered.

MEDICAL IMAGE COMPRESSION

A PROJECT REPORT

Submitted in partial fulfillment of the
requirement for the award of the degree
of

BACHELOR OF TECHNOLOGY
in
ELECTRICAL AND ELECTRONICS ENGINEERING

By

Paras Prateek Bhatnagar
Paramjeet Singh Jamwal
Preeti Kumari
Nisha Rajani

DEPARTMENT OF ELECTRICAL ENGINEERING
COLLEGE OF ENGINEERING ROORKEE
ROORKEE – 247667 (INDIA)

MAY, 2011

Candidate's Deceleration

We hereby, certify that the work which is being presented in the report entitled, "***MEDICAL IMAGE COMPRESSION***", in the partial fulfillment of the requirements for the award of the degree of BACHELOR OF TECHNOLOGY in ELECTRICAL AND ELECTRONICS ENGINEERING, submitted in the Department of Electrical Engineering, College of Engineering Roorkee, affiliated to Uttarakhand Technical University, Dehradun (India), is an authentic record of our own work carried out for a period of nine months , from August'10 to May'11, under the supervision of ***Mr. Akhilendra Singh Yadav***, Head of Department, Department of Electrical Engineering and ***Mr. Ashutosh Shukla***, Assistant Professor, Department of Electrical Engineering, College of Engineering Roorkee , Roorkee (India).

The matter embodied in this project report has not been submitted by u for the award of any other degree or diploma.

Dated : May 11, 2011

(Paras Prateek Bhatnagar) (Paramjeet Singh Jamwal)

(Preeti Kumari) (Nisha Rajani)

This is to certify that the above statement made by the candidates is correct to the best of our knowledge.

(Mr. Akhilendra Singh Yadav)
Head of Department, Deptt. of Electrical Engg. ,
College Of Engineering Roorkee,
Roorkee – 247667 (INDIA)

(Mr. Ashutosh Shukla)
Asst. Professor, Deptt. of Electrical Engg. ,
College of Engineering Roorkee,
Roorkee – 247667 (INDIA)

Acknowledgement

We would like to express our profound and sincere gratitude to our project guides, ***Mr. Akhilendra Singh Yadav***, Head of Department, Department of Electrical Engineering and ***Mr. Ashutosh Shukla***, Assistant Professor, Department of Electrical Engineering, College of Engineering Roorkee, for their constant and valuable guidance, inspiration, forbearance and keen interest during this project work.

We take this opportunity to thank ***Mrs. Anuradha***, Assistant Professor, Department of Electrical Engineering for providing the departmental facilities for carrying out this work.

We are also very grateful for the forbearance shown by ***Mr. Vishnu Saran Nayak***, Assistant Professor, Department of Electronics Engineering, for his concern and advice, during the period of our project.

We would also like to thank the ***UACEE (Universal Association of Computers and Electronics Engineers)*** for the acceptance of the paper titled "Unit Embedded Zerotree Wavelet" in ***ICACCN'11***, submitted by all four of us and its publication in their international journal. This has been the main source of moral boost for us.

Finally, we would like to acknowledge the immeasurable contribution of our ***parents***, without their constant inspiration and comradeship this work would never have been over. After completion of this project we can confidently say that this experience has not only enriched us with technical knowledge but also enhanced the maturity of thoughts and vision.

(Paras Prateek Bhatnagar) (Paramjeet Singh Jamwal)

(Preeti Kumari) (Nisha Rajani)

Dated : May 11, 2011

Contents

* Paras Prateek Bhatnagar, Preeti Kumari, Paramjeet Singh Jamwal and Nisha Rajani,"*Unit Embedded Zerotree Wavelet Coding*", "*International Conference on Advanced Computing , Communication and Networks*" , UACEE, 2011, pp 167-171.

Abstract

Image compression is the application of data compression on digital images. In effect, the objective is to reduce redundancy of the image data in order to be able to store or transmit data in an efficient form.

Image compression can be Lossy or lossless. Lossless compression is sometimes preferred for medical imaging, technical drawings, icons or comics. This is because lossy compression methods, especially when used at low bit rates, introduce compression artifacts. Lossless compression methods may also be preferred for high value content, such as medical imagery or image scans made for archival purposes. Lossy methods are especially suitable for natural images such as photos in applications where minor loss of fidelity is acceptable to achieve a substantial reduction in bit rate. The lossy compression that produces imperceptible differences can be called visually lossless. The best image quality at a given bit-rate or compression rate is the main goal of image compression.

Lossless data compression is a class of data compression algorithms that allows the exact original data to be reconstructed from the compressed data. The term lossless is in contrast to lossy data compression, which only allows an approximation of the original data to be reconstructed in exchange for better compression rates.

A lossy compression method is one where compressing data and then decompressing it retrieves data that is different from the original, but is close enough to be useful in some way. Lossy compression is most commonly used to compress multimedia data, especially in applications such as streaming media and internet telephony. By contrast, lossless compression is required for text and data files, such as bank records, text articles, etc. In many cases it is advantageous to make a master lossless file which can then be used to produce compressed files for different purposes.

Medical imaging is the technique and process used to create images of the human body for clinical purposes or medical diagnostics. The image data can take many forms, such as video sequences, views from multiple cameras, or multi-dimensional data from a medical scanner.

List of Figures and Tables Used

1. Introduction

The work presented in this project is dedicated to the implementation of the most popular image compression methods available and concluding the best amongst them. The work is carried out by comparison of both lossy and lossless methods. Moreover, this works illustrates a modified algorithm which improves the coding time of the image, which is named as "Unit Embedded Zerotree Wavelet" algorithm.

1.1 Literature Review

With advancement in technology, Digital imagining has become a part and parcel of our lives. The main problem being faced in the field of digital imaging is turning to be the arrangement of such huge digital information gathered every single second. The best way to arrange such huge amount of information is by application of digital compression of the gathered information. Such a methodology tends to reduce the storage space by taking advantage of data redundancy and special methods based on human vision systems.

The art of image compression begin in 1960s by simple run length encoding methods whereby the redundant data is prevented from being repeated. However soon it was felt that a more efficient method would be required in future which would not rely merely on run length encoding methods. Soon afterwards many methods were implemented but none of them was found to be as efficient as the DCT based method proposed by the Joint Photographic Experts Group, which came to known as JPEG. W.B. Pennenbaker and J.L. Mitchell (1993) [2] and G. Wallace (1991) [3], covers the main aspects of JPEG, Still Image Compression Standard. Soon the JPEG standard became the manifesto of the image compression standards and is widely used even today in web graphics and digital cameras.

With the advancement in field of medicine and the application of digital imaging in the field of medicine, soon it was felt that a more efficient standard would be required. The medical images contain only a small amount of significant information .Most of the information contained in the medical images was of no use. So the need of new standard was felt which only compresses the significant information which rest of the information was just left compressed at a poor quality being just visually visible. This standard came to be known as the Region of Interest. Shoji Hirano and Shusaku Tsumoto (2005) [4], introduces the rough representation of a ROI in medical images.

Lately, the DWT has gained wide popularity due to its excellent decorrelation properties. Many modern image compression systems embody the DWT as the transform stage. It is widely recognized that the biorthogonal filters are among the best filters for DWT-based image compression. Lossless image compression techniques find applications in fields such as medical imaging, preservation of artwork, remote sensing etc. Day-by-day DWT is becoming more and more popular for digital image compression. Biorthogonal (5, 3) and (9, 7) filters have been chosen to be the standard filters used in the JPEG2000 codec standard. After DWT was introduced, several codec algorithms were proposed to compress the transform coefficients as much as possible. Among them, Embedded Zerotree Wavelet (EZW) as presented by Jerome M. Shapiro (1993) [5], Set Partitioning in Hierarchical Trees (SPIHT) and

Embedded Bock Coding with Optimized Truncation (EBCOT) are the most famous ones. The embedded zerotree wavelet algorithm (EZW) is a simple, yet remarkably effective, image compression algorithm, having the property that the bits in the bit stream are generated in order of importance, yielding a fully embedded code. Using an embedded coding algorithm, an encoder can terminate the encoding at any point thereby allowing a target rate or target distortion metric to be met exactly. Also, given a bit stream, the decoder can cease decoding at any point in the bit stream and still produce exactly the same image that would have been encoded at the bit rate corresponding to the truncated bit stream.

With the implementation of the EZW algorithm, it was felt that an algorithm which could code lossless images at a faster rate would be needed .Thus, the Unit EZW was implemented which works on the principal of fragmentation. Paras Prateek Bhatnagar, Preeti Kumari, Paramjeet Singh Jamwal and Nisha Rajani (2011) [1] illustrated this algorithm by comparing the improvement in coding times by using the Unit EZW algorithm over the original EZW algorithm. With even more advancement in technology, future researches must replicate such findings to cope up with the challenges, which are still to be faced.

1.2 Organizing of Project Work

The complete project work has been divided into ten chapters on the basis of the content covered.

The first chapter introduces the work covered. This chapter presents the aim of the project along with the literature review .The literature review presents the study of the various research papers that was conducted before the project was started. Also a brief historical background of image compression and the detailed organization structure of the project report are presented in this chapter.

The second chapter introduces the basics of Medical Image Compression. It lays down the definition of various topics which must be clear before the work is presented. This chapter includes topics such as Digital Signal Processing, Digital Image Processing and Image Compression which form a superset of the present work. It also lays down the definition of Medical Image Compression along with a brief overview of the algorithms used in the present work.

The third chapter introduces the Joint Pictures Experts Group Algorithm. Along with the detailed explanation of the algorithm, the results obtained have been presented. This chapter also presents the effect of varying the compression ratio on the visual quality of the image along with an encoding example.

Similarly the forth chapter introduces the Region of Interest Algorithm. Here also detailed explanation of the algorithm has been carried out. Moreover the results of the ROI algorithm are also presented. The chapter ends with a comparison of the results of both the lossy algorithms so that a sharp comparison may be made to conclude the better algorithm.

The fifth and the sixth chapter presents the lossless algorithms covered in the project. These algorithms include the Embedded Zerotree Wavelet Algorithm along with a modified algorithm named as the Unit Embedded Zerotree Wavelet Algorithm. The detailed expatiation of these algorithms has been presented along with the results. The sixth chapter ends with a comparison of coding time using both the algorithms so that better of the two algorithms may be concluded.

The next three chapters are dedicated to explain the application, advantages and disadvantages of the Digital Image Compression. These chapters present a detailed explanation of the topics concerned.

The last chapter ends the project report by concluding the better of the compared algorithm in both the segments i.e. the lossy and the lossless segment. The chapter presents the reason of considering an algorithm over the other.

The appendix and references have been covered at the end of the project report.

2. Medical Image Compression

Medical imaging is often perceived to designate the set of techniques that noninvasively produce images of the internal aspect of the body. In this restricted sense, medical imaging can be seen as the solution of mathematical inverse problems. This means that cause (the properties of living tissue) is inferred from effect (the observed signal). In the case of ultrasonography the probe consists of ultrasonic pressure waves and echoes inside the tissue show the internal structure. In the case of projection radiography, the probe is X-ray radiation which is absorbed at different rates in different tissue types such as bone, muscle and fat.

2.1 Digital Signal Processing

Digital signal processing (DSP) is concerned with the representation of discrete time signals by a sequence of numbers or symbols and the processing of these signals. Digital signal processing and analog signal processing are subfields of signal processing. DSP includes subfields like: audio and speech signal processing, sonar and radar signal processing, sensor array processing, spectral estimation, statistical signal processing, digital image processing, signal processing for communications, control of systems, biomedical signal processing, seismic data processing, etc.

The goal of DSP is usually to measure, filter and/or compress continuous real-world analog signals. The first step is usually to convert the signal from an analog to a digital form, by *sampling* it using an analog-to-digital converter (ADC), which turns the analog signal into a stream of numbers. However, often, the required output signal is another analog output signal, which requires a digital-to-analog converter (DAC). Even if this process is more complex than analog processing and has a discrete value range, the application of computational power to digital signal processing allows for many advantages over analog processing in many applications, such as error detection and correction in transmission as well as data compression.

2.2 Digital Image Processing

Digital image processing is the use of computer algorithms to perform image processing on digital images. As a subcategory or field of digital signal processing, digital image processing has many advantages over analog image processing. It allows a much wider range of algorithms to be applied to the input data and can avoid problems such as the build-up of noise and signal distortion during processing. Since images are defined over two dimensions digital image processing may be modeled in the form of Multidimensional Systems.

2.3 Image Compression

Image compression is the application of data compression on digital images. In effect, the objective is to reduce redundancy of the image data in order to be able to store or transmit data in an efficient form. Image compression can be Lossy or lossless. Lossless compression is sometimes preferred for *medical imaging*, technical drawings, icons or comics. This is because lossy compression methods, especially when used at low bit rates, introduce compression artefacts. Lossless compression methods may also be preferred for high value content, such as medical imagery or image scans made for archival purposes. Lossy methods are especially suitable for natural images such as photos in applications where minor loss of fidelity is acceptable to achieve a substantial reduction in bit rate. The lossy compression that produces imperceptible differences can be called visually lossless.

2.4 Medical Image Compression

In the clinical context, "invisible light" medical imaging is generally equated to radiology or "clinical imaging" and the medical practitioner responsible for interpreting (and sometimes acquiring) the images are a radiologist. "Visible light" medical imaging involves digital video or still pictures that can be seen without special equipment. Dermatology and wound care are two modalities that utilize visible light imagery. Diagnostic radiography designates the technical aspects of medical imaging and in particular the acquisition of medical images. The radiographer or *radiologic technologist* is usually responsible for acquiring medical images of diagnostic quality, although some radiological interventions are performed by radiologists. While radiology is an evaluation of anatomy, nuclear medicine provides functional assessment.

As a field of scientific investigation, medical imaging constitutes a sub-discipline of biomedical engineering, medical physics or medicine depending on the context: Research and development in the area of instrumentation, image acquisition (e.g. radiography), modeling and quantification are usually the preserve of biomedical engineering, medical physics and computer science; Research into the application and interpretation of medical images is usually the preserve of radiology and the medical sub-discipline relevant to medical condition or area of medical science (neuroscience, cardiology, psychiatry, psychology, etc.) under investigation. Many of the techniques developed for medical imaging also have scientific and industrial applications.

2.5 Algorithms Used

Compression algorithms used may be broadly classified into two categories namely the lossy compression and the lossless compression, both of these algorithms suffer from their own advantages and disadvantages.

A lossy compression method is one where compressing data and then decompressing it retrieves data that is different from the original, but is close enough to be useful in some way. Lossy compression is most commonly used to compress multimedia data, especially in applications such as streaming media and internet telephony. By contrast, lossless compression is required for text and data files, such as bank records, text articles, etc. In many cases it is advantageous to make a master lossless file which can then be used to produce compressed files for different purposes; for example a multi-megabyte file can be used at full size to produce a full-page advertisement in a glossy magazine, and a 10 kilobyte lossy copy made for a small image on a web page.

Lossless data compression is a class of data compression algorithms that allows the exact original data to be reconstructed from the compressed data. The term *lossless* is in contrast to lossy data compression, which only allows an approximation of the original data to be reconstructed in exchange for better compression rates. Lossless compression is used when it is important that the original and the decompressed data be identical, or when no assumption can be made on whether certain deviation is uncritical. Typical examples are executable programs and source code. Some image file formats, like PNG or GIF, use only lossless compression, while others like TIFF may use either lossless or lossy methods.

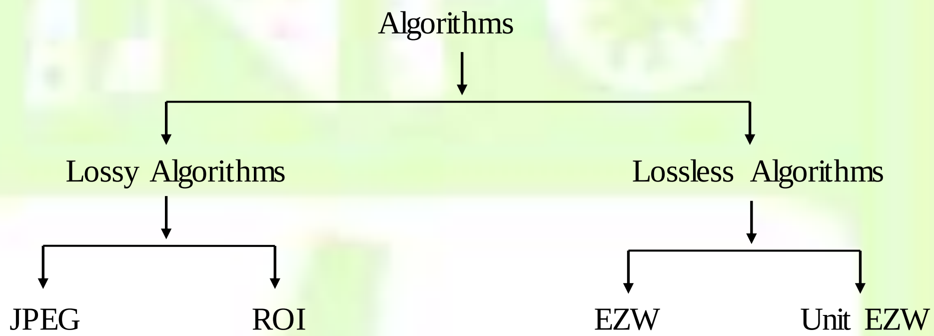

Figure 1. Figure showing the classification of the compression algorithms used in the present work.

3. Joint Photographic Experts Group Compression Algorithm

The JPEG compression algorithm is at its best on photographs and paintings of realistic scenes with smooth variations of tone and colour. For web usage, where the bandwidth used by an image is important, JPEG is very popular. JPEG is also the most common format saved by digital cameras. On the other hand, JPEG is *not* as well suited for line drawings and other textual or iconic graphics, where the sharp contrasts between adjacent pixels cause noticeable artefacts. JPEG is also not well suited to files that will undergo multiple edits, as some image quality will usually be lost each time the image is decompressed and recompressed, particularly if the image is cropped or shifted, or if encoding parameters are changed.

As JPEG is a lossy compression method, which removes information from the image, it must not be used in astronomical imaging or other purposes where the exact reproduction of the data is required. Lossless formats must be used instead.

3.1 Discrete Cosine Transformation

The DCT is a time to frequency domain transformation. The DCT coefficients and the inverse DCT coefficients form a linear pair. DCT temporarily increases the bit-depth of the image, since the DCT coefficients of an 8-bit/component image take up to 11 or more bits (depending on fidelity of the DCT calculation) to store. This may force the codec to temporarily use 16-bit bins to hold these coefficients, doubling the size of the image representation at this point; they are typically reduced back to 8-bit values by the quantization step. The temporary increase in size at this stage is not a performance concern for most JPEG implementations, because typically only a very small part of the image is stored in full DCT form at any given time during the image encoding or decoding process. The 2-D DCT is obtained using the formula given below:

$$p_{xy}=\frac{1}{4}\sum_{i=0}^{7}\sum_{j=0}^{7}C_iC_jG_{ij}\cos(\frac{(2x+1)i\pi}{16})\cos(\frac{(2x+1)j\pi}{16})$$

The DCT process produces a rather larger value at the top-left. This is called the DC coefficient. For a 8x8 image block, the remaining 63 coefficients are called the AC coefficients. The advantage of the DCT is its tendency to aggregate most of the signal in one corner of the result, as may be seen above. The quantization step to follow accentuates this effect while simultaneously reducing the overall size of the DCT coefficients, resulting in a signal that is easy to compress efficiently in the entropy stage.

3.2 Encoding Algorithm

The basic flowchart showing the complete JPEG algorithm is enumerated in Figure 2.The processes used in this chart have been explained in the subsequent sections of this report.

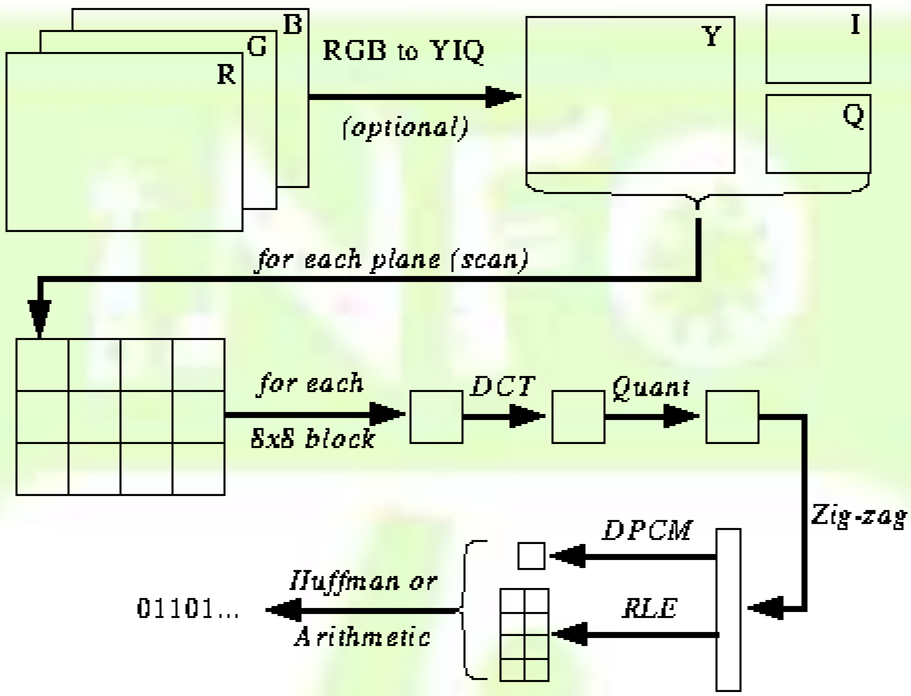

Figure 2. Figure showing the flowchart for JPEG Compression algorithm.

Colour space transformation

First, the image should be converted from RGB into a different colour space called YCbCr. It has three components Y, Cb and Cr: the Y component represents the brightness of a pixel, the Cb and Cr components represent the chrominance (split into blue and red components). The YCbCr colour space conversion allows greater compression without a significant effect on perceptual image quality. The compression is more efficient because the brightness information, which is more important to the eventual perceptual quality of the image, is confined to a single channel, more closely representing the human visual system.

This conversion to YCbCr is specified in the JFIF standard, and should be performed for the resulting JPEG file to have maximum compatibility. However, some JPEG implementations in "highest quality" mode do not apply this step and instead keep the colour information in the RGB colour model, where the image is stored in separate channels for red, green and blue luminance. This results in less efficient compression, and would not likely be used if file size were an issue.

Downsampling

Due to the densities of colour- and brightness-sensitive receptors in the human eye, humans can see considerably more fine detail in the brightness of an image (the Y component) than in the colour of an image (the Cb and Cr components). Using this knowledge, encoders can be designed to compress images more efficiently. The transformation into the YCbCr colour model enables the next step, which is to reduce the spatial resolution of the Cb and Cr components .The ratios at which the Downsampling can be done on JPEG are 4:4:4 (no downsampling), 4:2:2 (reduce by factor of 2 in horizontal direction), and most commonly 4:2:0 (reduce by factor of 2 in horizontal and vertical directions). For the rest of the compression process, Y, Cb and Cr are processed separately and in a very similar manner.

Block splitting

After subsampling, each channel must be split into 8×8 blocks of pixels. Depending on chroma subsampling, this yields. MCU blocks of size 8×8 (4:4:4 – no subsampling), 16×8 (4:2:2), or most commonly 16×16 (4:2:0).If the data for a channel does not represent an integer number of blocks then the encoder must fill the remaining area of the incomplete blocks with some form of dummy data. Filling the edge pixels with a fixed colour (typically black) creates ringing artefacts along the visible part of the border; repeating the edge pixels is a common technique that reduces the visible border, but it can still create artefacts.

Discrete cosine transform

Next, each component (Y, Cb, Cr) of each 8×8 block is converted to a frequency-domain representation, using a normalized, two-dimensional type-II discrete cosine transform (DCT). Before computing the DCT of the sub image, its grey values are shifted from a positive range to one cantered around zero. For an 8-bit image each pixel has 256 possible values: $[0,255]$. To centre on zero it is necessary to subtract by half the number of possible values, or 128. Subtracting 128 from each pixel value yields pixel values on $[-128,127]$

Quantization

The human eye is good at seeing small differences in brightness over a relatively large area, but not so good at distinguishing the exact strength of a high frequency brightness variation. This allows one to greatly reduce the amount of information in the high frequency components. This is done by simply dividing each component in the frequency domain by a constant for that component, and then rounding to the nearest integer. This is the main lossy operation in the whole process. As a result of this, it is typically the case that many of the higher frequency components are rounded to zero, and many of the rest become small positive or negative numbers, which take many fewer bits to store.

Entropy coding

Entropy coding is a special form of lossless data compression. It involves arranging the image components in a "zigzag" order employing run-length encoding (RLE) algorithm that groups similar frequencies together, inserting length coding zeros, and then using Huffman coding on what is left.The JPEG standard also allows, but does not require, the use of arithmetic coding, which is mathematically superior to Huffman coding. However, this feature is rarely used as it is covered by patents and because it is much slower to encode and decode compared to Huffman coding. Arithmetic coding typically makes files about 5% smaller. If the i-th block is represented by Bi and positions within each block are represented by (p,q) where p = 0, 1, ..., 7 and q = 0, 1, ..., 7, then any coefficient in the DCT image can be represented as Bi(p,q). Thus, in the above scheme, the order of encoding pixels (for the i-th block) is Bi(0,0), Bi(0,1), Bi(1,0), Bi(2,0), Bi(1,1), Bi(0,2), Bi(0,3), Bi(1,2) and so on. This encoding mode is called baseline *sequential* encoding. Baseline JPEG also supports *progressive* encoding. While sequential encoding encodes coefficients of a single block at a time (in a zigzag manner), progressive encoding encodes similar-positioned coefficients of all blocks in one go, followed by the next positioned coefficients of all blocks, and so on. So, if the image is divided into N 8×8 blocks {B0,B1,B2, ..., Bn-1}, then progressive encoding encodes Bi(0,0) for all blocks, i.e., for all i = 0, 1, 2, ..., N-1. This is followed by encoding Bi(0,1) coefficient of all blocks, followed by Bi(1,0)-th coefficient of all blocks, then Bi(2,0)-th coefficient of all blocks, and so on. It should be noted here that once all similar-positioned coefficients have been encoded, the next position to be encoded is the one occurring next in the zigzag traversal as indicated in the figure above. It has been found that Baseline Progressive JPEG encoding usually gives better compression as compared to Baseline Sequential JPEG due to the ability to use different Huffman tables (see below) tailored for different frequencies on each "scan" or "pass" (which includes similar-positioned coefficients), though the difference is not too large.

In the rest of the article, it is assumed that the coefficient pattern generated is due to sequential mode. In order to encode the above generated coefficient pattern, JPEG uses Huffman encoding. JPEG has a special Huffman code word for ending the sequence prematurely when the remaining coefficients are zero. JPEG's other code words represent combinations of (a) the number of significant bits of a coefficient, including sign, and (b) the number of consecutive zero coefficients that precede it. (Once you know how many bits to expect, it takes 1 bit to represent the choices {-1, +1}, 2 bits to represent the choices {-3, -2, +2, +3}, and so forth.) In our example block, most of the quantized coefficients are small numbers that are not preceded immediately by a zero coefficient. These more-frequent cases will be represented by shorter code words. The JPEG standard provides general-purpose Huffman tables; encoders may also choose to generate Huffman tables optimized for the actual frequency distributions in images being encoded.

3.3 Decoding Algorithm

Decoding means to display the image back from its compressed form .It consists of doing all the above in reverse. Taking the DCT coefficient matrix (after adding the difference of the DC coefficient back in) and taking the entry-for-entry product with the quantization matrix from above results in a matrix which closely resembles the original DCT coefficient matrix for the top-left portion. Taking the inverse DCT results in an image with values (still shifted down by 128). Adding 128 to the obtained matrix results in an image which resembles closely with the original image.

The error is most noticeable in the bottom-left corner where the bottom-left pixel becomes darker than the pixel to its immediate right.

3.4 An Example

Consider a 8 x 8 image as follows :

$$\begin{bmatrix} 52 & 55 & 61 & 66 & 70 & 61 & 64 & 73 \\ 63 & 59 & 55 & 90 & 109 & 85 & 69 & 72 \\ 62 & 59 & 68 & 113 & 144 & 104 & 66 & 73 \\ 63 & 58 & 71 & 122 & 154 & 106 & 70 & 69 \\ 67 & 61 & 68 & 104 & 126 & 88 & 68 & 70 \\ 79 & 65 & 60 & 70 & 77 & 68 & 58 & 75 \\ 85 & 71 & 64 & 59 & 55 & 61 & 65 & 83 \\ 87 & 79 & 69 & 68 & 65 & 76 & 78 & 94 \end{bmatrix}$$

1) Subtracting -128 from the image :

$$\begin{bmatrix} -76 & -73 & -67 & -62 & -58 & -67 & -64 & -55 \\ -65 & -69 & -73 & -38 & -19 & -43 & -59 & -56 \\ -66 & -69 & -60 & -15 & 16 & -24 & -62 & -55 \\ -65 & -70 & -57 & -6 & 26 & -22 & -58 & -59 \\ -61 & -67 & -60 & -24 & -2 & -40 & -60 & -58 \\ -49 & -63 & -68 & -58 & -51 & -60 & -70 & -53 \\ -43 & -57 & -64 & -69 & -73 & -67 & -63 & -45 \\ -41 & -49 & -59 & -60 & -63 & -52 & -50 & -34 \end{bmatrix}$$

2) Taking DCT of the image :

$$\begin{bmatrix} -415 & -30 & -61 & 27 & 56 & -20 & -2 & 0 \\ 4 & -22 & -61 & 10 & 13 & -7 & -9 & 5 \\ -47 & 7 & 77 & -25 & -29 & 10 & 5 & -6 \\ -49 & 12 & 34 & -15 & -10 & 6 & 2 & 2 \\ 12 & -7 & -13 & -4 & -2 & 2 & -3 & 3 \\ -8 & 3 & 2 & -6 & -2 & 1 & 4 & 2 \\ -1 & 0 & 0 & -2 & -1 & -3 & 4 & -1 \\ 0 & 0 & -1 & -4 & -1 & 0 & 1 & 2 \end{bmatrix}$$

3) Dividing the image by quantization matrix and rounding :

$$\begin{bmatrix} -26 & -3 & -6 & 2 & 2 & -1 & 0 & 0 \\ 0 & -2 & -4 & 1 & 1 & 0 & 0 & 0 \\ -3 & 1 & 5 & -1 & -1 & 0 & 0 & 0 \\ -4 & 1 & 2 & -1 & 0 & 0 & 0 & 0 \\ 1 & 0 & 0 & 0 & 0 & 0 & 0 & 0 \\ 0 & 0 & 0 & 0 & 0 & 0 & 0 & 0 \\ 0 & 0 & 0 & 0 & 0 & 0 & 0 & 0 \\ 0 & 0 & 0 & 0 & 0 & 0 & 0 & 0 \end{bmatrix}$$

4) Taking the zigzag order :

$$\begin{array}{llllll} -26 \\ -3 & 0 \\ -3 & -2 & -6 \\ 2 & -4 & 1 & -4 \\ 1 & 1 & 5 & 1 & 2 \\ -1 & 1 & -1 & 2 & 0 & 0 \\ 0 & 0 & 0 & -1 & -1 & \text{EOB} \end{array}$$

5) Performing RLE and Huffman Coding :

Output :
110001010100111001000101100001011010001100110001100100110010100101100000010000110111
101000001010

Input Size : 64 bytes

Output Size : 12 bytes

Compression Ratio : 5.33:1

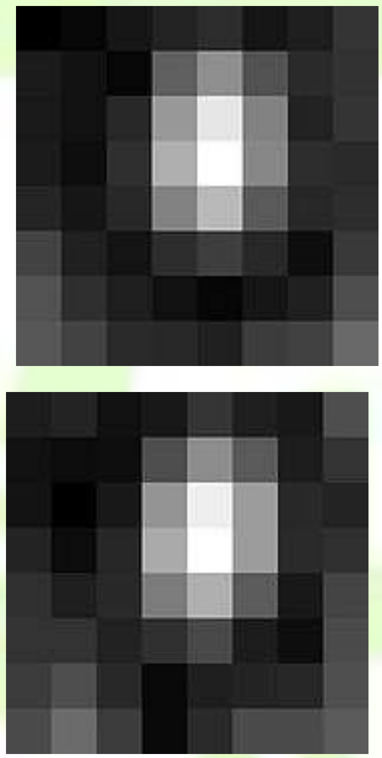

Figure 3. Figure showing the original 8x8 image (top) and its decoded version (bottom). The visible difference occurs in the lower right blocks.

3.5 Effects of JPEG Compression

JPEG compression artifacts blend well into photographs with detailed non-uniform textures, allowing higher compression ratios. Notice how a higher compression ratio first affects the high-frequency textures in the upper-left corner of the image, and how the contrasting lines become fuzzier. The very high compression ratio severely affects the quality of the image, although the overall colours and image form are still recognizable. However, the precision of colours suffer less (for a human eye) than the precision of contours (based on luminance). This justifies the fact that images should be first transformed in a colour model separating the luminance from the chromatic information, before sub sampling the chromatic planes (which may also use lower quality quantization) in order to preserve the precision of the luminance plane with more information bits. The uncompressed MRI image below (2,62,144 pixels) would require 7,86,432 bytes (excluding all other information headers).

Image	***Enlarged View***	***Quality***	***Size (KB)***	**Compression Ratio**
		***Good Quality*** (Quality = 90 %)	98.02	7.832:1
		***Average Quality*** *(Quality = 50 %)*	41.27	18.608:1
		***Medium Quality*** (Quality = 30 %)	31.51	24.371:1

		***Low Quality*** *(Quality = 10 %)*	19.09	40.225:1

3.6 Compression Results

A) X-Ray Image

CR	MSE	PSNR	BITRATE
9.47	8.493	38.843	0.84477297
13.28	18.562	35.445	0.60240964
16.39	28.236	33.623	0.4881025
18.88	37.066	32.441	0.42372881
21.23	45.124	31.587	0.37682525
23.85	54.211	30.79	0.33542977
27.63	68.82	29.754	0.28954035
33.58	95.391	28.336	0.23823705
44.28	159.28	26.109	0.18066847

Figure 4a. Figure showing the tabular variation of parameters with bitrate using JPEG algorithm for X-Ray Image.

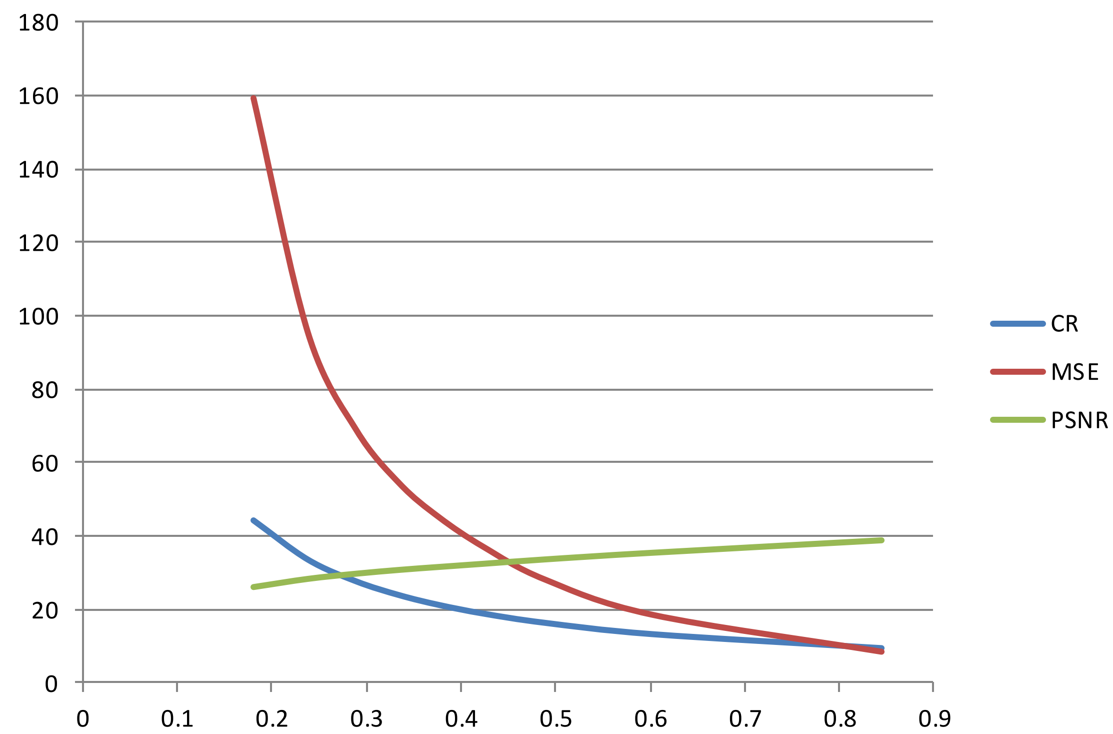

Figure 4b. Figure showing the graphical variation of parameters with bitrate using JPEG algorithm for X-Ray Image.

B) CAT-Scan Image

CR	MSE	PSNR	BITRATE
9.29	8.372	38.903	0.86114101
12.73	18.577	35.441	0.62843676
15.35	29.086	33.494	0.52117264
17.6	39.453	32.17	0.45454545
19.39	49.482	31.186	0.41258381
21.57	62.365	30.181	0.37088549
25.03	81.216	29.034	0.31961646
29.97	113.5	27.581	0.2669336
40.42	199.48	25.132	0.19792182

Figure 5a. Figure showing the tabular variation of parameters with bitrate using JPEG algorithm for CAT-Scan Image.

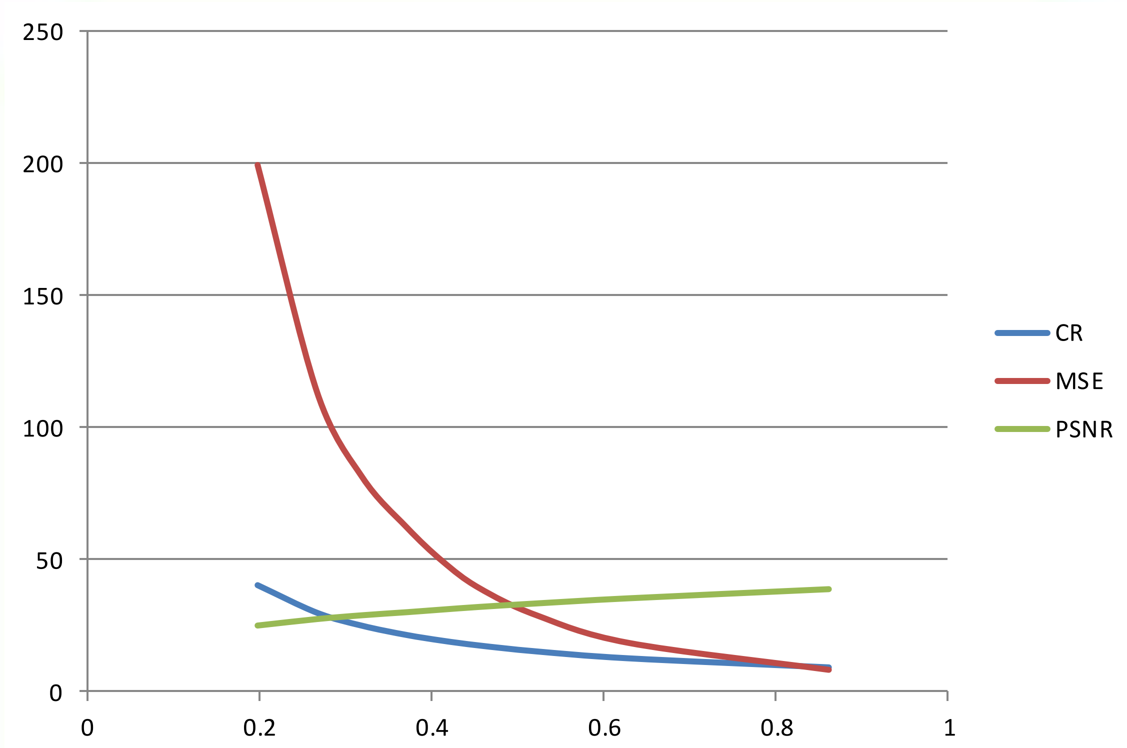

Figure 5b. Figure showing the graphical variation of parameters with bitrate using JPEG algorithm for CAT-Scan Image.

C) MRI Image

CR	MSE	PSNR	BITRATE
7.832	11.879	37.383	1.021
11.283	26.952	33.825	0.709
14.192	39.215	32.196	0.563
16.582	49.868	31.153	0.482
18.608	58.937	30.427	0.429
24.371	85.938	28.789	0.328
29.563	115.86	27.491	0.271
40.225	195.43	25.221	0.199

Figure 6a. Figure showing the tabular variation of parameters with bitrate using JPEG algorithm for MRI Image.

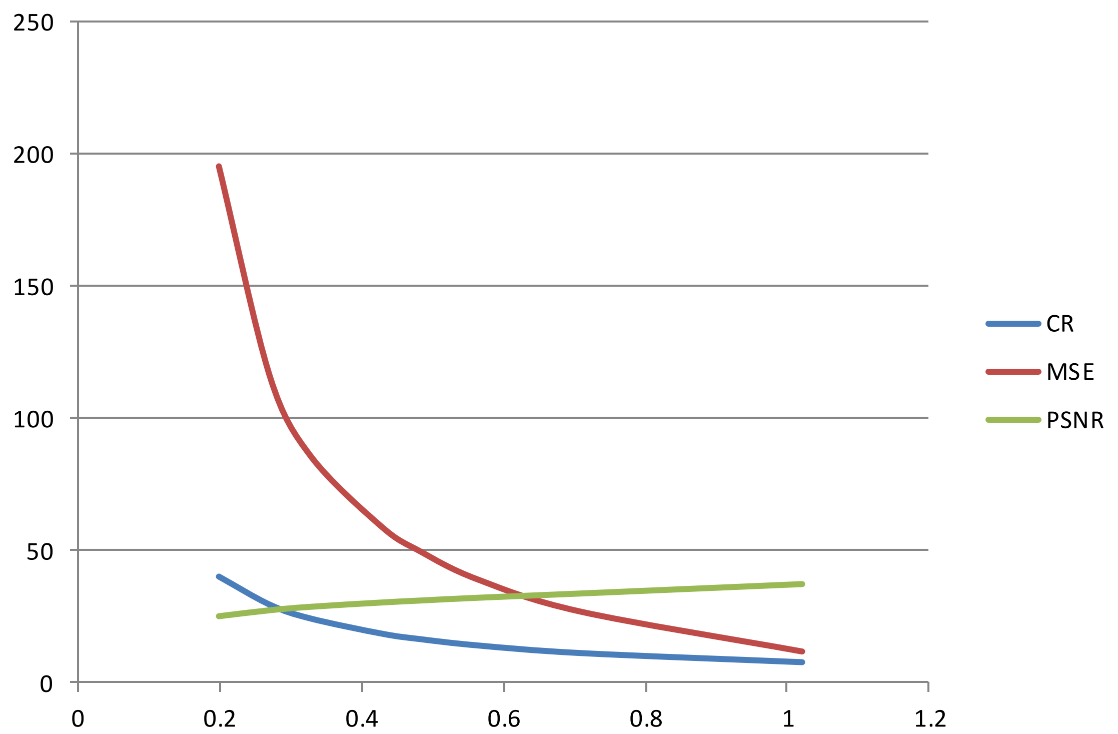

Figure 6b. Figure showing the graphical variation of parameters with bitrate using JPEG algorithm for MRI Image.

D) BARBARA Image

CR	MSE	PSNR	BITRATE
7.355	7.764	39.23	1.08769545
10.361	33.01	32.944	0.77212624
13.166	52.568	30.924	0.6076257
15.608	73.661	29.458	0.51255766
17.868	91.91	28.497	0.44772778
20.569	115.18	27.517	0.3889348
24.665	150.13	26.366	0.32434624
32.556	206.46	24.982	0.24573043
49.398	304.55	23.294	0.16194988

Figure 7a. Figure showing the tabular variation of parameters with bitrate using JPEG algorithm for BARBARA Image.

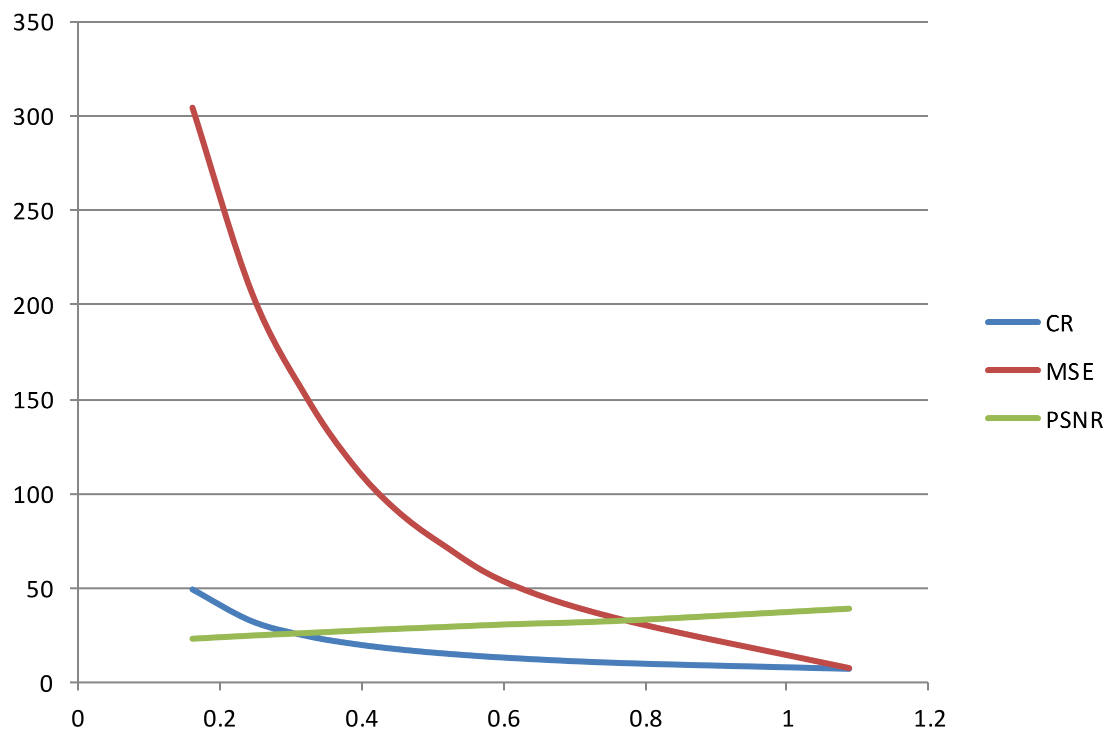

Figure 7b. Figure showing the graphical variation of parameters with bitrate using JPEG algorithm for BARBARA Image.

4. Region of Interest Compression Algorithm

A Region of Interest, often abbreviated ROI, is a selected subset of samples within a dataset identified for a particular purpose. The concept of an ROI is commonly used in medical imaging. For example, the boundaries of a tumor may be defined on an image or in a volume, for the purpose of measuring its size. The endocardial border may be defined on an image, perhaps during different phases of the cardiac cycle, say end-systole and end-diastole, for the purpose of assessing cardiac function.

There are three fundamentally different means of encoding an ROI:

Burned in to the dataset, with a value that may or may not be outside the normal range of normally occurring values

As separate purely graphic information, such as with vector or bitmap (rasterized) drawing elements, perhaps with some accompanying plain (unstructured) text annotation

As separate structured semantic information (such as coded value types) with a set of spatial and/or temporal coordinates

Medical imaging standards such as DICOM provide general and application-specific mechanisms to support various use-cases.

For DICOM images:

Burned in graphics and text may occur within the normal pixel value

Bitmap (rasterized) overlay graphics and text may be present in unused high bits of the pixel data or in a separate attribute (deprecated)

Vector graphics may be encoded in separate image attributes as curves (deprecated)

Unstructured vector graphics and text as well as bitmap (rasterized) overlay graphics may be encoded in a separate object as a presentation state that references the image object to which it is to be applied

Structured data may be encoded in a separate object as a structured report in the form of a tree of name-value pairs of coded or text concepts possibly associated with derived quantitative information can reference spatial and/or temporal coordinates that in turn reference the image objects to which they apply

As far as non-medical standards are concerned, in addition to the purely graphic markup languages and vector graphic and 3D drawing file formats that are widely available, and which carry no specific ROI semantics, some standards such as JPEG 2000 specifically provide mechanisms to label and/or compress to a different degree of fidelity, what they refer to as regions of interest.

4.1 Compression Results

A) MRI Image

CR	MSE	PSNR	BITRATE
18.09	14.84	36.417	0.442233
23.773	33.899	32.829	0.336516
27.886	46.923	31.417	0.286882
30.929	57.592	30.579	0.258657
33.055	65.947	29.939	0.242021
37.241	84.541	28.86	0.214817
42.199	118.52	27.393	0.189578

Figure 8a. Figure showing the ROI and tabular variation of parameters with bitrate using ROI algorithm for MRI Image.

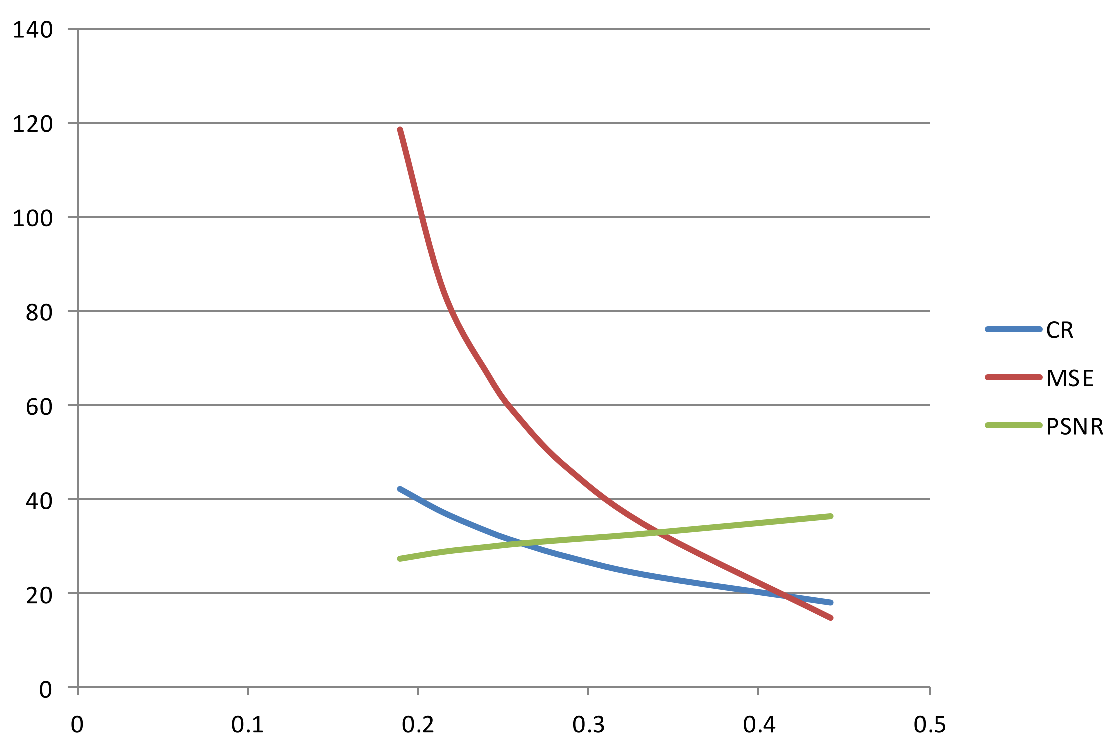

Figure 8b. Figure showing the graphical variation of parameters with bitrate using ROI algorithm for MRI Image.

B) X-Ray Image

CR	MSE	PSNR	BITRATE
14.74	11.433	37.549	0.542741
19.8	24.68	34.207	0.40404
23.629	36.552	32.502	0.338567
26.6	47.059	31.404	0.300752
29.136	56.434	30.615	0.274574
34.325	77.315	29.248	0.233066
41.25	115.14	27.519	0.193939

Figure 9a. Figure showing the ROI and tabular variation of parameters with bitrate using ROI algorithm for X-Ray Image.

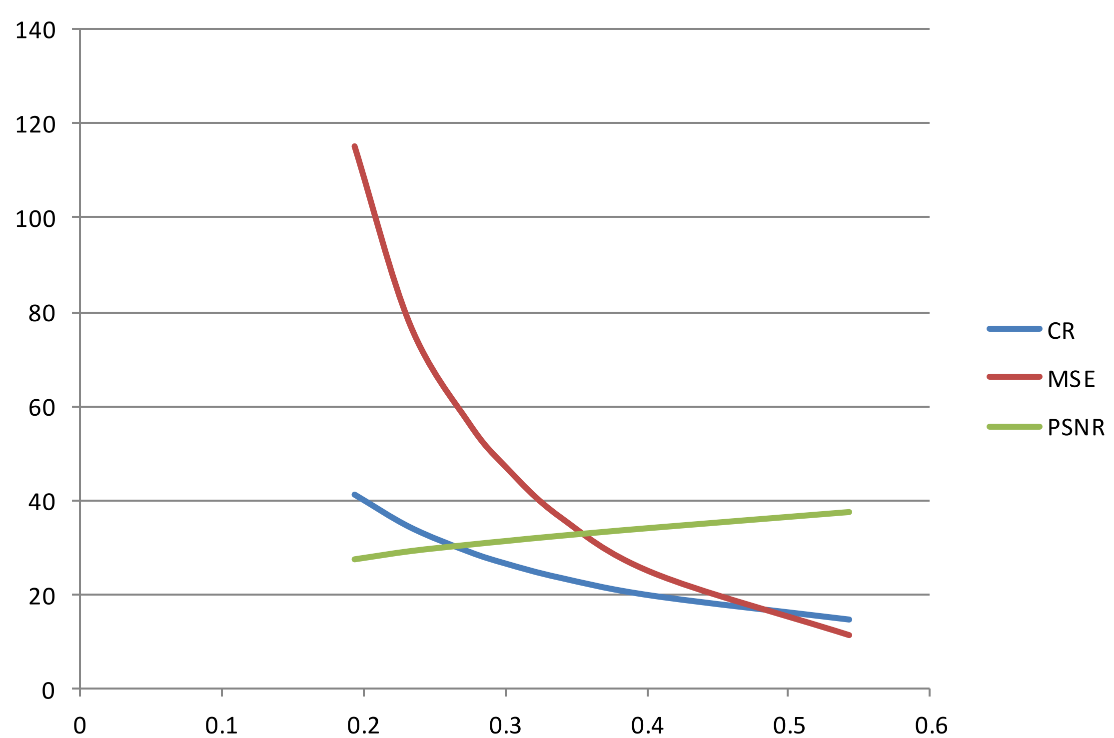

Figure 9b. Figure showing the graphical variation of parameters with bitrate using ROI algorithm for X-Ray Image.

C) CAT-Scan Image

CR	MSE	PSNR	BITRATE
11.579	6.643	39.907	0.690906
16.405	14.196	36.609	0.487656
19.688	21.16	34.876	0.406339
22.137	27.484	33.74	0.361386
24.066	33.45	32.887	0.332419
27.962	48.175	31.303	0.286103
33.47	76.172	29.313	0.23902

Figure 10a. Figure showing the ROI and tabular variation of parameters with bitrate using ROI algorithm for CAT-Scan Image.

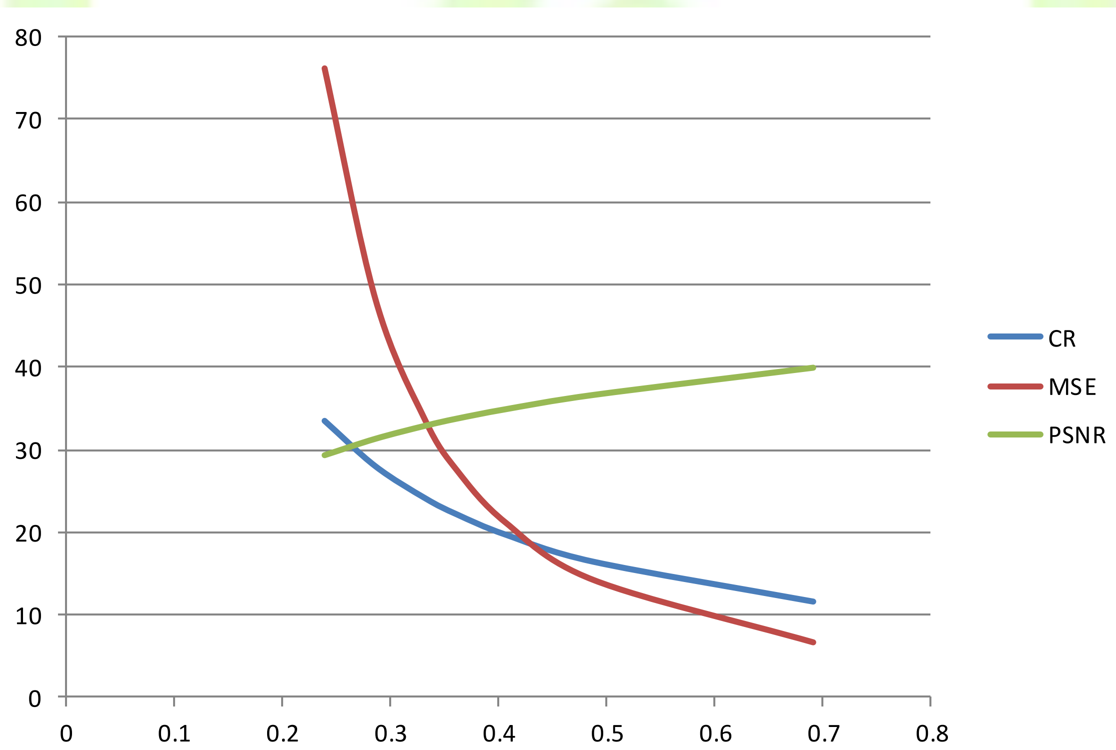

Figure 10b. Figure showing the graphical variation of parameters with bitrate using ROI algorithm for CAT-Scan Image.

4.2 Comparison with JPEG Algorithm

A) MRI Image

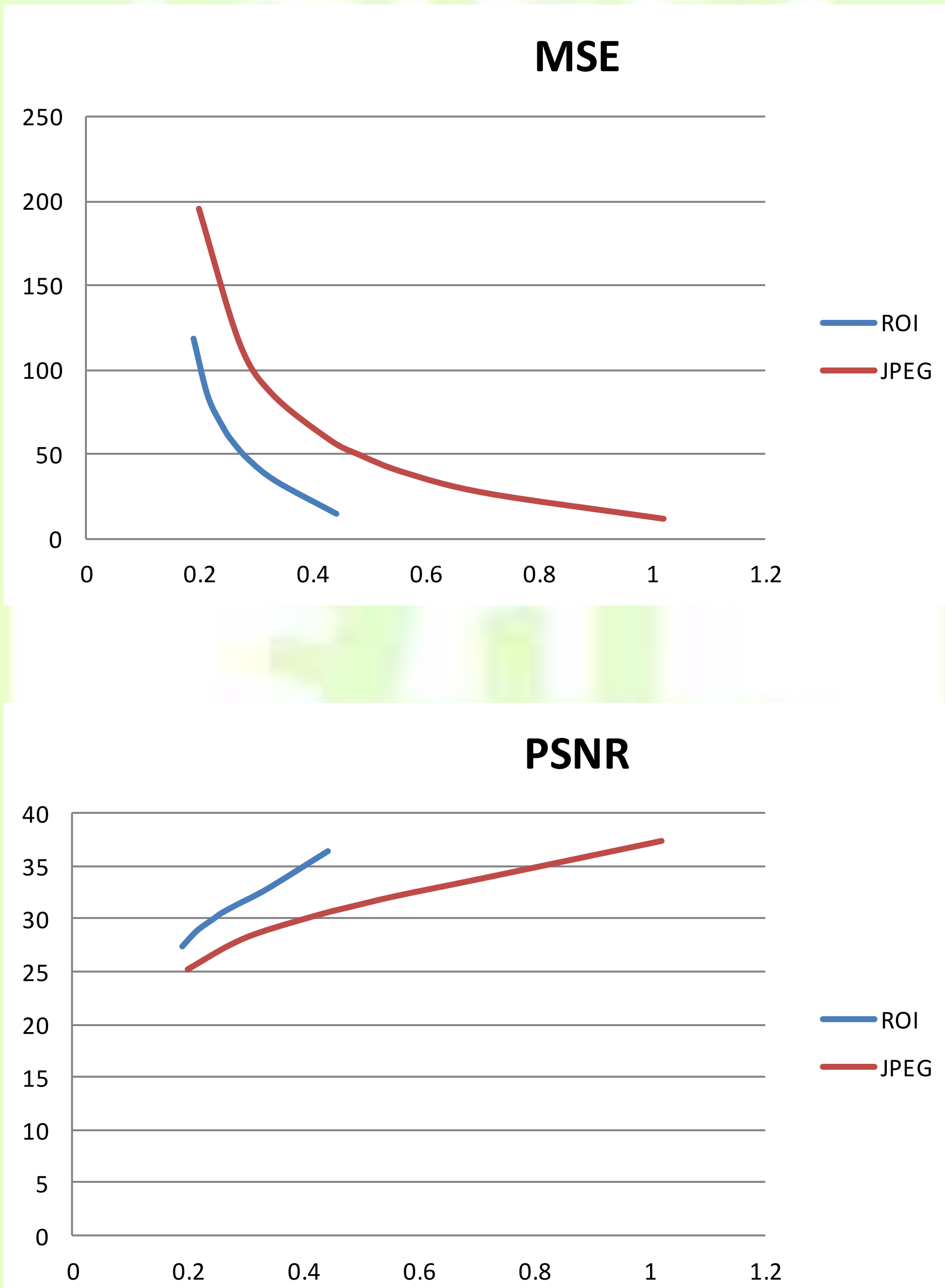

Figure 11. Figure showing the graphical comparison of variation of parameters with bitrate using JPEG and ROI algorithm for MRI Image.

B) X-Ray Image

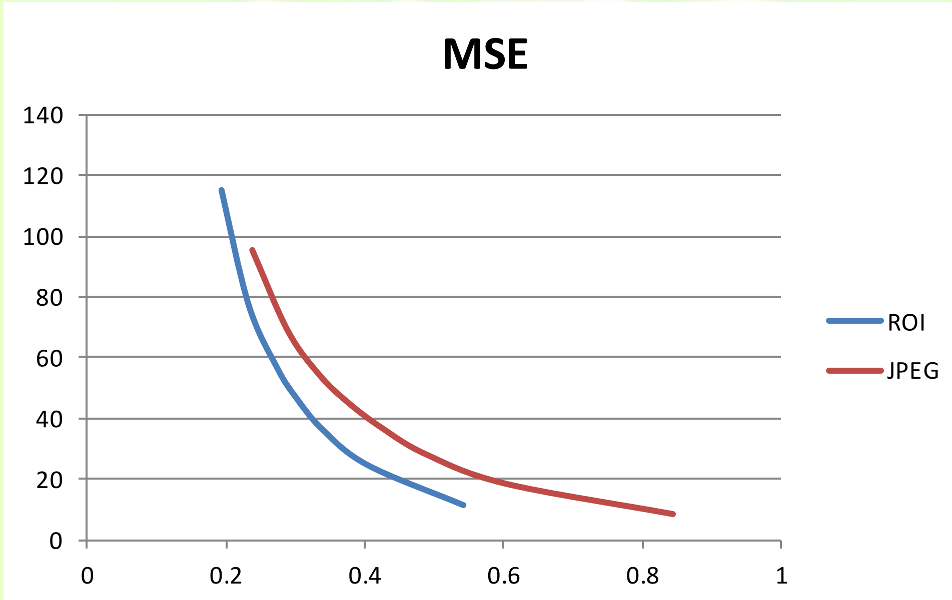

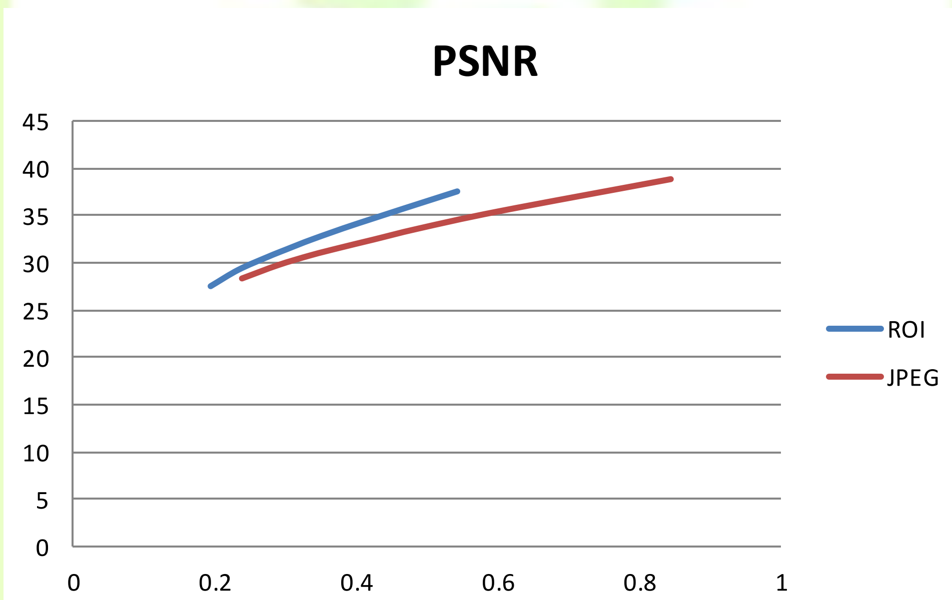

Figure 12. Figure showing the graphical comparison of variation of parameters with bitrate using JPEG and ROI algorithm for X-Ray Image.

C) CAT-Scan Image

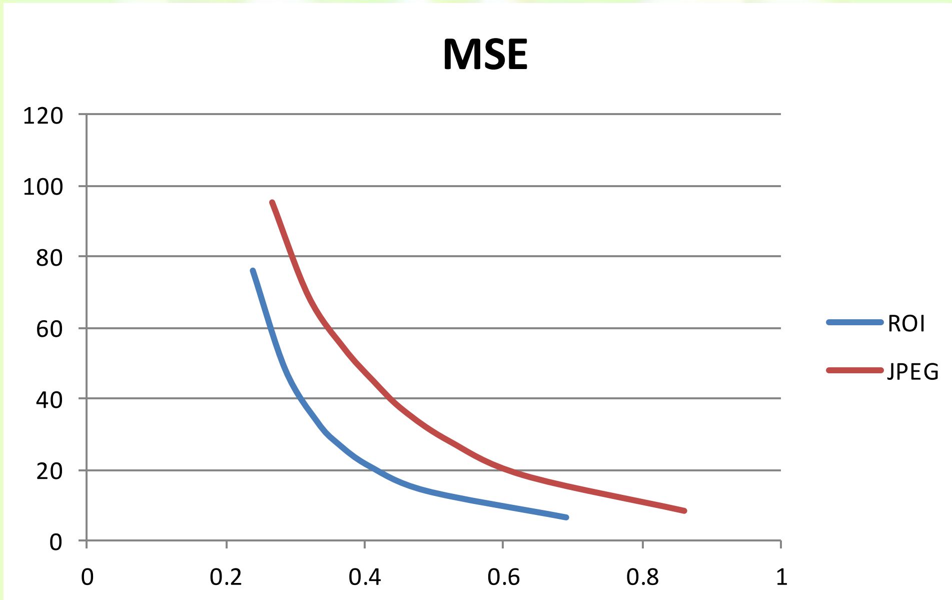

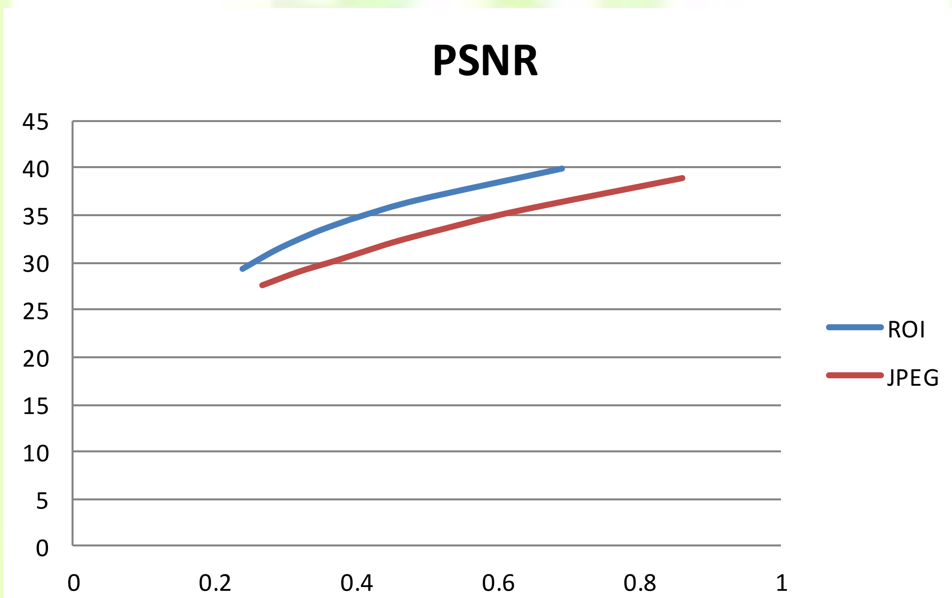

Figure 13. Figure showing the graphical comparison of variation of parameters with bitrate using JPEG and ROI algorithm for CAT-Scan Image.

5. Embedded Zerotree Wavelet Compression Algorithm

The EMBDDED ZEROTREE WAVELET (EZW) algorithm, as presented by J. Shapiro, is a simple yet powerful algorithm, in which bit-streams are generated in order of their significance in containing the image information. TRANSFORM coding forms an integral part of the image compression techniques. Transform Coding involves a reversible, linear and unique set of coefficients, which are often quantized and then coded. Wavelet decomposition makes the energy distributed throughout the entire image to be clustered in a few sub bands, thereby creating a special parent-child-grandchild relationship (in the wavelet decomposed coefficients) known as TREE. Few such trees having a special relationship tend to become ZEROTREES, as explained in later section. This technique thereby takes advantage of the hierarchical structure of the wavelet decomposed sub images, using the parent-child-grandchild relationships for compression.

Another significant feature is the embedded coding which helps to transmit the image progressively thereby with each new set of next step encoded coefficients improving the details of the already decoded image. Using an embedded code, a coder can terminate the encoding at any desired step taking into account a desired parameter like bit-rate, as against the image quality. Similarly, for a given bit stream, the decoder can stop decoding at any step thereby producing reconstructed image corresponding to a lower-rate encoding. Optimally, for a given bit-rate, the non-embedded code must be more efficient than the embedded code, as it is free from those constraints, which are imposed by the embedded coding. However, overweighting this disadvantage, a large number of advantages like better PSNR and reduced MSE are associated with embedded coders. The EZW algorithm gives a good performance in terms of time taken for encoding, when relatively images of smaller dimensions are coded using it. However, as the image dimensions increases the time taken for encoding goes on increasing with it.

5.1 Wavelet Decomposition

The first step in embedded wavelet zerotree coding involves decomposition of the original image into wavelet decomposed images using 2-D discrete wavelet transform. The 2-D wavelet transforms the image into four sub-images using special filters which are applied along the rows and then along the columns. This result in four sub-bands named as low-low, high-low, low-high and high-high. These sub-images are named as LL1, HL1, LH1, HH1 .The low-low sub-band may be further decomposed and divided into four sub-bands. These sub-images are obtained by using vertical and horizontal filters.

As a result of this decomposition, the entire image energy gets squeezed into the LL1 sub-band. The HL1, LH1 and the HH1 sub-band contains only the directional information of the original image. The wavelet filters are so designed that the coefficients in the sub-bands are mostly not correlated with each other. Moreover, in case of an image most of the information exists in the low frequency components while the higher frequency components add only intricate details to the image. The filters used in present work for obtaining the discrete wavelet transform, are based on the *Daubechies* filters. After the first level of wavelet decomposition the LL1 sub-band is again decomposed by using the same discrete wavelet transform into four another sub-band labeled as LL2,HL2,LH2 and HH2.This process is repeated a desired number of times until a finer resolved image is obtained. The present work is carried out by using 3 levels of wavelet decomposition. The third level of decomposition is obtained from the LL2 sub-band as shown in Figure 15.

Figure 14. Figure showing (a) The original woman image (b) The 2-D wavelet decomposed representation of the woman image .The bands are labeled as LL1,HL1,LH1,HH1 following from top-left to bottom-right. The LL1 sub-band contains the most significant image coefficients, while HL1, LH1 and HH1 sub-bands contain only the directional information.

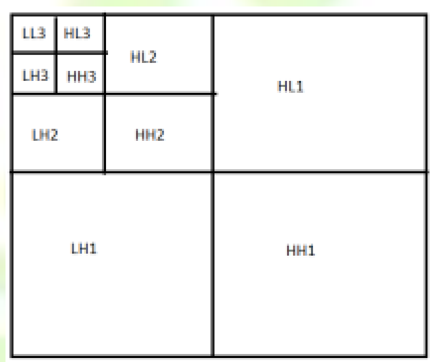

Figure 15. Figure showing the three levels of wavelet decomposition.
The third decomposition level is obtained by further decomposition of LL2 sub-band. This decomposition clusters the maximum energy in the LL3 sub-band.

5.2 Tree Structure of Wavelet Coefficients

In a hierarchical sub-band structure, each coefficient at a given scale is related to a set of coefficients at the next finer scale of similar orientation. However, the highest frequency sub-bands are exceptions, since there is no existence of a finer scale beyond them. The coefficients at the coarser scale are known as *parent* and the coefficients at the finer scale in similar orientation and same spatial location are known as *children*. For a given parent, the set of all coefficients, at each finer scale having similar orientation and spatial locations is known as descendants. The wavelet decomposition of each band creates four sub-bands. Thus, each coefficient in the parent band is linked to four coefficients in the child sub-bands (except in LL3). This hierarchical structure is known as *Quad-Tree*. For a three level decomposed images as in Figure 2, each coefficient in HL3,LH3 & HH3 is linked to four child coefficients in HL2,LH2 & HH2;which are further linked to sixteen coefficients in HL1,LH1 & HH1.This entire tree structure consisting of one coefficient in HL3,four coefficients in HL2 and sixteen coefficients in HL1 , is known as a Quad-tree as shown in Figure 3.A *zero-tree*, may be defined against a threshold, as a quad-tree having all its children coefficients, including its parent coefficient, lesser than the threshold. The zerotree concept arises from the fact that if a DWT coefficient at a coarse scale is insignificant, then normally all its higher frequency descendants are also likely to be insignificant.

A zerotree must therefore have a root structure, which is insignificant at a threshold. Since in a wavelet decomposed sub-image the maximum energy gets accumulated in the higher order sub-bands, so normally the children coefficients are smaller than the corresponding parent coefficient of the quad-tree, thereby creating a large number of zero-trees. This is illustrated by an example in Figure 17, as against a threshold of 32, here the circled coefficients represents a zero-tree.

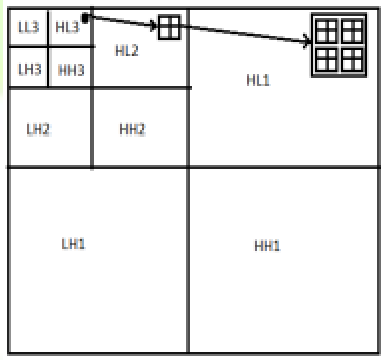

Figure 16. Figure showing a quad-tree obtained after three levels of wavelet decomposition. The arrow points from the parent to child to grand-child. Similar relationship exists for LH3 & HH3 sub-band also. However this relationship does not exist in LL3 sub-band.

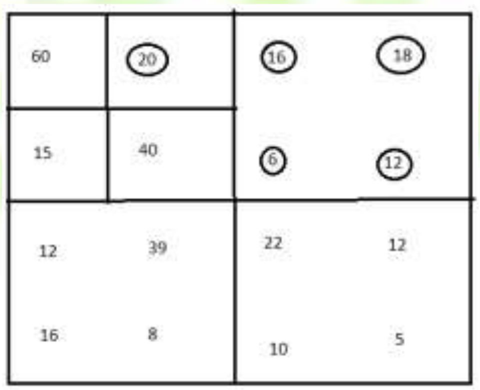

Figure 17. Figure showing an example of zero-tree structure for two level wavelet decomposed image of 4x4(dimensions). The example assumes a threshold value of *32*.The *circled* coefficients represents a zero-tree. The coefficient values of *39* and *40* in the *LH1* and *HH2* sub-bands respectively, prevent the corresponding quad-trees to turn into zero-trees.

5.3 Encoding Algorithm

The EZW algorithm is based on the following observations – When an image, having a low pass spectrum is wavelet decomposed, its energy in the LL sub-band increases with each level of decomposition and higher valued coefficients are more significant as compared to lower valued coefficients. The original algorithm begins encoding by decomposing the image to be encoded using the 2-D discrete wavelet transformation, a desired number of times. In the present work the image has been decomposed for three wavelet levels using filters based on the Daubechies filters as in .Next, the algorithm starts by calculating a threshold coefficient (in the power of 2), less than or equal to the maximum magnitude of the coefficients in the image. The algorithm codes using two passes. The first pass is known as the *Dominant Pass*.

This dominant pass creates a list containing coefficients known as Subordinate list. Then, this Subordinate list undergoes through another pass known as *Subordinate Pass* .The image coefficients are scanned in a prescribed order known as *Morton* scanning order as shown in Figure 5.The lower frequency sub-bands are scanned before the higher frequency sub-bands. Then the scanning continues to the next finer scale. This ensures that the all parent coefficients are scanned before the child coefficients. This process continues till the highest frequency sub-band is covered. This order is to be calculated, depending on the dimensions of the image. The method exploits the fact that a tree once identified to be a zero-tree is exempted from coding and is assigned a symbol once only , thereby all its descendents are prevented from being scanned again. The dominant pass works on the simple concept of significance. A coefficient becomes significant with respect to a given threshold if its magnitude is greater than or equal to the threshold. At the start, each coefficient is assumed to be insignificant and progressively, more and more significant coefficients are detected. In the dominant pass, the magnitude of the coefficient scanned is compared against the threshold.

On comparison two conditions arise – either the scanned coefficient is significant with respect to the threshold or it is insignificant. If former condition is satisfied then again the coefficient checked for the sign coding. If this coefficient is positive it is assigned a symbol '*p*' otherwise it is assigned a symbol '*n*'. Moreover, this coefficient is added to a subordinate list, which is to be next scanned in the sub-ordinate pass. If the latter condition is satisfied then the entire tree-structure is considered .If the tree structure is a zero-tree, then it is assigned a symbol't', and is marked a zero-tree. Otherwise, a non zero-tree structure is coded as an isolated zero, and is assigned a symbol '*z*'. The dominant pass thereby creates two sets – one containing the coefficients marked using the four symbols, known as significance map and the other containing a list of coefficients having a significant magnitude than the present threshold, known as subordinate list. This coding reduces the cost of encoding the using the similarity property . Though,2D-DWT essentially decorrelates the coefficients, however the occurrence of insignificant coefficients is not an independent event. Rather,it is easier to predict insignificance, than to predict significant details. Zerotree coding therefore exploits this redundancy among such insignificant coefficients.The following subordinate pass scans all the coefficients of the sub-ordinate list which has been created or concatenated during the present dominant passes. The coefficients in this sub-ordinate list are retained during each pass

.After each pass the coefficients found significant during the previous dominant pass are added to this list. This pass is followed by a subordinate pass, during which the coefficients shortlisted during the dominant pass, are scanned again in order to add increased precision to image detail. This is done by splitting the region of uncertainty into two halves - one of them, being greater than half the present threshold and the other one being smaller. For the former half the symbol '1' is assigned while for the latter half the symbol '0' is assigned. The coefficients in the sub-ordinate list are sorted in such an order, as to enable the decoder to carry out the same sorting. The process alternates between both the passes and the present threshold is halved at each pass. In this manner all the coefficients are scanned and the process stops when the present threshold tends to become unity or at a stage, based on any desired image parameter (like the bit-rate or PSNR). The coefficients which were found significant during the present dominant pass are replaced by zero and the process is repeated. The stream of symbols generated from the dominant pass is then compressed using any entropy coding algorithms like the *HUFFMAN* coding or *ARITHMETIC* coding. The present work uses Huffman coding. The symbols generated during the subordinate pass need not to be entropy coded. Actually, EZW encoding reorders the wavelet coefficients in such a way that they can be compressed very efficiently. Therefore the EZW encoder is always followed by an entropy encoder. Since the wavelet coefficients are reordered, in accordance of their importance in determining the image structure, so the decoding algorithm requires the scanning order in which the image was encoded.

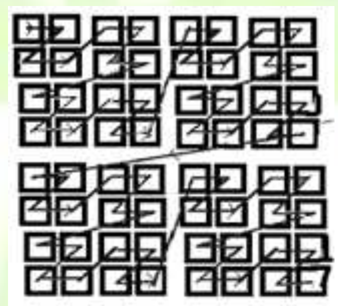

Figure 18. Figure showing scanning order for a 8x8 image .The scanning begins in the order : LL3,HL3,LH3,HH3,HL2,LH2,HH2,HL1,LH1 & HH1.The scanning order continues in the direction of arrow known as *Morton* scanning.

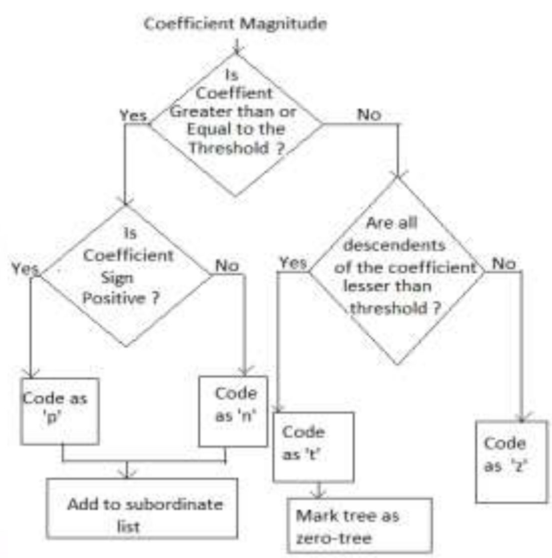

Figure 19. Figure showing flowchart for encoding coefficient during the dominant pass. This pass creates two output sets – one containing the four coded symbols and a sub-ordinate list set.

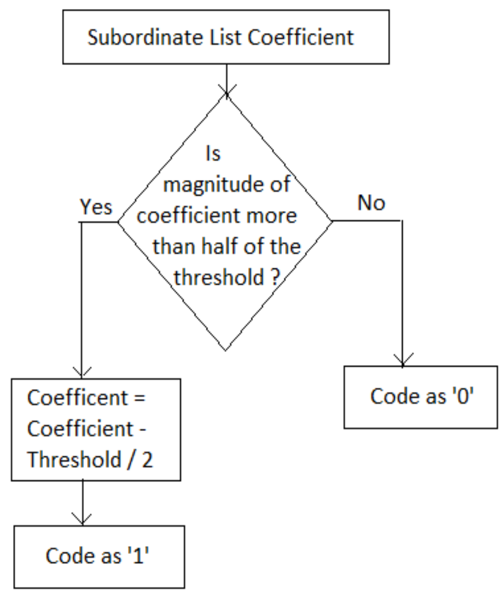

Figure 20. Figure showing flowchart for encoding subordinate list coefficient during the subordinate pass. This pass creates a single set containing the symbols ‘1’ and ‘0’.

5.4 An Example

Consider a 8 x 8 matrix having a wavelet decomposition level of three:

63	-34	49	10	7	13	-12	7
-31	23	14	-13	3	4	6	-1
15	14	3	-12	5	-7	3	9
-9	-7	-14	8	4	-2	3	2
-5	9	-1	47	4	6	-2	2
3	0	-3	2	3	-2	0	4
2	-3	6	-4	3	6	3	6
5	11	5	6	0	3	-4	4

Initial Threshold: 32

Dominant Pass 1: pnztpttttztttttttptt

Sub-ordinate Pass 1: 1010

Threshold: 16

Dominant Pass 2: ztnptttttttt

Sub-ordinate Pass 2: 100110

Threshold: 8

Dominant Pass 3:zzzzzppnppnttnnptpttnttttttttpttptttttttttpttttttttttt

Sub-ordinate Pass 3: 10011101111011011000

Threshold: 4

Dominant Pass 4: zzzzzzztztznzzzzpttptpptpnptnttttptpnppppttttptptttpnp

Sub-ordinate Pass 4: 110111110110010000011101101000100101011OO

Threshold: 2

Dominant Pass 5: zzzzztzzzzztpzzzttpttttnptppttptttnppnttttpnnpttpttppttt

Sub-ordinate Pass 5: 10111100110100010111110101101100100000000110110110011000111

Threshold: 1

Dominant Pass 6: zzzttztttztttttnnttt

Output after Huffman Coding :
1110110100111000001000000000111000100110111011110101010101011101110110111011101100011
01101110011100011000000000111000011100000000001110111101010101010101001001011010101O
10111000111001110111001110110111001100000011100111011011101110111011100000011100111O
000111011011101010100110100111011110110110001101111101100100000111011010001001010110
0

Input Size : 64 bytes

Output Size : 43 bytes

Compression Ratio : 1.49:1

6. Unit Embedded Zerotree Wavelet Compression Algorithm

The original EZW algorithm scans the entire wavelet decomposed image, at a stroke, during each pass. Unit EZW presents a modified method for coding images using EZW method, which works on the principal of fragmentation. This method takes the smallest unit cell, generated from the wavelet decomposed image, to encode at a time .This makes the encoding times independent of the level of wavelet decomposition. Results show that this algorithm is more efficient in performance, in terms of encoding times, as compared to the original algorithm. Moreover, the difference between the encoding times using the original and Unit EZW method tends to increase with an increase in the dimensions of the image under test.

6.1 Unit Cell

The algorithm relies heavily on the concept of a unit cell. A unit cell may be defined as the smallest possible square matrix generated from the wavelet decomposed image, having the same level of wavelet decomposition structure as the original image. For a three level wavelet decomposed sub-image, the unit cell must be a square matrix, having the order of eight. A unit cell is composed of a single coefficient from the lowest frequency & the coarsest parent sub-band, followed by its quad-tree coefficients from the next higher frequency & finer child sub-band. This process continues till the finest scale sub-band has been reached.

6.2 Encoding Algorithm

Similar to the original algorithm, this algorithm begins the encoding process, by the wavelet decomposition of the image, a desired number of times. The threshold is calculated for the entire image, once only and the same is used throughout the process. From the wavelet decomposed sub-image unit cells are generated. These generated unit cells are then coded using the original EZW coding algorithm. These unit cells are then coded serially. For the embedded coding, the first dominant pass coefficients of all unit cells are combined followed by the next first sub-ordinate pass. The stream generated during dominant pass undergoes through a *RUN-LENGTH* coder. This run-length coding is necessary because the generated bit-stream has a high order of redundancy, which arises due to the fact, that a single threshold value is utilized for each unit-cell. This run-length coding is followed by entropy coding. Similar to the original algorithm the bit-stream generated during the sub-ordinate pass, needs not be run-length or entropy coded. This is followed by the next dominant and sub-ordinate pass and the process is repeated based on any desired image parameter. Once this parameter is obtained the encoder stops. The decoder must be aware of the order in which the unit cells were encoded, in order to be able to reconstruct the original image.

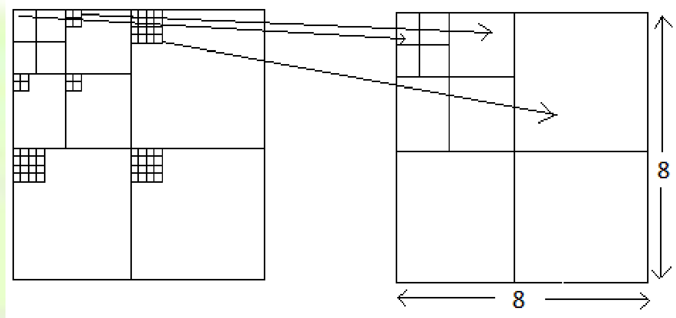

Figure 21. Figure showing formation of a unit cell from a wavelet decomposed sub-image. The arrow points from the sub-image to the unit cell. Similar relationship exists for elements in the LH, HH & HL sub-bands also.

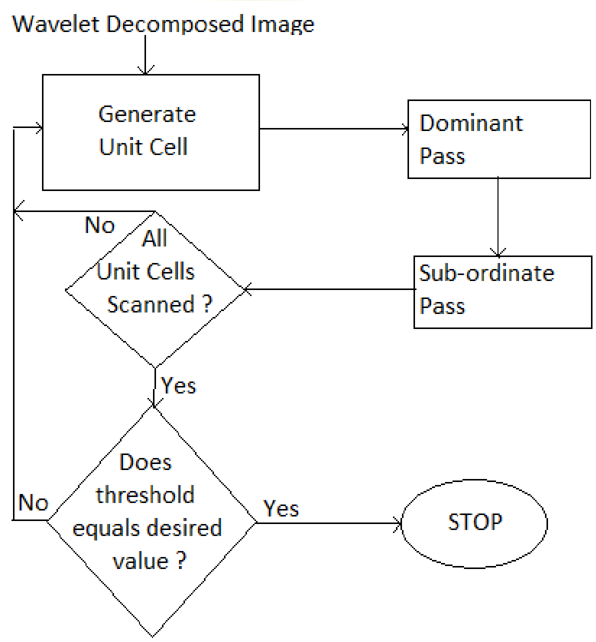

Figure 22. Figure showing the flowchart for the Unit EZW Algorithm

6.3 *Comparison with existing EZW Algorithm*

The results have been obtained for different test-images having varying dimensions. The results were obtained on the same machine for three levels of wavelet decomposition. For the original algorithm the entire image was scanned and the coding time was noted, while for the proposed algorithm, unit cells were composed, scanned and coded and again the coding time was noted. Results for the same have been shown in Figure 23. The results show a considerable improvement in the coding time using the proposed algorithm as compared to original algorithm.

Image	Original EZW algorithm					Unit EZW algorithm				
	Dimensions (Pixels × Pixels)	*32 × 32*	*64 × 64*	*128 × 128*	*256 × 256*	*Dimensions (Pixels × Pixels)*	*32 × 32*	*64 × 64*	*128 × 128*	*256 × 256*
LENA_GRAY		1.092	4.540	20.062	210.617		0.952	3.479	13.120	52.073
BARBARA_GRAY		1.108	4.477	19.407	213.425		0.983	3.572	13.915	54.632
CAMRAMAN		1.139	4.618	20.639	200.960		0.998	3.588	13.463	53.867
GOLDHILL		1.136	4.680	20.779	216.670		0.996	3.510	13.541	54.226
PEPPERS_GRAY		1.186	4.524	19.812	214.626		1.030	3.650	14.258	54.632

Figure 23. Figure showing the coding time for original and Unit EZW algorithm (in seconds)

Image	Dimensions (Pixels × Pixels)			
	32 × 32	*64 × 64*	*128 × 128*	*256 × 256*
LENA_GRAY	12.821	23.370	34.603	75.276
BARBARA_GRAY	11.282	20.214	28.299	74.402
CAMRAMAN	12.379	22.304	34.769	73.195
GOLDHILL	12.324	25.000	34.833	74.973
PEPPERS_GRAY	13.153	19.319	28.034	74.545

Figure 24. Figure showing the improvement in coding time for Unit EZW algorithm over the original algorithm (in percent)

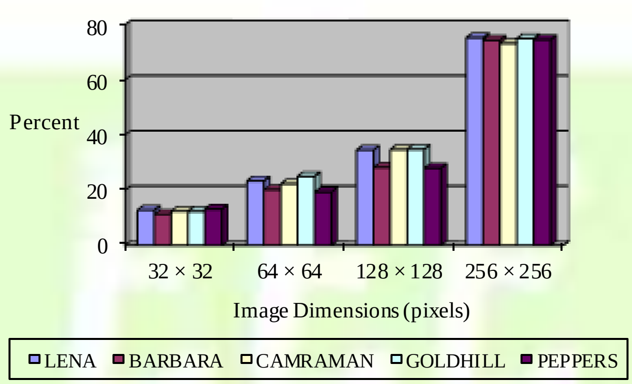

Figure 25. Figure showing the improvement in coding time using unit EZW algorithm over original algorithm.

7. Applications of Digital Image Compression

- **Computer vision:** Computer vision is concerned with the theory behind artificial systems that extract information from images. The image data can take many forms, such as video sequences, views from multiple cameras, or multi-dimensional data from a medical scanner.

- **Optical sorting:** Optical Sorting is a process of visually sorting a product though the use of Photo detector, Camera, or the standard Mark 1 Human eye ball.

- **Augmented Reality:** Augmented reality (AR) is a term for a live direct or indirect view of a physical real-world environment whose elements are augmented by virtual computer-generated imagery.

- **Face detection:** Face detection is a computer technology that determines the locations and sizes of human faces in digital images. It detects facial features and ignores anything else, such as buildings, trees and bodies.

- **Feature detection:** In computer vision and image processing the concept of feature detection refers to methods that aim at computing abstractions of image information and making local decisions at every image point whether there is an image feature of a given type at that point or not.

- **Lane departure warning system:** In road-transport terminology, a lane departure warning system is a mechanism designed to warn a driver when the vehicle begins to move out of its lane on freeways and arterial roads.

- **Medical image processing:** Medical imaging is the technique and process used to create images of the human body for clinical purposes or medical.

- **Remote sensing:** Remote sensing is the acquisition of information of a phenomenon, by the use of real-time sensing device(s) that are not in physical or intimate contact with the object.

8. Advantages of Digital Image Compression

- **Post - processing of image:** Post-processing of the image allows the operator to manipulate the pixel shades to correct image density and contrast, as well as perform other processing functions that could result in improved diagnosis and fewer repeated examinations.

- **Easy storage and retrieval of image:** With the advent of electronic record systems, images can be stored in the computer memory and easily retrieved on the same computer screen and can be saved indefinitely or be printed on paper or film if necessary.

- **Ease of sharing data:** All digital imaging systems can be networked into practice management software programs facilitating integration of data. With networks, the images can be viewed in more than one room and can be used in conjunction with pictures obtained with an optical camera to enhance the patients' understanding of treatment.

- **More use of the same data:** Digital imaging allows the electronic transmission of images to third-party providers, referring dentists, consultants, and insurance carriers via a network.

- **Environmental friendly:** Digital imaging is also environmentally friendly since it does not require chemical processing. It is well known that used film processing chemicals contaminate the water supply system with harmful metals such as the silver found in used fixer solution.

- **Reduction in radiation:** Radiation dose reduction is also a benefit derived from the use of digital systems. Some manufacturers have claimed a 90% decrease in radiation exposure, but the real savings depend on comparisons.

9. Disadvantages of Digital Image Compression

- **High initial cost:** The initial cost can be high depending on the system used, the number of detectors purchased, etc.

- **Need of extra knowledge:** Competency using the software can take time to master depending on the level of computer literacy of team members.

- **Limitation on shape and size of detectors:** The detectors, as well as the phosphor plates, cannot be sterilized or autoclaved and in some cases CCD/CMOS detectors pose positioning limitations because of their size and rigidity. This is not the case with phosphor plates; however, if a patient has a small mouth, the plates cannot be bent because they will become permanently damaged.

- **High maintenance cost:** Phosphor plates cost an average of $25 to replace, and CCD/CMOS detectors can cost more than $5,000 per unit. Thus, digital processing system requires more maintenance as compared to traditional systems.

- **Need for standardization:** Since digital imaging in dentistry is not standardized, professionals are unable to exchange information without going through an intermediary process. Hopefully, this will change within the next few years as manufacturers of digital equipment become DICOM compliant.

10. Conclusion

To conclude the project work a brief comparison of all the algorithms covered under both the lossy and lossless methods will be made.

Two of the lossy compression algorithms have been presented. The JPEG algorithm have the advantages of the coding algorithm being lesser complicated than the ROI algorithm, along with it is associated the advantage of JPEG algorithm being a standard manifesto. The JPEG algorithm is used widely in digital cameras and web usage. Moreover the JPEG algorithm has the advantage of having lesser coding times in comparison with the ROI method, primarily due to the fact that in JPEG the entire image is coded in a shot while ROI first divides the image into the Interest region and the background which need to be separately coded at different quality factors.

The ROI algorithm has the advantages of having better compression ratios along with a higher Picture Signal to Noise Ratio and a lesser Mean Square Errors. Moreover there is a better scope of ROI being implemented in the medical field because of the fact that most of the part of a medical image is of no use for medical purpose. The significant information is contained in a small part which is selected as ROI and coded at much higher quality. Thus, conclusion may be made that in field of medical image compression, ROI is much better performer than JPEG. While, in case of general digital imagining JPEG is a better performer than ROI.

Considering the case of lossless methods the primary matter of concern turns out to be the coding time. The EZW algorithm though being one of the most popular quad-tree coding algorithm, suffers from the fact that it requires a large coding time for images of higher dimensions. In this case the Unit EZW algorithm uses a modified algorithm which reduces the coding time while maintaining all the features of the EZW algorithm like the embedded coding and zerotree concept. Thus, in this category Unit EZW algorithm may be concluded as the better performer.

The future scope of the present project may be understood to be application of such Unit algorithms using other quad-tree approaches like the SPIHT and the NLS. Moreover, many more challenges will surely arise in near future, that are still to be dealt with.

A) X-Ray Image

NAME : X-RAY
TYPE : BITMAP
BYTES PER PIXEL : 24
SIZE : 768 KB
DIMENSIONS : 512 x 512

B) CAT-Scan Image

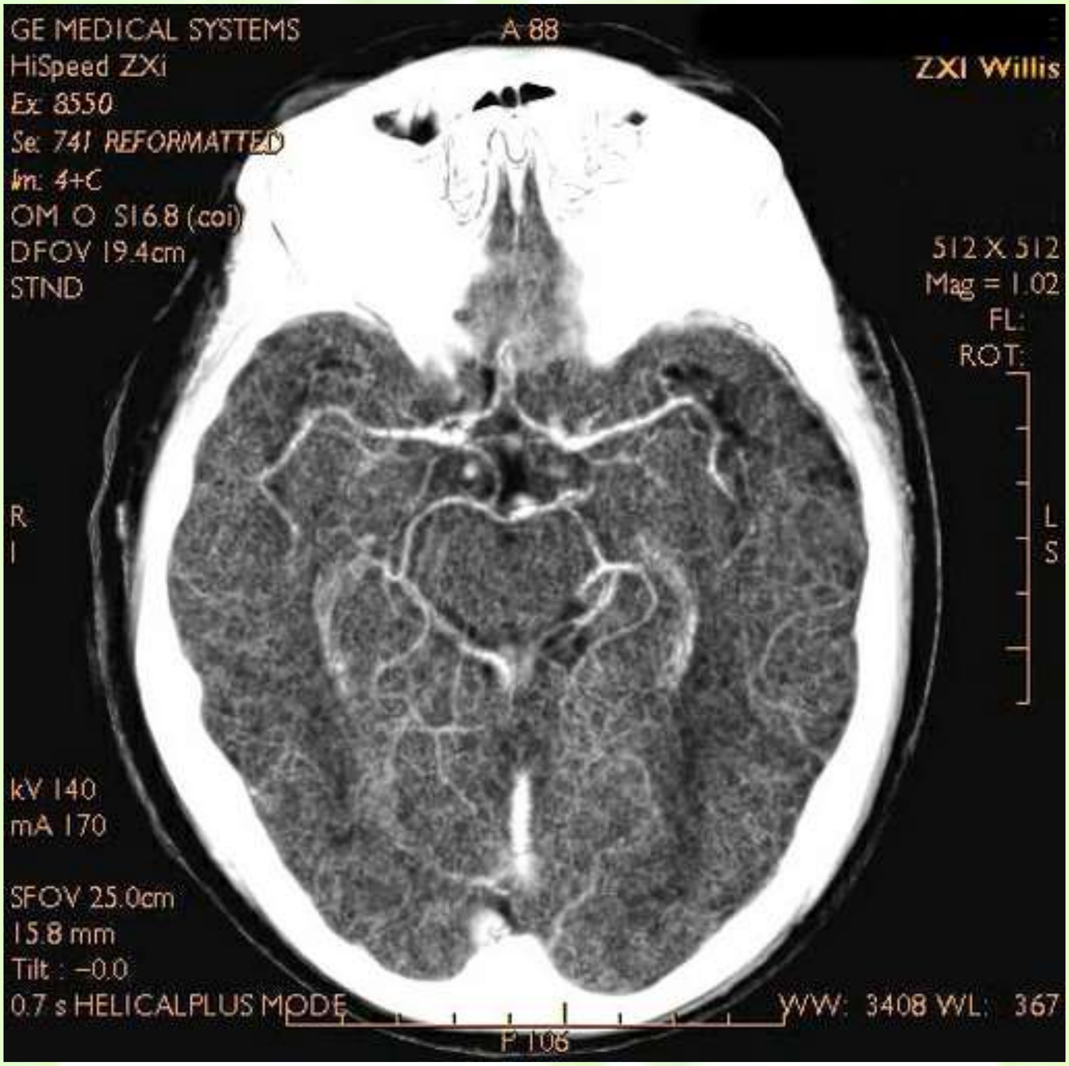

NAME : CAT-Scan
TYPE : BITMAP
BYTES PER PIXEL : 24
SIZE : 768 KB
DIMENSIONS : 512 x 512

C) MRI Image

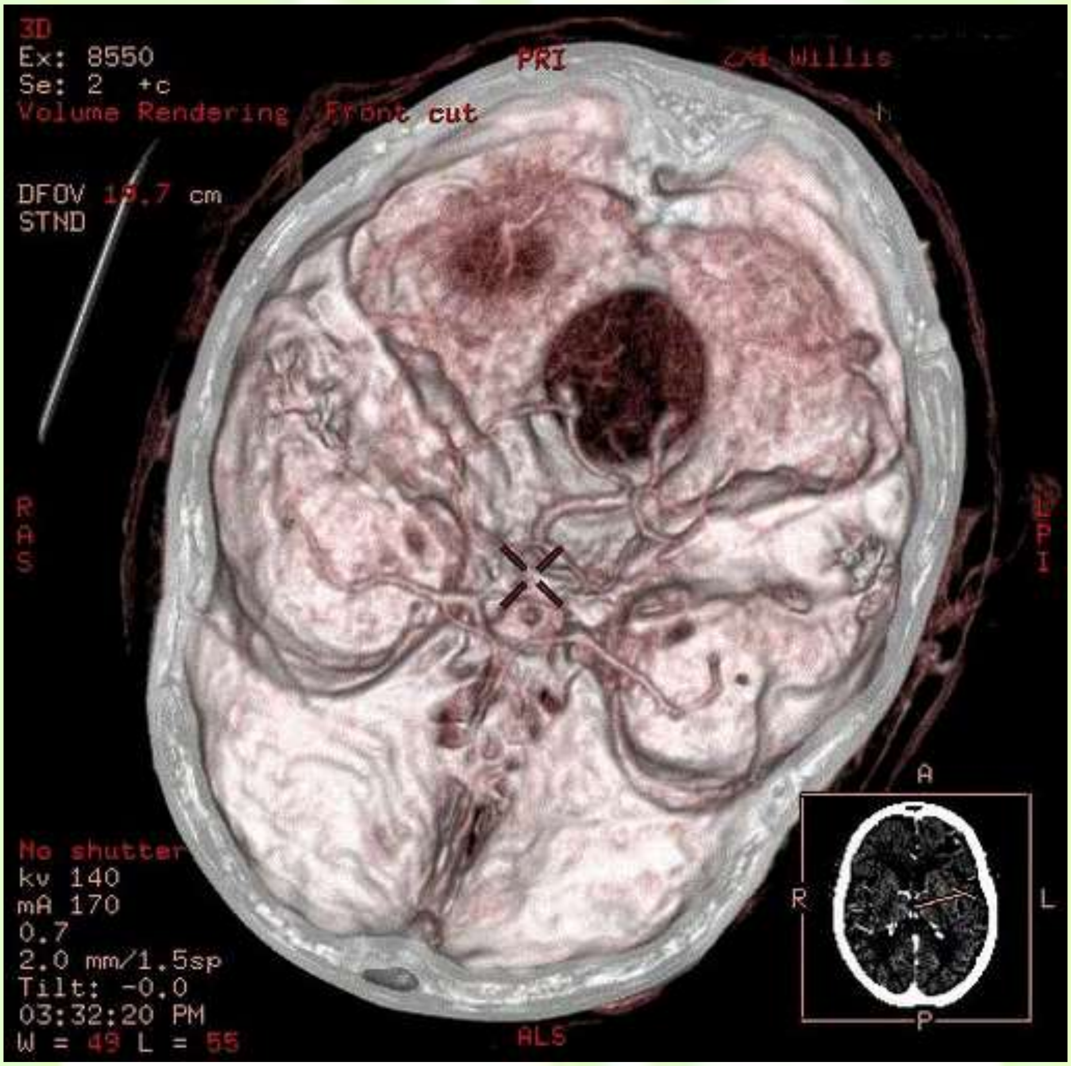

NAME *:* MRI
TYPE *:* BITMAP
BYTES PER PIXEL *:* 24
SIZE *:* 768 KB
DIMENSIONS *:* 512 x 512

D) BARBARA Image

NAME : BARBARA
TYPE : BITMAP
BYTES PER PIXEL : 24
SIZE : 192 KB
DIMENSIONS : 256 x 256

E) LENA Image

NAME : LENA
TYPE : BITMAP
BYTES PER PIXEL : 24
SIZE : 768 KB
DIMENSIONS : 512 x 512

A) LENA_GRAY Image

NAME : LENA_GRAY
TYPE : BITMAP
BYTES PER PIXEL : 8
SIZE : 65 KB
DIMENSIONS : 256 x 256

B) BARBARA_GRAY Image

NAME : BARBARA_GRAY
TYPE : BITMAP
BYTES PER PIXEL : 8
SIZE : 65 KB
DIMENSIONS : 256 x 256

C) CAMARAMAN Image

NAME : CAMARAMAN
TYPE : BITMAP
BYTES PER PIXEL : 8
SIZE : 65 KB
DIMENSIONS : 256 x 256

D) GOLDHILL Image

NAME : GOLDHILL
TYPE : BITMAP
BYTES PER PIXEL : 8
SIZE : 65 KB
DIMENSIONS : 256 x 256

E) PEPPERS_GRAY Image

NAME *:* PEPPERS_GRAY
TYPE *:* BITMAP
BYTES PER PIXEL *:* 8
SIZE *:* 65 KB
DIMENSIONS *:* 256 x 256

i. Appendix C. *JPEG Quantization Tables*

A) Luminance Quantization Table

16	11	10	16	24	40	51	61
12	12	14	19	26	58	60	55
14	13	16	24	40	57	69	56
14	17	22	29	51	87	80	62
18	22	37	56	68	109	103	77
24	35	55	64	81	104	113	92
49	64	78	87	103	121	120	101
72	92	95	98	112	100	103	99

B) Chrominance Quantization Table

17	18	24	47	99	99	99	99
18	21	26	66	99	99	99	99
24	26	56	99	99	99	99	99
47	66	99	99	99	99	99	99
99	99	99	99	99	99	99	99
99	99	99	99	99	99	99	99
99	99	99	99	99	99	99	99
99	99	99	99	99	99	99	99

A) Daubechies Wavelet

Named after Ingrid Daubechies, the Daubechies wavelets are a family of orthogonal wavelets defining a discrete wavelet transform and characterized by a maximal number of vanishing moments for some given support. With each wavelet type of this class, there is a scaling function which generates an orthogonal multiresolution analysis.

In general the Daubechies wavelets are chosen to have the highest number *A* of vanishing moments, (this does not imply the best smoothness) for given support width $N=2A$, and among the 2^{A-1} possible solutions the one is chosen whose scaling filter has extremal phase. The wavelet transform is also easy to put into practice using the fast wavelet transform. Daubechies wavelets are widely used in solving a broad range of problems, e.g. self-similarity properties of a signal or fractal problems, signal discontinuities, etc.

The Daubechies wavelets are not defined in terms of the resulting scaling and wavelet functions; in fact, they are not possible to write down in closed form. The graphs below are generated using the cascade algorithm, a numeric technique consisting of simply inverse-transforming [1 0 0 0 0 ...] an appropriate number of times.

Wavelet and scaling function :

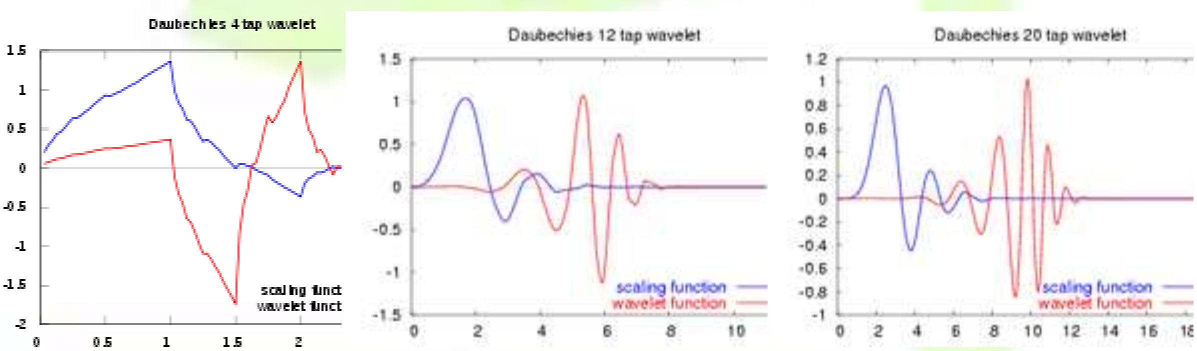

Amplitudes of the frequency spectra of the above functions :

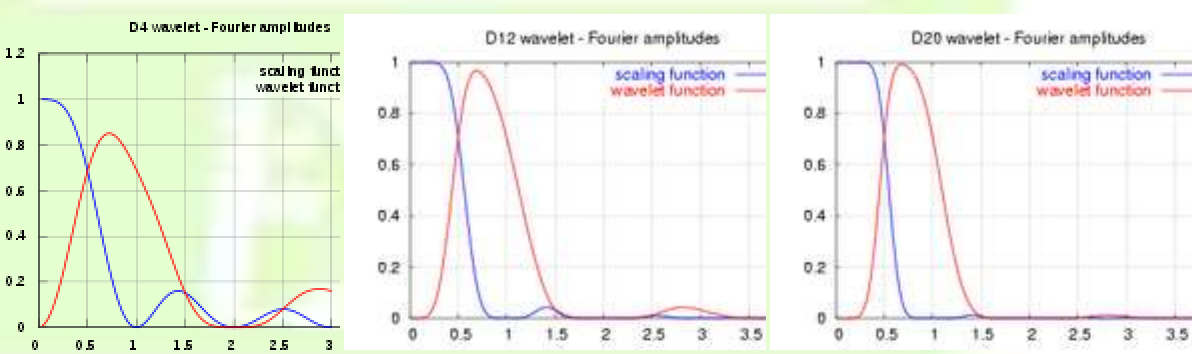

B) Orthogonal Wavelet

An orthogonal wavelet is a wavelet where the associated wavelet transform is orthogonal. That is the inverse wavelet transform is the adjoint of the wavelet transform. If this condition is weakened you may end up with biorthogonal wavelets.The scaling function is a refinable function. That is, it is a fractal functional equation, called the refinement equation:

$$\phi(x) = \sum_{k=0}^{N-1} a_k \phi(2x-k),$$

where the sequence $(a_0, \ldots, a_{N-1})$ of real numbers is called a scaling sequence or scaling mask. The wavelet proper is obtained by a similar linear combination,

$$\psi(x) = \sum_{k=0}^{M-1} b_k \phi(2x-k),$$

where the sequence $(b_0, \ldots, b_{M-1})$ of real numbers is called a wavelet sequence or wavelet mask. A necessary condition for the *orthogonality* of the wavelets is that the scaling sequence is orthogonal to any shifts of it by an even number of coefficients:

$$\sum_{n\in\mathbb{Z}} a_n a_{n+2m} = 2\delta_{m,0}$$

In this case there is the same number $M=N$ of coefficients in the scaling as in the wavelet sequence, the wavelet sequence can be determined as $b_n = (-1)^n a_{N-1-n}$. In some cases the opposite sign is chosen.

necessary condition for the existence of a solution to the refinement equation is that some power $(1+Z)^A$, $A>0$, divides the polynomial $a(Z) := a_0 + a_1 Z + \ldots + a_{N-1} Z^{N-1}$.The maximally possible power A is called polynomial approximation order (or pol. app. power) or number of vanishing moments. It describes the ability to represent polynomials up to degree $A-1$ with linear combinations of integer translates of the scaling function.

B) Biorthogonal Wavelet

A biorthogonal wavelet is a wavelet where the associated wavelet transform is invertible but not necessarily orthogonal. Designing biorthogonal wavelets allows more degrees of freedom than orthogonal wavelets. One additional degree of freedom is the possibility to construct symmetric wavelet functions.

In the biorthogonal case, there are two scaling functions $\phi, \tilde{\phi}$, which may generate different multiresolution analyses, and accordingly two different wavelet functions $\psi, \tilde{\psi}$ So the numbers *M* and *N* of coefficients in the scaling sequences $a, \tilde{a}$ may differ. The scaling sequences must satisfy the following biorthogonality condition

$$\sum_{n \in \mathbb{Z}} a_n \tilde{a}_{n+2m} = 2 \cdot \delta_{m,0}.$$

Then the wavelet sequences can be determined as $b_n = (-1)^n \tilde{a}_{M-1-n}$, $n = 0, \ldots, M-1$ and $\tilde{b}_n = (-1)^n a_{M-1-n}$, $n = 0, \ldots, N-1$

2-D	Two Dimensional
ADC	Analog to Digital Converter
AR	Augmented Reality
BPP	Bits Per Pixel
CAT	Computed Axial Tomography
CCD	Charge Coupled Device
CMOS	Complementary Metal Oxide Semiconductor
CR	Compression Ratio
DAC	Digital to Analog Converter
DCT	Discrete Cosine Transformation
DICOM	Digital Imaging and Communications in Medicine
DSP	Digital Signal Processing
DWT	Discrete Wavelet Transformation
EBCOT	Embedded Block Coding with Optimized Truncation
EOB	End Of Block
EZW	Embedded Zerotree Wavelet
GIF	Graphic Interchange Format
ICACCN	International Conference on Advanced Computing , Communications and Networks
JFIF	JPEG File Interchange Format
JPEG	Joint Photographic Experts Group
KB	Kilo Bytes
LPF	Low Pass Filter
MRI	Magnetic Resonance Imaging
MSE	Mean Square Error
PNG	Portable Network Graphics
PSNR	Picture Signal to Noise Ratio
RGB	Red Green Blue
RLE	Run Length Encoding

ROI	Region of Interest
SPIHT	Set Partitioning in Hierarchical Trees
TIFF	Tagged Image File Format
UACEE	Universal Association of Computers and Electronics Engineers

ii. Works Cited

[1] Paras Prateek Bhatnagar, Preeti Kumari, Paramjeet Singh Jamwal, Nisha Rajani and Akhilendra Singh Yadav,"Unit Embedded Zerotree Wavelet Coding", International Conference on Advanced Computing , Communication and Networks, UACEE, 2013, pp 167-171.

[2] W.B. Pennenbaker and J.L. Mitchell, "JPEG Still Image Data Compression Standard," New York, Van Nostrand Reinhold, 1993.

[3] G. Wallace, "The JPEG still picture compression standard," *Communications of the ACM*, Vol. 34, pp. 30-44, 1991.

[4] Shoji Hirano , Shusaku Tsumoto, "Rough representation of a region of interest in medical images", International Journal of Approximate Reasoning, 40 (2005).pp 23–34.

[5] Jerome M. Shapiro, "Embedded image coding using zero trees of wavelet coefficients", IEEE Trans. Signal Process. 41 (12), (December 1993) 3445-3462.

[6] Daubechies, I. (1992), ten lectures on wavelets, CBMS-NSF conference series in applied mathematics. SIAM Ed.

[7] Module 5, "Embedded Wavelet Coding", Lesson 13, "Wavelet Approach", Version 2, ECE IIT, Kharagpur.

[8] C. Valens, "EZW Encoding Tutorial" [Online].Available: http://polyvalens.pagesperso-orange.fr/clemens/download/ezwe_26022004.pdf

[9] Vinay U. Kale, Shirish M. Deshmukh, "Visually Improved Image Compression by Combining EZW Encoding with Texture Modeling using Huffman Encoder", IJCSI International Journal of Computer Science Issues, Vol. 7, Issue 3, No 11, May 2010,p. 28-38.

[10] Yushin Cho and William A. Pearlman, "QUANTIFYING THE CODING POWER OF ZEROTREES OFWAVELET COEFFICIENTS: A DEGREE-K ZEROTREE MODEL", Rensselaer Polytechnic Institute, Troy, NY, USA.

[11] Xiangang Li, EZW MatLab Code [Online].Available: http://polyvalens.pagesperso-orange.fr/clemens/download/ezwmatlab2.zip.

[12] Janaki. R and Dr.Tamilarasi.A, "Still Image Compression by Combining EZW Encoding with Huffman Encoder", International Journal of Computer Applications (0975 – 8887), Volume 13– No.7, January 2011, p.1-7.

[13] Arian Munteanu, Jan Cornelis, Geert Van der Auwera and Paul Cristea, "Wavelet Image Compression—The Quadtree Coding Approach", IEEE TRANSACTIONS ON INFORMATION TECHNOLOGY IN BIOMEDICINE, VOL. 3, NO. 3, SEPTEMBER 1999,pp 176-185.

[14] C.-Y. Teng, D. L. Neuhoff, J. A. Storer, and M. Cohn, "Quadtree-guided wavelet image coding," in Proc. IEEE Data Compression Conf., 1996, pp. 406–415.

[15] G. J. Sullivan and R. L. Baker, "Efficient quadtree coding of images and F. Golchin and K. Paliwal, "Quadtree based classification with arithmetic and trellis coded quantization for subband image coding," in Proc. Int. Conf. ASSP, 1997, pp. 2921–2924.

[16] R. L. Joshi, V. J. Crump, and T. R. Fischer, "Image subband coding using arithmetic coded trellis coded quantization," IEEE Trans. Circuits yst. Video Technol., vol. 6, pp. 515–523, 1995.

SPECT & PET

NAGARAJU.B

- **Radionuclides** are unstable nuclei
- Having a neutron excess or deficit, are radioactive → 'decay' to become stable nuclei, with the emission of any combination of alpha, beta, and gamma radiation.

Production of radionuclides:

- **Natural radionuclides:** few, sufficiently long lived, e.g. uranium, radium, and radon.

- **Radionuclides in medical imaging** → produced artificially, in the following way

- Some radionucleids produced by additional neutron forced into a stable nucleus:
  - Nucleus has a neutron excess → unstable.
  - In a ***nuclear reactor***,
  - e.g. with **Molybdenum (Mo)**:

  $_{98}Mo + n \rightarrow {}_{99}Mo$

  - Same atomic number.
  - Mass number increased by 1.
  - Radionuclides produced by this process have same chemical properties and called "an isotope" .

- Radionuclides produced by additional proton forced into a stable nucleus → knocking out a neutron:
  - Nucleus has a *neutron deficit* → unstable.
  - In a ***cyclotron*** which accelerates positively charged ions: e.g. protons or alpha particles.
  - e.g. with **Boron (B)**:

  $${}_{11}B + p \rightarrow {}_{11}C + n$$

  - Atomic number increased by 1.
  - Same mass number.

Radioactive decay

- ***Nuclides with a neutron excess:***

  β - Decay

  • Neutron change into a proton & an electron → the electron is ejected from the nucleus with high energy **"-ve beta particle"**

  n → p + β -

  • For example, ***Iodine-131 (131I, Z= 53)*** → ***Xenon-131 (131Xe, Z= 54)***.

  • Same mass number.

  • Atomic number increased by 1 .

  •The daughter nucleus mostly produced with excess energy with immediate loss of energy with the emission of one or more **γ** photons.

- **Isomeric transition**: in this some radionucleids the gamma ray is not emitted until an appreciable time after the emission of beta particle.
- For ex: ^{99}Mo decays by emission of –ve beta particle, the daughter nucleus Tc remains in exited stable for variable length of time, it is said to be metastable and is written as ^{99m}Tc.
- Its decay to ground state , ^{99}Tc, is most often with emission of gamma ray of energy 140kev.

- ***Nuclides with a neutron deficit:***

β + Decay

• A proton change into a neutron and a positive electron → the latter is ejected from the nucleus with high energy **"+ve β particle"**.

p → n + β+

• For example,

Carbon-11 (11C, Z= 6)* → *Boron-11 (11B, Z= 5).

• Same Mass and charge.

• The atomic number decreased by 1 .

•The daughter nucleus, if excited → loses excess energy by the emission of gamma photons till reaches the ground state.

- **K-electron capture (EC)**

  • The nucleus capturing an extra-nuclear electron from the nearest (K) shell → increase its
  number of neutrons relative to the number of protons.

  p + e → n

  • Same Mass and charge.

  The atomic number decreased by 1 .

  •The daughter nuclide will emit **characteristic X-rays** when the hole so created in the Kshell is filled by an electron from an outer shell ± **gamma rays** if still excited.

  • **Iodine-123 (123I)** decays by electron capture and emits **160 keV gamma** and **28 keV Xrays**, but **no β-particles**.

Radiopharmaceuticals

- Radiopharmaceuticals are the radioactive substances or radioactive drugs for diagnostic or therapeutic interventions.it contains
- a radioactive isotope that can be injected safely into the body, and
- a carrier molecule which delivers the isotope to the area to be treated or examined.
- Isotope during its conversion to stable forms emits radiation.

SPECT

- Single-photon emission computed tomography (SPECT) provides three-dimensional (3D) image information about the distribution of a radiopharmaceutical injected into the patient for diagnostic purposes.
- By combining conventional scintigraphic and computed tomographic methods, SPECT images present 3D functional information about the patient in more detail and higher contrast than found in planar scintigrams.

- A typical SPECT system consists of one or more scintillation cameras that acquire multiple two-dimensional planar projection images around the patient. The projection data are reconstructed into 3D images. The collimator of the scintillation camera has substantial effects on the spatial resolution and detection efficiency of the SPECT system.
- Physical factors such as photon attenuation and scatter affect the quantitative accuracy and quality of SPECT images, and various methods have been developed to compensate for these image-degrading effects.

- SPECT studies use standard radionuclides (eg, technetium-99m or iodine-123) and simpler imaging instrumentation. These standard radionuclides commonly emit gamma-ray photons with energies that are much lower than 511 keV. A typical example is Tc-99m, which emits 140 keV photons.
- An exception is the widely used myocardial agent, thallium-201, whose decay to mercury-201 results in the emission of characteristic mercury x rays with an average energy of about 72 keV.

In a typical conventional scintigraphy system which is used in SPECT. A given radioisotope-labeled pharmaceutical is injected into the patient.

Depending on the biodistribution properties of the pharmaceutical, the radioactivity is distributed in specific organs and normal or abnormal tissues.

Gamma-ray photons emitted from the radiopharmaceutical interact with matter inside the patient’s body. Those photons that exit the patient’s body and pass through the holes of a collimator are detected by a position-sensitive detector.

- Typically a scintillation (or Anger) camera mounted on a rotating gantry. A typical large field-of-view scintillation camera consists of a 0.95-cm-thick, 40-cm-collimeter sodium iodide crystal and an array of photomultiplier tubes at its back. The detected photons are transformed into visible light (ie, scintillations), which is converted into electrical signals by the photomultiplier tubes.
- The magnitudes of the electrical signals are proportional to the energies of the photons. A pulse height analyzer evaluates the energies of the detected photons and accepts only those that fall within a preset energy window, which is centered at the energy peak of the primary photons; thus, scattered photons and their adversive effects are rejected.

- The effectiveness of this scatter rejection depends on the energy resolution of the detector and the width of the energy window. Finally, a two-dimensional(2D) projection image of the three-dimensional (3D) radioactivity distribution is formed from the registered photon counts .

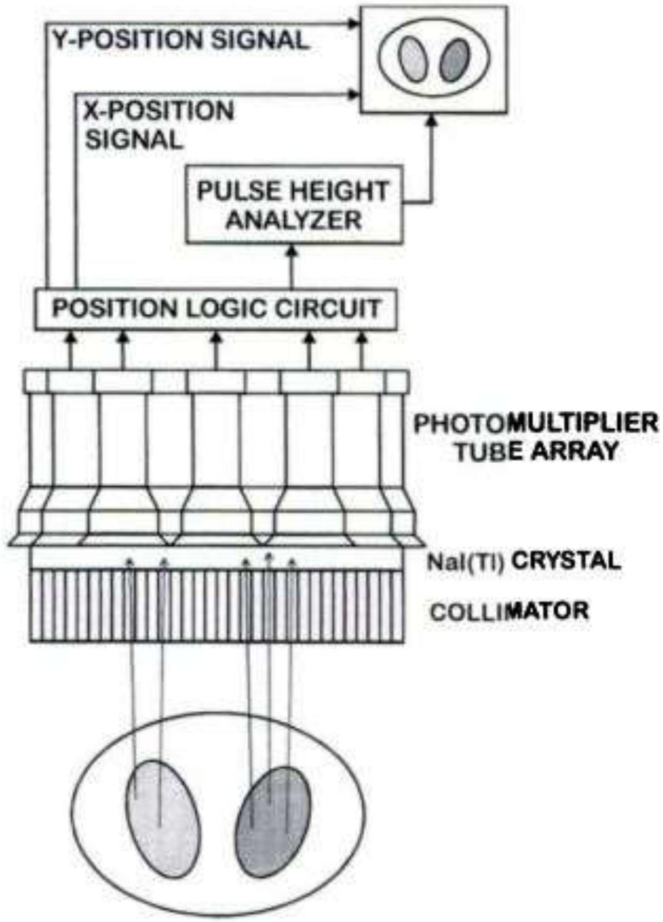

Figure 1. Diagram of the components of a typical conventional scintigraphy system.

PHYSICAL AND INSTRUMENTATION **FACTORS** THAT AFFECT SPECT IM**AGES**

- A number of factors substantially affect the quality and quantitative accuracy of SPECT images.
- They include physical factors, which are related to the interaction of photons emitted from the radiopharmaceuticals with matter inside the patient, and instrumentation factors, which are related to the SPECT imaging system.
- For photon energies commonly used in scintigraphy and SPECT are photoelectric and Compton scatter are the major interactions of radiation with matter.

- In a photoelectric interaction, the photon is totally absorbed by an atom. In a Compton scatter interaction, the photon changes its direction of travel, with partial loss of its original energy.

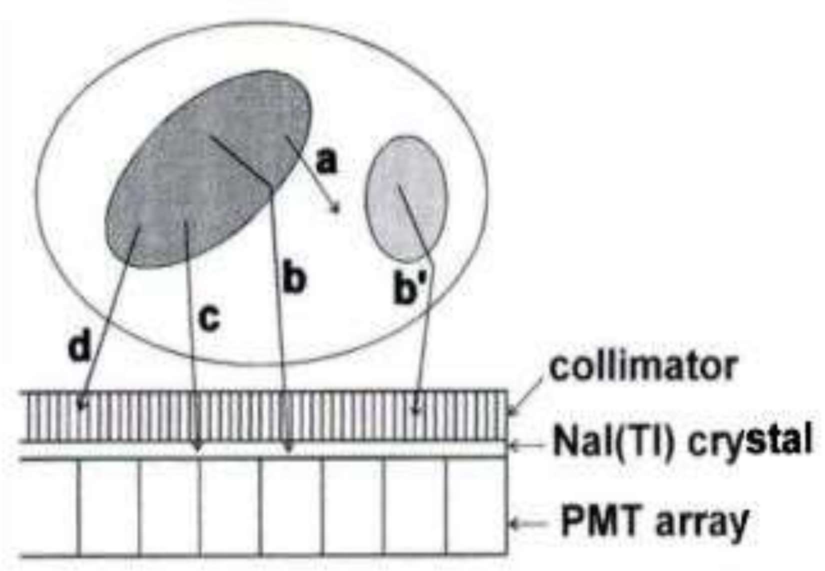

- Photon attenuation can be defined as the reduction of the number of primary photons that pass through a given thickness of material. Photon attenuation is caused by photoelectric and Compton scatter interactions in the material.
- The amount of attenuation depends on the incident photon energy and on the thickness and attenuation coefficient of the material. For example, the 140-keV photons from Tc-99m lose half of their original number in about 4.5 cm of water or soft tissue. As a result, photon attenuation substantially affects the quantitative accuracy of scintigraphic and SPECT images.

- Image reconstruction is done from the data acquired.
- There are the two reconstruction algorithma used in SPECT.
  - FILTERED BACK PROJECTION
  - ITERATIVE RECONSTRUCTION

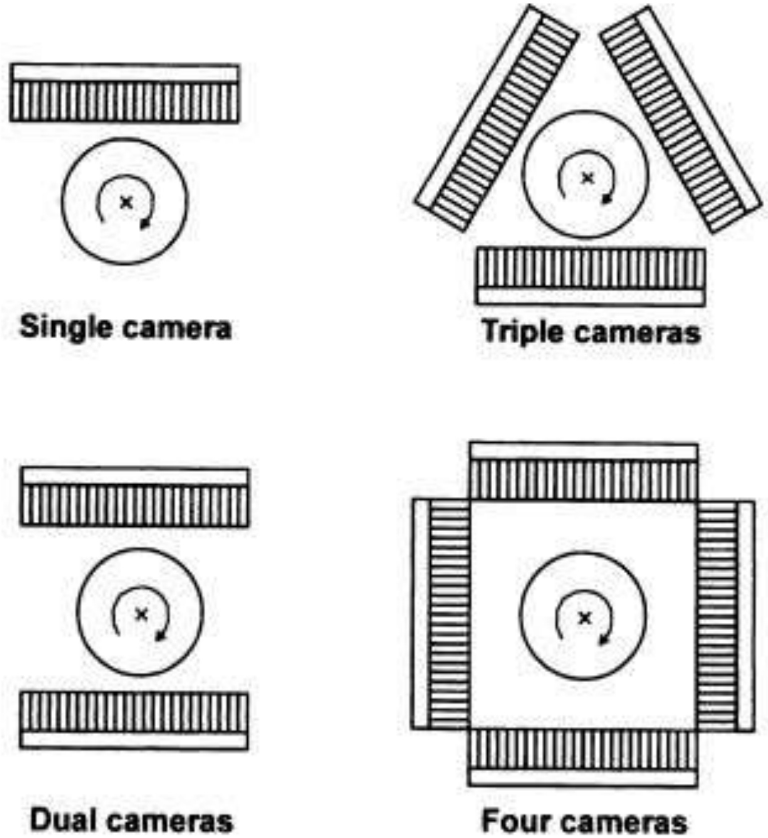

Figure 3. Diagrams show typical configurations of commercial SPECT imaging systems. The increased number of scintillation cameras around the patient results in increased detection efficiency or improved spatial resolution.

Radionuclides Commonly Used in Scintigraphy and SPECT

Radionuclide	Half-life	Energies of Primary Photons (keV)
Technetium-99m	6 h	140
Thallium-201	73 h	~72
Gallium-67	3.3 d	88, 185, 300
Iodine-131	8.04 d	365
Iodine-123	13.2 h	159
Xenon-127	36.4 d	172, 203, 375
Xenon-133	5.25 d	81, 161

Common clinical applications

Study	Radioisotope	Emission energy (keV)	Half-life	Radiopharmaceutical
Bone scan	technetium-99m	140	6 hours	Phosphonates / Bisphosphonates
Myocardial perfusion scan	technetium-99m	140	6 hours	tetrofosmin; Sestamibi
Sestamibi parathyroid scan	technetium-99m	140	6 hours	Sestamibi
Brain scan	technetium-99m	140	6 hours	HMPAO; ECD
Neuroendocrine or neurological tumor scan	iodine-123 or iodine-131	159	13 hours or 8 days	MIBG
White cell scan	indium-111 & technetium-99m	171 & 245	67 hours	*in vitro* labelled leucocytes

PRINCIPLE OF PET

- The concept of PET is to radiolabel a bio-compound, inject it into the patient, and then measure its bio-distribution as a function of time to determine physiologic quantities associated with the biocompound.
- All PET compounds are radiolabeled with positron-emitting radionuclides.
- These radionuclides have decay characteristics that enable localization in the body.
- A positron is emitted from the nucleus, travels a short distance, and annihilates with its antiparticle (an electron), which results in two 5 I l-keV photons traveling in opposite directions.
- After both photons are detected, the activity is localized somewhere along the line defined by the two detectors.

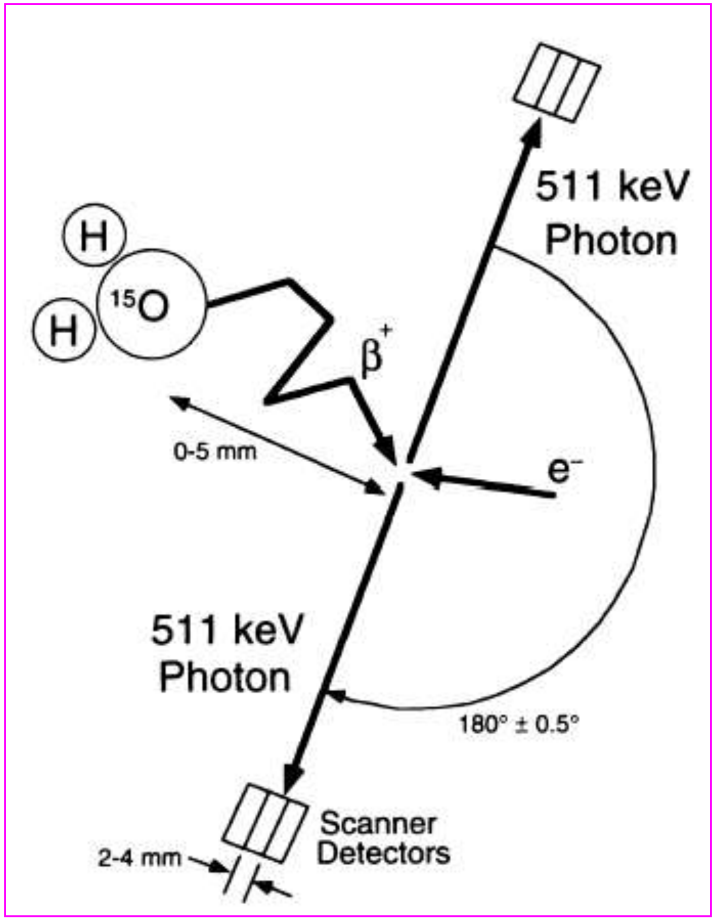
511 keV
Photon
H
15O
H
β+
0-5 mm
e-
511 keV
Photon
180° ± 0.5°
Scanner
Detectors
2-4 mm

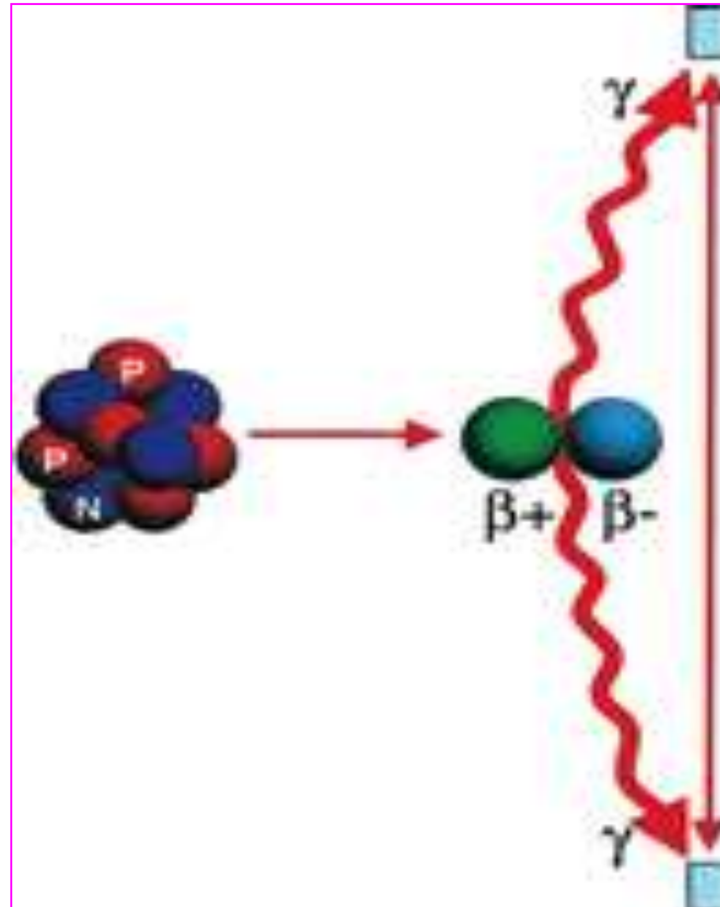
γ
P
P
N
β+
β-
γ

A PET study consists of

- producing radiotracers
- Synthesizing radiopharmaceuticals from the tracers
- administering the radiopharmaceutical to a patient
- measuring the resulting radioactivity distribution in an organ of interest
- interpreting activity distribution as a function of physiologic parameters.

PRODUCTION OF RADIONUCLIDE

- PET radionuclides are positron emitters.
- There are 5 convenient nuclides-

	HALF LIFE (min)
Rubidium- 82	1.23
Fluorine – 18	109
Oxygen- 15	2
Nitrogen- 13	10
Carbon- 11	20

Commonly produced isotopes : “F O N C”

SYNTHESIS OF F-18 &FDG

- Over 500 PET compounds have been synthesized since 1970.
- Natural substrates such as amino acids, analogues ,fluorinated glucose &drugs.
- MC used is a glucose analogue, 2-[F18]fluoro-2-deoxy-D-glucose (FDG).

Why is 18 F the most used positron emitter?

- 18F is a small atom.
- its addition to a molecule does not deform it to the point where it is not recognized by the body anymore
- has a half-life of 109 minutes.
- This is long enough to perform a complicated chemistry (labelling) , and to allow transport over some distance.
- It is also not long enough to keep the radiation burden to patient low

USES

Fluorodeoxyglucose

[18F]-labeled 2-deoxyglucose (FDG) is used in neurology, cardiology and oncology to study glucose metabolism. FDG is potentially useful in differentiating benign from malignant forms of lesions because of the high metabolic activity of many types of aggressive tumors.

Oxygen

[15O]-labeled water is used to evaluate myocardial oxygen consumption and oxygen extraction fraction. It can also be used to measure tumor necrosis.

- **Ammonia**
  [13N]-labeled ammonia can be used to measure blood flow.

- **Leucine**
  [11C]-labeled methionine and leucine can be used to evaluate amino acid uptake and protein synthesis, providing an indicator of tumor viability.

- **Fluorine Ion**
  Radiolabeled fluorine ion [18F-] was once a standard agent for clinical bone scanning.

Principle of metabolic imaging with FDG

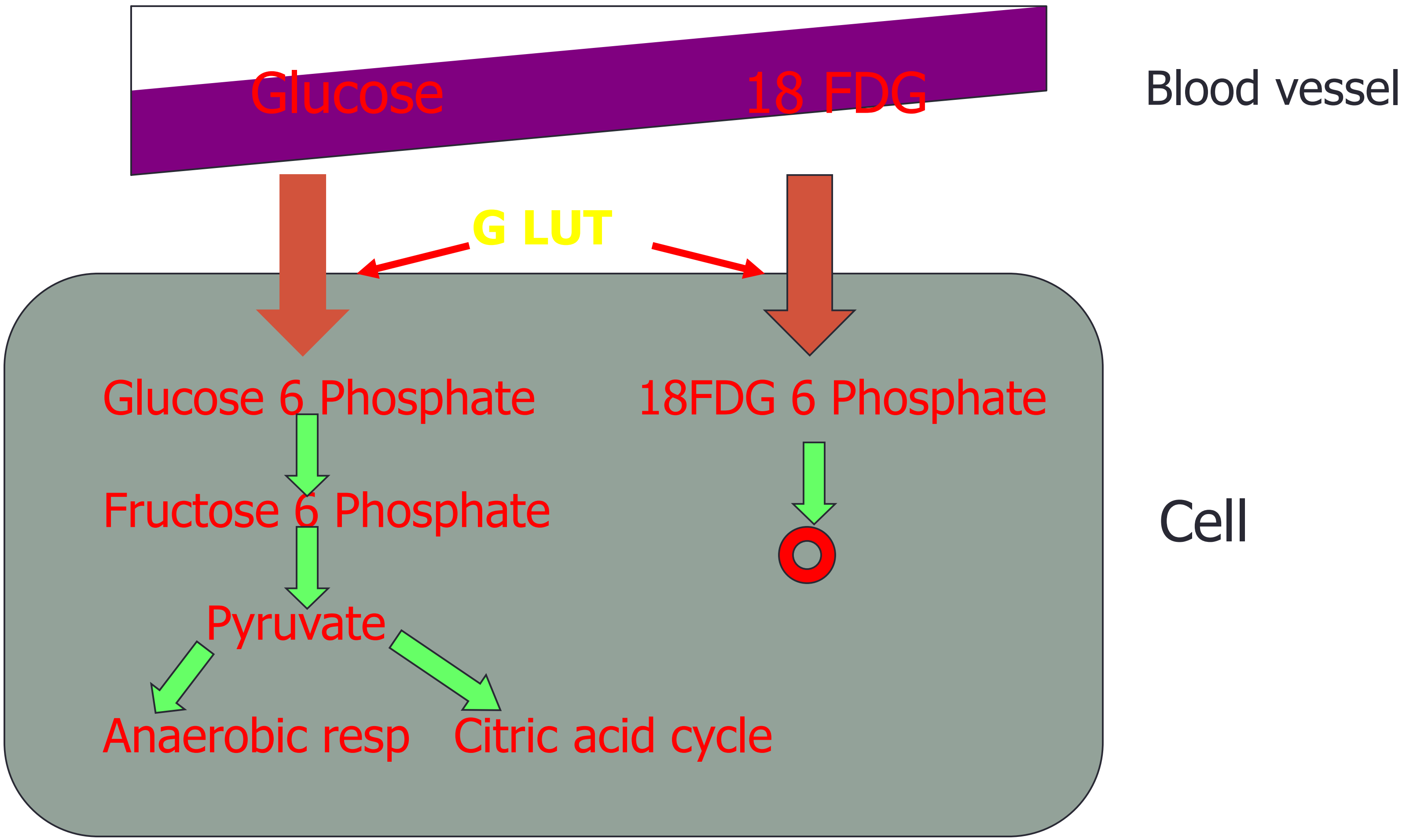

- A positron emission tomography (PET) scanner is a large machine with a round, doughnut shaped hole in the middle
- Within this machine are multiple rings of detectors that record the emission of energy from the radiotracer in our body.
- A nearby computer aids in creating the images from the data obtained by the camera or scanner.

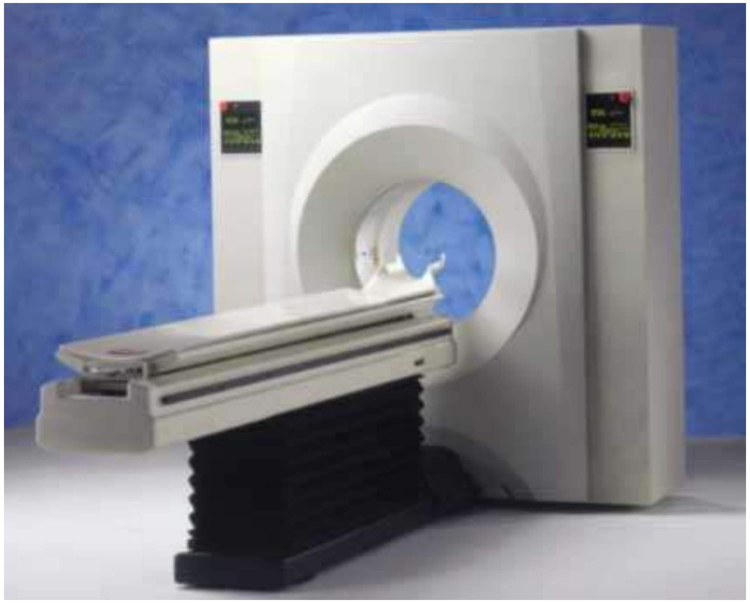

SCANNER DESIGN….

- Detectors are 18-40 rings of crystals forming a cylindrical field of view about 15cm long that can acquire many slices of coincidence data
- PET scanners use crystals with higher density & higher Z numbers due to sensitivity
- Group of crystals is put together into a block
- Four PMT’s to each block of crystal
- Use “electronic collimation” to detect location of annihilation event

- Localizing the site of impact is achieved by measuring the light detected in each PMT
- Signal is then amplified
- System must be able to determine which signals come from paired 511keV photons and record the time of detection (timing discriminator)
- Coincidence circuit then examines signals to confirm it if it occurred with in the time window

CRYSTALS USED IN PET

- BaF_2 – Barium Flouride*(0.8ns)*
- BGO – Bismuth Germinate Oxide*(300ns)*
- LSO – Lutetium Orthosilicate*(40ns)*
- GSO – Gadolineum Orthosilicate*(60ns)*
- YLSO – Yttrium Lutetium Orthosilicate*(40ns)*

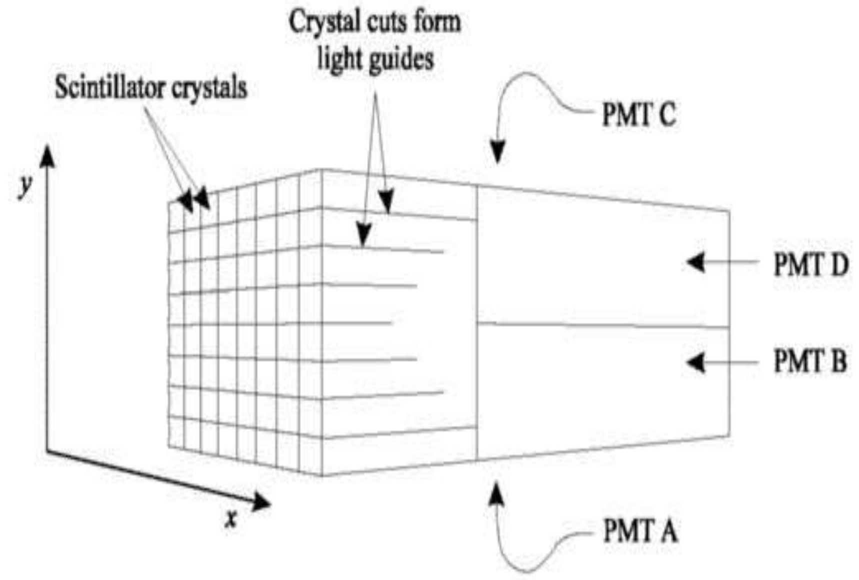

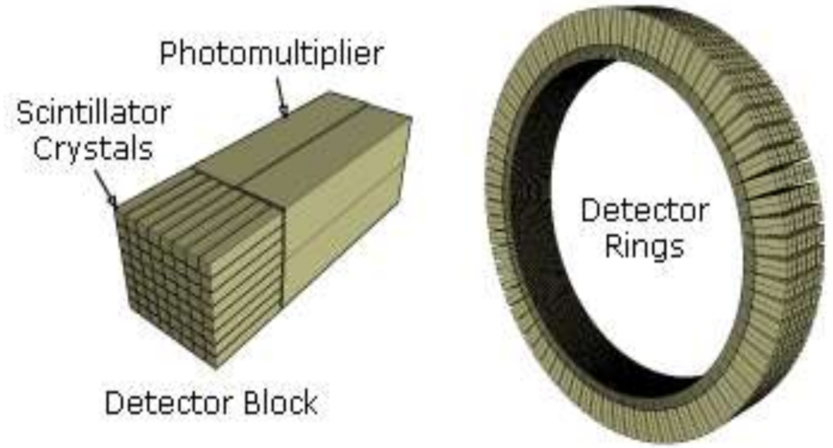

COINCIDENCE DETECTION

- Photons should arrive with in a certain time of one another
- A coincidence timing window allows detection of the PMT electrical signal from photon pair (4-12ns)
- If it falls within timing window it is registered as a true event
- When two different annihilation events are detected with in the timing window is known as “random event”

DATA ACQUSITION

- The detection of photon pairs by opposing crystals create one event .
- Millions of these event will be stored with in sinograms and used to reconstruct the image
- Spatial resolution is determined by the size of crystal and their separation and is typically 3-5mm
- PET is 50-100 times more sensitive and produces higher quality than a SPECT
- Reconstruction is similar to SPECT

RECONSTRUCTION

- PET reconstruction can be performed with a variety of algorithms
- Filtered back projection
- Iterative reconstruction(ordered subset reconstruction)

ATTENUATION CORRECTION

- Mathematical attenuation correction techniques may be used if tissue attenuation is the same at all areas within a transaxial slice .
- Measured attenuation may be performed by two methods:
  - Transmission scan using a radioactive source rotating it around the patient
  - CT scan to measure tissue density
- The ability to correct for attenuation improves quality and permits absolute quantification of radioactivity in the body

- **<u>Resolution in PET is determined by three factors:</u>**
  - distance the positron travels before it annihilates with an electron,
  - variation in angle between the two annihilation photons, and
  - physical size of the detectors.

- A positron will travel between 0.5 and 2 mm in tissue before annihilation, depending on its energy.

- Typical detector sizes are 1 -3 mm.

- The best possible resolution of a PET scanner is 1-2mm. Typical clinical scanners have a resolution of approximately 4-7 mm.

PET vs. CT & MRI

PET	CT and MRI
Shows extent of disease	Detects changes in body structure
Can help in monitoring treatment and shows it's effectiveness	Simply confirms the presence of a mass
Reveals disease earlier, can diagnose faster	
Can detect whether a mass is benign or malignant	
Can detect abnomalities before there is an anatomical change	

SAFETY ASPECTS OF PET

- PET has 511Kev gamma rays energy, that is 3 times of 140Kev gamma ray energy of Technitium99m
- Due to their high energy 16 times more lead is required to obtain the same stopping effect for 511Kev photons as compared to 140Kev photons

So Tungsten shielding is used for Positron emitting radionuclide.
It provides 1.4 times the shielding capability for the same thickness of Lead

CONTRA INDICATIONS

- Pregnancy
- Use of caffeine, tobacco, or alcohol in past 24hours before scan
- Using sedatives
- Using medicines that change metabolism ex: ***INSULIN*.**

PET-CT FUSION

- FDG PET is a strictly functional modality and lacks anatomic landmarks.
- Unless anatomic correlation is available to delineate normal structures, pathologic sites of FDG accumulation can easily be confused with normal physiologic uptake, leading to false-positive or false-negative findings.
- **Coregistration** of PET scans with CT using a combined PET-CT scanner improves the overall sensitivity and specificity of information provided by PET or CT alone .
- advantage is ability to correlate findings at two complementary imaging modalities in a comprehensive examination. Hence, PET-CT provides more **precise anatomic definition for both the physiologic and pathologic uptake seen at FDG PET**

Distance betwn pet and ct scanner

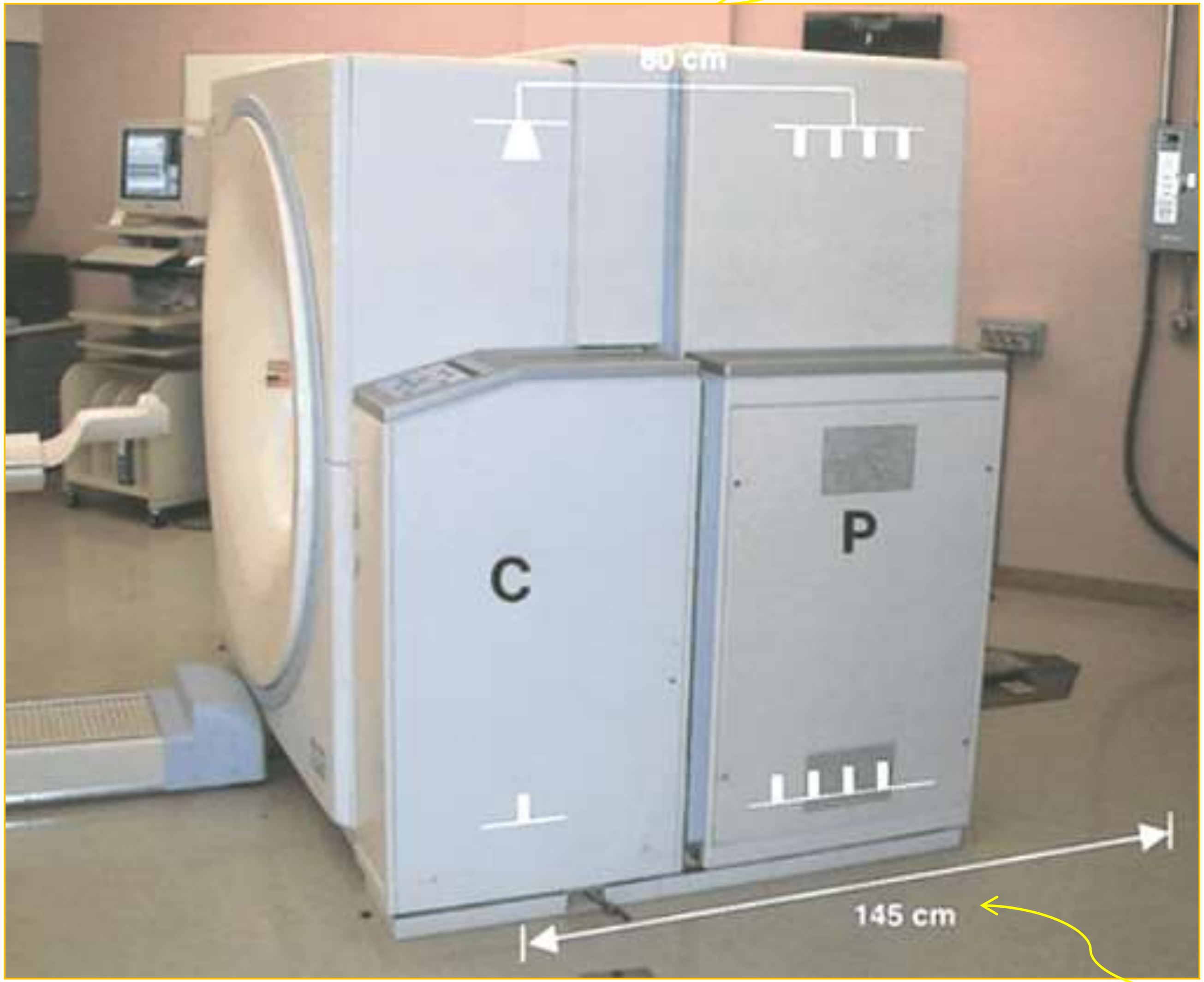

Max coverage during combined study

SCANNING TECHNIQUE

- Nil orally for approximately 4–6 hours
- avoid caffeinated or alcoholic beverages but can have water during this period.
- blood glucose level of less than 150 mg/dL is desirable.
- Avoid strenuous activity to avoid physiologic muscle uptake of FDG
- water-soluble iodinated contrast media orally for bowel opacification **except for head and neck study**.
- 10 mCi injected intravenously
- Patient activity and speech are limited for 20 minutes immediately following injection
- Pet study is started 60 mins after injection.

CT TECHNIQUE

- Contrast material–enhanced helical CT is performed following injection of **125 m**L of a contrast medium at a rate of 4 mL/sec by using a power injector .
- Whole-body PET-CT study scanning begins at the level of the skull base and extends caudally to the level of the symphysis pubis.

PET TECHNIQUE

- The PET scanner is located behind the CT scanner and housed in the same extended-length gantry. PET is performed following the CT study without moving the patient in the caudocranial direction, starting at the thighs to limit artifacts from the FDG metabolite excretion into the urinary system

Typical scout image obtained during an FDG PET-CT study. The blue-purple rectangle represents CT coverage during the study, and each overlapping green rectangle represents PET coverage.

INTERPRETATION OF IMAGES

- PET provides images of quantitative uptake of the radionuclide injected that can give the concentration of radiotracer activity in kilobecquerels per milliliter .

- Methods for assessment of radiotracer uptake –
  - visual inspection
  - **standardized uptake value (SUV)**
  - glucose metabolic rate

LIMITATIONS AND ARTIFACTS OF PET-CT

- 1.Patient motion may cause confusion as to the correct position of the origin of the detected photon.
- Patient motion is minimized by –
  - carefully instructing patients not to move during the study;
  - placing them in a comfortable position before the start of the study;
  - ensuring that they are not taking diuretics, which may otherwise require them to evacuate the bladder during the study;
  - having patients empty their bladder before the start of the study or catheterizing the bladder.

ADVANTAGES OF PET-CT

1. helpful in accurate localization of small areas of increased radiotracer activity that would have been difficult or not possible to localize on PET images alone .
2. helps in distinguishing structures that normally show high metabolic activity from those with abnormally increased activity.
3. PET-CT combines the advantages of the excellent functional information provided by PET and the superb spatial and contrast resolution of CT
4. Finally, attenuation correction for quantitative or semi quantitative assessment of data is possible by using the CT data,

PET/MRI: TECHNICAL EVOLUTION

- The idea to combine PET and MRI arose as early as the mid 1990s, even before PET/CT was introduced.

- The PET/MRI combination requires 3 risky technologic steps that modify state-of-the-art PET and MRI.
    1. First, the photomultiplier technology must be replaced with magnetic field–insensitive photodiodes .
    2. Second, compact PET detectors must be constructed so that it shouldn't interfere with the field gradients or MR radiofrequency.
    3. Finally, the MRI scanner must be adapted to accommodate the PET detectors and to allow simultaneous data acquisition without mutual interference.

Scanner Design

- Based on the technologic challenges to combine PET and MRI into a single gantry, Philips and Siemens proposed 2 fundamentally different prototype PET/MRI designs.
- In the **Siemens prototypes** include 4 dedicated brain PET scanners that fit into a standard 3-T clinical MRI scanner.
- The PET/MRI system, together with a dedicated radiofrequency head coil, allows simultaneous PET/MRI data acquisition of the human brain or body extremities.
- **Philips** developed a PET/MRI design in which the gantries are approximately 2.5 m apart but share a common patient handling system. This implementation does not allow for simultaneous data acquisition and, therefore, results in longer examination times.

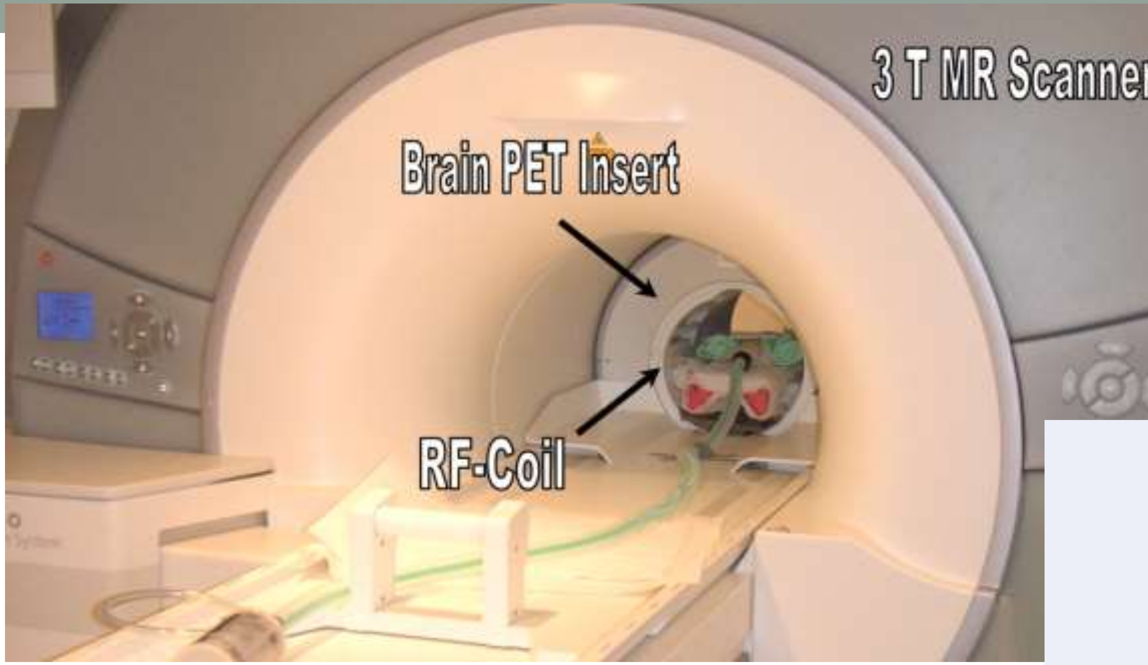
3 T MR Scanner
Brain PET Insert
RF-Coil

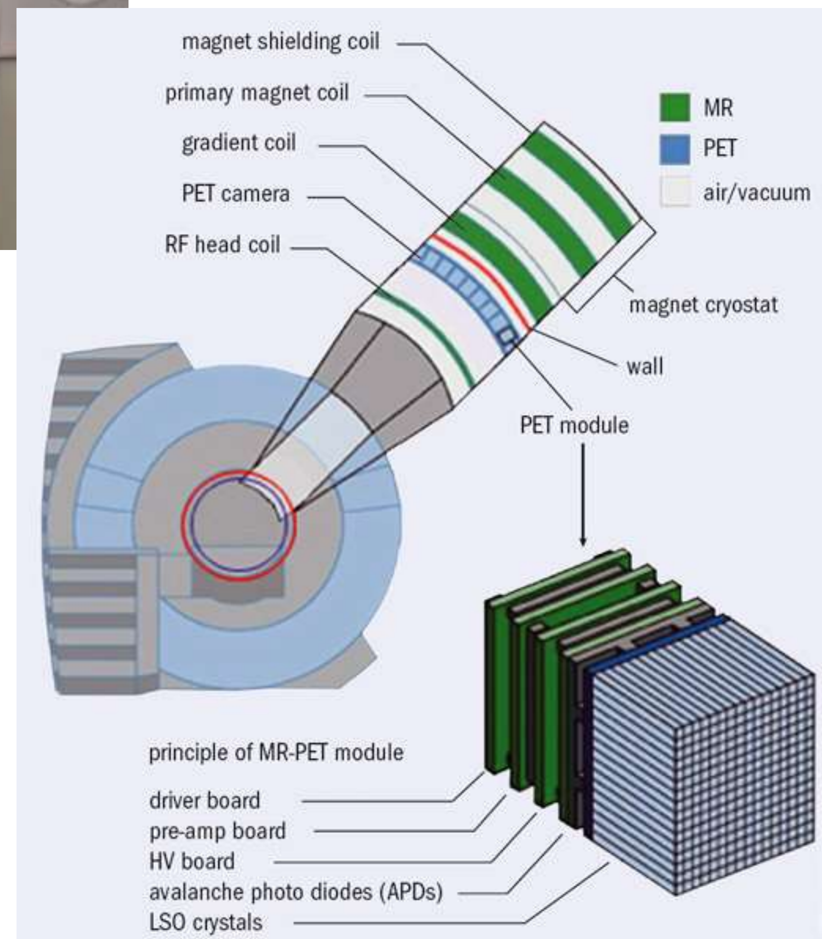
magnet shielding coil
primary magnet coil
gradient coil
PET camera
RF head coil
MR
PET
air/vacuum
magnet cryostat
wall
PET module
principle of MR-PET module
driver board
pre-amp board
HV board
avalanche photo diodes (APDs)
LSO crystals

CLINICAL POTENTIAL OF PET/MRI

- It is reasonable to expect that brain PET/MRI will provide new insights in the field of neuroscience and neurologic disorders, such as neuro degeneration, brain ischemia, neuro oncologyor seizures .
- It is feasible with current prototypes and future-generation systems to simultaneously study brain function, metabolism, oxygen consumption, and perfusion.
- In oncology, an accurate spatial match between PET and MRI data is mandatory for both radiation therapy planning and biopsy guidance.
- Combining PET with cardiac MRI may enable detection and differentiation of vulnerable plaques and diseased myocardium.

Advantage of PET/MRI over PET/CT

1. is not associated with significant radiation exposure
2. has a much higher soft tissue contrast.
3. MRI allows for additional techniques - such as angiography, functional MRI ,diffusion ,spectroscopy and perfusion techniques within one single examination.

PHYSIOLOGIC VERSES PATHOLOGIC FDG UPTAKE

- There are several sites of normal physiologic accumulation of FDG. FDG accumulation is most intense in the **cerebral cortex, basal ganglia, thalamus, and cerebellum.** The myocardium expresses insulin-sensitive glucose transporters, which facilitate the transport of glucose into muscle. A recent meal often causes intense myocardial FDG uptake because of the associated elevated serum insulin levels

- Because FDG appears in the glomerular filtrate and, unlike glucose, is not reabsorbed in the tubules, intense FDG activity is seen in the intrarenal collecting systems, ureters, and bladder

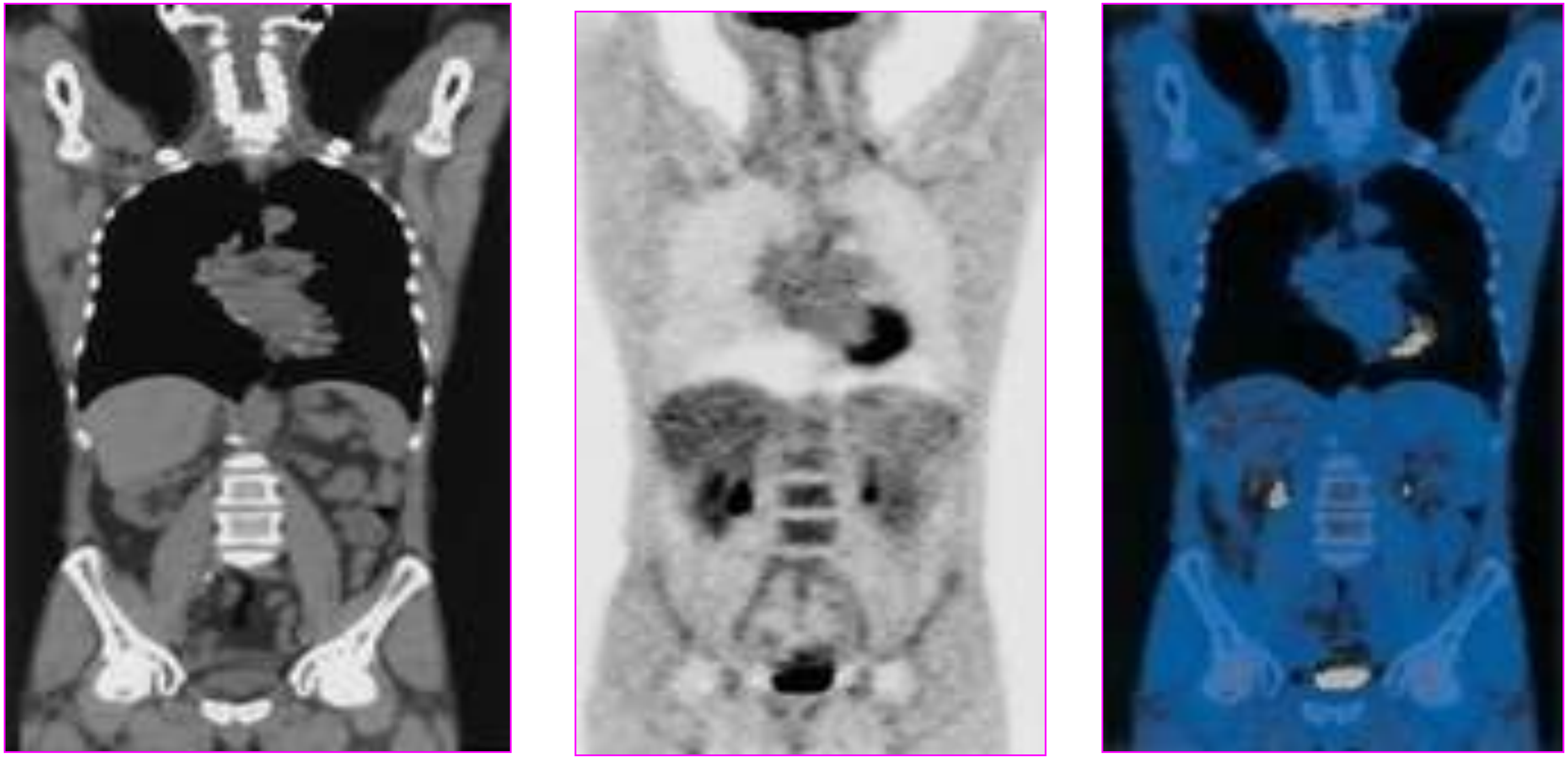

Physiologic FDG uptake

- **Some clinical applications where PET used:**

- **The Role of PET/CT in Lymphoma**
- Assess response to therapy/residual disease
- Identify recurrent disease
- Initial diagnosis and staging
- Identify suitable sites for biopsy
- Disease surveillance
- Radiotherapy planning

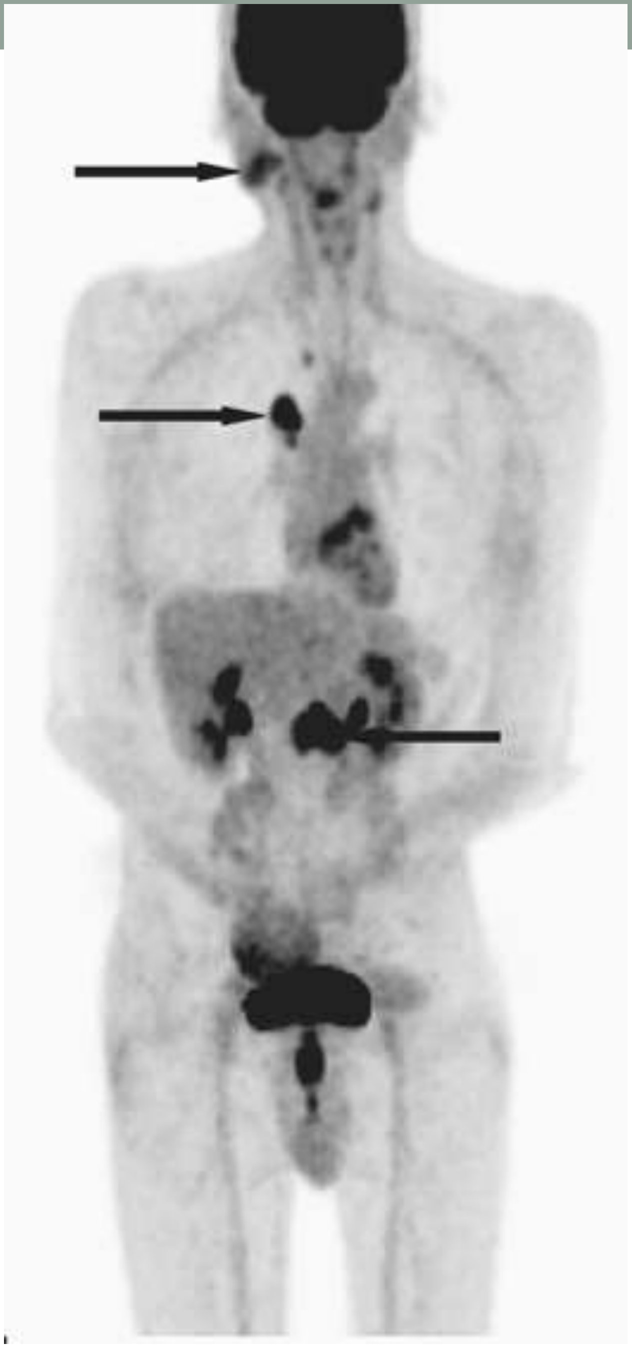

An example of stage 4 disease. NHL with disease in the mediastinum, neck, and abdomen

- **ASSESSMENT OF TREATMENT RESPONSE**

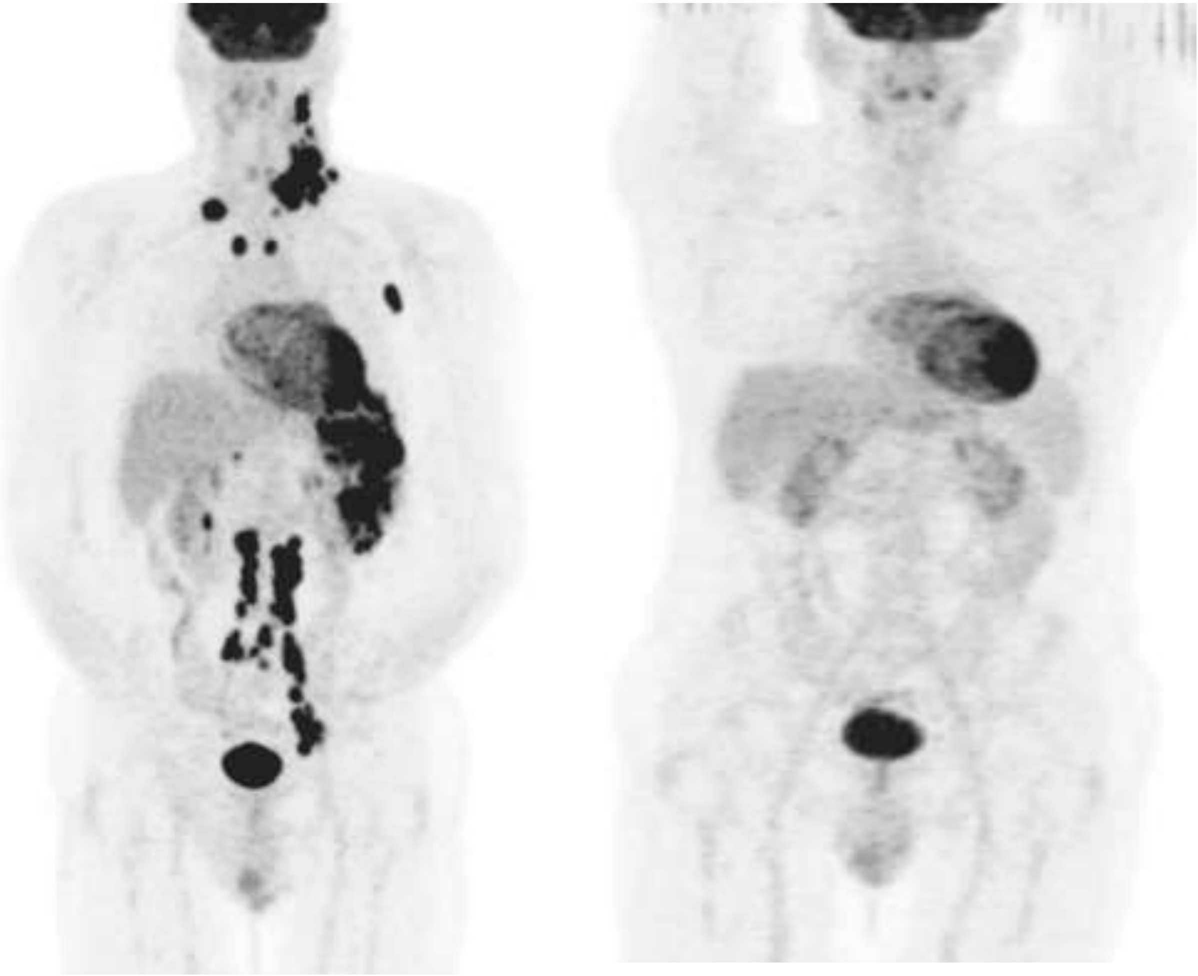

Pretherapy and post therapy studies showing a complete metabolic response to therapy.

NEURO-ONCOLOGY

- Tumor recurrence versus radiation necrosis
- Diagnosis
- Grading
- Monitoring response to therapy
- Radiotherapy planning
- Biopsy planning

SEIZURE FOCUS IDENTIFICATION

STROKE

DEMENTIAS

OTHER APPLICATIONS

- Brain injury- vascular, trauma
- Psychiatry- depression, schizophrenia,anxiety
- Movement disorders with 18F-dopa
- Miscellaneous- infection, substance abuse,eating disorders

Biopsy Planning

PET

CT

PET/CT

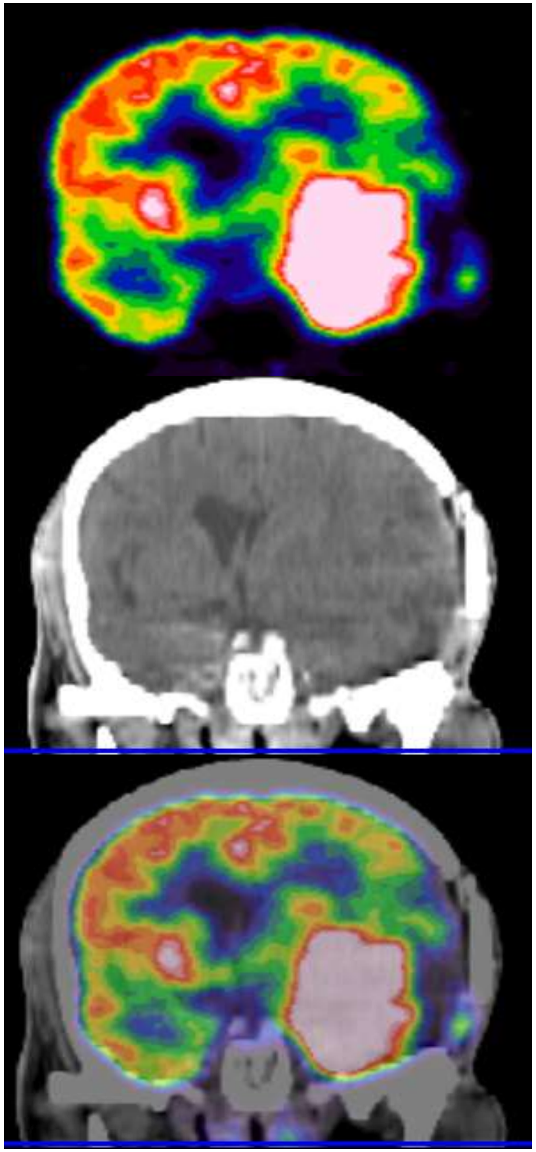

Localizing

the most

viable tissue

in the lesion

PET in Brain Disorders

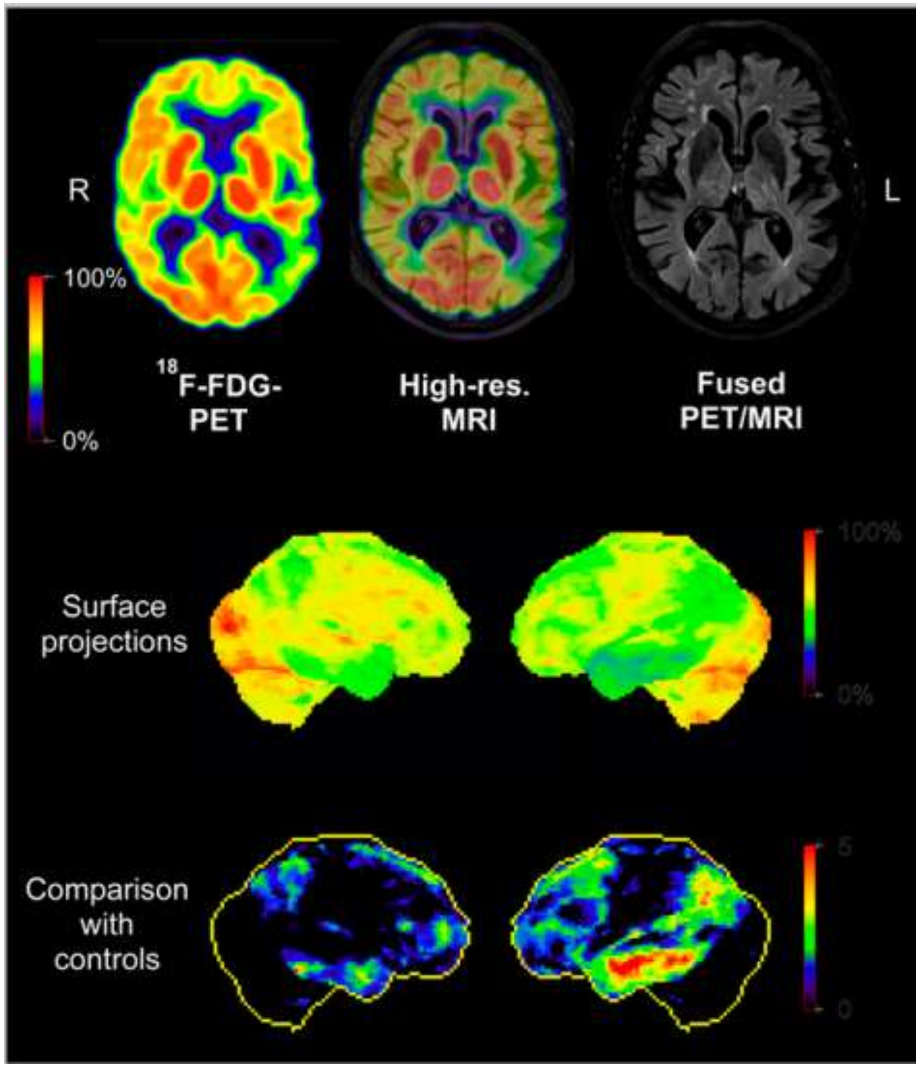

Simultaneous PET/MRI study in Alzheimer disease

Hypo metabolism in left temporal lobe secondary to epilepsy

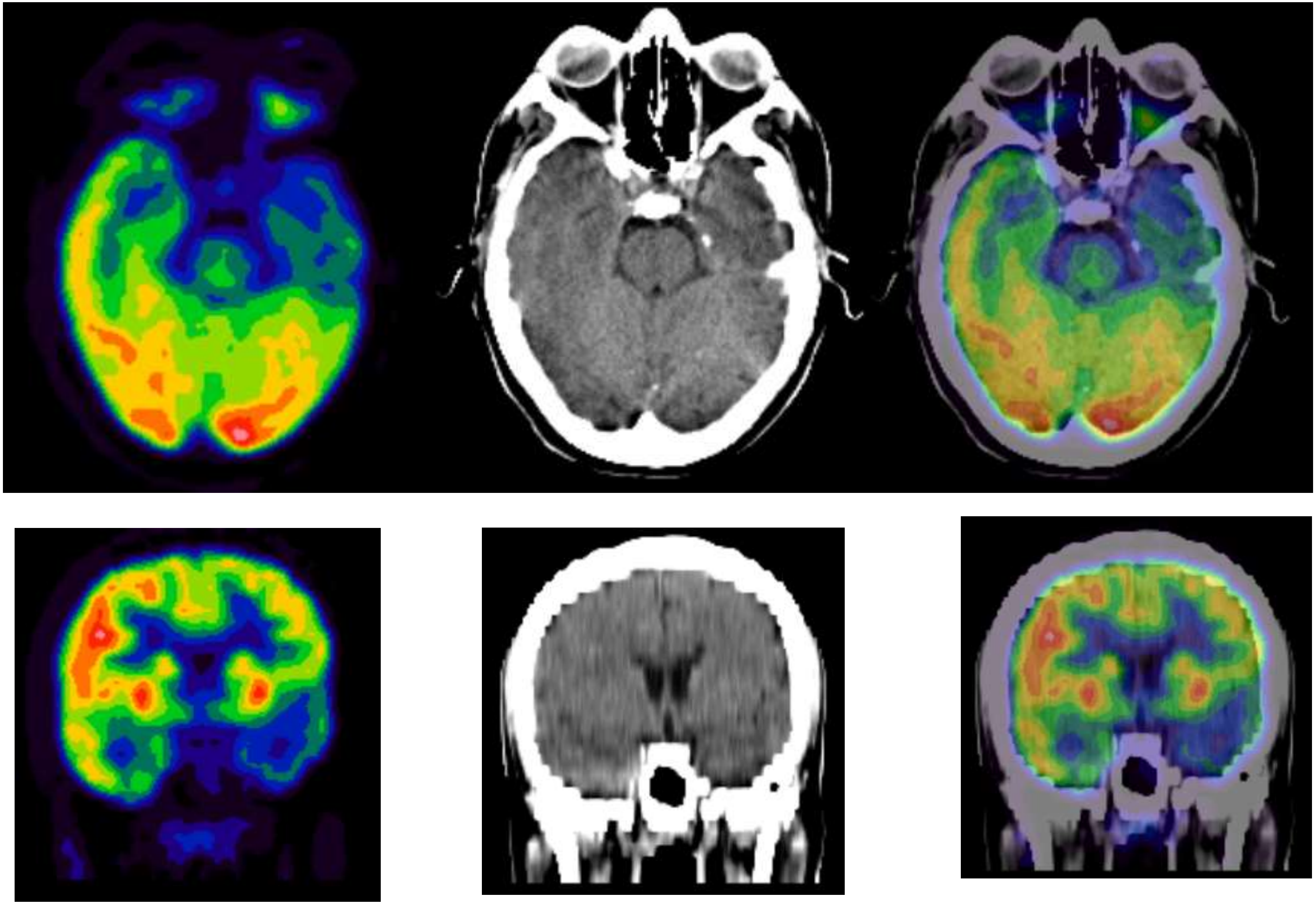

CARDIAC PET and PET CT IMAGING

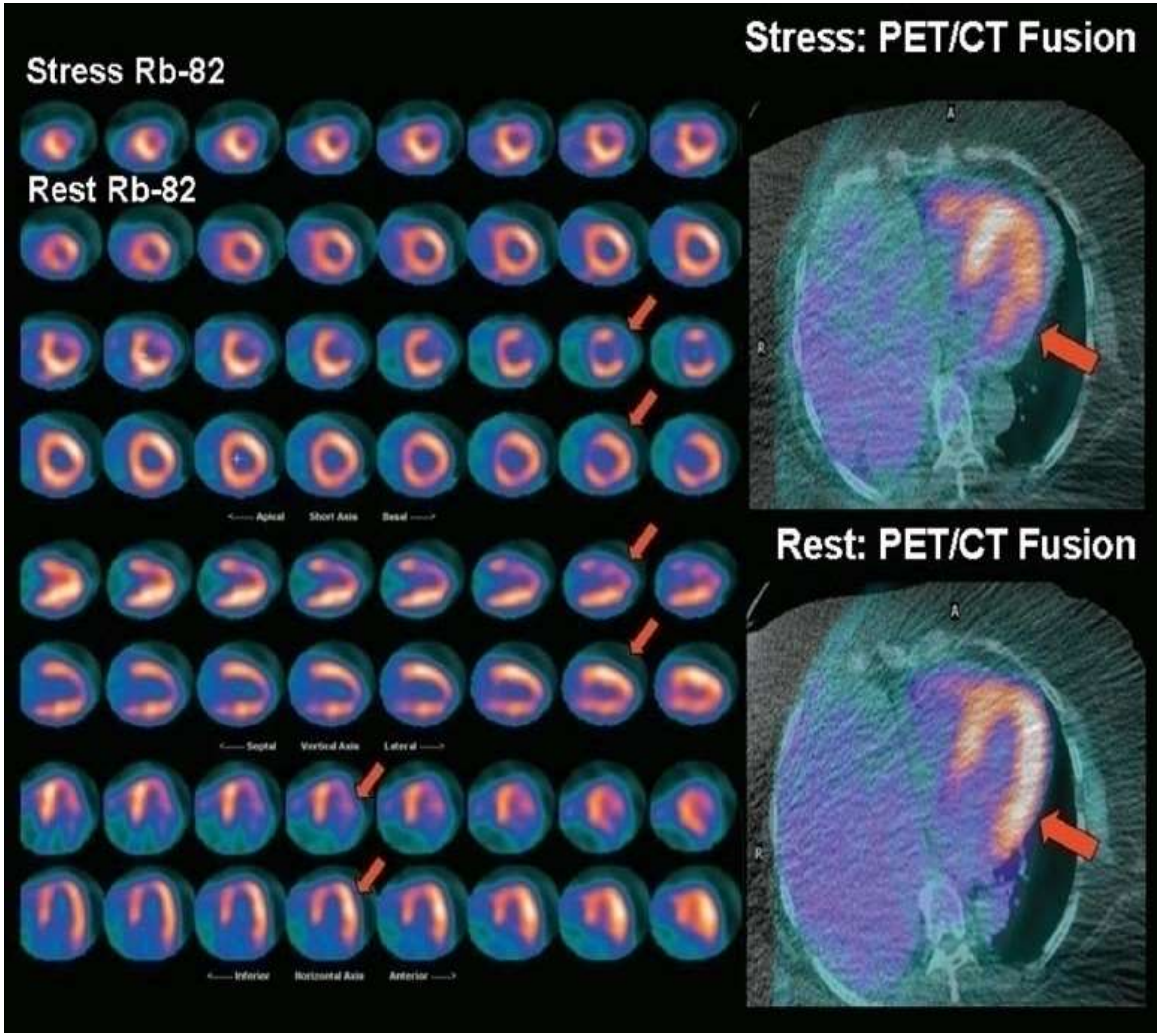

The stress images show a severe perfusion defect throughout the anterolateral wall that is completely reversible at rest

PET vs. SPECT

- PET have superior sensitivity and resolution
- Greater flexibility of incorporating positron labels into biomolecules
- PET is more expensive and requires the presence of an onsite cyclotron

PEM

- Positron Emission Mammography
- PEM is a specialized & improved form of PET for imaging breasts and other small body parts.
- Camera and detectors are closer to the area affected with cancer which produces a very sharp detailed image of tumors and cancerous tissue.
- Can see cancers as small as 1.5 – 2mm about the width of a grain of rice.
- Also allows for the earlier detection of elusive cancers such as DCIS (ductal carcinoma in situ).

PEM

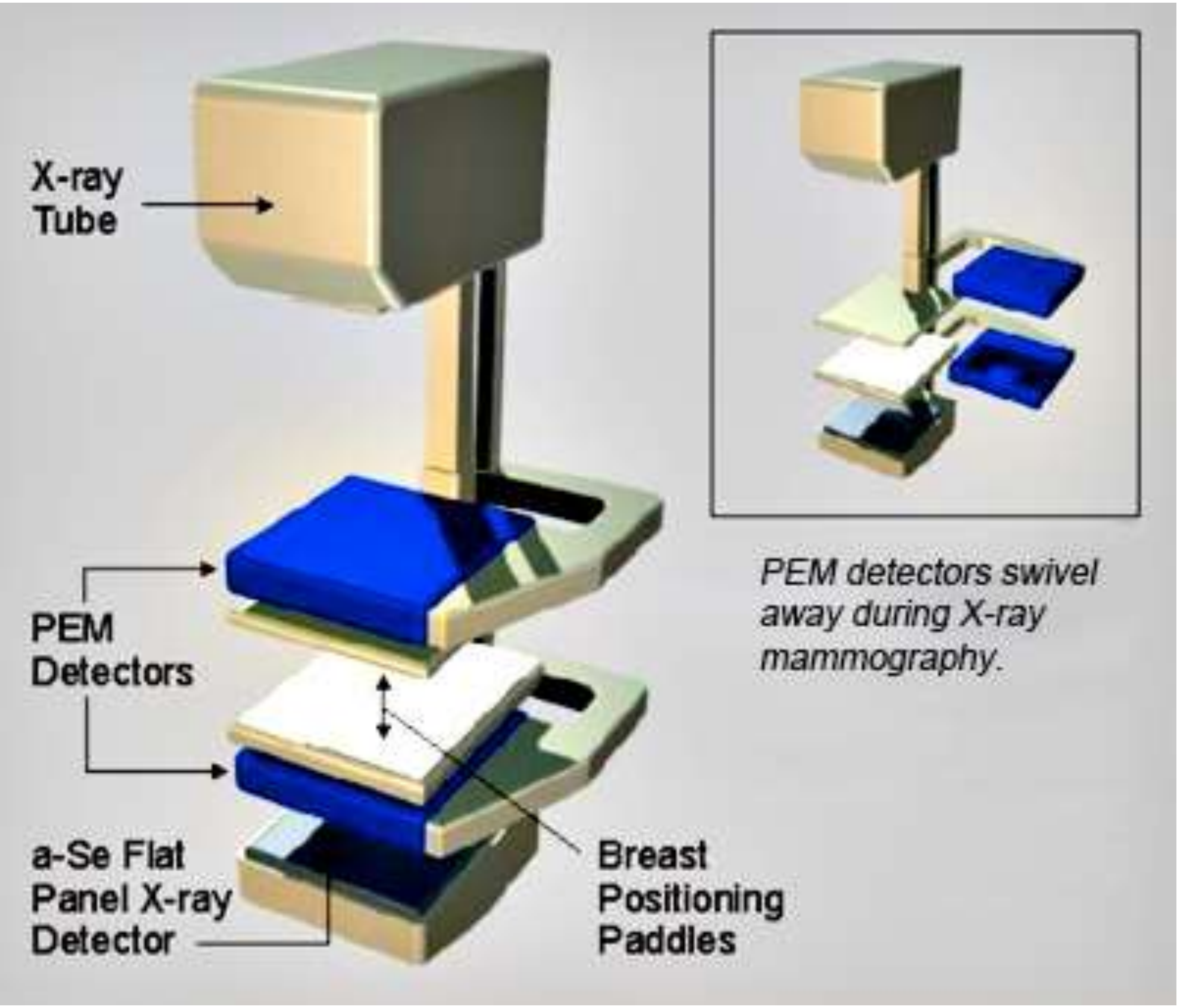

X-ray Tube
PEM Detectors
a-Se Flat Panel X-ray Detector
Breast Positioning Paddles
PEM detectors swivel away during X-ray mammography.

- Differences between whole-body PET and PEM

- better spatial resolution (1-2 mm vs. 5-10 mm). This comes at the cost of field-of-view
- Photon-Detection Sensitivity
- Closer proximity of PEM detectors increases geometric sensitivity
- Allows lower dose/faster imaging/longer uptake time


Thank you!

SPECT & PET

NAGARAJU.B

- **Radionuclides** are unstable nuclei
- Having a neutron excess or deficit, are radioactive → 'decay' to become stable nuclei, with the emission of any combination of alpha, beta, and gamma radiation.

Production of radionuclides:

• **Natural radionuclides:** few, sufficiently long lived, e.g. uranium, radium, and radon.

• **Radionuclides in medical imaging** → produced artificially, in the following way

- Some radionucleids produced by additional neutron forced into a stable nucleus:
  - Nucleus has a neutron excess → unstable.
  - In a ***nuclear reactor***,
  - e.g. with **Molybdenum (Mo)**:

$_{98}Mo + n \rightarrow {}_{99}Mo$

  - Same atomic number.
  - Mass number increased by 1.
  - Radionuclides produced by this process have same chemical properties and called "an isotope" .

- Radionuclides produced by additional proton forced into a stable nucleus → knocking out a neutron:
  - Nucleus has a *neutron deficit* → unstable.
  - In a ***cyclotron*** which accelerates positively charged ions: e.g. protons or alpha particles.
  - e.g. with **Boron (B)**:

$$_{11}B + p \rightarrow {}_{11}C + n$$

  - Atomic number increased by 1.
  - Same mass number.

Radioactive decay

- ***Nuclides with a neutron excess:***
  β - Decay
  • Neutron change into a proton & an electron → the electron is ejected from the nucleus with high energy **“-ve beta particle”**
  n → p + β -
  • For example, ***Iodine-131 (131I, Z= 53)*** → ***Xenon-131 (131Xe, Z= 54)***.
  • Same mass number.
  • Atomic number increased by 1 .
  •The daughter nucleus mostly produced with excess energy with immediate loss of energy with the emission of one or more **γ** photons.

- **Isomeric transition**: in this some radionucleids the gamma ray is not emitted until an appreciable time after the emission of beta particle.
- For ex: ^{99}Mo decays by emission of –ve beta particle, the daughter nucleus Tc remains in exited stable for variable length of time, it is said to be metastable and is written as ^{99m}Tc.
- Its decay to ground state , ^{99}Tc, is most often with emission of gamma ray of energy 140kev.

- ***Nuclides with a neutron deficit:***
  β + Decay
  • A proton change into a neutron and a positive electron → the latter is ejected from the
  nucleus with high energy **"+ve β particle"**.
  p → n + β+
  • For example,
  Carbon-11 (11C, Z= 6) → ***Boron-11 (11B, Z= 5).***
  • Same Mass and charge.
  • The atomic number decreased by 1 .
  •The daughter nucleus, if excited → loses excess energy by the emission of gamma photons till reaches the ground state.

- **K-electron capture (EC)**

• The nucleus capturing an extra-nuclear electron from the nearest (K) shell → increase its
number of neutrons relative to the number of protons.

p + e → n

• Same Mass and charge.

The atomic number decreased by 1 .

•The daughter nuclide will emit **characteristic X-rays** when the hole so created in the Kshell is filled by an electron from an outer shell ± **gamma rays** if still excited.

• **Iodine-123 (123I)** decays by electron capture and emits **160 keV gamma** and **28 keV Xrays**, but **no β-particles**.

Radiopharmaceuticals

- Radiopharmaceuticals are the radioactive substances or radioactive drugs for diagnostic or therapeutic interventions.it contains
- a radioactive isotope that can be injected safely into the body, and
- a carrier molecule which delivers the isotope to the area to be treated or examined.
- Isotope during its conversion to stable forms emits radiation.

SPECT

- Single-photon emission computed tomography (SPECT) provides three-dimensional (3D) image information about the distribution of a radiopharmaceutical injected into the patient for diagnostic purposes.
- By combining conventional scintigraphic and computed tomographic methods, SPECT images present 3D functional information about the patient in more detail and higher contrast than found in planar scintigrams.

- A typical SPECT system consists of one or more scintillation cameras that acquire multiple two-dimensional planar projection images around the patient. The projection data are reconstructed into 3D images. The collimator of the scintillation camera has substantial effects on the spatial resolution and detection efficiency of the SPECT system.
- Physical factors such as photon attenuation and scatter affect the quantitative accuracy and quality of SPECT images, and various methods have been developed to compensate for these image-degrading effects.

- SPECT studies use standard radionuclides (eg, technetium-99m or iodine-123) and simpler imaging instrumentation. These standard radionuclides commonly emit gamma-ray photons with energies that are much lower than 511 keV. A typical example is Tc-99m, which emits 140 keV photons.
- An exception is the widely used myocardial agent, thallium-201, whose decay to mercury-201 results in the emission of characteristic mercury x rays with an average energy of about 72 keV.

In a typical conventional scintigraphy system which is used in SPECT. A given radioisotope-labeled pharmaceutical is injected into the patient.

Depending on the biodistribution properties of the pharmaceutical, the radioactivity is distributed in specific organs and normal or abnormal tissues.

Gamma-ray photons emitted from the radiopharmaceutical interact with matter inside the patient’s body. Those photons that exit the patient’s body and pass through the holes of a collimator are detected by a position-sensitive detector.

- Typically a scintillation (or Anger) camera mounted on a rotating gantry. A typical large field-of-view scintillation camera consists of a 0.95-cm-thick, 40-cm-collimeter sodium iodide crystal and an array of photomultiplier tubes at its back. The detected photons are transformed into visible light (ie, scintillations), which is converted into electrical signals by the photomultiplier tubes.
- The magnitudes of the electrical signals are proportional to the energies of the photons. A pulse height analyzer evaluates the energies of the detected photons and accepts only those that fall within a preset energy window, which is centered at the energy peak of the primary photons; thus, scattered photons and their adversive effects are rejected.

- The effectiveness of this scatter rejection depends on the energy resolution of the detector and the width of the energy window. Finally, a two-dimensional(2D) projection image of the three-dimensional (3D) radioactivity distribution is formed from the registered photon counts .

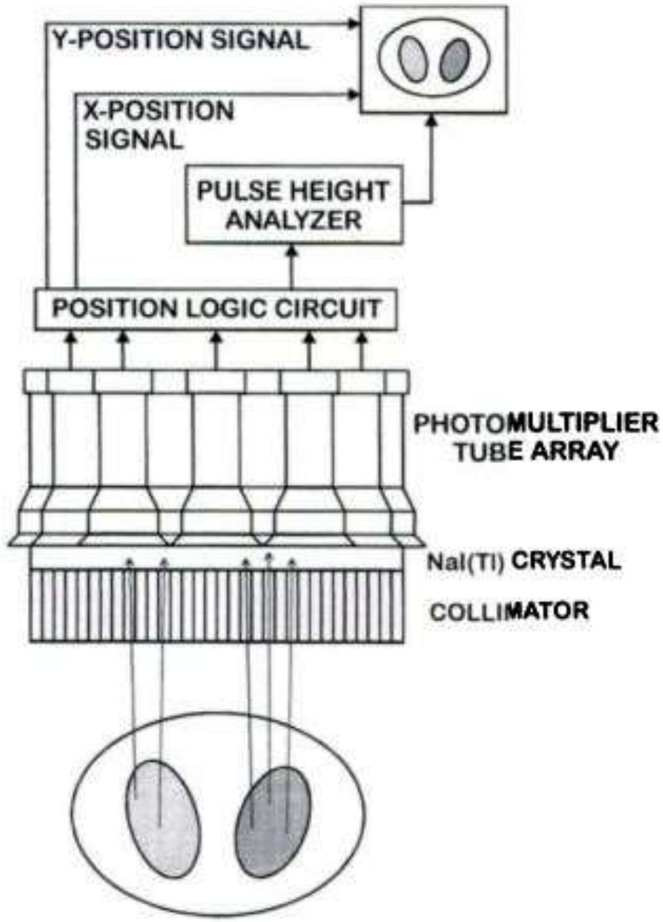

Figure 1. Diagram of the components of a typical conventional scintigraphy system.

PHYSICAL AND INSTRUMENTATION **FACTORS** THAT AFFECT SPECT IM**AGES**

- A number of factors substantially affect the quality and quantitative accuracy of SPECT images.
- They include physical factors, which are related to the interaction of photons emitted from the radiopharmaceuticals with matter inside the patient, and instrumentation factors, which are related to the SPECT imaging system.
- For photon energies commonly used in scintigraphy and SPECT are photoelectric and Compton scatter are the major interactions of radiation with matter.

- In a photoelectric interaction, the photon is totally absorbed by an atom. In a Compton scatter interaction, the photon changes its direction of travel, with partial loss of its original energy.

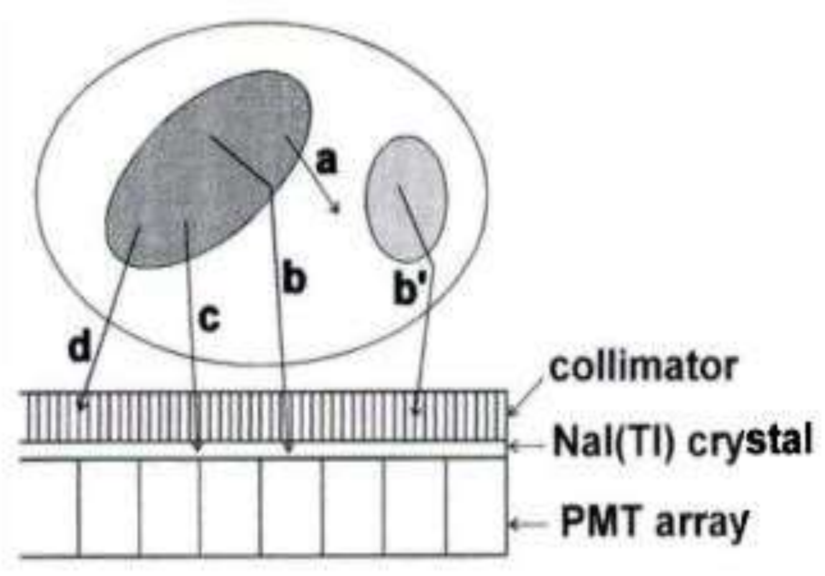

- Photon attenuation can be defined as the reduction of the number of primary photons that pass through a given thickness of material. Photon attenuation is caused by photoelectric and Compton scatter interactions in the material.
- The amount of attenuation depends on the incident photon energy and on the thickness and attenuation coefficient of the material. For example, the 140-keV photons from Tc-99m lose half of their original number in about 4.5 cm of water or soft tissue. As a result, photon attenuation substantially affects the quantitative accuracy of scintigraphic and SPECT images.

- Image reconstruction is done from the data acquired.
- There are the two reconstruction algorithma used in SPECT.
  - FILTERED BACK PROJECTION
  - ITERATIVE RECONSTRUCTION

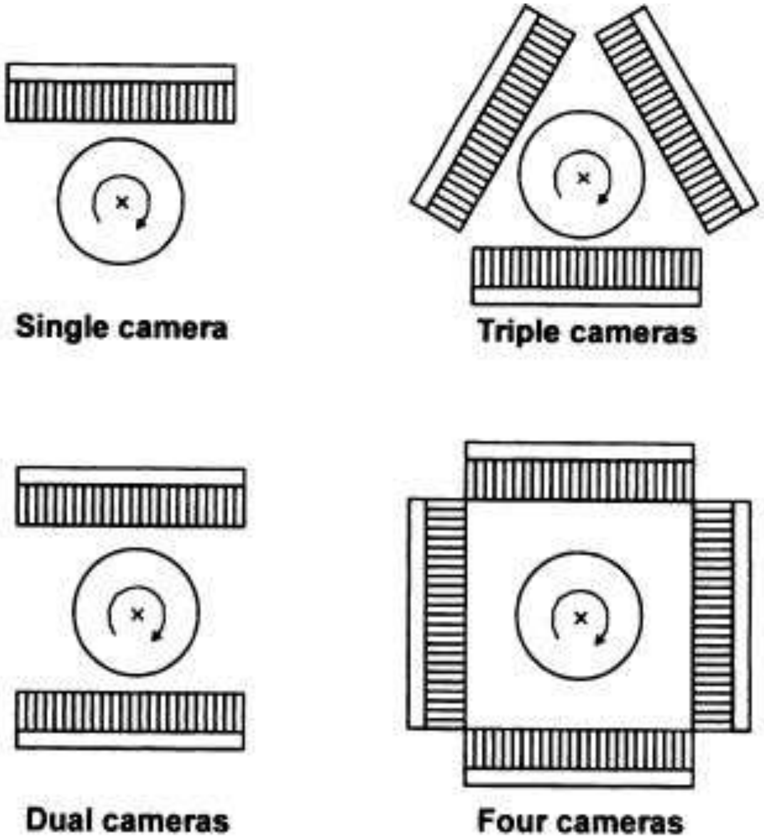

Figure 3. Diagrams show typical configurations of commercial SPECT imaging systems. The increased number of scintillation cameras around the patient results in increased detection efficiency or improved spatial resolution.

Radionuclides Commonly Used in Scintigraphy and SPECT

Radionuclide	Half-life	Energies of Primary Photons (keV)
Technetium-99m	6 h	140
Thallium-201	73 h	~72
Gallium-67	3.3 d	88, 185, 300
Iodine-131	8.04 d	365
Iodine-123	13.2 h	159
Xenon-127	36.4 d	172, 203, 375
Xenon-133	5.25 d	81, 161

Common clinical applications

Study	Radioisotope	Emission energy (keV)	Half-life	Radiopharmaceutical
Bone scan	technetium-99m	140	6 hours	Phosphonates / Bisphosphonates
Myocardial perfusion scan	technetium-99m	140	6 hours	tetrofosmin; Sestamibi
Sestamibi parathyroid scan	technetium-99m	140	6 hours	Sestamibi
Brain scan	technetium-99m	140	6 hours	HMPAO; ECD
Neuroendocrine or neurological tumor scan	iodine-123 or iodine-131	159	13 hours or 8 days	MIBG
White cell scan	indium-111 & technetium-99m	171 & 245	67 hours	*in vitro* labelled leucocytes

PRINCIPLE OF PET

- The concept of PET is to radiolabel a bio-compound, inject it into the patient, and then measure its bio-distribution as a function of time to determine physiologic quantities associated with the biocompound.
- All PET compounds are radiolabeled with positron-emitting radionuclides.
- These radionuclides have decay characteristics that enable localization in the body.
- A positron is emitted from the nucleus, travels a short distance, and annihilates with its antiparticle (an electron), which results in two 5 I l-keV photons traveling in opposite directions.
- After both photons are detected, the activity is localized somewhere along the line defined by the two detectors.

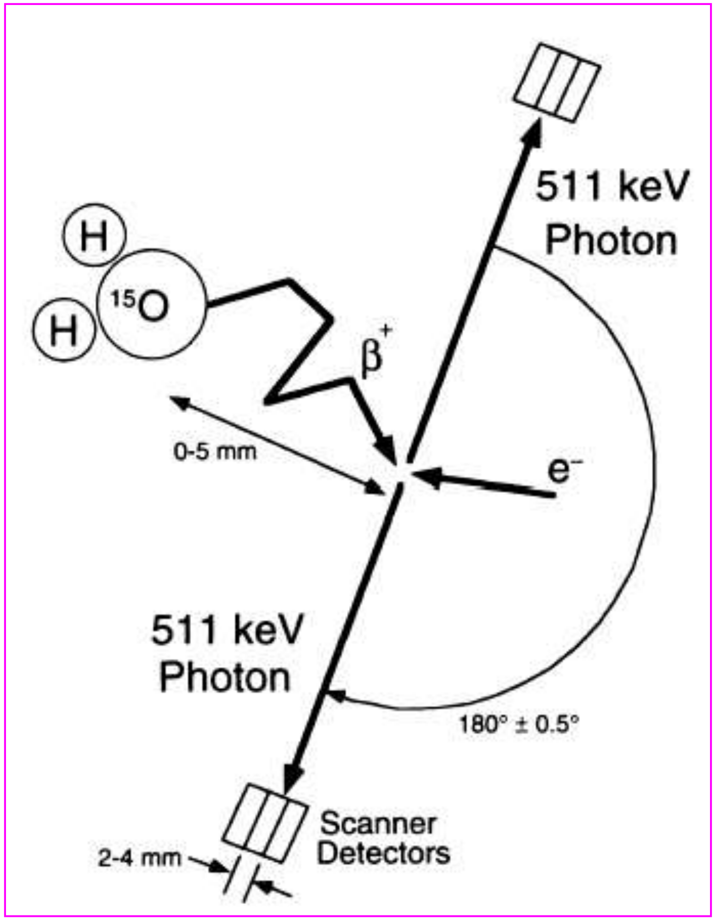

511 keV
Photon
H
15O
H
β+
0-5 mm
e-
511 keV
Photon
180° ± 0.5°
Scanner
Detectors
2-4 mm

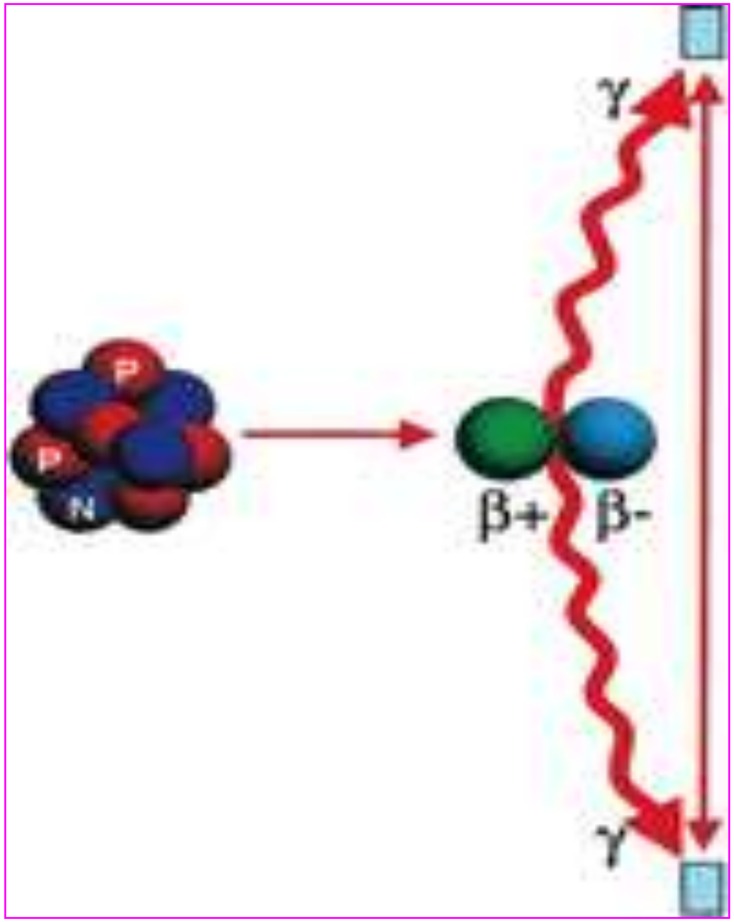

γ
P
P
N
β+
β-
γ

A PET study consists of

- producing radiotracers
- Synthesizing radiopharmaceuticals from the tracers
- administering the radiopharmaceutical to a patient
- measuring the resulting radioactivity distribution in an organ of interest
- interpreting activity distribution as a function of physiologic parameters.

PRODUCTION OF RADIONUCLIDE

- PET radionuclides are positron emitters.
- There are 5 convenient nuclides-

	HALF LIFE (min)
Rubidium- 82	1.23
Fluorine – 18	109
Oxygen- 15	2
Nitrogen- 13	10
Carbon- 11	20

Commonly produced isotopes : “F O N C”

SYNTHESIS OF F-18 &FDG

- Over 500 PET compounds have been synthesized since 1970.
- Natural substrates such as amino acids, analogues ,fluorinated glucose &drugs.
- MC used is a glucose analogue, 2-[F18]fluoro-2-deoxy-D-glucose (FDG).

Why is 18 F the most used positron emitter?

- 18F is a small atom.
- its addition to a molecule does not deform it to the point where it is not recognized by the body anymore
- has a half-life of 109 minutes.
- This is long enough to perform a complicated chemistry (labelling) , and to allow transport over some distance.
- It is also not long enough to keep the radiation burden to patient low

USES

Fluorodeoxyglucose

[18F]-labeled 2-deoxyglucose (FDG) is used in neurology, cardiology and oncology to study glucose metabolism. FDG is potentially useful in differentiating benign from malignant forms of lesions because of the high metabolic activity of many types of aggressive tumors.

Oxygen

[15O]-labeled water is used to evaluate myocardial oxygen consumption and oxygen extraction fraction. It can also be used to measure tumor necrosis.

- **Ammonia**
  [13N]-labeled ammonia can be used to measure blood flow.

- **Leucine**
  [11C]-labeled methionine and leucine can be used to evaluate amino acid uptake and protein synthesis, providing an indicator of tumor viability.

- **Fluorine Ion**
  Radiolabeled fluorine ion [18F-] was once a standard agent for clinical bone scanning.

Principle of metabolic imaging with FDG

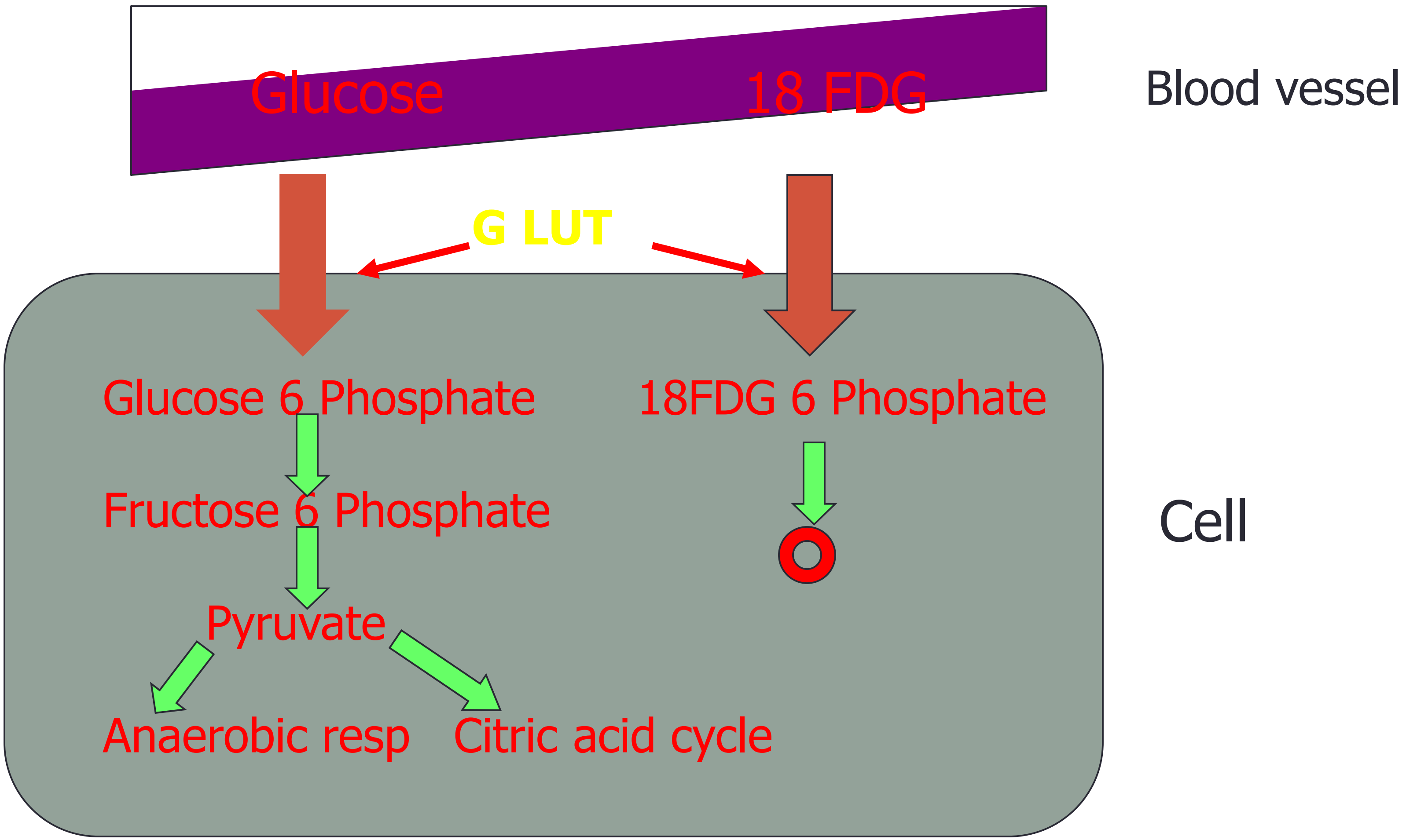

- A positron emission tomography (PET) scanner is a large machine with a round, doughnut shaped hole in the middle
- Within this machine are multiple rings of detectors that record the emission of energy from the radiotracer in our body.
- A nearby computer aids in creating the images from the data obtained by the camera or scanner.

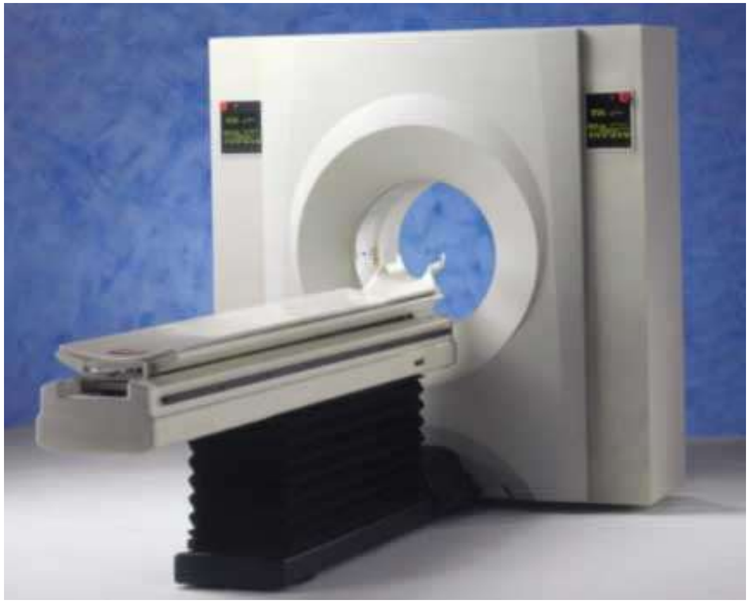

SCANNER DESIGN….

- Detectors are 18-40 rings of crystals forming a cylindrical field of view about 15cm long that can acquire many slices of coincidence data
- PET scanners use crystals with higher density & higher Z numbers due to sensitivity
- Group of crystals is put together into a block
- Four PMT's to each block of crystal
- Use "electronic collimation" to detect location of annihilation event

- Localizing the site of impact is achieved by measuring the light detected in each PMT
- Signal is then amplified
- System must be able to determine which signals come from paired 511keV photons and record the time of detection (timing discriminator)
- Coincidence circuit then examines signals to confirm it if it occurred with in the time window

CRYSTALS USED IN PET

- BaF_2 – Barium Flouride*(0.8ns)*
- BGO – Bismuth Germinate Oxide*(300ns)*
- LSO – Lutetium Orthosilicate*(40ns)*
- GSO – Gadolineum Orthosilicate*(60ns)*
- YLSO – Yttrium Lutetium Orthosilicate*(40ns)*

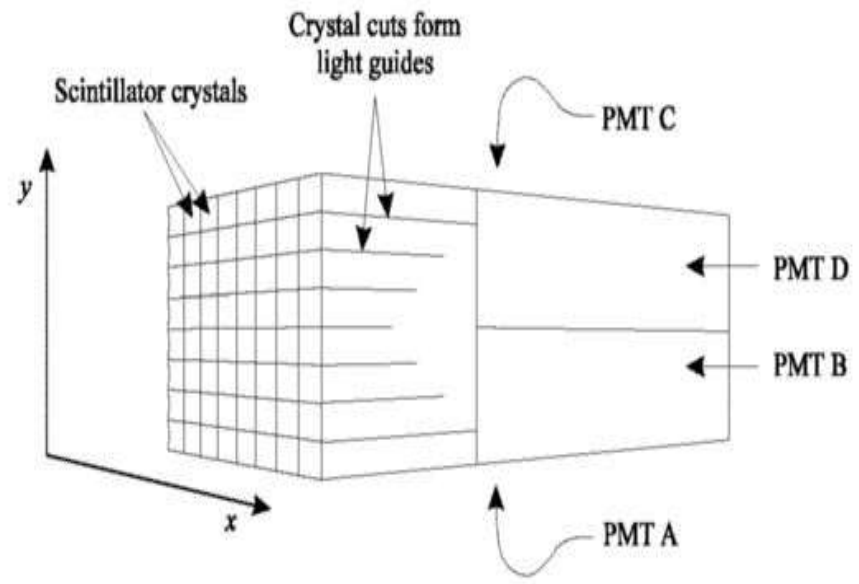

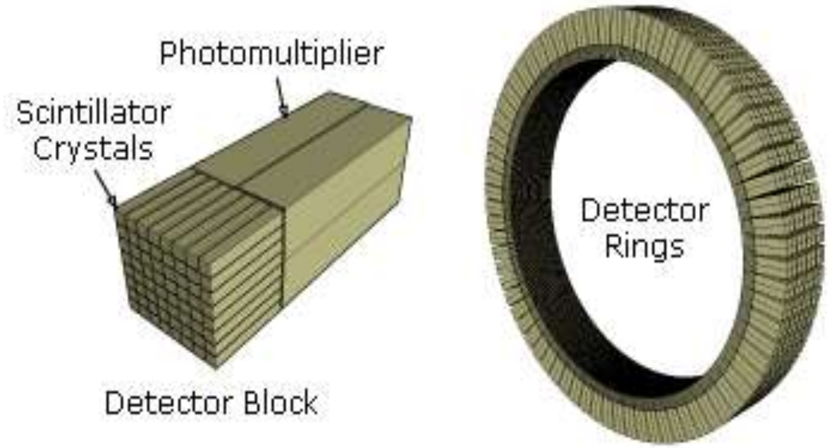

COINCIDENCE DETECTION

- Photons should arrive with in a certain time of one another
- A coincidence timing window allows detection of the PMT electrical signal from photon pair (4-12ns)
- If it falls within timing window it is registered as a true event
- When two different annihilation events are detected with in the timing window is known as “random event”

DATA ACQUSITION

- The detection of photon pairs by opposing crystals create one event .
- Millions of these event will be stored with in sinograms and used to reconstruct the image
- Spatial resolution is determined by the size of crystal and their separation and is typically 3-5mm
- PET is 50-100 times more sensitive and produces higher quality than a SPECT
- Reconstruction is similar to SPECT

RECONSTRUCTION

- PET reconstruction can be performed with a variety of algorithms
- Filtered back projection
- Iterative reconstruction(ordered subset reconstruction)

ATTENUATION CORRECTION

- Mathematical attenuation correction techniques may be used if tissue attenuation is the same at all areas within a transaxial slice .
- Measured attenuation may be performed by two methods:
  - Transmission scan using a radioactive source rotating it around the patient
  - CT scan to measure tissue density
- The ability to correct for attenuation improves quality and permits absolute quantification of radioactivity in the body

- **<u>Resolution in PET is determined by three factors:</u>**
  - distance the positron travels before it annihilates with an electron,
  - variation in angle between the two annihilation photons, and
  - physical size of the detectors.

- A positron will travel between 0.5 and 2 mm in tissue before annihilation, depending on its energy.

- Typical detector sizes are 1 -3 mm.

- The best possible resolution of a PET scanner is 1-2mm. Typical clinical scanners have a resolution of approximately 4-7 mm.

PET vs. CT & MRI

PET	CT and MRI
Shows extent of disease	Detects changes in body structure
Can help in monitoring treatment and shows it's effectiveness	Simply confirms the presence of a mass
Reveals disease earlier, can diagnose faster	
Can detect whether a mass is benign or malignant	
Can detect abnomalities before there is an anatomical change	

SAFETY ASPECTS OF PET

- PET has 511Kev gamma rays energy, that is 3 times of 140Kev gamma ray energy of Technitium99m
- Due to their high energy 16 times more lead is required to obtain the same stopping effect for 511Kev photons as compared to 140Kev photons

So Tungsten shielding is used for Positron emitting radionuclide.

It provides 1.4 times the shielding capability for the same thickness of Lead

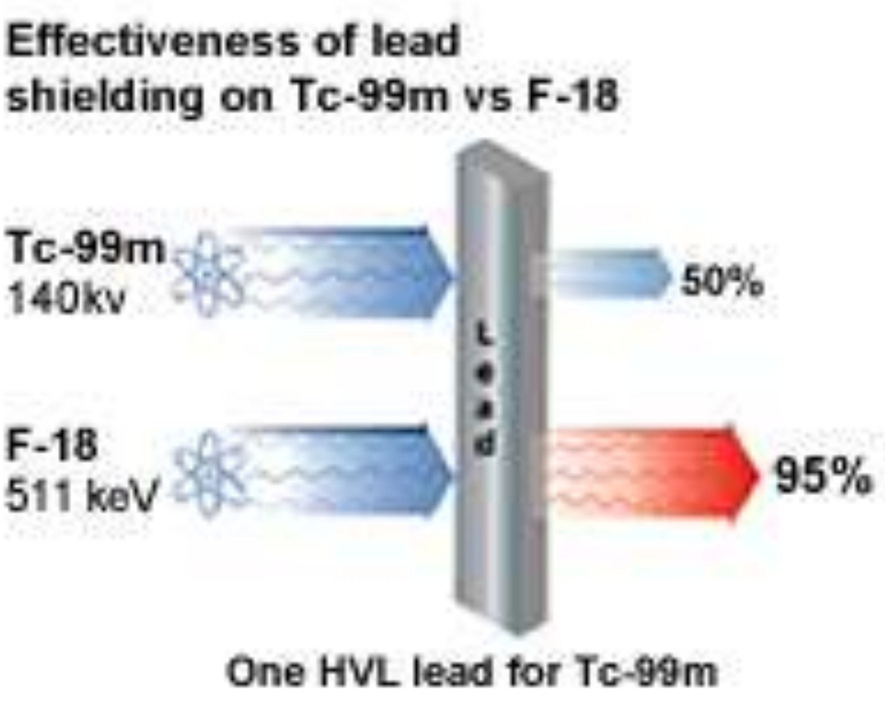

CONTRA INDICATIONS

- Pregnancy
- Use of caffeine, tobacco, or alcohol in past 24hours before scan
- Using sedatives
- Using medicines that change metabolism ex: ***INSULIN.***

PET-CT FUSION

- FDG PET is a strictly functional modality and lacks anatomic landmarks.
- Unless anatomic correlation is available to delineate normal structures, pathologic sites of FDG accumulation can easily be confused with normal physiologic uptake, leading to false-positive or false-negative findings.
- **Coregistration** of PET scans with CT using a combined PET-CT scanner improves the overall sensitivity and specificity of information provided by PET or CT alone .
- advantage is ability to correlate findings at two complementary imaging modalities in a comprehensive examination. Hence, PET-CT provides more **precise anatomic definition for both the physiologic and pathologic uptake seen at FDG PET**

Distance betwn pet and ct scanner

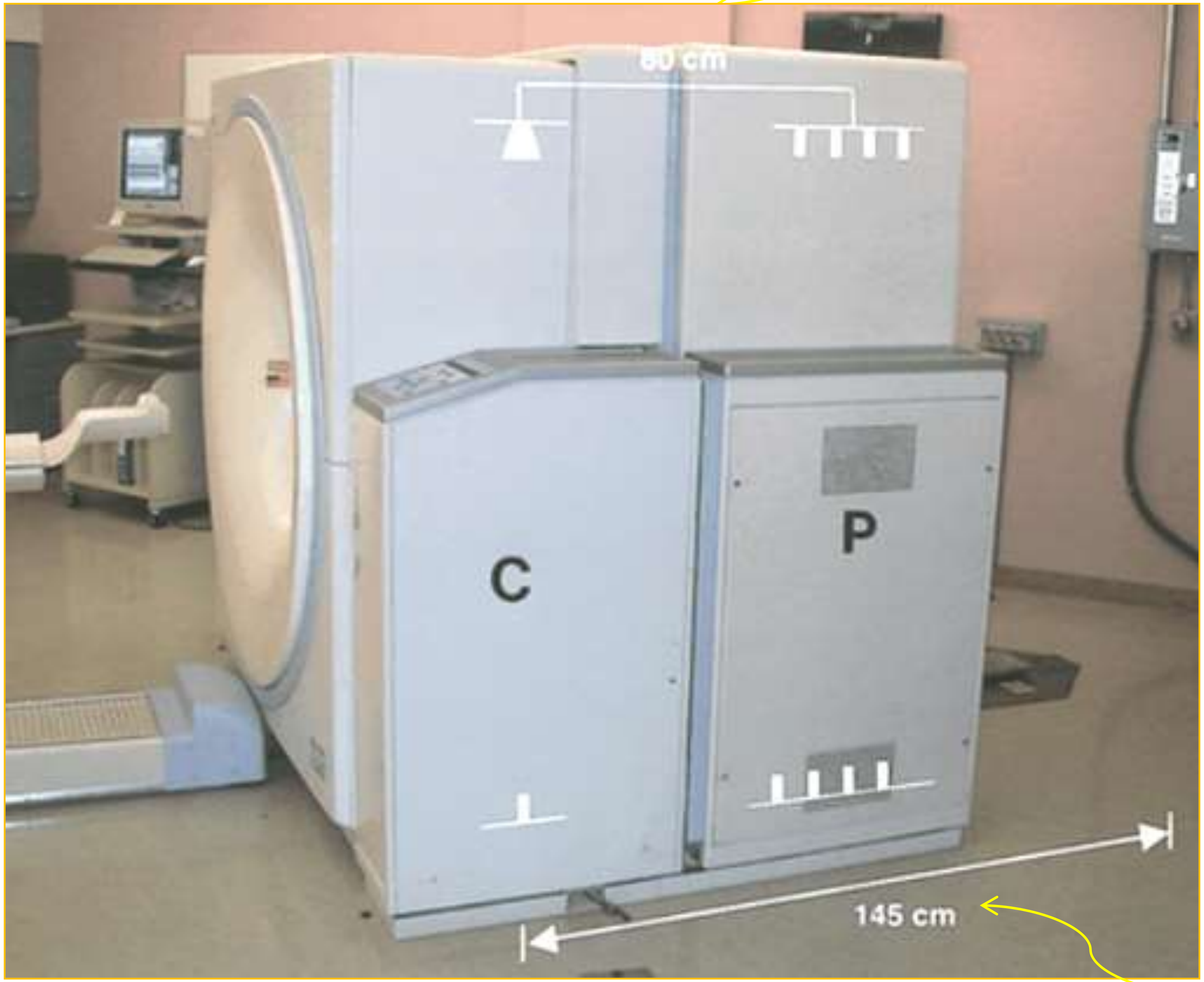

Max coverage during combined study

SCANNING TECHNIQUE

- Nil orally for approximately 4–6 hours
- avoid caffeinated or alcoholic beverages but can have water during this period.
- blood glucose level of less than 150 mg/dL is desirable.
- Avoid strenuous activity to avoid physiologic muscle uptake of FDG
- water-soluble iodinated contrast media orally for bowel opacification **except for head and neck study**.
- 10 mCi injected intravenously
- Patient activity and speech are limited for 20 minutes immediately following injection
- Pet study is started 60 mins after injection.

CT TECHNIQUE

- Contrast material–enhanced helical CT is performed following injection of **125 m**L of a contrast medium at a rate of 4 mL/sec by using a power injector .
- Whole-body PET-CT study scanning begins at the level of the skull base and extends caudally to the level of the symphysis pubis.

PET TECHNIQUE

- The PET scanner is located behind the CT scanner and housed in the same extended-length gantry. PET is performed following the CT study without moving the patient in the caudocranial direction, starting at the thighs to limit artifacts from the FDG metabolite excretion into the urinary system

Typical scout image obtained during an FDG PET-CT study. The blue-purple rectangle represents CT coverage during the study, and each overlapping green rectangle represents PET coverage.

INTERPRETATION OF IMAGES

- PET provides images of quantitative uptake of the radionuclide injected that can give the concentration of radiotracer activity in kilobecquerels per milliliter .

- Methods for assessment of radiotracer uptake –
  - visual inspection
  - **standardized uptake value (SUV)**
  - glucose metabolic rate

LIMITATIONS AND ARTIFACTS OF PET-CT

- 1.Patient motion may cause confusion as to the correct position of the origin of the detected photon.
- Patient motion is minimized by –
    - carefully instructing patients not to move during the study;
    - placing them in a comfortable position before the start of the study;
    - ensuring that they are not taking diuretics, which may otherwise require them to evacuate the bladder during the study;
    - having patients empty their bladder before the start of the study or catheterizing the bladder.

ADVANTAGES OF PET-CT

1. helpful in accurate localization of small areas of increased radiotracer activity that would have been difficult or not possible to localize on PET images alone .
2. helps in distinguishing structures that normally show high metabolic activity from those with abnormally increased activity.
3. PET-CT combines the advantages of the excellent functional information provided by PET and the superb spatial and contrast resolution of CT
4. Finally, attenuation correction for quantitative or semi quantitative assessment of data is possible by using the CT data,

PET/MRI: TECHNICAL EVOLUTION

- The idea to combine PET and MRI arose as early as the mid 1990s, even before PET/CT was introduced.

- The PET/MRI combination requires 3 risky technologic steps that modify state-of-the-art PET and MRI.
  1. First, the photomultiplier technology must be replaced with magnetic field–insensitive photodiodes .
  2. Second, compact PET detectors must be constructed so that it shouldn't interfere with the field gradients or MR radiofrequency.
  3. Finally, the MRI scanner must be adapted to accommodate the PET detectors and to allow simultaneous data acquisition without mutual interference.

Scanner Design

- Based on the technologic challenges to combine PET and MRI into a single gantry, Philips and Siemens proposed 2 fundamentally different prototype PET/MRI designs.
- In the **Siemens prototypes** include 4 dedicated brain PET scanners that fit into a standard 3-T clinical MRI scanner.
- The PET/MRI system, together with a dedicated radiofrequency head coil, allows simultaneous PET/MRI data acquisition of the human brain or body extremities.
- **Philips** developed a PET/MRI design in which the gantries are approximately 2.5 m apart but share a common patient handling system. This implementation does not allow for simultaneous data acquisition and, therefore, results in longer examination times.

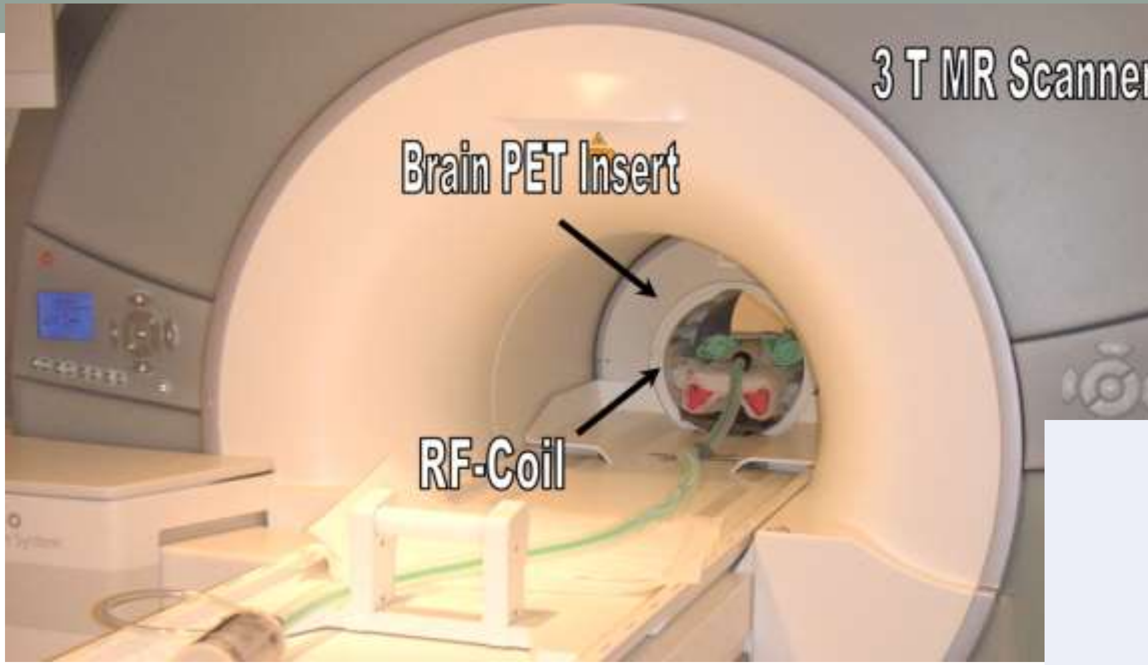
3 T MR Scanner
Brain PET Insert
RF-Coil

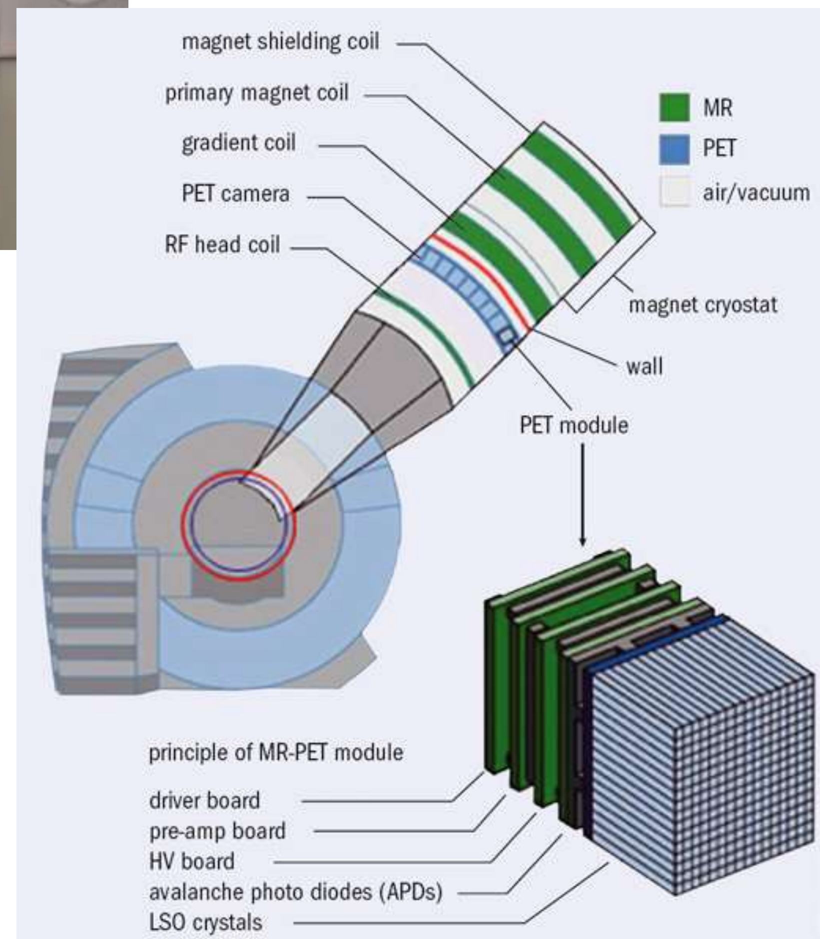
magnet shielding coil
primary magnet coil
gradient coil
PET camera
RF head coil
MR
PET
air/vacuum
magnet cryostat
wall
PET module
principle of MR-PET module
driver board
pre-amp board
HV board
avalanche photo diodes (APDs)
LSO crystals

CLINICAL POTENTIAL OF PET/MRI

- It is reasonable to expect that brain PET/MRI will provide new insights in the field of neuroscience and neurologic disorders, such as neuro degeneration, brain ischemia, neuro oncologyor seizures .
- It is feasible with current prototypes and future-generation systems to simultaneously study brain function, metabolism, oxygen consumption, and perfusion.
- In oncology, an accurate spatial match between PET and MRI data is mandatory for both radiation therapy planning and biopsy guidance.
- Combining PET with cardiac MRI may enable detection and differentiation of vulnerable plaques and diseased myocardium.

Advantage of PET/MRI over PET/CT

1. is not associated with significant radiation exposure
2. has a much higher soft tissue contrast.
3. MRI allows for additional techniques - such as angiography, functional MRI ,diffusion ,spectroscopy and perfusion techniques within one single examination.

PHYSIOLOGIC VERSES PATHOLOGIC FDG UPTAKE

- There are several sites of normal physiologic accumulation of FDG. FDG accumulation is most intense in the **cerebral cortex, basal ganglia, thalamus, and cerebellum.** The myocardium expresses insulin-sensitive glucose transporters, which facilitate the transport of glucose into muscle. A recent meal often causes intense myocardial FDG uptake because of the associated elevated serum insulin levels

- Because FDG appears in the glomerular filtrate and, unlike glucose, is not reabsorbed in the tubules, intense FDG activity is seen in the intrarenal collecting systems, ureters, and bladder

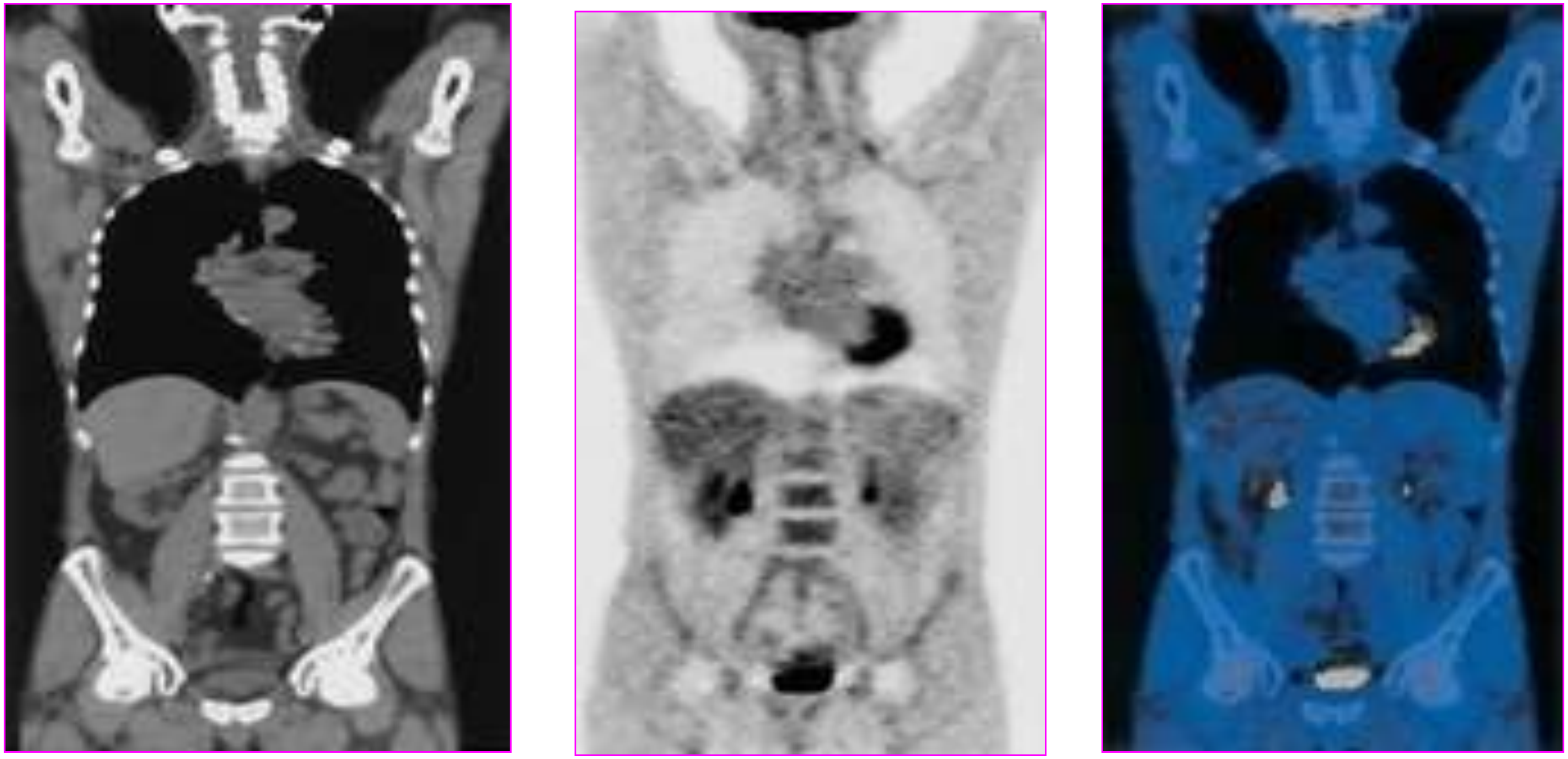

Physiologic FDG uptake

- **Some clinical applications where PET used:**

- **The Role of PET/CT in Lymphoma**
- Assess response to therapy/residual disease
- Identify recurrent disease
- Initial diagnosis and staging
- Identify suitable sites for biopsy
- Disease surveillance
- Radiotherapy planning

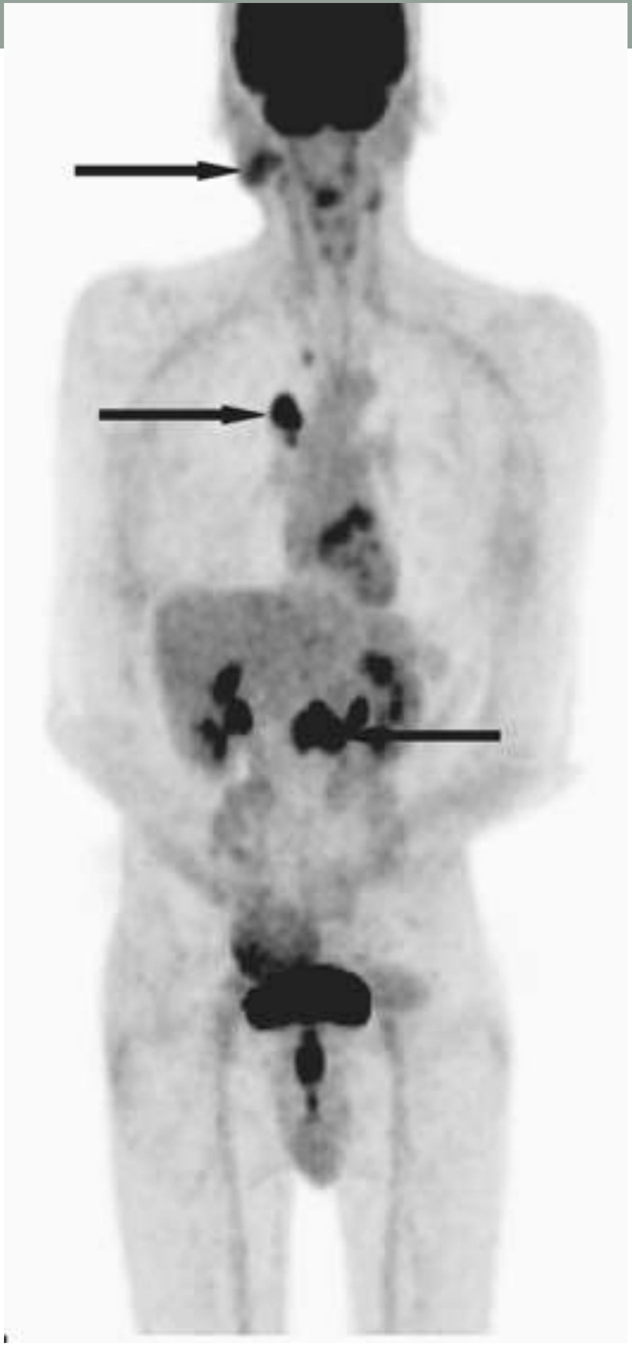

An example of stage 4 disease. NHL with disease in the mediastinum, neck, and abdomen

- **ASSESSMENT OF TREATMENT RESPONSE**

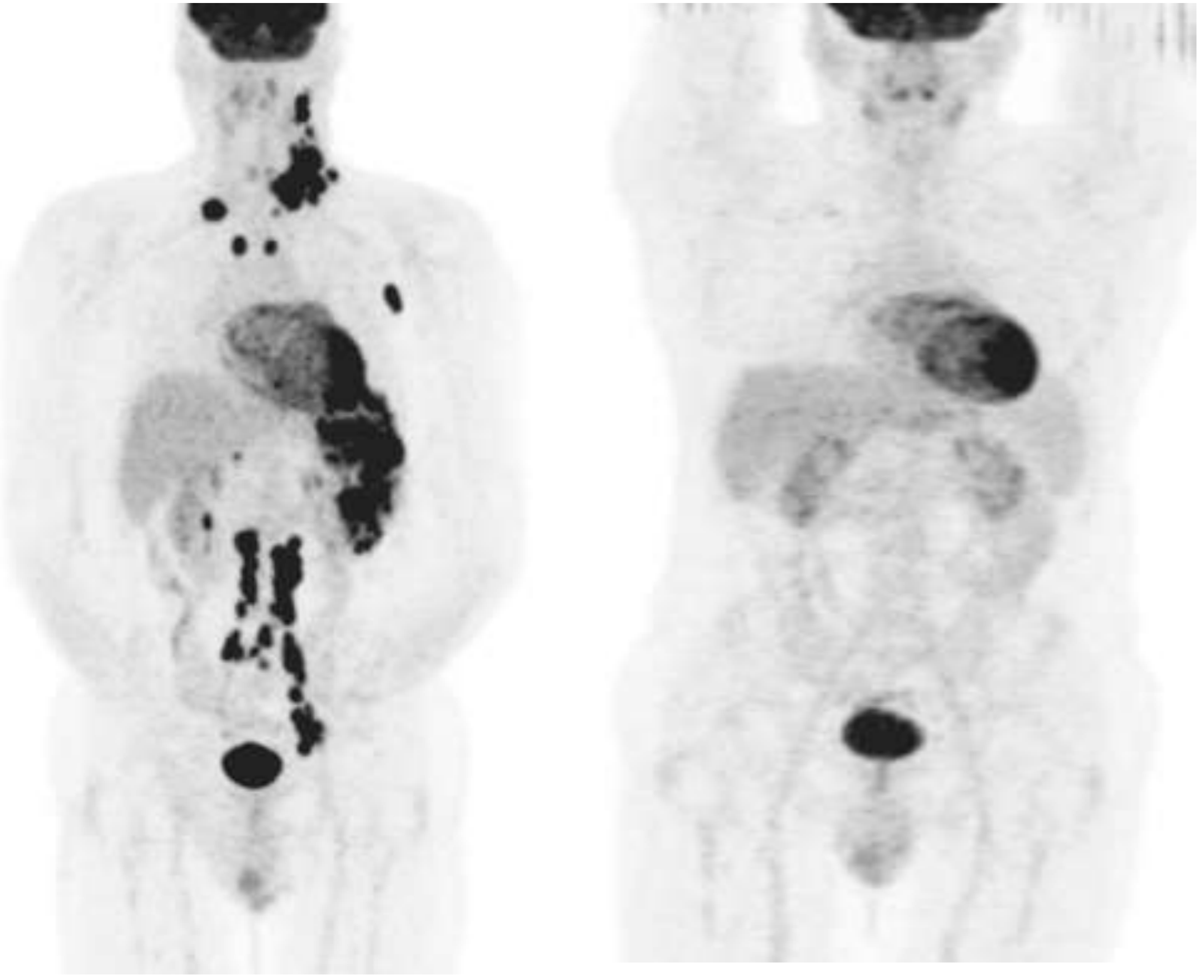

Pretherapy and post therapy studies showing a complete metabolic response to therapy.

NEURO-ONCOLOGY

- Tumor recurrence versus radiation necrosis
- Diagnosis
- Grading
- Monitoring response to therapy
- Radiotherapy planning
- Biopsy planning

SEIZURE FOCUS IDENTIFICATION

STROKE

DEMENTIAS

OTHER APPLICATIONS

- Brain injury- vascular, trauma
- Psychiatry- depression, schizophrenia,anxiety
- Movement disorders with 18F-dopa
- Miscellaneous- infection, substance abuse,eating disorders

Biopsy Planning

PET

CT

PET/CT

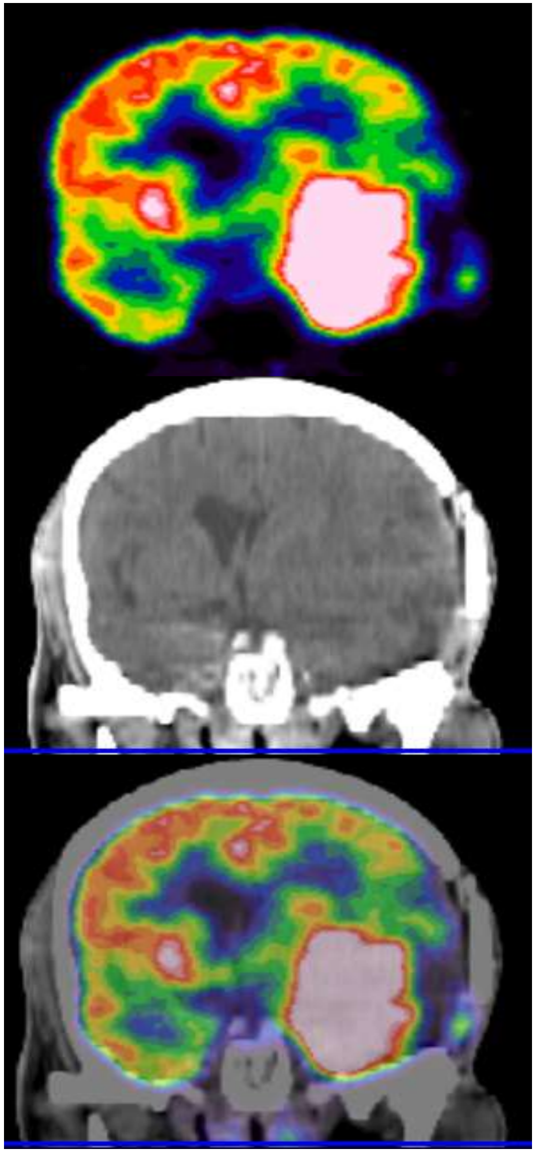

Localizing

the most

viable tissue

in the lesion

PET in Brain Disorders

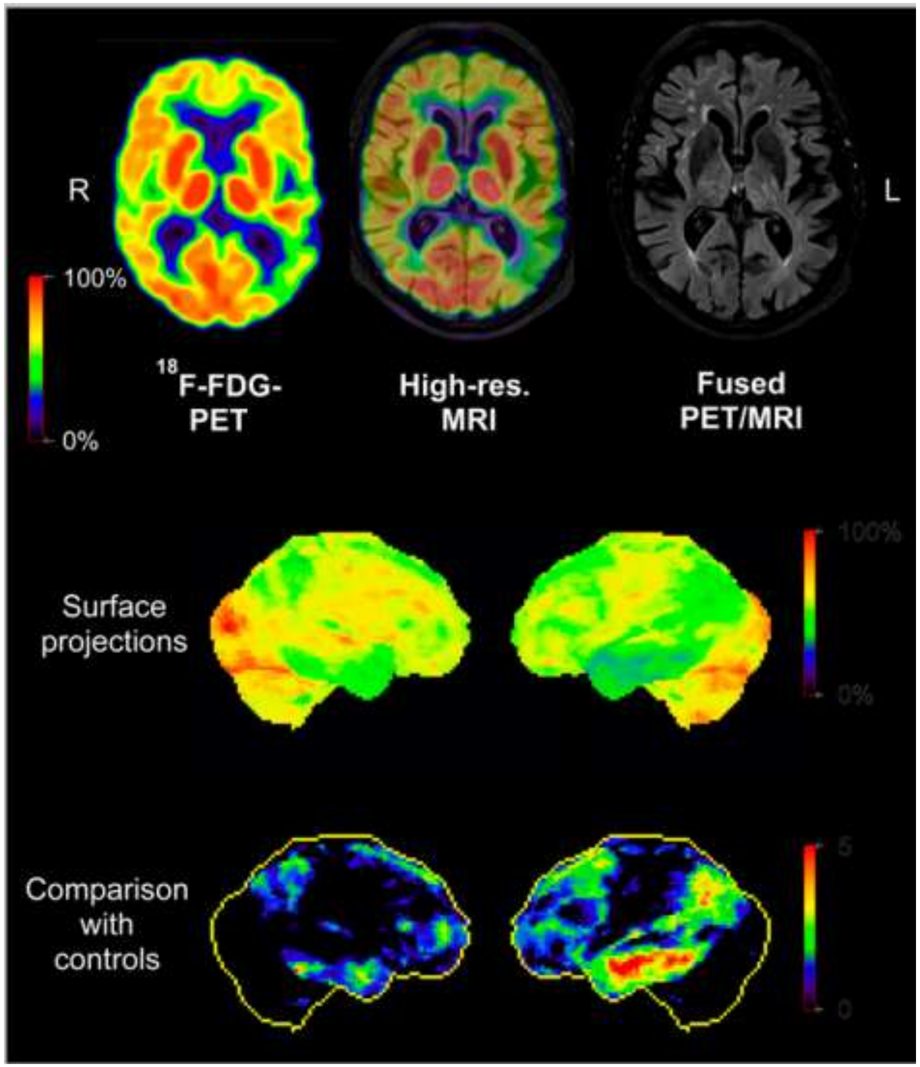

Simultaneous PET/MRI study in Alzheimer disease

Hypo metabolism in left temporal lobe secondary to epilepsy

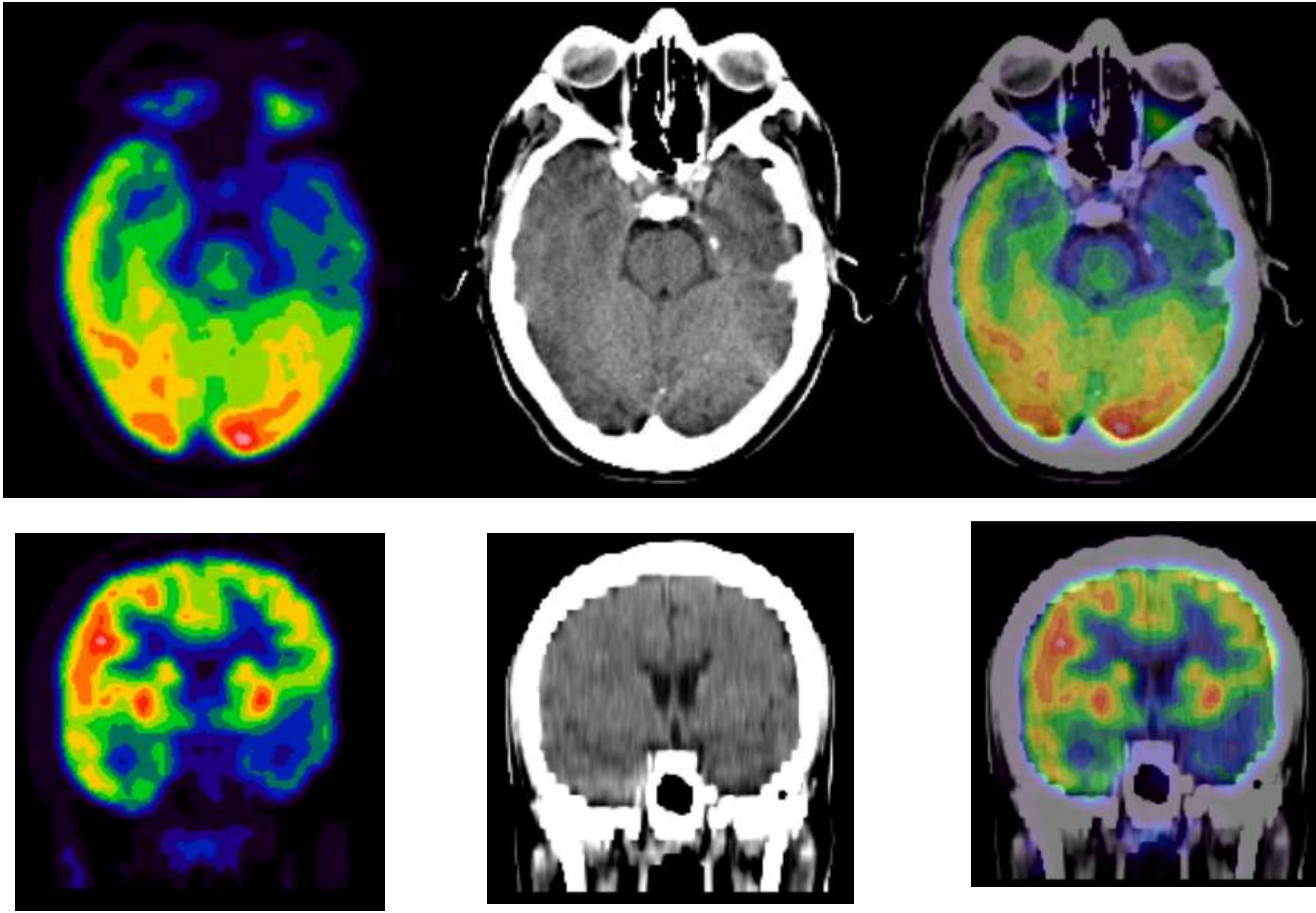

CARDIAC PET and PET CT IMAGING

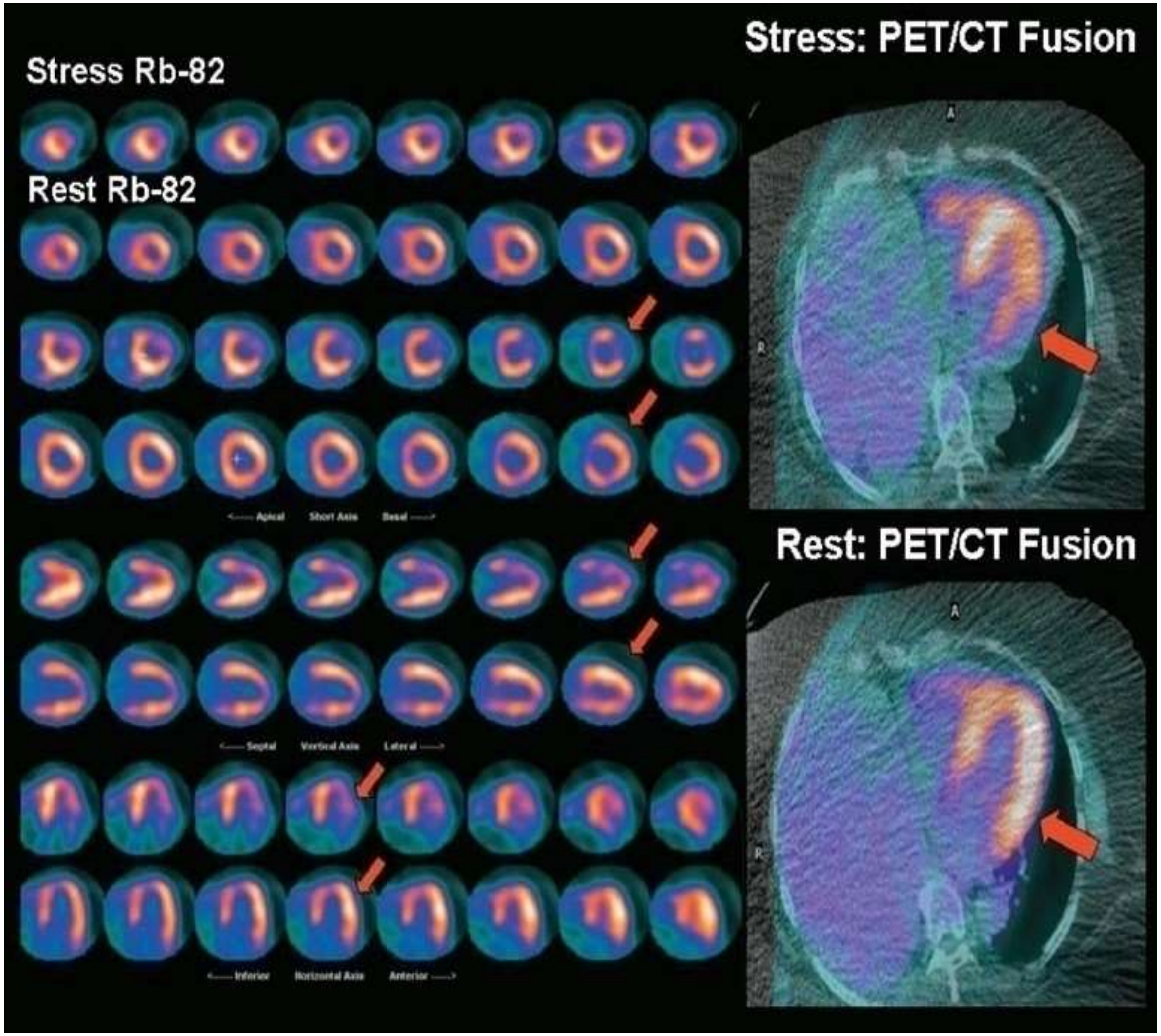

The stress images show a severe perfusion defect throughout the anterolateral wall that is completely reversible at rest

PET vs. SPECT

- PET have superior sensitivity and resolution
- Greater flexibility of incorporating positron labels into biomolecules
- PET is more expensive and requires the presence of an onsite cyclotron

PEM

- Positron Emission Mammography
- PEM is a specialized & improved form of PET for imaging breasts and other small body parts.
- Camera and detectors are closer to the area affected with cancer which produces a very sharp detailed image of tumors and cancerous tissue.
- Can see cancers as small as 1.5 – 2mm about the width of a grain of rice.
- Also allows for the earlier detection of elusive cancers such as DCIS (ductal carcinoma in situ).

PEM

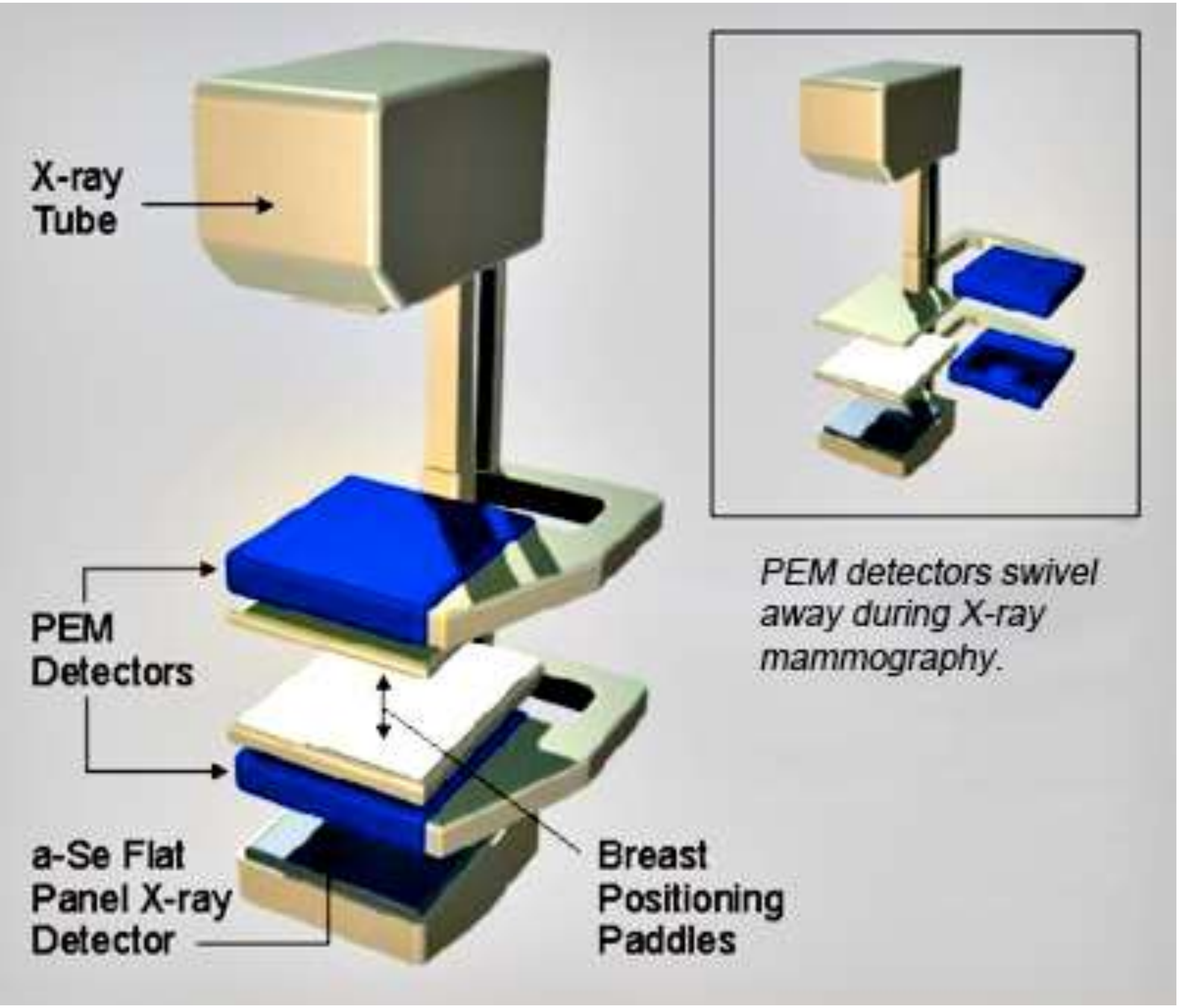
X-ray Tube
PEM Detectors
a-Se Flat Panel X-ray Detector
Breast Positioning Paddles
PEM detectors swivel away during X-ray mammography.

- Differences between whole-body PET and PEM

- better spatial resolution (1-2 mm vs. 5-10 mm). This comes at the cost of field-of-view
- Photon-Detection Sensitivity
- Closer proximity of PEM detectors increases geometric sensitivity
- Allows lower dose/faster imaging/longer uptake time


Thank you!

SPECT TECHNOLOGY

INTRODUCTION

- Emission Computed Tomography is a technique where by multi cross sectional images of tissue function can be produced
- The technique of SPECT is generally considered as two separate modalities.SINGLE PHOTON Emission Computed Tomography involves the use single gamma ray emitted per nuclear disintegration.
- Positron Emission Tomography makes use of radio isotopes such as gallium-68, when two gamma rays each of 511KeV, are emitted simultaneously.

SPECT

- **What is SPECT?**

  SPECT is short for single photon emission computed tomography. As its name suggests (single photon emission) gamma rays are the sources of the information rather than X-ray emission in the conventional CT scan.

- **Why SPECT?**

  Similar to X-ray, CT, MRI, etc SPECT allows us to visualize functional information about patient's specific organ or body system.

THEORY AND INSTRUMENTATION

- SPECT is a technology used in nuclear medicine where the patient is injected with a radiopharmaceutical which will emit gamma rays.
- We seek the position and concentration of radionuclide distribution by the rotation of a photon detector array around the body which acquires data from multiple angles.

CONT…

- Each of the cameras collects a matrix of values which correspond to the number of gamma counts detected in that direction at the one angle.

- Images can be reprojected into a three dimensional one that can be viewed in a dynamic rotating format on computer monitors, facilitating the demonstration of pertinent findings to the referring physicians

GAMMA CAMERA

- The instrument used in nuclear medicine for the detection of gamma rays is known as gamma Camera

- The components making up the gamma camera are
  1. Camera Collimator
  2. Scintillation Detector
  3. Photomultiplier Tube
  4. Positron Circuitry
  5. Data Analysis Computer

Cont…

2. Improvement in these parameters is a constant goal of the SPECT researcher. Improvement in both of these parameters simultaneously is rarely achieved in practice.

Collimation

Computers in radiology and nuclear medicine

Image acquisition

ADVANTAGES

- Localization of defects is more precise and more clearly seen by the inexperienced eye.
- Extend and size of defects is better defined.
- Images free of background.

SPECT APPLICATIONS

- Heart imaging
- Brain Imaging
- SPECT imaging
- Tumor detection
- Bone Scans

POSITRON EMISSION TOMOGRAPHY

- In the simplest PET camera two modified sophisticated cameras called Anger cameras are placed on opposite sides of the patient.

- This increases the collection angle and reduces the collection times which are the limitations of SPECT In PET, radiopharmaceuticals are labeled with positron emitting isotopes.

COMPARISON OF PET AND SPECT

- SPECT imaging is inferior to PET because of attainable resolution and sensitivity. Different radionuclide is used for SPECT imaging that emits a single photon rather than positron emission as in PET.

- The use of collimator results in a tremendous decrease in the detection efficiency as compared to PET.

CONCLUSION

- SPECT being a nuclear medicine imaging modality , it has all the advantages and disadvantages of nuclear medicine can be highly beneficial or dangerous on the application , so is SPECT .

- In spite of this , Today , nearly all cardiac patients receive a planar ECT or SPECT as part of their work-up to detect and stage coronary artery disease.

THANK YOU

QUERIES…

IMAGE TRANSFORMS

Dr Kamalraj Subramaniam
Associate Professor
Department of Biomedical Engg
FOE
Karpagam Academy of Higher Education

Image Transforms

- Transform is basically the representation of the signal. Signal is represented in terms of basis function
- It Need not be always from time domain to frequency domain.

Role of Image Transforms

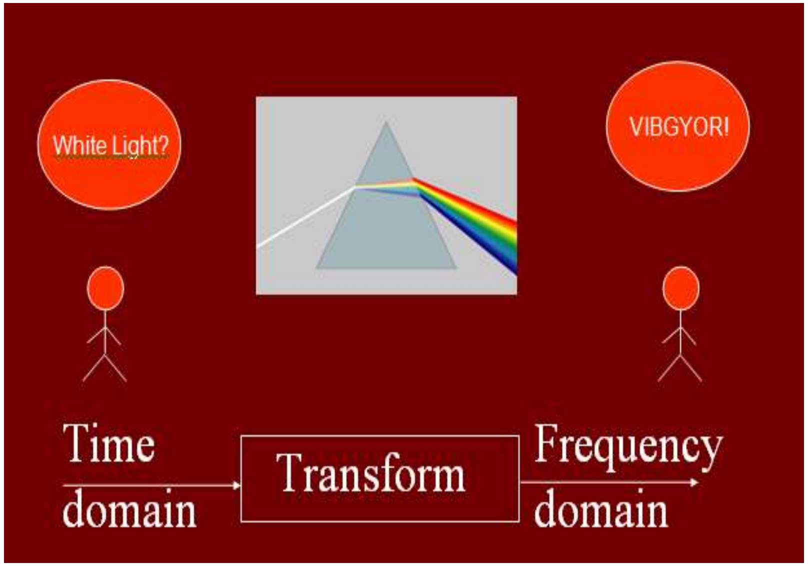

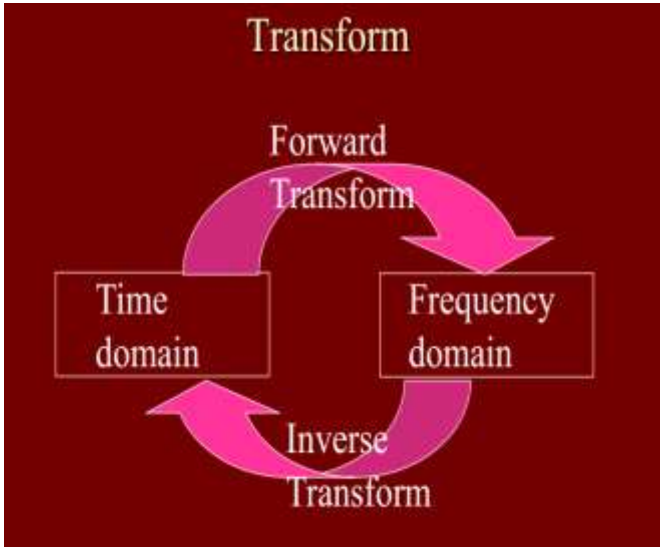

Classification of Image Transform

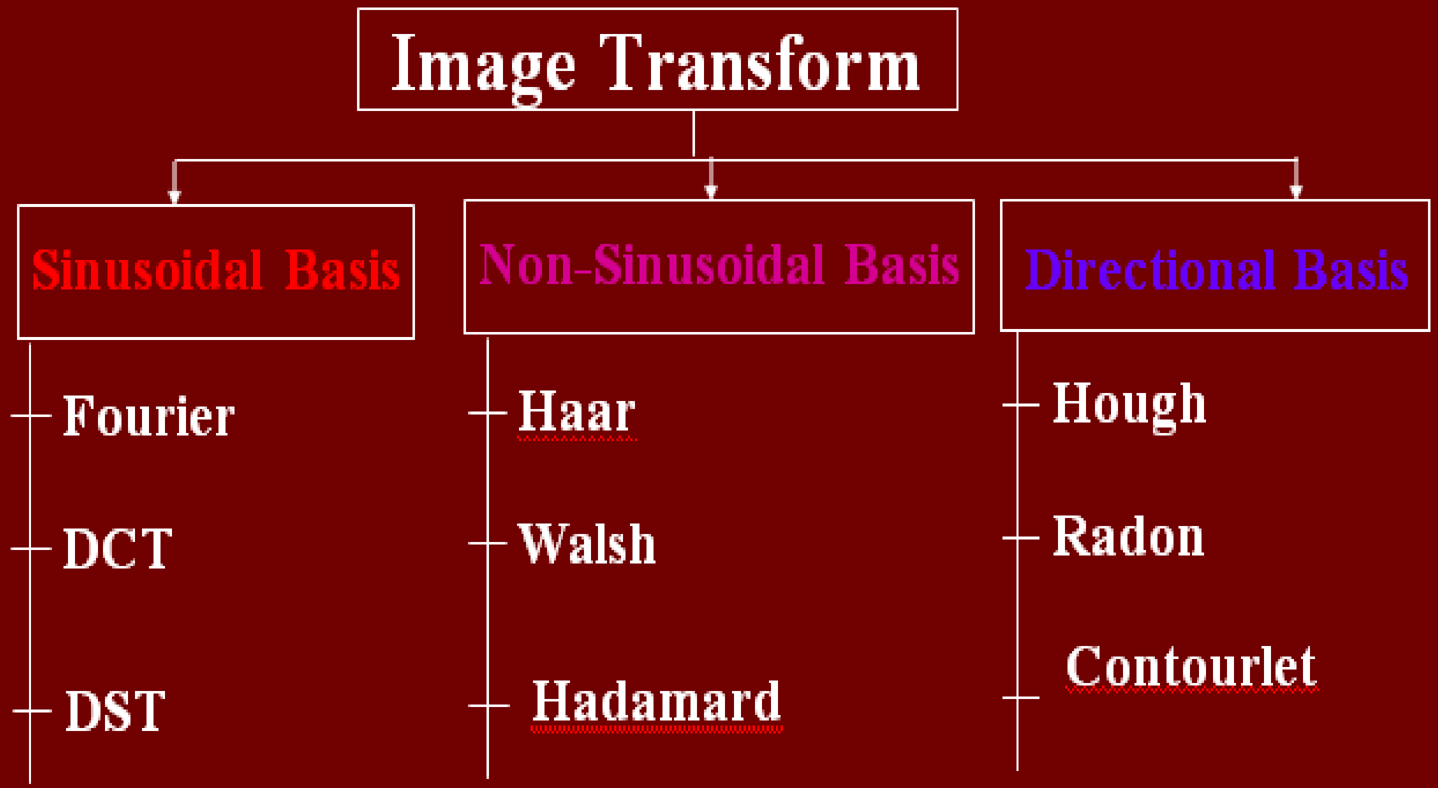

2D DFT

2D DFT from 1D DFT

$x[n] \xrightarrow{\text{1D-DFT}} X[k]$

$f[m,n] \xrightarrow{\text{2D-DFT}} F[k,l]$

$$X[k] = \sum_{n=0}^{N-1} x[n]\, e^{-j\frac{2\pi}{N}kn}$$

$$F[k,l] = \sum_{m=0}^{N-1} \sum_{n=0}^{N-1} f[m,n]\, e^{-j\frac{2\pi}{N}mk}\, e^{-j\frac{2\pi}{N}nl}$$

2-D Discrete Fourier Transform (DFT)

- 2-D DFT of an N×N image $\{u(m, n)\}$ is a separable transform defined as:

$$v(k,l) = \sum_{m=0}^{N-1} \sum_{n=0}^{N-1} u(m,n) W_N^{km} W_N^{ln}, \quad 0 \le k,l \le N-1$$

$$W_N \equiv \exp\left\{\frac{-j2\pi}{N}\right\}$$

- The 2-D DFT inverse transform is given as:

$$v(k,l) = \sum_{m=0}^{N-1} \sum_{n=0}^{N-1} u(m,n) W_N^{km} W_N^{ln}, \quad 0 \le k,l \le N-1$$

- In matrix notation: **V** = **FUF** and **U** = **F*VF***

Properties of 2-D DFT

[The $N^2 \times N^2$ matrix $\mathcal{F}$ represents the N×N 2-D unitary DFT]

- **Symmetric and unitary**

  $\mathcal{F}^T = \mathcal{F}$ and $\mathcal{F}^{-1} = \mathcal{F}^*$

- **Periodic extensions**

  $$v(k + N, l + N) = v(k, l) \qquad \forall k, l$$
  $$u(m + N, n+N) = u(m, n) \qquad \forall m, n$$

- **Sampled Fourier spectrum**

  If $\bar{u}(m,n) = u(m,n),\ 0 \le m,n \le N-1$,and $\bar{u}(m,n) = 0$ otherwise, then:

  $$\tilde{U}\left(\frac{2\pi k}{N}, \frac{2\pi l}{N}\right) = DFT\{u(m,n)\} = v(k,lx)$$

  where $\tilde{U}(\omega_1, \omega_2)$ is the Fourier transform of $\bar{u}(m,n)$

- **Fast transform**

  Since 2-D DFT is separable, it is equivalent to 2N 1-D unitary DFTs, each of which can be performed in $O(N \log_2 N)$ via the FFT. Hence the total number of operations is $O(N^2 \log_2 N)$.

Cosine transform

Discrete Cosine Transform (DCT)

- The N×N DCT matrix **C** = {$c(k, n)$}, is defined as

$$c(k,n)=\begin{cases}\dfrac{1}{\sqrt{N}}, & k=0,\ 0\le n\le N-1\\[2ex] \sqrt{\dfrac{2}{N}}\cos\dfrac{\pi(2n+1)k}{2N}, & 1\le k\le N-1,\ 0\le n\le N-1\end{cases}$$

- Properties of DCT:

1. Real and orthogonal
2. **$\mathbf{C} = \mathbf{C}^* \Rightarrow \mathbf{C}^{-1} = \mathbf{C}^T$**
3. **Not** the real part of the unitary DFT
4. Fast transform
5. Excellent energy compaction.
6. The basis vector of the DCT (rows of **C**) are eigen-vectors of symmetric traditional matrix $\mathbf{Q}_r$
7. DCT is very close to the KL (Karhunen-Loeve) transform of a first-order stationary Markov sequence.

$$\mathbf{Q}_r=\begin{bmatrix}1-\alpha & -\alpha & 0 & \mathbf{0}\\ -\alpha & 1 & \ddots & \\ 0 & \ddots & 1 & -\alpha\\ \mathbf{0} & -\alpha & & 1-\alpha\end{bmatrix}$$

1-D DISCRETE COSINE TRANSFORM

$$C(u) = a(u)\sum_{x=0}^{N-1} f(x)\cos\left[\frac{(2x+1)u\pi}{2N}\right]$$

$$u = 0, 1, \ldots, N-1$$

$$a(u) = \begin{cases} \sqrt{\frac{1}{N}} & u = 0 \\ \sqrt{\frac{2}{N}} & u = 1, \ldots, N-1 \end{cases}$$

2-D DCT

$$C(u,v) = a(u)a(v)\sum_{x=0}^{N-1}\sum_{y=0}^{N-1} f(x,y)\cos\left[\frac{(2x+1)u\pi}{2N}\right]\cos\left[\frac{(2y+1)v\pi}{2N}\right]$$

$$f(x,y) = \sum_{u=0}^{N-1}\sum_{v=0}^{N-1} a(u)a(v)C(u,v)\cos\left[\frac{(2x+1)u\pi}{2N}\right]\cos\left[\frac{(2y+1)v\pi}{2N}\right]$$

$$u, v = 0, 1, \ldots, N-1$$

Sine transform

Discrete Sine Transform (DST)

- The N×N DST matrix $\boldsymbol{\Psi} = \{\psi(k, n)\}$, is defined as

$$\psi(k,n)=\sqrt{\frac{2}{N+1}}\sin\frac{\pi(k+1)(n+1)}{N+1},\quad 0\le k,n\le N-1$$

- Properties of DST:
  1. DST is real, symmetric, and orthogonal:
  $$\boldsymbol{\Psi}^* = \boldsymbol{\Psi} = \boldsymbol{\Psi}^T = \boldsymbol{\Psi}^{-1}$$
  2. DST is not the imaginary part of the unitary DFT
  3. DST is a fast transform
  4. The basis vectors of the DFT are the eigenvectors of the symmetric tridiagonal Toeplitz matrix **Q**
  5. DST is close to the KL transform of first order stationary Markov sequences.
  6. DST leads to a fast KL transform algorithm for Markov sequence, whose boundary values are given.

Hadamard Transform

- The Hadamard transform also known as **Walsh–Hadamard transform.** It is used for image compression.
- It is an example **Fourier transforms** which performs an orthogonal, symmetric, involutive, and linear operation on 2^m real numbers.
- Also the Hadamard matrices are purely real.

Hadamard Transform

- Elements of Hadamard matrices take only the binary values ±1. The Hadamard transform matrices, $\mathbf{H}_n$, are N×N matrices, where N≡2n, n ∈ I+.
- Kronecker product recursion

$$\mathbf{H}_1 = \frac{1}{\sqrt{2}}\begin{bmatrix} 1 & 1 \\ 1 & -1 \end{bmatrix} \qquad \mathbf{H}_n = \mathbf{H}_{n-1} \otimes \mathbf{H}_1 = \frac{1}{\sqrt{2}}\begin{bmatrix} \mathbf{H}_{n-1} & \mathbf{H}_{n-1} \\ \mathbf{H}_{n-1} & -\mathbf{H}_{n-1} \end{bmatrix}$$

- Properties of Hadamard Transform:
  - The Hadamard transform is real, symmetric, and orthogonal:

$$\mathbf{H}^* = \mathbf{H} = \mathbf{HT} = \mathbf{H}^{-1}$$

  - The Hadamard transform is a fast transform {O (N log2N)}
  - The Hadamard transform has good energy compaction

Haar Transform

Haar Transform

- The Haar functions $h_k(x)$ are defined on a continuous interval, $x \in [-1,1]$ and for $k = 0, 1, \ldots, N-1$ where $N=2^n$.
- The integer k can be uniquely decomposed as: $k = 2^p + q - 1$, where $0 \le p \le n-1$; $q=0,1$ for $p=0$ and $1 \le q \le 2^p$ for $p \ne 0$.
- For Example, when N = 4 (or n=2) we have

k	0	1	2	3
p	0	0	1	1
q	0	1	1	2

Representing k by (p,q), the Haar functions are defined as:

$$h_0(x) \equiv h_{0,0}(x) = \frac{1}{\sqrt{N}},\ x \in [0,1]$$

$$h_k(x) \equiv h_{p,q}(x) = \frac{1}{\sqrt{N}} \begin{cases} 2^{p/2}, & \frac{q-1}{2^p} \le x < \frac{q-1/2}{2^p} \\ -2^{p/2}, & \frac{q-1/2}{2^p} \le x < \frac{q}{2^p} \\ 0 & \text{,daerah lain untuk } x \in [0,1] \end{cases}$$

Haar Transform

- For N=2 dan N=4:

$$\mathbf{Hr}_2 = \frac{1}{\sqrt{2}} \begin{bmatrix} 1 & 1 \\ 1 & -1 \end{bmatrix} \qquad \mathbf{Hr}_8 = \frac{1}{\sqrt{4}} \begin{bmatrix} 1 & 1 & 1 & 1 \\ 2 & 1 & -1 & -1 \\ \sqrt{2} & -\sqrt{2} & 0 & 0 \\ 0 & 0 & \sqrt{2} & -\sqrt{2} \end{bmatrix}$$

- Properties of Haar Transform:
  1. Real and orthogonal: $\mathbf{Hr} = \mathbf{Hr}^*$ dan $\mathbf{Hr}^{-1} = \mathbf{Hr}^T$
  2. Very fast transform : O(N) operation on Nx1 vector.
  3. Poor energy compaction for images

Slant Transform and its properties

Slant Transform

- The N×N Slant transform matrices are defined by the recursion

$$\mathbf{S}_N = \frac{1}{\sqrt{2}}\begin{bmatrix} 1 & 0 & \mathbf{0} & 1 & 0 & \mathbf{0} \\ a_N & b_N & & -a_N & b_N & \\ \mathbf{0} & & \mathbf{I}_{(N/2)-2} & \mathbf{0} & & \mathbf{I}_{(N/2)-2} \\ 1 & 0 & \mathbf{0} & 1 & 0 & \mathbf{0} \\ -b_N & a_N & & b_N & a_N & \\ \mathbf{0} & & \mathbf{I}_{(N/2)-2} & \mathbf{0} & & -\mathbf{I}_{(N/2)-2} \end{bmatrix}\begin{bmatrix} \mathbf{S}_{N-1} & \mathbf{0} \\ \mathbf{0} & \mathbf{S}_{N-1} \end{bmatrix} \qquad \mathbf{S}_1 = \frac{1}{\sqrt{2}}\begin{bmatrix} 1 & 1 \\ 1 & -1 \end{bmatrix}$$

where $N=2^n$ and $\mathbf{I}_M$ denotes an M×M identity matrix

- Parameters a_n dan b_n are defined by the recursions:

$$b_n = (1 + 4a^2_{n-1})^{-1/2} \quad a_1 = 1$$
$$a_n = 2b_n a_{n-1}$$

- The 4×4 Slant transformation matrix: $\mathbf{S}_2 = \frac{1}{2}\begin{bmatrix} 1 & 1 & 1 & 1 \\ \frac{3}{\sqrt{5}} & \frac{1}{\sqrt{5}} & \frac{-1}{\sqrt{5}} & \frac{-3}{\sqrt{5}} \\ 1 & -1 & -1 & 1 \\ \frac{1}{\sqrt{5}} & \frac{-3}{\sqrt{5}} & \frac{3}{\sqrt{5}} & \frac{-1}{\sqrt{5}} \end{bmatrix}$

Slant Transform Properties

- Properties:
  1. Real and orthogonal: $\mathbf{S} = \mathbf{S}^*$ and $\mathbf{S}^{-1} = \mathbf{S}^T$
  2. A fast transform: $O(N \log_2 N)$
  3. Good energy compaction

KL Transforms and their properties

KARHUNEN-LOEVE (KLT) (continuous signals)
OR
HOTELLING TRANSFORM (discrete signals)

The term KLT is the most widely used

The concepts of ***eigenvalue*** and ***eigevector*** are necessary to understand the KL transform.

If $\underline{C}$ is a matrix of dimension $n \times n$, then a scalar λ is called an eigenvalue of $\underline{C}$ if there is a nonzero vector $\underline{e}$ in R^n such that

$$\underline{C}\,\underline{e} = \lambda \underline{e}$$

The vector $\underline{e}$ is called an eigenvector of the matrix $\underline{C}$ corresponding to the eigenvalue λ.

THE CASE OF MANY REALISATIONS OF A SIGNAL OR IMAGE

Consider a population of random vectors of the form

$$\underline{x} = \begin{bmatrix} x_1 \\ x_2 \\ \vdots \\ x_n \end{bmatrix}$$

x_i may represent an image

The population may refer to the number of pixels in each image.

The *mean vector* of the population is defined as

$$\underline{m}_x = E\{\underline{x}\} \Rightarrow \begin{bmatrix} m_1 \\ m_2 \\ \vdots \\ m_n \end{bmatrix} = \begin{bmatrix} E\{x_1\} \\ E\{x_2\} \\ \vdots \\ E\{x_n\} \end{bmatrix}$$

The *covariance matrix* of the population is defined as

$$\underline{C}_x = E\left\{(\underline{x} - \underline{m}_x)(\underline{x} - \underline{m}_x)^T\right\}$$

For M vectors from a random population, where M is large enough

$$\underline{m}_x = \frac{1}{M} \sum_{k=1}^{M} \underline{x}_k$$

Let $\underline{A}$ be a matrix whose rows are formed from the eigenvectors of $\underline{C}_x$.

The first row of $\underline{A}$ is the eigenvector corresponding to the largest eigenvalue, and the last row the eigenvector corresponding to the smallest eigenvalue.

Suppose that $\underline{A}$ is a transformation matrix that maps the vectors $\underline{x}'s$ into vectors $\underline{y}'s$ by using the following transformation

$$\underline{y} = \underline{A}(\underline{x} - \underline{m}_x)$$

The above transform is called the ***Karhunen-Loeve*** or ***Hotelling*** transform.

$$\underline{y} = \underline{A}(\underline{x} - \underline{m}_x)$$

$$\underline{m}_y = \underline{0}$$

$$\underline{C}_y = \underline{A}\underline{C}_x\underline{A}^T$$

$$\underline{C}_y = \begin{bmatrix} \lambda_1 & & & 0 \\ & \lambda_2 & & \\ & & \ddots & \\ 0 & & & \lambda_n \end{bmatrix}$$

The off-diagonal elements of the covariance matrix are 0, so the elements of the $\underline{y}$ vectors are uncorrelated !

To reconstruct the original vectors $\underline{x}$ from its corresponding $\underline{y}$

$$\underline{A}^{-1} = \underline{A}^{T}$$
$$\underline{x} = \underline{A}^{T}\, \underline{y} + \underline{m}_x$$

We form a matrix $\underline{A}_K$ from the K eigenvectors corresponding to the K largest eigenvalues, yielding a transformation matrix of order $K \times n$.

The $\underline{y}$ vectors would then be K dimensional.

The reconstruction of the original vector $\underline{\hat{x}}$ is

$$\underline{\hat{x}} = \underline{A}_K{}^{T}\, \underline{y} + \underline{m}_x$$

It can be proven that the mean square error between the perfect reconstruction $\underline{x}$ and the approximate reconstruction $\hat{\underline{x}}$ is given by the expression

$$e_{ms} = \left\| \underline{x} - \hat{\underline{x}} \right\|^2 = \sum_{j=1}^{n} \lambda_j - \sum_{j=1}^{K} \lambda_j = \sum_{j=K+1}^{n} \lambda_j$$

By using $\underline{A}_K$ instead of $\underline{A}$ for the KL transform we achieve compression of the available data.

THE CASE OF ONE REALISATION OF A SIGNAL OR IMAGE

We assume that the 2-D signal (image) is ***ergodic***.

Usually we divide the image into blocks and we apply the KLT in each block.

Mean vector inside the block:

$$m_f = \frac{1}{M^2} \sum_{k=1}^{M^2} \underline{f}(k)$$

Covariance matrix of the 2-D random field inside the block is $\underline{C}_f = \{c_{ij}\}$:

$$c_{ii} = \frac{1}{M^2} \sum_{k=1}^{M^2} \underline{f}(k)\underline{f}(k) - m_f^{\ 2}$$

$$c_{ij} = c_{i-j} = \frac{1}{M^2} \sum_{k=1}^{M^2} \underline{f}(k)\underline{f}(k+i-j) - m_f^{\ 2}$$

Drawbacks of KL Transform

Despite its favourable theoretical properties, the KLT is not used in practice, because:

i) Its basis functions depend on the covariance matrix of the image, and hence they have to recomputed and transmitted for every image.

ii) Perfect decorrelation is not possible, since images can rarely be modelled as realisations of ergodic fields.

iii) There are no fast computational algorithms for its implementation.


#D2578
THANK YOU
FOR YOUR
ATTENTION
PRESENTATIONLOAD

IMAGE RESTORATION AND RECONSTRUCTION OF MEDICAL IMAGES

Dr Kamalraj Subramaniam
Associate Professor
Department of Biomedical Engg
FOE
Karpagam Academy of Higher Education

Image Restoration

- Restoration is a process of reconstructing or recovering an image that has been degraded by using a priori knowledge of the degradation phenomenon.
- Thus restoration techniques are oriented towards modeling the degradation and applying the inverse process in order to recover the original image.

Image Degradation Model

- Objective: To restore a degraded/distorted image to its original content and quality.

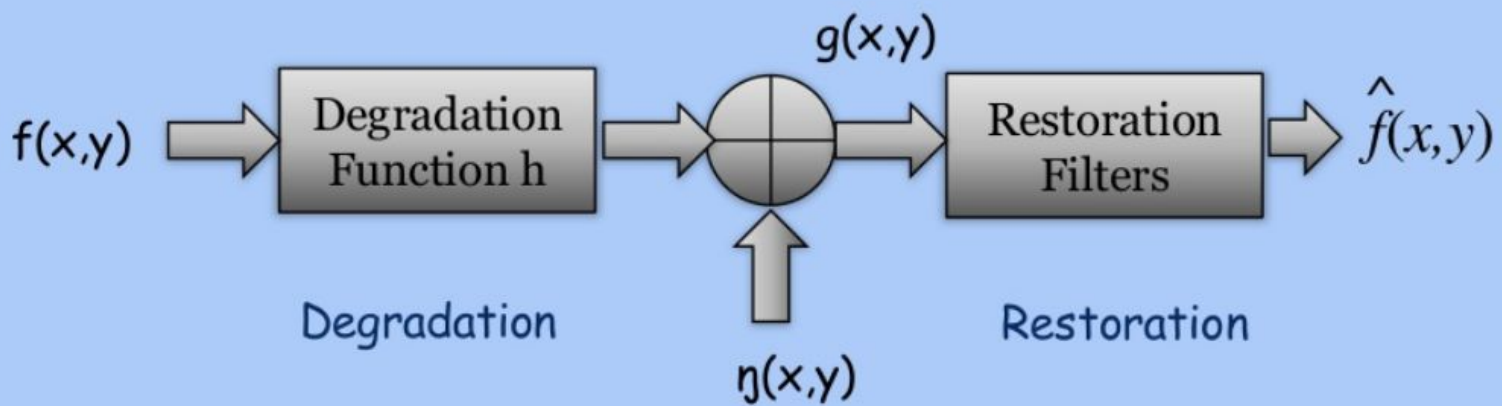

- Spatial Domain: $g(x,y)=h(x,y)*f(x,y)+ \eta(x,y)$
- Frequency Domain: $G(u,v)=H(u,v)F(u,v)+ \eta(u,v)$
- Matrix: $G=HF+\eta$

Constrained Restoration

- It is also known as maximum square error approach n = g-Hf.
- To estimate the original image f^, noise n has to be maximized and f^ = g/H.

Unconstrained Restoration

- It is also known as least square error approach. n = g-Hf To estimate the original image f^, noise n has to be minimized and f^ = g/H Where, H = system operator.
- f^ = estimated input image. g = degraded image.

Inverse Filtering

- Inverse filtering is the process of recovering the input of the system from its output.
- The simplest approach to restoration is direct inverse filtering, an estimate F^(u,v) of the transform of the original image simply by dividing the transform of the degraded image G^(u,v) by the degradation function.
- F^ (u,v) = G^(u,v)/H(u,v)

Image Restoration by Inverse Filtering

The purpose of image restoration is to estimate or recover the scene without image degradation or distortion caused by non-ideal image system (e.g. the optics of the camera system). Inverse filtering is one of the techniques used for image restoration to obtain a recovered image $f'(x,y)$ from the image data $g(x,y)$ so that $f'(x,y) = f(x,y)$ in the ideal situation $n(x,y) = 0$ and $h(x,y) * h'(x,y) = \delta(x,y)$ or $H(\omega_x, \omega_y) H'(\omega_x, \omega_y) = 1$.

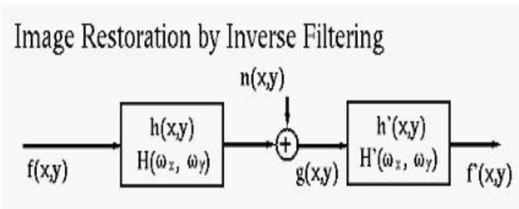

The camera system for image acquisition can be modeled mathematically by

$$g(x,y) = \int_0^T \int\int_{-\infty}^{\infty} h(x,y,x',y',t) f(x',y',t) dx'dy'dt + n(x,y)$$

where T is the exposure time, $n(x,y)$ is some additive noise, and $h(x,y,x',y',t)$ is a function characterizing the distortion introduced by the imaging system, caused by, for example, limited aperture, out of focus, random atmospheric turbulence, and/or relative motion. If the system is ideal, spatial and time invariant, and noise-free, i.e.,

$$h(x,y,x',y',t) = \delta(x-x', y-y')$$

then the imaging process becomes

$$g(x,y) = \int_0^T f(x,y,t) dt$$

If the signal is also time invariant (a stationary scene), i.e., $f(x,y,t) = f(x,y)$, the image obtained is simply

$$g(x,y) = T\, f(x,y)$$

We consider the correction of some possible distortions that may occur during image acquisition.

Least-Mean-Square (LMS) Algorithm.

$$\begin{pmatrix}\text{update value}\\ \text{of tap - weigth}\\ \text{vector}\end{pmatrix} = \begin{pmatrix}\text{old value}\\ \text{of tap - weight}\\ \text{vector}\end{pmatrix} + \begin{pmatrix}\text{learning -}\\ \text{rate}\\ \text{parameter}\end{pmatrix}\begin{pmatrix}tap -\\ input\\ vector\end{pmatrix}\begin{pmatrix}error\\ signal\end{pmatrix}$$

In the family of stochastic gradient algorithms

Approximation of the steepest – descent method

Based on the MMSE criterion.(Minimum Mean square Error)

Adaptive process containing two important signals:

1.) Filtering process, producing output signal.

2.) Desired signal (Training sequence)

Adaptive process: Recursive adjustment of filter tap weights

The LMS Algorithm consists of two basic processes that is followed in the adaptive equalization processes:

Training : It refers to adapting to the training sequence.

Tracking: keeps track of the changing characteristics of the channel.

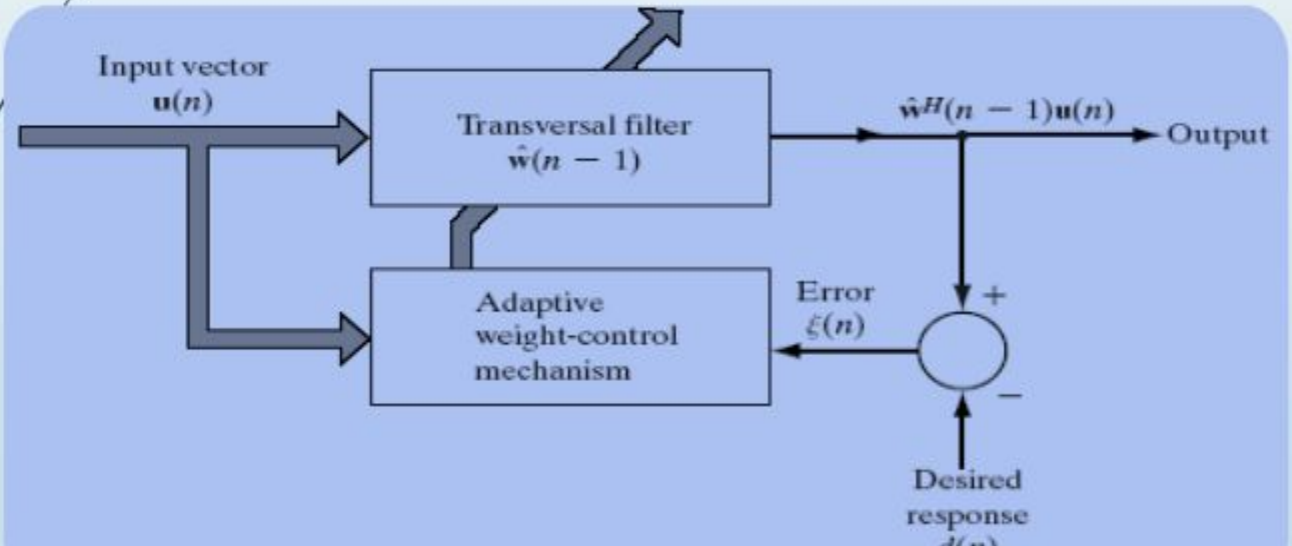

(a)

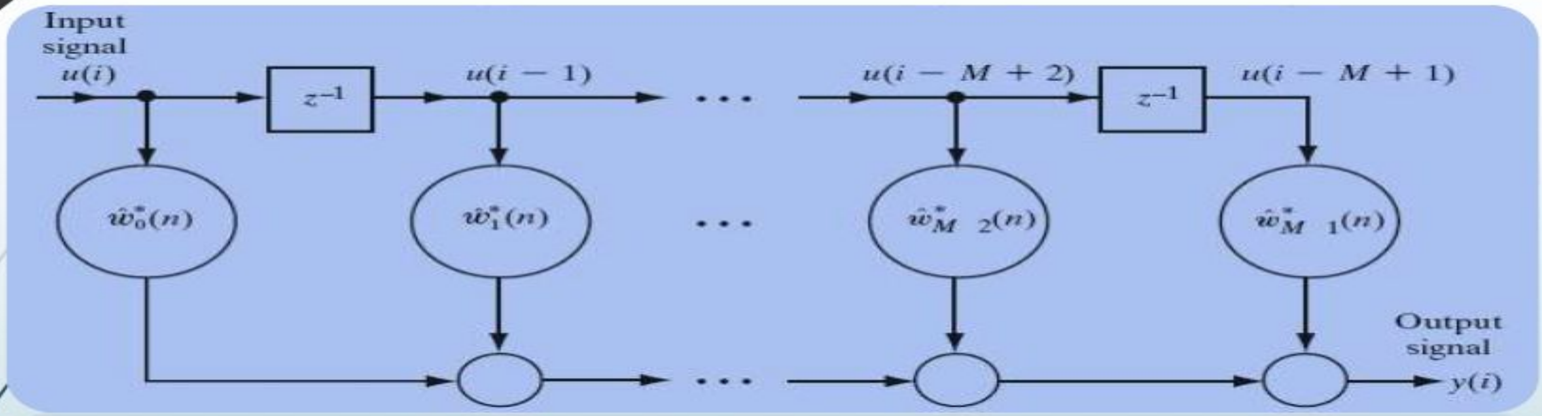

Transversal Filter

LMS Algorithm Steps:

Filter output $$z[n]=\sum_{k=0}^{M-1}u[n-k]w_k^*[n]$$

Estimation error $$e[n]=d[n]-z[n]$$

Tap-weight adaptation

$$w_k[n+1]=w_k[n]+\mu u[n-k]e^*[n]$$

Stability of LMS:

- The LMS algorithm is convergent in the mean square if and only if the step-size parameter satisfy

$$0 < \mu < \frac{1}{\lambda_{max}}$$

Here λ_{max} is the largest Eigen value of the correlation matrix of the input data.

- More practical test for stability is

$$0 < \mu < \frac{1}{\text{input signal power}}$$

- Larger values for step size

Increases adaptation rate (faster adaptation)

Increases residual mean-squared error

LMS – Advantage:

- Simplicity of implementation
- Not neglecting the noise like Zero forcing equalizer
- Stable and robust performance against different signal conditions

LMS – Disadvantage:

- Slow Convergence
- Demands using of training sequence as reference ,thus decreasing the communication BW.

Random Transform

Radon Transform

- Computes the projection of an image matrix along specific axes

$$R(\rho, \theta) = \int_L f(x, y) dL$$

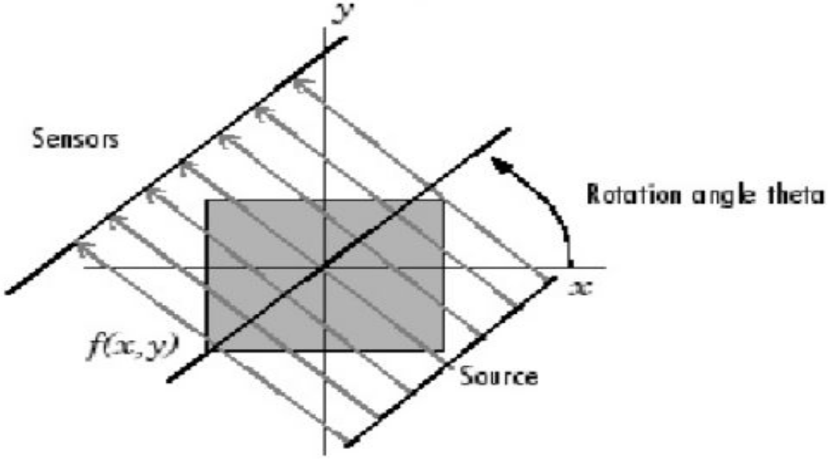

Filter Bank Projection

- A Digital filter bank is a collection of filters having a common input or output.
- 2 types of filter banks

  Analysis filter bank

  Synthesis filter bank

1-D AND 2-D FILTER BANKS

1-D FILTER BANK

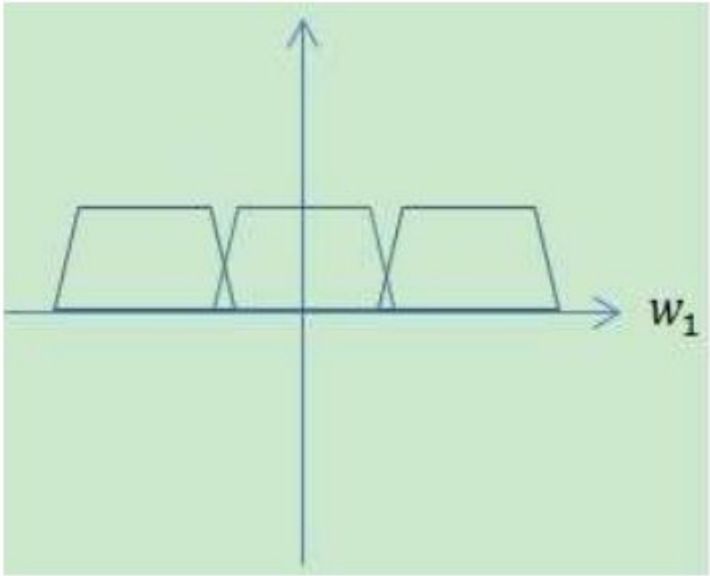

2-D FILTER BANK

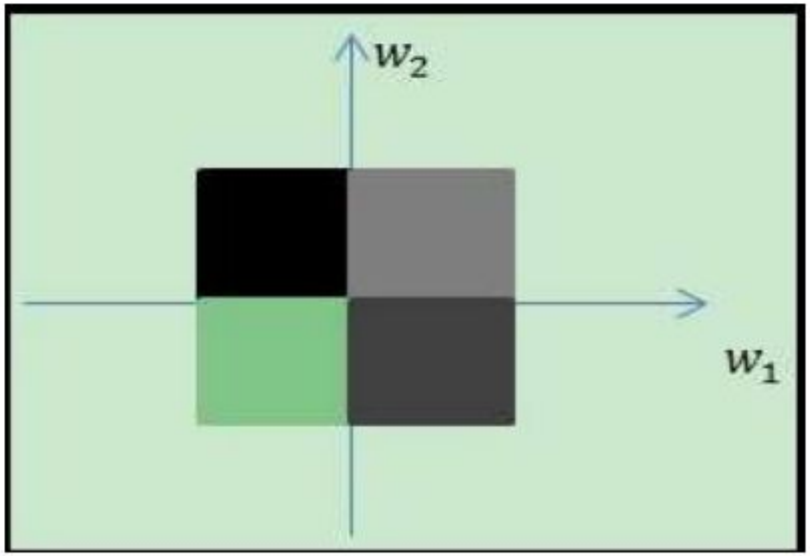

MULTIDIMENSIONAL ANALYSIS AND SYNTHESIS FILTER BANKS

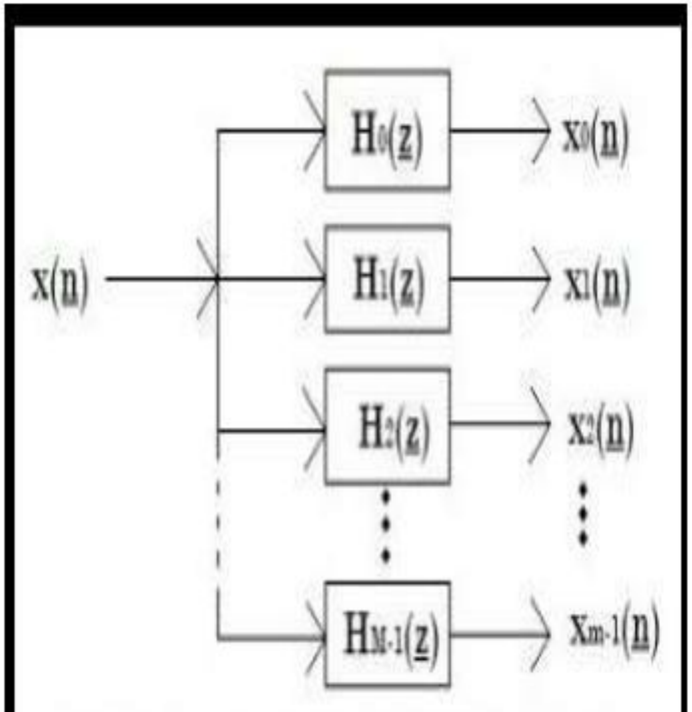

Multidimensional Analysis Filter Banks

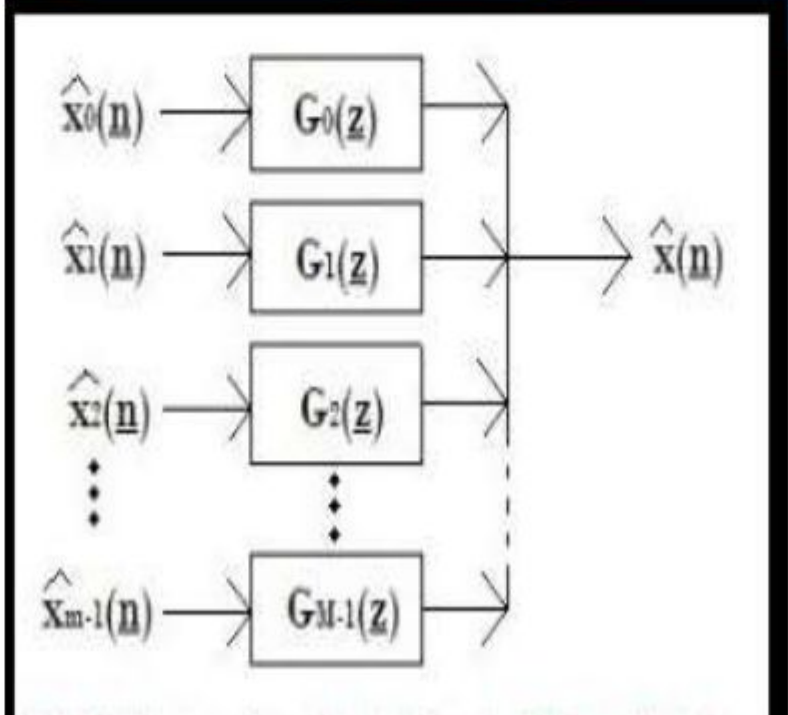

Multidimensional Synthesis Filter Banks

Thank You!!!

CHAPTER 2

IMAGE COMPRESSION TECHNIQUES

2.1 GENERAL

Image compression algorithms are broadly classified into lossless and lossy algorithms. The lossless algorithm preserves the original data, such that the original and the decompressed images are exactly equal. In a lossy compression, the decompressed image will not be identical to the original one. There are sub-classes for both the approaches. This chapter gives an overview of the lossless and lossy algorithms, entropy coding techniques, image quality measures and the simulation environment.

2.2 PRINCIPLE OF IMAGE COMPRESSION

The objective of an image compression algorithm is to reduce the number of bits required to represent an image, by removing the redundant information. There are three types of redundancies that can be exploited by the compression algorithms; inter-pixel, psycho-visual and coding redundancies (Gonzalez & Woods 2002). The image compression is realized by removing one or more of these redundancies.

Inter-pixel redundancies arise due to the correlation of the neighbouring pixels within an image. Predictive and transform coding techniques are normally employed for removing the inter-pixel redundancies. Psycho-visual redundancy is associated with the visual information. Since the human eye is less sensitive to high frequency components, these components can be treated as psycho-visually redundant, and hence ,can be removed from the image without affecting the visual quality. The end result of the removal of data in this way is a loss of quantitative information; hence it is called as quantisation. Quantisation is an irreversible operation and leads to lossy compression. The coding redundancy is removed by the use of entropy encoding techniques, such as Huffman coding and Arithmetic coding.

2.3 PREDICTIVE TECHNIQUES

Predictive coding techniques utilize the inter-pixel correlation present in the images. The DPCM is the first predictive coding technique that exploits the spatial correlation characteristics of images. Instead of encoding the actual pixel, the DPCM coder extracts the new information in each pixel, which is the difference between the current pixel and the predicted pixel value. The new information is sent for further encoding.

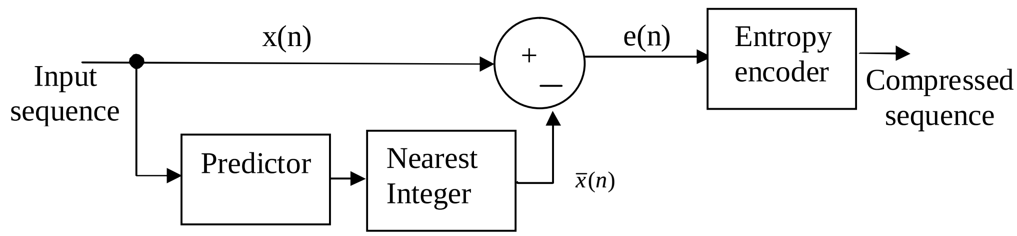

(a) Encoder

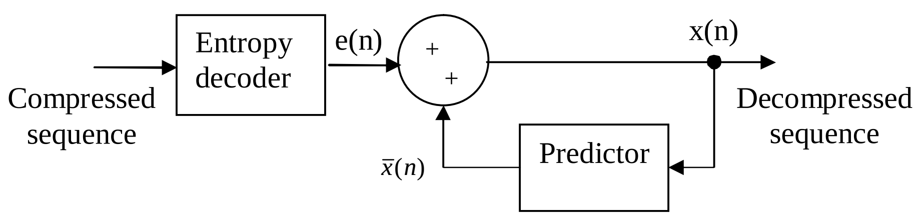

(b) Decoder

Figure 2.1 The Lossless DPCM coder

The encoder and the decoder shown in Figure 2.1 have a similar type of predictor unit. In order to encode an image, each consecutive pixel is fed as input to the encoder. The predictor unit predicts the expected value of the current pixel based on a weighted linear combination of the neighbouring pixels. Let the current pixel be x(n) (Jain, 1989) . The predicted pixel $\bar{x}(n)$ is given by Equation (2.1) as,

$$\bar{x}(n) = \sum_{k=1}^{m} p_k x(n) \tag{2.1}$$

where p_k are the prediction coefficients with i=1,2...m. The predicted pixel values are rounded off to the nearest integer, to generate integer difference values. The difference between the original pixel value and the predicted value is the prediction error for that pixel, which is sent to the entropy encoder. The prediction error e(n) is calculated by using Equation (2.2).

$$e(n) = x(n) - \bar{x}(n) \tag{2.2}$$

The image formed by using the prediction error values is referred to as the difference image or the prediction residual image. The entropy of the residual image is much lower than that of the original image. The prediction coefficients are generally computed using the Yule-Walker equations. The lossy compression is implemented in the DPCM coder by quantising the difference image.

The most widely used predictive coder is the JPEG-LS (Joint Photographic Experts Group-Lossless Standard), which is also the current standard for the lossless and near-loss compression of continuous tone images. The JPEG-LS is briefly explained in Section 2.3.1.

2.3.1 THE JPEG-LS

The algorithm behind the JPEG-LS is Low Complexity lossless compression for Images (LOCO-I). This algorithm uses a probability modelling scheme, which consists of a prediction step, determination of a context, and a probabilistic model for the prediction residual.

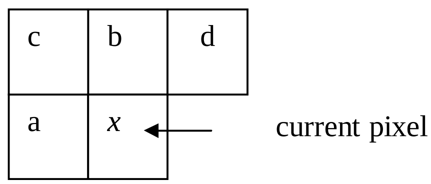

Figure 2.2 Neighbours of the current pixel x

Let *x* denote the current pixel. Figure 2.2 shows the neighbouring pixels a, b, c and d, which form the causal template for *x*. The causal template is used to detect the localised horizontal or vertical edges in the image. The predicted value for the current pixel *x* is obtained by switching between the three predictors (Weinberger et al 1996) as given in Equation (2.3).

$$x = \begin{cases} \min(a,b) & \text{if } c \geq \max(a,b) \\ \max(a,b) & \text{if } c \leq \min(a,b) \\ a+b-c & \text{otherwise} \end{cases} \tag{2.3}$$

If a vertical edge is present to the left of *x*, then the predictor selects *b*, and selects *a* if there is a horizontal edge above *x*. If there is no edge, the third option *a+b-c* is chosen. Since the values guessed by the predictor are the median of the three fixed predictors a, b and a+b-c, the predictor is named as the Median Edge Detector (MED).

2.3.1.1 Context modelling/determination

The context modelling in JPEG-LS is performed to reduce the number of coding parameters, which consist of a number of contexts and the number of free parameters defining the coding distribution at each context.

The prediction residuals of an image can be modelled using a Two Sided Geometric Distribution (TSGD), centred at zero. The TSGD centred at zero generates a bimodal distribution, with equal peaks at -1 and 0. Let ε denote the prediction residual. The range of ε lies in between $-\alpha$ and $+\alpha$, where α gives the size of the image alphabet. Since ε can take only α possible values, the range of α is reduced to $-(\frac{\alpha}{2})$ to $+ (\frac{\alpha}{2})-1$. This reduction is equivalent to cutting the tails of the geometric distribution without affecting the distribution significantly.

The difference values g_1=d-b, g_2=b-c and g_3=c-a are calculated to find the contexts. These values represent the local gradient, and give an idea about the smoothness and the edge activity in the image around the current pixel. These contexts are quantised by applying a quantiser, thus reducing the total number of contexts. The number of context regions are further optimised by using the symmetry property. The symmetry is preserved by indexing the regions as $-T,\ldots-1,0,+1,\ldots+T$, thus generating totally $(2T+1)^3$ contexts. The regions of opposite signs are merged to reduce the number of contexts to $\frac{(2T+1)^3}{2}$. A total of 365 contexts are defined in the JPEG-LS when T is equal to four.

Once the context modeling is performed, a Golomb-Rice encoder is used to implement the entropy encoding, which is optimal for a geometric distribution. There is no need to store the code table in a Golomb-Rice coder, whereas the Huffman coding uses a code table. Given a positive value *m*, the Golomb-Rice coder encodes a positive integer ‘n’ into two parts, a binary representation n mod m, and a unary representation $\left\lfloor \frac{n}{m} \right\rfloor$. The complexity of the encoding process is reduced by choosing the value of m as the power of 2.

2.3.2 The CALIC

The CALIC is a spatial domain approach for the lossless and the near-lossless compression of the images. This coder was developed in response to the requirement for a new lossless image compression standard by the JPEG group. The prediction in the CALIC algorithm is made by considering two previous scan lines. A buffer which can store two lines of pixel values is thus sufficient during encoding.

The CALIC encoder employs a gradient based adaptive non-linear predictor, named the Gradient-Adjusted Predictor (GAP). The GAP weights the neighbouring pixels of the current pixel x(m,n) according to the gradients. Two types of gradients, namely, the horizontal gradient (d_h) and the vertical gradient (d_v), are computed using Equations (2.4) and (2.5) respectively (Wu & Memon 1997).

$$d_h=|x[m-1,n]-x[m-2,n]|+|x[m,n-1]-x[m-1,n-1]|+|x[m+1,n-1]-x[m,n-1]| \tag{2.4}$$

$$d_v= |x[m-1,n] - x[m-1,n-1]|+ |x[m,n-1] -x[m,n-2]|+ |x[m+1,n-1]-x[m+1,n-2]| \tag{2.5}$$

The prediction process is carried out by using the following procedure, to get a predicted pixel $\overline{x}(m,n)$:-

If (d_v-d_h>80) {sharp horizontal edge}
$\overline{x}(m,n) = w$
else if (d_v-d_h<-80) {sharp vertical edge}

$\bar{x}(m,n)$ = n

else {

$\bar{x}(m,n)$ = (w+n)/2 +(ne - nw)/4

if (d_v - d_n>32) {horizontal edge}

$\bar{x}(m,n)$ = ($\bar{x}(m,n)$ +w) /2

else if (d_v-d_h>8) {weak horizontal edge}

$\bar{x}(m,n)$ = (3. $\bar{x}(m,n)$ +w)/4

else if (d_v-d_h<-32) {vertical edge}

$\bar{x}(m,n)$ = ($\bar{x}(m,n)$ +n)/2

else if (d_v-d_h<-8) {weak vertical edge}

$\bar{x}(m,n)$ = (3. $\bar{x}(m,n)$ /4

}

where

n = *x*(m, n-1) , w =*x*(m-1, n) , ne = *x*(m+1, n-1)

nw = *x*(m-1, n-1) , nn = *x*(m, n-2), ww =x(m-2, n)

The context of the current pixel x(m,n) is formed as a vector, which is given in Equation (2.6).

$$Y= [N, W, NW, NE, NN, WW, NNE] \tag{2.6}$$

Figure 2.3 shows the positions of the pixels which form the vector Y.

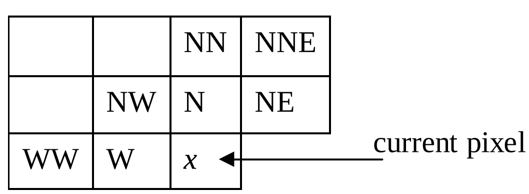

Figure 2.3 Context of the pixel x

The predicted value $\bar{x}(m,n)$ is compared with each component of this vector, Y. If Y(k) < $\bar{x}(m,n)$, then it is replaced with 1, else with 0. The pixel vector Y now becomes a binary vector, B= [b_7 b_6….. b_1b_0]. This one byte pattern B indicates the behaviour of the error. Since the vector is eight bits long, totally 256 vectors are possible. The dependency between the vectors has been analysed through context quantization, to reduce the total number of vectors from 256 to 144.

The predicted value $\overline{x}(m,n)$ is further adjusted by finding the residual error $|x - \overline{x}|$ and forming eight different error energy contexts. These contexts are formed by quantising an error energy estimator δ into eight bins, as shown in Equation (2.6).

$$\delta = d_h + d_v + 2\,|x - \overline{x}| \tag{2.7}$$

The energy estimate δ is divided into four levels to get four context error energies, which are further quantised using an eight level quantizer. The quantised context and the quantised context energy are combined to form a compound modelling context C(δ, β). This makes the context a function of two features; the spatial texture, and the energy in the prediction errors. The final context is formed as shown in Equation (2.8).

$$C(\delta, \beta) = \{x_1 x_0 \;\; b_7 b_6 \ldots\ldots b_1 b_0\} \tag{2.8}$$

where x_1x_0 represent the four levels of the energy. Considering these 4 levels, the total number of contexts becomes 576. This step completes the context modelling of the prediction error. The modelled error is encoded, using an arithmetic coder before transmission.

Among the various context based techniques, the CALIC gives the highest compression ratio. However, it has higher computational complexity than the JPEG-LS.

2.4 TRANSFORM BASED TECHNIQUES

Transform based coding is another method to eliminate the inter-pixel redundancies present in the images. The transforms have the energy compaction property; they pack the most information into a few transform coefficients. The remaining coefficients may be quantised with imperceptible distortion in the reconstructed image. The quantisation is performed by dividing the transform coefficients by the values from a quantisation table, which is designed based on the properties of the human visual system. The transforms used in image compression applications can be classified as block based and wavelet based methods. The block based transforms are constructed using the Discrete Cosine Transform (DCT), and the wavelet transforms are generated by using scaling and wavelet functions. The JPEG is based on the DCT, while the JPEG-2000 uses the DWT for the image coding. A short description of the JPEG and the JPEG2000 coders is given in Sections 2.4.1 and 2.4.2 respectively.

2.4.1 THE JPEG

The JPEG compression algorithm is the most commonly used lossy compression method for the compression of still images. This algorithm uses the DCT, and the coder is optimised for the photographic images. It has four compression modes namely, sequential, progressive, hierarchical and lossless. The sequential mode of JPEG compression is the most widely used method.

In the sequential mode, the compression process starts with the level shifting of the image pixels. Then, the image is divided into 8x8 blocks. The pixels in each block are transformed from the spatial domain to the transform domain using the DCT to produce 64 transform coefficients per block. Since the values of many of these coefficients are small, they are quantised by using a perceptually weighted quantisation table. The quantised coefficients are zig-zag scanned, so that they are arranged in the increasing order of the frequency. After identifying the DC and AC transform coefficients, the DC coefficients are encoded using a DPCM encoder, and the AC coefficients are encoded using a run-length encoder. Finally, the coefficients are entropy coded to generate the bit stream.

The lossy compression ratio is controlled in the JPEG encoder using a quality factor Q, which controls the values in the quantisation table. However, the method remains lossy even when Q assumes the value of hundred. There is a lossless option for the JPEG, which uses a predictive approach, and is not very successful due to a small compression ratio.

2.4.2 THE JPEG 2000

The JPEG 2000 is the current international standard for still image compression. The JPEG approach processes the image block by block, leading to blocky artefacts for low bit rates. Since the wavelet transform is applied to the entire image, the blocky effect is completely eliminated. Even for a block-based wavelet transformation, the blocky effect is significantly reduced. The JPEG 2000 has both lossless and lossy options.

In the JPEG 2000 coding, the compression process starts by shifting the level of the pixels. The level shifted image is divided into rectangular regions called tiles. A single tile is equivalent to using the image as a whole. The tiling process helps to extract the regions of the images, and to encode them independently. The tiling process is illustrated in Figure 2.4.

After the tiling process, the DWT is applied to each tile for generating the transform coefficients. The wavelet transform coefficients are subjected to the quantisation process, to get lossy compression for the image. Sub-band quantisation techniques are normally employed. The quantised wavelet coefficients are grouped using a context model to increase the efficiency of the compression. Further, entropy encoding is performed using the arithmetic coder to generate a compressed bit stream. The bit stream is assembled into packets and transmitted.

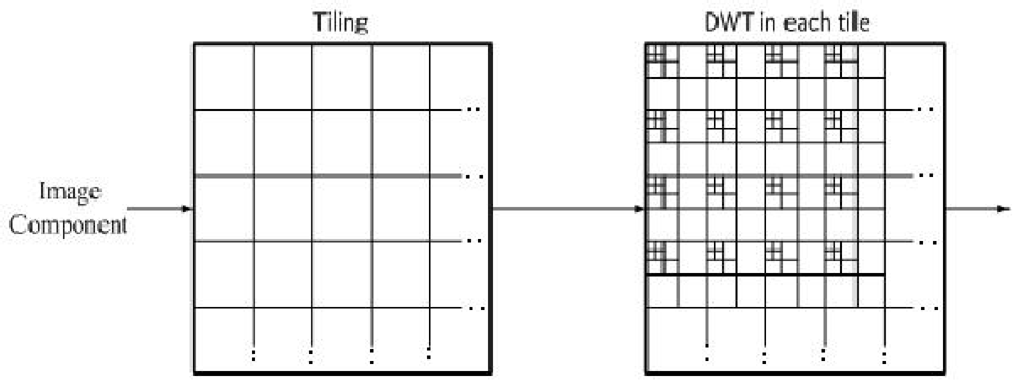

Figure 2.4 Tiling in the JPEG 2000

The main features of the JPEG 2000 coder are scalability, error resilience and the facility for Region of Interest (ROI) coding. The scalability is the ability to decode the image at various resolutions. While the low performance decoders decode the low resolution image at the basic quality, the high performance ones decode the image at full resolution at higher quality. The error resilience feature is added to facilitate the transmission of the compressed image over noisy channels. Data partitioning and resynchronisation tools are added in the coder to deal with channel errors. The ROI coding facility allows the coding of a certain part of the image with better quality than the rest of the image.

Since the JPEG 2000 is based on the DWT, a brief overview of this transform is given in Section 2.4.2.1.

2.4.2.1 The discrete wavelet transform

Consider a discrete sequence f(u), which is expressed as a linear combination of basis functions as given (Gonzalez & Woods 2002) in Equation (2.9).

$$f(u) = \sum_k a_k \phi_k(u) \tag{2.9}$$

where k is the index of the finite or infinite sum, $\varphi_k(u)$ are the basis functions and a_k are the expansion coefficients. If the expansion functions a_k are orthonormal, they can be calculated as the inner product of the basis function $\varphi_k(u)$ and f(u), as given by Equation (2.10) .

$$a_k = < \varphi_k(u), f(u)> \tag{2.10}$$

A set of basis functions $\{\varphi_{j,k}(u)\}$ can be generated by the integer translations, and binary scaling of the function $\varphi(u)$. The j value determines the width of $\varphi_{j,k}(u)$ and k decides the position of the function $\varphi_{j,k}(u)$ along the x-axis.. Since the shape of $\varphi_{j,k}(u)$ varies with j, $\varphi(u)$ is called a scaling function. The scaling functions are determined using the expression given in Equation (2.11).

$$\varphi(u) = \sum_n h_\varphi(n)\sqrt{2}\varphi(2u - n) \tag{2.11}$$

The $h_\phi(n)$ coefficients are called scaling function coefficients. For a scaling function, a wavelet function $\psi(u)$ can be defined. The set $\{\psi_{j,k}(u)\}$ is defined as,

$$\psi_{j,k}(u) = 2^{j/2}\,\psi(2^j u - k) \quad \text{for all } k \in Z \tag{2.12}$$

The wavelet functions are defined such that < $\varphi_{j,k}(u)$, $\psi_{j,l}(u)$ > = 0. Similar to the scaling function, the wavelet functions can be also expressed as a weighted sum of shifted scaling functions.

$$\psi(u) = \sum_n h_\Psi(n)\sqrt{2}\varphi(2u-n) \qquad (2.13)$$

In Equation (2.13), $h_\psi(n)$ are called the wavelet function coefficients and they are related to $h_\varphi(n)$ as,

$$h_\psi(n) = (-1)^n\, h_\varphi(1 - n) \qquad (2.14)$$

This relationship shows that, the wavelet function coefficients can be generated from the scaling function coefficients. In the multi resolution analysis, a scaling function is used to generate a series of approximations of a function, and the wavelet function is used to encode the difference between neighbouring approximations. Using the scaling functions and the wavelet functions, a given function f(u) can be expanded and written, as shown in Equation (2.15).

$$f(u) = \frac{1}{\sqrt{M}}\sum_k W_\phi(j_0,k)\ \phi_{j0,k}(u) + \frac{1}{\sqrt{M}}\sum_{j=j0}^{\infty}\sum_k W_\psi(j,k)\ \psi_{j,k}(u) \qquad (2.15)$$

where u=0,1.., M-1. The value $\frac{1}{\sqrt{M}}$ is a normalisation factor. The symbol j_0 indicates an arbitrary starting scale. The $W_\varphi(j_0,k)$ are called the approximation coefficients and $W_\psi(j,k)$ are the detail or wavelet coefficients. This means that, the function *f(u)* can be represented using the approximation coefficients and detail coefficients.

Let $W_\phi(j,k)$ and $W_\psi(j,k)$ represent the scale j approximation and detail coefficients respectively. They can be computed by convolving the scale (j+1) approximation coefficient $W_\phi(j+1,k)$ with the time reversed scaling and wavelet coefficient vectors $h_\phi(-n)$ and $h_\psi(-n)$, and sub-sampling the results. Since the convolutions are evaluated at n=2k, this is equivalent to filtering and down-sampling by two. The filter bank used for this type of filtering is called the analysis filter bank, which is shown in Figure 2.5.

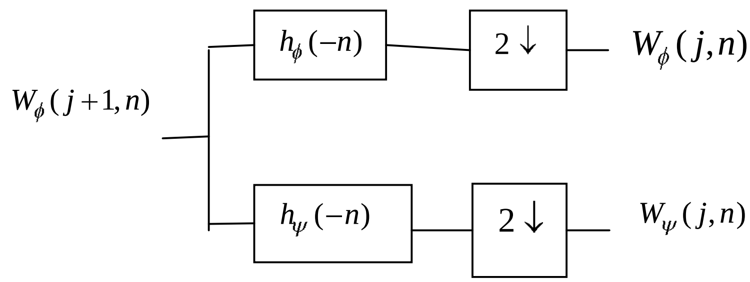

Figure 2.5 The 1-D DWT analysis filter bank

The 1-D wavelet transform can be extended to two dimensional functions like images, by using a 2-D scaling function and three 2-D wavelet functions. However, if the 2-D transform is separable, then the 2-D functions can be expressed as the product of 1-D functions. The separable transforms are computationally efficient with a time complexity of $O(N^2)$ when compared to the complexity of $O(N^4)$ of the 2-D transforms. Let the 2-D scaling function be $\varphi(u,v)$ and the three 2-D wavelet functions be $\psi_{LH}(u,v)$, $\psi_{HL}(u,v)$ and $\psi_{HH}(u,v)$. Using the separability property, these functions can be expressed as the product of the 1-D scaling function φ and the 1-D wavelet function ψ. The 2-D separable scaling function and the wavelet functions are given as,

$$\Phi(u,v) = \varphi(u)\varphi(v) \tag{2.16}$$

$$\psi_{LH}(u,v) = \psi(u)\ \varphi(v) \tag{2.17}$$

$$\psi_{HL}(u,v) = \varphi(u)\ \psi\ (v) \tag{2.18}$$

$$\psi_{HH}(u,v) = \psi\ (u)\ \psi\ (v) \tag{2.19}$$

These wavelet functions can be used to measure the variations in the images along different directions. The function $\psi_{LH}(u,v)$ measures the variations along columns (horizontal edges), while the function $\psi_{HL}(u,v)$ finds the variations along rows (vertical edges) and $\psi_{HH}(u,v)$ finds the diagonal variations.

Let f(u,v) be a two dimensional function of size MxN. Using separable two dimensional scaling and wavelet functions, the 2-D DWT of f(u,v) is given by Equations (2.20) and (2.21)

$$W_{\phi}(j_0,m,n) = \frac{1}{\sqrt{MN}} \sum_{u=0}^{M-1} \sum_{v=0}^{N-1} f(u,v)\ \phi_{j0,m,n}(u,v) \tag{2.20}$$

$$W_{\psi}^{t}(j,m,n) = \frac{1}{\sqrt{MN}} \sum_{u=0}^{M-1} \sum_{v=0}^{N-1} f(u,v)\ \psi_{j,m,n}^{t}(u,v) \qquad t=\{LH,HL,HH\} \tag{2.21}$$

The superscript index t is used to indicate the three wavelets given in Equations (2.17) to (2.19). Typical value for j_0 is zero and j=0, 1,…, J-1. The value J is selected such that $M=N=2^J$ and m, n= 2^j -1. Similar to the 1-D DWT, the 2-D DWT can be implemented using filters and down-sampling blocks. This implementation is shown in Figure 2.6.

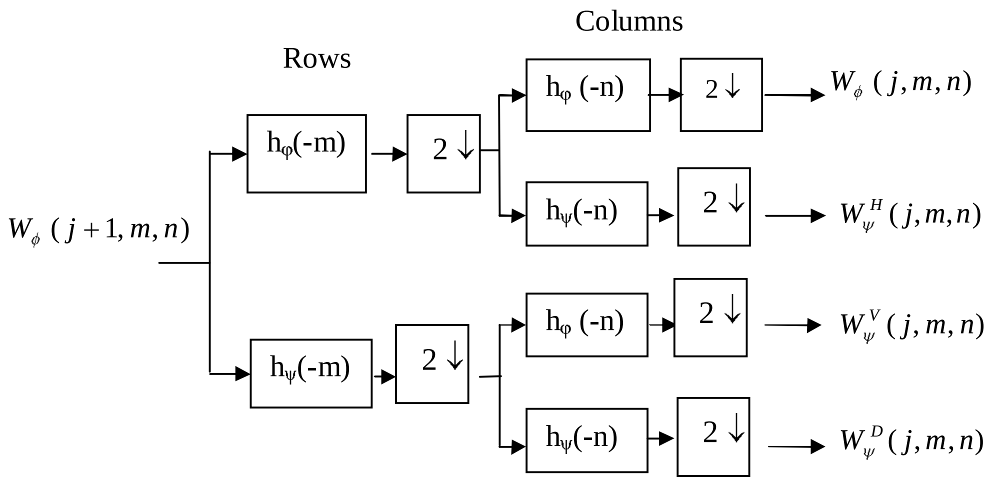

Figure 2.6 The 2-D discrete wavelet transform

In order to decompose an image using the 2-D DWT, the 1-D transform is first applied to the rows of the image, and then applied to the columns of the row transformed image. The application of the 1-D transform to each row gives one approximation sub band and one detailed sub band (L and H sub bands). By applying the 1-D transform on these L and H sub bands, four sub bands are generated; the approximation sub band (LL), horizontal sub band(HL), vertical sub band (LH) and detail sub band(HH). The LL is the low frequency version of the original image, called as the approximation image, while the LH, HL, HH are referred to as the high frequency sub bands. This is the first level of decomposition, and is shown in Figure 2.7.

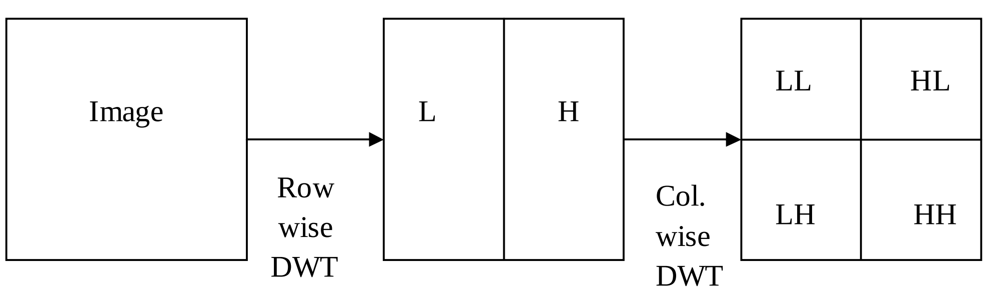

Figure 2.7 Single level wavelet decomposition

For the second level of decomposition, the 1-D transform is applied to the rows and columns of the approximation image. Figure 2.8 shows the two level wavelet decomposition process. This process is called as pyramidal decomposition.

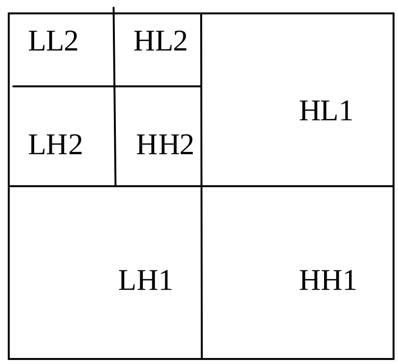

Figure 2.8 Two level wavelet decomposition

A two level wavelet decomposition of a CT brain image is shown in Figure 2.9.

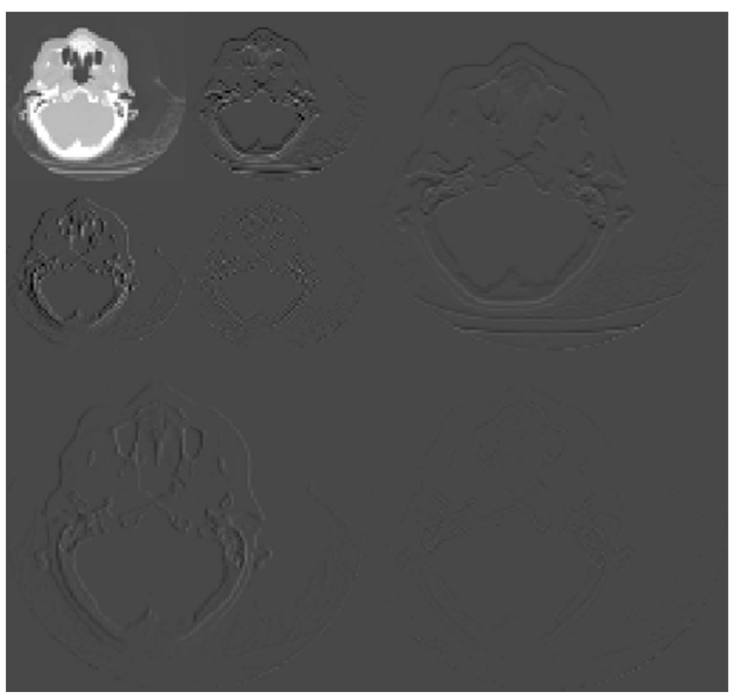

Figure 2.9 Two level decomposition of a CT brain image

The energy compaction property of the wavelets is highly useful for image compression. When a transform is applied to an image, if more energy is contained in a few transform coefficients, then good energy compaction is achieved. One measure of energy compaction is the transform Coding Gain (CG), which is defined as the ratio of the arithmetic mean to the geometric mean of the variances of all the transform coefficients. The high value of CG indicates that the transform can provide improved energy compaction in the transform domain.

2.4.2.2 Biorthogonal filters in wavelets

The orthogonality and the symmetry are the two properties required for a wavelet transform, when it is used for an image compression application. The orthogonality ensures the required energy compaction in the transform domain. The symmetry provides the linear phase, which is required to eliminate the phase distortion and the border artefacts in the filtered image. The filter bank of an orthogonal wavelet cannot have both symmetry and the orthogonality simultaneously. In other words, orthogonal wavelets cannot be symmetric. The only exception is the Haar wavelet, which has a filter length of two.

It is possible to construct symmetric wavelets by relaxing the orthogonality conditions. Biorthogonal wavelets fall into this category. The symmetric property of the filter pair is important in handling the edges in the images, as it reduces the border/edge artefacts. This symmetric property makes the biorthogonal filters greatly suitable for image coding than the orthogonal filters. In addition to the symmetry requirement, the design of filters also affects the compression performance. The analysis filter should be designed to maximise the coding gain, while the synthesis filter should be optimised for the smooth reconstruction of the image. This means that the design objectives of both filters are different.

Since the analysis and the synthesis functions of the biorthogonal filter have different frequency responses, it is possible to design these filters with different cost functions. In general, the analysis filters have higher number of vanishing moments than the synthesis filter, to achieve good energy compaction in the low frequency sub band. The synthesis filters have more zeros than the analysis filter, for obtaining a smooth synthesis basis function.

A set of biorthogonal filters, which exhibit close behaviour to the orthogonal filters is the Cohen-Daubechies-Feaveau (CDF) 9/7 filters. In the JPEG 2000 standard, this filter is used for lossy compression, and the LeGall 5/3 filter is used for lossless compression. The 5/3 analysis filter has 5 taps in the low pass filter and 3 taps in the high pass filter.

The support and the vanishing moment are the two parameters used in selecting a particular transform for image compression. A small support means that the analysis filter length is short and has fewer computations. Besides, if the length of the filter is long, it will lead to ringing artefacts around the edges. A high value for the vanishing moment implies an increased compression performance. The 5/3 transform has two vanishing moments, while the 2/6 transform with a similar support has three vanishing moments.

2.4.2.3 The lifting wavelet transform

The main difference between the classical wavelet transform and the lifting scheme is that, the latter does not use the Fourier Transform (Daubechies & Sweldens 1998), and allows fast implementation of the wavelet transform. Chao et al (1996) have shown that, many transforms increase the range of values after the transformation. The lifting approach permits in-place calculations and there are no extra coefficients. Since the

IWT filter coefficients are dyadic, the division and multiplication are shift operations (Adams & Kossentni 2000). In the lifting approach, the computations are still made using the floating point numbers, but the final result is obtained in the integer form.

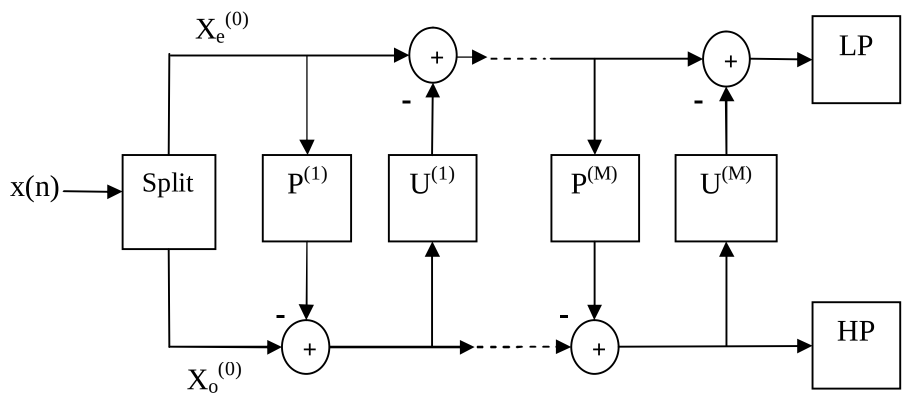

Figure 2.10 Forward lifting wavelet transform

The computation of the forward lifting wavelet transform consists of several stages of lifting steps in pair, namely, predict P (dual lifting), and update U (primal lifting). The repeated steps of the lifting wavelet transform for M stages are shown in Figure 2.10.

Initially a lazy wavelet transform is used to split the signal into even and odd components. A Haar wavelet is an ideal choice for a lazy wavelet. Let the input signal be x(n). Let $X_e^{(0)}$ and $X_o^{(0)}$ represent the even and odd data samples respectively. The split signal components are now given as,

$$X_e^{(0)} = x\{2i\} \tag{2.22}$$

$$X_o^{(0)} = x\{2i+1\} \tag{2.23}$$

The prediction step, which is also called as dual lifting, exploits the correlation between the adjacent pixels. Since the adjacent pixels are usually correlated, the separated even and odd samples also exhibit correlation. Hence, one can predict the odd samples using the even samples and vice-versa. Since the odd and even samples are highly correlated, such a prediction will de-correlate the signal. It is required to store only the part of X_o that varies from X_e, which is the prediction error. Effectively, X_0 is replaced by the prediction error values by using a prediction operator P. The prediction operation is implemented by applying the prediction filter to the even samples and subtracting the predicted value $P(X_e)$ from the odd ones to generate new X_o values for the i^{th} step, as given in Equation (2.24).

$$X_o^{(i)} \leftarrow X_o^{(i-1)} - P(X_e^{(i-1)}) \tag{2.24}$$

Since the values calculated using Equation (2.24) are the difference between the two components, the new X_o coefficients essentially contain the detail information.

In the update step, the mean value is calculated. The update operation is implemented by the application of an update filter to the odd samples and adding the resultant values to the even samples. The new X_e values are the approximation coefficients, as defined by Equation (2.25).

$$X_e^{(i)} \leftarrow X_e^{(i-1)} + U(X_o^{(i-1)}) \tag{2.25}$$

With repeated application of the lifting steps, the even samples will become the low pass coefficients and the odd samples will become the high pass coefficients. The number of lifting steps is decided by the length of the original filters.

2.4 THE INTEGER WAVELET TRANSFORM

The input pixels of an image are generally unsigned integers. The application of the wavelet transform generates floating point coefficients, which are not suitable for lossless applications. The lifting scheme can be modified to implement the integer operation (Calderbank et al 1997), by adding rounding operations to the lifting stages.

$$X_o^{(i)} \leftarrow X_o^{(i-1)} - \left\lfloor P(X_e^{(i-1)}) \right\rfloor \tag{2.26}$$

$$X_e^{(i)} \leftarrow X_e^{(i-1)} + \left\lfloor U(X_o^{(i-1)}) \right\rfloor \tag{2.27}$$

These steps result in the integer wavelet transform (IWT). Since they are formed using the lifting steps, the IWT is fully invertible. Since the lifting based IWT leads to a lossless coding, it is particularly suitable for the compression of medical images.

The use of IWT for the lossless compression of images was first demonstrated by Calderbank et al (1997, 1998). In addition to the lossless compression facility, the implementation of the integer computations in the hardware becomes simple. The lifting steps reduce the computational complexity of the filter bank by a factor of 4, when compared to the standard filter bank construction. This makes the lifting approach computationally efficient. Since it is an in-place calculation, an additional memory is not required to store the wavelet coefficients. The order in which the transform is applied is important to ensure the proper functioning of the IWT. If the forward transform is applied first to the rows and then to the columns, then the inverse transform should be applied in the reverse order. If the order is changed, then the invertibility is not guaranteed.

2.5 ENTROPY CODING TECHNIQUES

Entropy coding techniques are generally used for eliminating the coding redundancy in the images. The Huffman coding and the arithmetic coding are widely used for entropy coding. Both the methods are variable length encoding techniques, and utilise the probability information of the symbols for the coding. These two algorithms are briefly explained in Sections 2.5.1 and 2.5.2.

2.5.1 The Huffman Coding

The Huffman coding uses a binary tree obtained from source symbols. Initially, the symbols are sorted in the descending order of their probabilities. This is the first stage in the coding. Next, the least two probabilities are added to form a new probability, and it replaces the least two probabilities. The new probability is placed in the second stage such that, all the probabilities are again in the descending order. These steps are repeated until all the probabilities are combined.

Next, a binary tree is constructed where the nodes represent the combined probabilities and the leaves represent the symbols. The root of the tree is 1, which is the sum of all probabilities. Traversing down the tree, a code 0 is assigned to the left branch and a code 1 is assigned to the right branch, till the last branch is reached. The collection of 0s and 1s from the root to the leaf gives the code for each symbol.

For large alphabets with a fair distribution of probabilities, Huffman coding is able to produce an average codeword length close to the entropy. However, it is inefficient when the alphabet is small, with skewed probabilities.

2.5.2 Arithmetic Coding

Arithmetic coding is an efficient technique for small alphabets and skewed probabilities. The Huffman coding is a fixed-to-variable scheme, whereas arithmetic coding is a variable-to-fixed coding scheme. It is supposed to be near-optimal coding. Unlike the Huffman coding, where each symbol has a codeword, the arithmetic coder generates a single codeword for all the symbols in the message, in the form of a binary fraction.

In order to encode a message, an initial half-open interval of [0,1) is considered. The probabilities of all the symbols are represented as cumulative probabilities in this interval. As the number of symbols in the message increases, the interval becomes small. When all the symbols in the message are encoded, the final interval obtained is the binary fraction.

The arithmetic coding offers higher efficiency than the Huffman coding, but it is slow. The Huffman coding is very efficient when the probabilities of the symbols are uniform. If the probabilities are powers of two, then the Huffman coding achieves the average codeword length equal to the entropy. Since the Huffman coding is less complex than the arithmetic coding, it is preferred in this research work.

2.6 PERFORMANCE METRICS

The performance of an image compression algorithm is evaluated using various metrics. One of the commonly used metrics is the Compression Ratio (CR), which is defined (Gonzalez & Woods 2002) as in Equation (2.28).

$$CR = \frac{n_1}{n_2} \tag{2.28}$$

where n_1 is the number of bits in the original image, and n_2 is the number of bits in the compressed image. Large values of CR mean that the size of the compressed image is small.

The amount of compression can also be measured by stating the bit rate (BR), which is expressed in terms of bits per pixel (bpp). The objective of any image compression algorithm is to reduce the bit rate. The bit rate of an image is related to the compression ratio as given in Equation (2.29).

$$\text{BR}= \frac{\text{Number of bits per pixel in the original image}}{\text{CR}} \tag{2.29}$$

For an 8-bit image, the bit rate can be expressed as,

$$BR = \frac{8}{CR} \tag{2.30}$$

The expression given in Equation (2.30) indicates that the high compression ratios reduce the bit rate.

2.7 IMAGE QUALITY METRICS

Since the quantisation process removes the information from an image, it is necessary to quantify the loss of information. The image fidelity assessment techniques are employed to measure this loss. The basic approaches for assessing the image fidelity can be classified as objective and subjective methods.

2.7.1 Objective Approaches

In an objective approach, the loss of information is expressed as a function of the input image and the decompressed image. It is a mathematical approach, and a number of objective fidelity criteria is available in the literature. These methods can be classified according to the availability of the original images. Most methods use a full-reference image, which means that the original image is known. In some applications, the original image is not available, or in some other cases, it is partially available. If the reference image is partially available, the assessment is referred to as reduced-reference assessment (Wang et al 2004). All the objective metrics explained in this chapter assume that a full reference image is available, and the assessment is known as the full-reference quality assessment. Some of the frequently used metrics falling under the full reference class are discussed.

2.7.1.1 The peak signal to noise ratio

One of the simplest objective quality measures is the Peak Signal to Noise Ratio (PSNR). The PSNR is calculated using the Mean Square Error (MSE) value between two images. Let u(m,n) and u'(m,n) represent the pixels in the original image and the decompressed image respectively. Then, the MSE and the PSNR are defined (Jain 1989) as given in Equations (2.31) and (2.32).

$$\text{MSE} = \frac{1}{MN}\sum_{m=1}^{M}\sum_{n=1}^{N} E\left[\left|u(m,n)-u^{|}(m,n)\right|^{2}\right] \tag{2.31}$$

$$\text{PSNR} = 20\log_{10}\ \frac{\text{maximum gray level in the original image}}{\text{MSE}} \tag{2.32}$$

For an eight bit input image, the maximum gray level is 255. In this case, the PSNR is defined as given in Equation (2.33).

$$\text{PSNR} = 20\log_{10}\frac{255}{MSE} \tag{2.33}$$

2.7.1.2 The visual signal to noise ratio

Although the PSNR is a standard metric for measuring image quality, it does not reveal the real quality perceived by the human eyes. This is because the PSNR does not consider the characteristics of the Human Visual System (HVS) into account. The low level processing unit in a HVS is nonlinear, and uses several masking parameters. The VSNR is an image fidelity metric which considers the HVS parameters.

The VSNR was introduced by Chandler & Hemami (2007) and developed from the observation that, for the same mean square error, the visual quality of two images could be different. Let U denotes the original image and $\overline{U}$ denotes the original image and the distorted image respectively. The error image E is obtained as,

$$E = U - \overline{U} \tag{2.34}$$

The DWT is applied to both U and E to obtain two sets of sub bands {sU} and {sE}. The spatial frequency vector f is calculated next using the display resolution and viewing distance. In order to determine the visibility of the distortions in $\overline{U}$, the contrast thresholds for the detection of the distortion are calculated for each band for the original image, U. If the actual contrast in the respective band of the error image E is less than the contrast threshold, then the distortions are below the visibility threshold. The algorithm takes the corresponding VSNR value as infinity and terminates. If the contrast is higher than the contrast threshold, then the distortion is said to be supra threshold; the algorithm executes a second stage to compute the VSNR value. The VSNR in decibels is given by Equation (2.35).

$$VSNR=10\log_{10}\frac{C^2(U)}{VD^2} \tag{2.35}$$

where C(U) denotes the contrast of the original image U, and VD is the visual distortion as a function of the perceived contrast d_{pc} and the global precedence d_{gp}. A parameter α determines the relative contribution of each contrast. The visual distortion (VD) is given by,

$$\text{VD} = \alpha d_{pc} + (1-\alpha)\frac{d_{gp}}{\sqrt{2}} \; \alpha d_{pc} + (1-\alpha)\frac{d_{gp}}{\sqrt{2}} \tag{2.36}$$

The limitation of the VSNR is that, it does not take into account the spatial localization of distortion. Besides, the metric operates only on the luminance of the distortion and does not consider the effects of chrominance distortion. Since the chrominance distortion need not be considered for a gray level image, this drawback will not affect the assessment procedure for the gray level images.

2.7.1.3 The structural similarity index

An image quality assessment algorithm, considered to be in line with the human perception, is the Structural Similarity (SSIM) index. Some of the previous studies have shown that the PSNR performs well in the analysis of noisy images, but is poor in describing the structural content of the images. The SSIM index gives a value near to 1 when two 8-bit test images ‘a’ and ‘b’ have a similar mean square error, but different visual quality. For a given pixel P, the SSIM index is calculated by considering a small window around the pixel. The statistical parameters are then calculated for the window to find the SSIM index for the given pixel. In order to eliminate the artefacts in the quality map, the standard square window is replaced by a Gaussian window with a standard deviation of 1.5 (Wang et al 2004).

The SSIM index for a pixel P is defined as,

$$SSIM(P) = \frac{(2\mu_a\mu_b + C_1)(2\sigma_{ab} + C_2)}{(\mu_a^2 + \mu_b^2 + C_1)(\sigma_a^2 + \sigma_b^2 + C_2)} \quad (2.37)$$

where μ_a and μ_b are the mean intensity of pixels within the window for the images *a* and *b* respectively. The symbols σ_a and σ_b are the variances of the images and σ_{ab} is the covariance between the images *a* and *b*. The constants C_1 and C_2 are for the regularization and are given by $C_1 = (K_1L)^2$ and $C_2 = (K_2L)^2$ where L is the dynamic range of the image. The scalar constants K_1 and K_2 have typical values of 0.01 and 0.03 respectively. The final value is given by the mean SSIM index of all the pixels in the complete image.

2.7.2 Subjective Approaches

The subjective criterion is based on the human visual perception. The decompressed images are viewed by a human observer and their visual evaluation is used to assess the image quality. In subjective quality assessment, the original and decompressed images are shown on a single screen to a group of observers and their evaluations are averaged on a rating scale. An example scale could contain the observations such as {excellent, good, fair, poor, unsatisfactory] with numerical weights {5, 4, 3, 2, 1} attached to each observation.

The objective methods are faster and easier when compared to the subjective approaches. Hence, they are widely employed. Also, these approaches are more useful for the lossy compression, where the artefacts are always visible after a certain level of compression. Since this thesis investigates the near-lossless and lossless approaches, there are no visible artefacts, and therefore, the subjective approaches are not used. However, the opinion of the medical experts has been taken for images compressed using near-lossless methods.

2.8 COMPARISON OF COMPRESSION METHODS

A summary of the advantages and disadvantages of various image compression methods is given in Table 2.1

Table 2.1 Comparison of compression methods

DOMAIN	Compression Method	Advantages	Disadvantages
SPATIAL	DPCM	minimum computational complexity	Medium compression ratio, no multi-resolution capability
	JPEG-LS	Medium compression ratio	Medium complexity
	CALIC	High compression ratio	High complexity
TRANSFORM	JPEG	Less complex than wavelet	No multi-resolution capability
	JPEG-2000	Multi-resolution Scalability ROI coding facility	More complex than JPEG

2.9 THE SIMULATION ENVIRONMENT

The image processing algorithms can be written using high level languages like C, C++, Java, MATLAB etc. The Matrix Laboratory (MATLAB) developed by Mathworks Inc. is highly preferred for the image processing algorithm development and simulation.

MATLAB is a high level language, capable of visualisation, modelling, programming and mathematical computations. The image processing toolbox available in MATLAB is exhaustive and has pre-defined functions to read and write the images. The coding is user friendly, and the existing codes written in other high level languages like C, C++ and Java can be called from within the program. Additionally, the MATLAB codes can be directly converted to hardware description languages like Verilog and VHDL, for implementation in the hardware. All these features make MATLAB an ideal tool for the testing and implementation of image processing algorithms. All the algorithms presented in this research work are developed in the MATLAB environment.

2.10 IMAGE DATASETS

The medical images used in this thesis work are collected from various hospitals. The angiogram images are collected from the Madras Medical Mission, Chennai. The CT abdomen, thorax and elbow images are collected from a hospital in Trivandrum, Kerala. The sample images from these datasets are shown in Appendix 1.

2.11 CONCLUSION

An overview of the image compression algorithms and the still image compression standards are explained in this Chapter. Various image compression algorithms are studied and their suitability for implementing the proposed objectives of the research work is identified. Since the DPCM has the least computational complexity, it has been chosen as one of the algorithms for the near-lossless and lossless compression of images. For lossless compression with multi-resolution, the IWT is chosen as it has less complexity than the DWT. various biorthogonal transforms are studied and their complexities are analysed. It is found that, the (5/3) transform and (2/6) transforms have less complexity and good compression performance. Hence, they are chosen for the implementation of various wavelet based schemes. Since the JPEG 2000 uses the 9/7 transform, it is also used for comparison.

The standard entropy coding methods such as Huffman coding and arithmetic coding are studied and compared. Some of the performance metrics and the image quality measures used in this thesis are also discussed.

question	opt1
The first application of digital image was in the -------.	medical field
Which is the subjective type image processing operation	Image restoration
Which processing is used to reduce the memory usage of an image during its storage	segmentation
Which is not related with the components of image processing system	image restoration
Which controls the amount of light that enters into the eye	pupil
.--------vision is called photopic or bright light vision ?	cones
Which light receptors in the eye are sensitive for color?	rods
Digitizing the co-ordinates values of an image is called --------.	sampling
Any two pixels connectivity is based on ------	their spatial coordinates
For a pixel p,q with coordinates (6,8) and (4,3). find D8 distance	6
When check board pattern becomes visible in an image?	Increasing spatial resolution
Compute the memory size required for storing the image of size 256x256 with 16 gray levels	256x256x4
What are bo(6),b1(6) and b2(6)?	0,1,1
Which transform kernels are based on the statistics of the data?	slant
Which transform has the same forward and inverse kernel?	slant
Which transform produces high compression ratio	slant
Which distance is called chessboard distance	D4 distance
What is meant by the sequency of a basis function matrix?	the number of sign changes in a row of the basis function matrix
Which operator is more suitable for edge detection?	power law
which distance is called city block distance?	D4 distance
Digital image is composed of --------	Pixels
Feature selection deals with-------	color processing
Which membrane in the eye serve as the major source of nutrition to the eye?	choroid
.Which vision is called scotopic or dim light vision	cones
Which tissue in an eye has more protein than any other in the eye?	Irish diaphragm
What is blind spot?	center part of the retina
What is the typical focal length of the human eye?	15mm to 20mm

What is subjective brightness?	brightness of the object
the weber ratio is expressed as	$\Delta Ic/I$
For good brightness discrimination the weber ratio should be -----	small
Digitizing gray level value is called -----	sampling
.If the size of the image is 25x25 and 5 bits /pixel , then what is the memory size required to store that image	25x25x5
What is the minimum size and gray level value of an image ,which is free from sampling check board errors and false contouring	512x512 with 32 gray levels
For the pixels p, q with co-ordinates (6,8) and (8,6) find the Euclidean distance	sqrt(6)
Consider the pixels p,q with co ordinates (6,8) and (4,3) find D4 distance	7
When false contouring results in an image?	Increasing spatial resolution
The magnitude of power spectrum in Fourier transform is given by	p(u.v) = |F(u,v)|
.In Haar transform the integer K is related with p and q as ------.	$K=2^q+p+1$
The two dimensional scaling of the DFT is defined as	(1/a) F(u,v)
The computation complexity of N point DCT via FFT is given by	$O(N\log_2 N)$
Which transform is used in JPEG compression standard	slant
An observer is looking at a tree 15 meter high at a distance of 100m.Find the size of the retinal image	4mm
How aliasing is eliminated in image processing?	by proper image acquisition method
What do you mean by orthogonality of a transform	the cross product of any two columns of the kernel matrix is zero
Write the sequence of the following matrix 1 1 0 1 1 1 -1 -1 1 -1 1 -1 1 -1 -1 1	0,1,3,2
The convolution property of 2D DFT is given by	f(m,n)*g(m,n) = F(u,v).G(u,v)
What is the computation complexity of DFT transform?	$O(N\log_2 N)$
What is the necessity of FFT?	to get spectrum without aliasing

What is the condition for m adjacency for any two pixels p and q?	q is in $N_4(p)$
.------- are sensitive for brightness information	cones
The transform which posses the highest energy compaction property is	Fourier transform
The transform which is widely used to detect lines in an image is	Fourier transform
Below the pixel values in a 4x4 gray level image. What is the minimum number of bits required to store each picture element	1
The minimum D4 and D8 distances between the pixels values 1 and 5 are $\begin{bmatrix} 1 & 2 & 4 & 8 \\ 2 & 6 & 4 & 2 \\ 3 & 3 & 4 & 5 \\ 2 & 2 & 4 & 6 \end{bmatrix}$	3,5
The number of bits necessary to represent a 256x256 image with 256 gray level is	524288
Which transform basis function matrix depends on the covariance matrix of the data.	Fourier transform
The discrete version of KL transform is	Fourier transform
The n^{th} order Hadamard transform is obtained by	H_n= Kronecker product of H_1 and H_{n-1}
In contrast stretching, the location of points (r1,s1)(r2,s2) are as follows r1=r2 and s1=0 and s2=L-1 (Maximum gray level) The resulting output image is -------.	binary image

opt2	opt3	opt4	opt5	opt6
news paper industry	printing	satellite picture analysis		
Image acquisition	Image enhancement	image segmentation		
representation	recognition	compression		
image displays	computers	image processing software		
Irish diaphragm	choroid	sclera		
rod	blind spot	rods and cones		
fovea	cones	rods and cones		
quantization	resizing	gray level transformation		
their gray levels	their colors	their neighborhood dimensions		
8	4	5		
decreasing spatial resolution	increasing gray level quantization	decreasing gray level quantization		
256x256x8	256x256x3	256x4		
1,1,0	0,1,0	1,0,1		
walsh	haar	K-L		
walsh	haar	K-L		
walsh	haar	K-L		
D8 distance	Euclidean distance	m path distance		
the number of sign changes in a column of the basis function matrix	total number of sign changes	total number of sign changes/2		
gradient	log	laplacian		
D8 distance	Euclidean distance	m path distance		
continuous gray levels	continuous spatial co ordinates	discrete spatial co ordinates		
extracting image components	extracting attributes	partitioning the image into its constituent parts		
sclera	retina	cornea		
rod	blind spot	rods and cones		
fovea	cilliary body	lens		
high cone density area	high rod density area	the absence of rods and cones in the retina		
20mm to 25mm	14mm to 17mm	10mm to 20mm		

intensity perceived by the human visual system	intensity above the thresold	intensity below the scotopic thresold
$\Delta Ic/2I$	$I/\Delta Ic$	$I/\Delta Ic$
0.5	high	2
quantization	resizing	gray level transformation
400	800	1k
512x512 with 64 gray levels	256x256 with 64 gray levels	256x256 with 128 gray levels
sqrt(5)	sqrt(8)	sqrt(3)
6	4	5
decreasing spatial resolution	increasing gray level quantization	decreasing gray level quantization
$p(u.v) = \|F(u,v)\|^2$	$p(u.v) = \|F(u,v)\|^{1/2}$	$p(u.v) = 0.5\|F(u,v)\|$
$K=2^p+q+1$	$K=2^q+p-1$	$K=2^p+q-1$
(1/b) F(u,v)	(2/ab) F(u,v)	(1/ab) F(u,v)
$O(\log_2 N)$	$O(N^2)$	$O(2N)$
walsh	haar	DCT
2.55mm	3mm	2mm
contrast stretching	low pass filtering the image	high pass filtering the image
the cross product of any two columns of the kernel matrix is not zero	the dot product of any two columns of the kernel matrix is zero	the dot product any two columns of the kernel matrix is not zero
2,1,3,0	0,2,3,1	1,0,2,3
$f(m,n)*g(m,n) = F(u,v)+G(u,v)$	$f(m,n)*g(m,n) = F(u,v)+G(u,v)$	$f(m,n)*g(m,n) = [F(u,v).G(u,v)]/2$
$O(\log_2 N)$	$O(N^2)$	$O(2N)$
to minimize false contouring	to reduce the computation complexity of DFT	to minimize check board pattern

q is in $N_D(p)$	q is in $N_4(p)$ or $N_D(P)$ and the set $N_4(p) \cap N_D(p)$	$N_4(p) \cap N_D(p) = \phi$
rods	Fovea	blind spot
walsh transform	cosine transform	Haar Transform
walsh transform	slant transform	KL Transform
2	3	4
5,3	6,4	4,3
324388	224288	124288
walsh transform	slant transform	KL Transform
walsh transform	slant transform	KL Transform
H_n= Kronecker product of H_1 and H_{n-2}	H_n= H1. H_{n-1}	H_n= Kronecker product of H_2 and H_{n-1}
negative image	high contrast image	low contrast image

answer

news paper industry
Image enhancement

compression

image restoration
Irish diaphragm
cones
cones

sampling

their gray levels
8
Increasing spatial resolution

256x256x4
1,0,1
walsh
slant
walsh
D4 distance

total number of sign changes/2
power law
D4 distance
continuous spatial co ordinates

color processing

sclera
rods and cones

lens

high rod density area
20mm to 25mm

brightness of the object
ΔIc/I

0.5

sampling

800
256x256 with 64 gray levels

sqrt(6)

5
decreasing spatial resolution

p(u.v) = 0.5|F(u,v)|
$K=2^p+q-1$
(1/a) F(u,v)
O(2N)
walsh

3mm

low pass filtering the image

the cross product of any two columns of the kernel matrix is zero

0,1,3,2
f(m,n)*g(m,n) = F(u,v)+G(u,v)
$O(N^2)$
to reduce the computation complexity of DFT

q is in $N_D(p)$
blind spot

walsh transform

slant transform

1

5,3

124288

KL Transform
Fourier transform

H_n= Kronecker product
of H_1 and H_{n-1}

negative image

question

1. From the following which image enhancement technique is based on point processing?

1	2	3	1	2
4	5	2	3	3
3	3	5	4	4
1	3	2	3	5
2	1	3	1	3

for the given pixel value in a 5x5 gray level image What is the value of the pixel at the location(3,3) after applying median filtering?

Which of the following filter will in general have the best performance in enhancing edges in an image?

The parameter that may change if all the pixels in an image are shuffled is

1	2	3	1	2
4	5	2	3	3
3	3	5	4	4
1	3	2	3	5
2	1	3	1	3

for the given pixel value in a 5x5 gray level image What is the value of the pixel at the location(3,3) after applying simple average filtering?

The operator which can be used to detect the edges in an image is

=1

otherwise

.Which filter is used to perform high pass filtering without the loss of the background information?

Which frequency domain filter is based on illumination –reflectance model?

Which filter is known as box filter?

.From the following which filter belongs to order statistics category?

From the following which is not a point processing enhancement technique?

.Which filter is more suitable for the removal of salt and pepper noise?

Which preprocessing operation moves the center of the spectrum to the point u=M/2 and v=N/2

What is the response of the butterworth low pass filter at D(u,v)=D0?

. What is the response of the butterworth low pass filter at D(u,v)=D0?

Which filter performs gray level compression and contrast enhancement while do filtering?

The fourier transform of the original imagef(x,y)and the blurred image g(x,y) are related in the frequency domain by the equation

Which order of the butterworth filter has no ringing effect?

.The transfer function of the Gaussian low pass filter is given by

The unsharp masking can be implemented in the frequency domain by using the composite filter

High boost filtering can be implemented as

The general form of log transformation is given by

Which transformation results spreading /Compressing of gray levels in an image?

.The basic form of power law transformation is given by

What values of γ in the power law transformation map a narrow range of dark input into a wider range of output values ?

What values of γ in the power law transformation map a wide range of bright input into a narrow range of output values ?

Perform bit plane slicing(Plane=2) for the following image pixel values 4,2,6

The sum of all components in a normalized histogram is equal to -----.

Which logic operator performs the operation same as that of the negative operation?

The low contrast image results due to --------.
Which operation enhances the specific range of gray levels?
.---------- are the basis for the numerous spatial domain processing techniques
An important application of Image averaging is in the field of -------.
The smallest meaningful mask size used in the spatial filtering is ----------.
The median filter represents the -------percentile of the ranked set of numbers.
The max filter represents the -------percentile of the ranked set of numbers.
. The min filter represents the -------percentile of the ranked set of numbers
The lapalcaian image enhancement is given by
In high boost filtering ,A=1 results --------.
The transfer function of a Butterworth low pass filtering of order n and with cut off frequency D_0 from the orgin is given by
What type of filters are used in frequency domain filtering?

opt 1	opt 2	
Pseudo coloring	filtering Homomorphic	
1	2	
Mean filter	median filter	
) Mean	entropy	
3.33	4.5	
adder	Integrator	
Laplacian filter	homomorphic filter	
Gaussian HPF	) Butterworth HPF	
Gaussian HPF	Butterworth HPF	
weighted average filter with all coefficents equal to one.	weighted average filter with all coefficents grater than one	
Min filter	Butterworth filter	
) gray level slicing	contrast strecting	
Max filter	) Median filter	
) (-1)*f(x,y)	) $(-1)^{x+y}$ *f(x,y)	
50% of its maximum value	66% of its maximum value	
50% of its maximum value	60.% of its maximum value	
Guassian low pass filter	Butterworth high pass filter	
a) G(u,v))=H(u,v)F(u,v)	a) G(u,v))=H(u,v)/F(u,v)	
) n=3	n=4	
$H(u,v)=exp(-D^2(u,v)/2\sigma^2)$	$H(u,v)=exp(-D^2(u,v)/2\sigma)$	
) $H_{hp}=1-H_{lp}(u,v)$	) $H_{hp}=1+H_{lp}(u,v)$	
$H_{hb}=(A+1)+ H_{hp}(u,v)$	) $H_{hb}=(A-1)+ H_{hp}(u,v)$	
) s= c log(1-r)	s= c log(1-2r)	
) Log Transformation	Threshold mapping	
$s= cr^{\gamma/2}$	) $s= cr^{\gamma}$	
a) $\gamma>1$	a) $^{\gamma}<1$	
a) $\gamma=10$ and above	a) $\gamma=0$	
a) 1,2,2	0,1,2	
	0	0.5

AND	OR	
camera movement	lack of dynamic range in the image sensor	
) bit plane slicing	contrast stretching	
Histograms	negative imaging	
Medical	) Industrial purpose	
) 5x5	3x3	
	0	25
	0	25
	0	25
$g(x,y)= 2f(x,y)-\nabla^2 f(x,y)$	$g(x,y)= f(x,y)+2\nabla^2 f(x,y)$	
Laplacian sharpening	) homomorphic filtering	
a) $H(u,v)= 2/[1-(2D(u,v)/ D_0)^{2n}]$	a) $H(u,v)= 1/[1-(D(u,v)/ D_0)^{2n}]$	
zerophase shift filters	phase shift filters	

opt 3	opt 4
Gray level slicing	Laplacian filtering
3	4
Lapalcian filter	mode filter
histogram	covariance
3	5
multiplier	differentiator
notch filter	Guassian filter
High boost filter	Homomorphic filtering
High boost filter	Homomorphic filtering
weighted average filter with all coefficents less than one	) weighted average filter with all coefficents rather than one
Ideal low pass filter	Homomorphic filter
Power law transformations	) Lapacian filtering
) Guassian filter	Mode filter
$(1)^{x+y}$ *f(x,y)	f(x,y)/(-1)
80% of its maximum value	) 77% of its maximum value
80% of its maximum value	77% of its maximum value
Laplacian filter	) Homomorphic filter
a) G(u,v))=F(u,v)/H(u,v)	G(u,v))=2H(u,v)F(u,v)
n=20	n=1
$H(u,v)=\exp(D^2(u,v)/2\sigma^2)$	) $H(u,v)=\exp(-D\ (u,v)/2\sigma)$
$H_{hp}=1-(H_{lp}(u,v)/2)$	$H_{hp}=1+2H_{lp}(u,v)$
$H_{hb}=(A+1)\ H_{hp}(u,v)$	$H_{hb}=(A-2)\ H_{hp}(u,v)$
s= c log(1+r)	s= log(1-r)
Power law transformation	contrast stretching
$s=(cr^{\gamma})/2$	$s=2cr^{\gamma}$
a) $\gamma=0$	γ =10 and above
a) $\gamma<1$	$\gamma>1$
a) 0,2,2	2,2,1
0.6	1

NOT	EX-OR	
bright illumination level	out of focusing of the lens	
gray level slicing	Histogram processing	
gray level transformations	bit plane slicing	
astronomy	range imaging	
6x6	4x4	
100		50
100		50
100		50
) $g(x,y)= f(x,y)-\nabla^2 f(x,y)$	$g(x,y)= f(x,y)-(\nabla^2 f(x,y))/2$	
Gaussian filtering	unsharp masking	
a) $H(u,v)= 1/[1+(D(u,v)/ D_0)^{2n}]$	$H(u,v)= 2/[1+(D(u,v)/ D_0)^{2n}]$	
) non symmetric and phase shift filters	symmetric and phase shift filters	

opt 5	opt 6	answer
		Gray level slicing
		3
		Lapalcian filter
		covariance
		3.33
		differentiator
		notch filter
		High boost filter
		Homomorphic filtering
		weighted average filter with all coefficents equal to one.
		Min filter
		) Lapacian filtering
		) Median filter
		) $(-1)^{x+y}$ *f(x,y)
		50% of its maximum value
		60.% of its maximum value
		) Homomorphic filter
		G(u,v))=H(u,v)F(u,v
		n=1
		) $H(u,v)=\exp(-D^2(u,v)/2\sigma^2)$
		) $H_{hp}=1-H_{lp}(u,v)$
		) $H_{hb}=(A-1)+ H_{hp}(u,v)$
		s= c log(1+r)
		Log Transformation
		) $s= cr^{\gamma}$
		a) $^{\gamma}$<1
		γ >1
		a) 0,2,2

NOT

lack of dynamic range in the image sensor
gray level slicing
Histograms
astronomy
3x3

50
100
0

) $g(x,y)= f(x,y)-\nabla^2 f(x,y)$
Laplacian sharpening

a) $H(u,v)= 1/[1+(D(u,v)/ D_0)^{2n}]$
symmetric and phase shift filters

question
Mathematical modeling of the image restoration process is given by
Which noise has constant spectrum in the frequency domain?
Which noise has good mathematical tractability in spatial and frequency domain?
Which noise arises due to electrical or electromechanical interference during image acquisition?
Which noise is known as salt and pepper noise?
Which noise can be estimated by simply subtracting the predicted image spectrum with the noisy image spec
The electric circuit noise and temperature sensor noises are modelled as ------.

The Rayleigh noise model is used to --------.
The gamma noise model is used to --------.
The exponential noise model is used to --------.

The wiener filter behaves like an inverse filter ---------.
.The singular values of the matrix 2 2

In the image restoration the blurred image is often modeled as -------.

The singular value decomposition of the matrix A is given by $A=UDV^T$. Identify the false statement.
All the eigen values of the unitary matrix will have a magnitude of
The matrix A can be decomposed into A= UDVT through singular value decomposition .If one
attempts to plot the shape of singular values -----.

.Which noise is known as gamma noise?
The special case of erlang pdf with b=1 results -------.
The mean of the uniform noise pdf is given by ------.
Which noise is used to characterize the noise phenomena in range imaging?
.In which applications the exponential noise phenomena model is used?
Which noise is considered as spatially dependent one?

When the image enhancement and image restoration becomes indistinguishable disciplines?
An image restoration using geometric mean filter is given by $\hat{f}(x,y)$ = ------.
Which filter works well for salt but fails for pepper noise?
What values of the order(Q) of the harmonic filter eliminates pepper noise?

What values of the order(Q) of the harmonic filter eliminates salt noise?
How contra harmonic filter reduces to arithmetic mean filter?
. How contra harmonic filter reduces to harmonic filter?
Which filters are suitable for random noise like Gaussian or uniform noise?
Which filter is useful for finding the brightest points in an image?
Which filter is useful for finding the darkest points in an image?
Which degradation function(filter) is used to model a mild ,uniform blurring in an image?
The estimation of H(u,v) by experimentation method is given by----.
What is the draw back in inverse filtering?

What is the concept involved in weiner filtering?

The restored value in the wiener filtering in given in the frequency domain by ------.
Which function is used to measure the smoothness of an image?
Wiener filter is also known as -------filter?

H(u,v)
Sη(u,v)
Sf(u,v)
F• (u,v)

a. Degradation function
b.power spectrum of the noise
c. restored image
d.power spectrum of undegraded image

Match the following

.--------noise parameters are estimated by inspection of the Fourier spectrum of the image.

Verify the following statements

Statement 1:Priori blur identification method is not sensitive to noise

Statement 2: The conjugate gradient method suffers from incorrect convergence to local minima.

.---------method is used to find ARMA model parameters.

In SVD, the matrix U can be computed trough the eigenvectors of ------- .

In SVD, the matrix V can be computed trough the eigenvectors of ------- .

From the following applications, which is not related to SVD.

The noise domination in the image due to inverse filtering is reduced by ----- filter.

Identify the filter whose transfer function is given by H(u,v) = 1/H if H > e

H(u,v)= 0 otherwise

The variance of the uniform noise is given by -----.

The variance of the exponential noise is given by -------.

Hubnagel and stanly defined the atmospheric turbulence model as ------

opt1	opt2
$g(x,y)=h(x,y)*f(x,y)+ \eta(x,y)$	$g(x,y)=h(x,y)* \eta(x,y)+ f(x,y)$
White noise	Gaussian Noise
White noise	Gaussian Noise
Periodic noise	Gaussian Noise
Periodic noise	Gaussian Noise
Gaussian Noise	Periodic noise
Gaussian Noise	Periodic noise
electromagnetic interference noises	laser imaging
electromagnetic interference noises	laser imaging
electromagnetic interference noises	laser imaging
in the presence of noise	in the absence of noise
(1,0)	(2,0)
original image + psf filter	original image - psf filter
The number of singular values depends	The singular values are the square
Unity	zero
a) Square	b) rectangle
Raleigh noise	exponential noise
exponential noise	Raleigh noise
μ=a-b	(a+b)/2
exponential noise	Raleigh noise
laser imaging	range imaging
exponential noise	Raleigh noise
image restoration using blind deconvolu	restoration in the presence of noise
) $[\Pi\ g(s,t)]^{1/mn}$	$[\Pi\ g(s,t)]^{mn}$
geometric mean filter	harmonic filter
positive values	negative values
positive values	negative values
by making Q=1	by making Q=-1
by making Q=1	by making Q=-1
Median filter	Harmonic filter
Min filter	median filter
Min filter	) median filter
Gaussian LPF	butterworth HPF
G(u,v)*A	G(u,v)/A
it provides very high signal amplification	noises are suppressed
to minimize the error between original image and estimated image	to minimize the square of the error between original image and estimated image
Laplacian	gamma
minimum means square error	Least square filter

(i)-a, (ii)-b, (iii)-d,(iv)-c

(i)-b, (ii)-a, (iii)-c, (iv)-d

impulse noise	uniform noise
Statement 1 and 2 are false	Statement 1 and 2 are true
conjugate gradient	simulated annealing
) A^TA	AA^T
) A^TA	AA^T
digital watermarking	face recognition
wiener filter	pseudo inverse filter
wiener filter	pseudo inverse filter
$\sigma^2=(b-a)^2/12$	$\sigma^2=(b+a)^2/12$
$\sigma^2=(2/a)^2$	$\sigma^2=(1/a)$
$H(u,v) = \exp(-(u^2+v^2)^{5/6})$	$H(u,v) = \exp(K(u^2+v^2)^{5/6})$

opt3	opt4
$g(x,y)=h(x,y)/f(x,y)^{*}\ \eta(x,y)$	$g(x,y)=h(x,y)^{*}f(x,y)-\eta(x,y)$
rajleigh noise	Exponential Noise
rajleigh noise	Exponential Noise
rajleigh noise	Exponential Noise
Impulse noise	Exponential Noise
Impulse noise	Exponential Noise
Impulse noise	Exponential Noise
noises in Image ranging applications	Sensor temperature noises
noises in Image ranging applications	Sensor temperature noises
noises in Image ranging applications	transient noises
in the presence of noise and degradation	wiener filter does not resemble inverse filter at any condition
(3,0)	(4,0)
original image/psf filter	convolution of original image with psf of blur.
The singular values are the square root of the eigen values of AAT.	The singular values are the squares of the eigen values of AAT.
infinity	equal to the rank of the matrix
c) straight line	d) parabola.
) Erlang noise	uniform noise
impulse noise	uniform noise
(a-b)/2	$(b-a)^2/2$
impulse noise	uniform noise
electro mechanical noise modeling	electric circuit noise modeling
impulse noise	periodic noise
restoration by frequency domain filtering	) restoration by inverse filtering
[• g(s,t)]	[Π g(s,t)]/2
contra harmonic filter	median filter
Q=0	Q=-1
Q=0	Q=-1
by making Q=0	by making Q=any positive value
by making Q=0	by making Q=any positive value
) geometric mean filter	contra harmonic filter
mean filter	max filter
mean filter	max filter
butterworth LPF	Gaussian LPF
$G(u,v)^2*A$	G(u,v)/2A
noises are amplified	it attenuates the useful signal
to minimize the means square of the error between original image and estimated image	to make the error between original image and estimated image to one.
gradient	Gaussian
constrained least square filter	geometric mean filter

(i)-a, (ii)-b, (iii)-c, (iv)-d

(i)-c, (ii)-b, (iii)-a, (iv)-c

periodic noise

exponential noise

Statement 1 is false and 2 is true

Statement 1 is true and 2 is false

maximum likelihood

validation

$(A^T)^2 A$

)($A^TA)/2$

$(A^T)^2 A$

)($A^TA)/2$

Image compression

) image enhancement

laplacian filter

constrained least square filter

laplacian filter

constrained least square filter

$\sigma^2=(b-a)/2$

$\sigma^2=(b-a)/12$

$\sigma^2=(1/a)^2$

$\sigma^2=(1/2a)^2$

H(u,v) = exp(--K(u2+v2)5/6)

$H(u,v) = \exp(--K(u^2+v^2))$

opt5	opt6	answer
		$g(x,y)=h(x,y)*f(x,y)+ \eta(x,y)$
		White noise
		Gaussian Noise
		Periodic noise
		Impulse noise
		Periodic noise
		Gaussian Noise
		noises in Image ranging applications
		laser imaging
		transient noises
		in the presence of noise
		(2,0)
		convolution of original image with psf of blur.
		The singular values are the square root of the eigen values of AAT.
		Unity
		c) straight line
		) Erlang noise
		) exponential noise
		(a+b)/2
		Raleigh noise
		laser imaging
		periodic noise
		) restoration in the presence of noise only condition using spatial filtering
		) $[\Pi\ g(s,t)]^{1/mn}$
		harmonic filter
		positive values
		negative values
		by making Q=0
		by making Q=-1
		) geometric mean filter
		max filter
		Min filter
		Gaussian LPF
		G(u,v)/A
		noises are amplified
		to minimize the means square of the error between original image and estimated image
		Laplacian
		minimum means square error

(i)-a, (ii)-b, (iii)-d,(iv)-c

periodic noise

Statement 1 is true and 2 is false

maximum likelihood

AA^T

A^TA

image enhancement

pseudo inverse filter

pseudo inverse filter

$\sigma^2=(b-a)^2/12$

$\sigma^2=(1/a)^2$

H(u,v) = exp(--K(u2+v2)5/6)

question
Which one of the following is a lossy coding?

In a DPCM coder which of the following is need to be quantized?

What does the definition of entropy tell us?
In an image compression system, 16,384 bits are used to represent a 128x128 image with 256 gray levels. What is the compression ratio for this system?
Statement 1:Entropy is a measure of average information.   Statement2: Entopy is maximum if the symbols are euiprobable
In a black and white image , the probability of occurrence of black and white pixel is 0.5.Then the entropy of the image in bits per sample is
The number of shades of gray in a six bit image is
If one fixes the vector dimension to be 2 and the bit rate as 2 bits/dimension then the number of code vectors is ------.
An example of dictionary based coding technique is ------.
The transform which is recommended in JPEG 2000 IS

The quantizer in an image compression system is a

The basic principle of variable length coding is to -----
P(a1)=0.1, p(a2)=0.3 p(a3)=0.25 , p(a4)=0.15 p(a5)= 0.20 .The following codes are assigned to the symbols a1=1,a2=001,a3=10 a4=001 and a5=10. The average code word length for this source is
A still image with uniform intensity exhibits
The relative data redundancy or redundant information is calculated by
The run length coding is used to exploit ------- redundancy.
.If the CR is 2.63 ,then what is the relative data redundancy?
.Which redundancy elimination results quantitative information loss?

What is the sampling ratio of Y, Cb and Cr signals in video coding??
The self information associated with the ransom event A is given by -----

What is the purpose of channel encoder?
Which reduces the coding ,interpixel and coding redundancy in the input image of a general compression system?
From the following which is the object based compression technique?
From the following which is called uniquely decodeable , instantaneous block code
Which code does not have a one to one correspondence between source symbols and code words?
From the following which code does not require prior knowledge about the probability of the symbols?
From the following which code is based on dictionary based approach

What is the drawback in LZW coding?

Which code is integrated in PDF file format?
What is the gray code for the binary code 01111111?

What is white block skipping?

Which is not related to the bit plane coding?
Incorporating variable length coding with run length coding results ------.
In a binary image , if the entropy of H0=0.4 L0=3
H1=0.5 L1=2
What is the approximate run length coding entropy?

Relative address coding is related to ------.
JPEG format is useful when ____________
Which is computationally simple transform in and also used for image compression
Which coding encodes the difference between current pixel and the predicted value of that pixel.

.In predictive coding technique the errors are often modeled as ----.
The first order estimate of the entropy of the prediction error image is ------ that of the original image
The lossy image compression technique provide high compression by compromising -------.
.In delta modulation the predictor is defined as ------.

Which compression technique is based on frequency domain modification?
The most popular sub image size used in transform based image coding is ----- .

Zonal coding is based on --------.
In transform coding the zeroth coefficient is modeled by a ------- density function.
Which image coding does not have sub image processing steps?
Which is the most commonly used wavelet in wavelet coding?

A P-scale fast wavelet transform has ------- number of filter bank iterations

What is dead zone in wavelet coding quantizer design?

What is the special feature of JBIG 1?
What is the pass mode code word in 2-D run lenth coding used in binary image compression standard?
From the following which is still image compression standard?
From the following which is video compression standard?
DCT is used in ------- compression standard
Which one is used to compress the image?
Which one is used to compress the video?
Digitizing the image intensity amplitude is called
Digital Video is a sequence of

opt1	opt2	opt3
Run length coding	uniform quantizer	Huffman coding
The reconstruction value	The difference between prediction value and the original value	The prediction value
The reconstruction value	The difference between prediction value and the original value	The prediction value
4	8	12
a) Statement 1 and 2 are wrong	a) Statement 1 and 2 are true	c) Statement 1 true and 2 are wrong
0.25	0.5	0.75
256	128	64
8	16	32
Huffman coding	run length coding	LZW coding
K-L Transform	K-L Transform	Walsh transform
lossless element which exploits the psycho visual redundancy	lossly element which exploits the psycho visual redundancy	lossless element which exploits the statistical redundancy
assign shorter code words to more probable symbols	) assign longer code words to more probable symbols	assign uniform code words to least probable symbols
1.7	2	1.8
good spatial redundancy	poor spatial redundancy	good coding redundancy
Rd=1+(1/CR)	) Rd=1-(1/CR)	Rd=1+CR
Interpixel	psycho visual	coding
0.5	0.62	0.9
Interpixel	psycho visual	coding
2:01:01	3:01:01	4:01:01
) $i(A)= \log_2 p(A)$	) $i(A)= -\log_{10} p(A)$	$i(A)= -\ln p(A)$
) increases the source encoder output	decreases the noise immunity of the source encoder output	) increases the noise immunity of the source encoder output
a) Channel encoder	a) Source encoder	a) Channel decoder
mpeg-1	mpeg-2	mpeg-4
arithmetic code	Huffman code	LZW code
arithmetic code	) Huffman code	LZW code
arithmetic code	) Huffman code	LZW code
arithmetic code	) Huffman code	LZW code
dictionary overflow	use of finite precision arithmetic	end message indicator

arithmetic code	) Huffman code	LZW code
) 01000000	) 01101000	) 01000011
black color is skipped while coding	white color is skipped while coding	Intermediate gray levels are skipped while coding
constant area coding	one dimensional run length coding	two dimensional run length coding
increases compression ratio	decreases compression ratio	increases distortion
0.25	0.18	0.5
contour tracing and coding	1-D runlength coding	2-D runlength coding
there are so many colors in the picture	there are not so many colors in the picture	we want to show more bright
Walsh Hadamard transform	DFT	DCT
Lossless predictive coding	Huffman coding	bit plane coding
Guassian PDF	zero mean uncorrelated Laplacian PDF	Ralyeigh PDF
grater than	equal to	less than
accuracy of the reconstructed image	decreased PSNR value	decreased MSE
fn= a f'n-1	fn= a f'n-1+1	fn= • /f'n-1
transform coding	predictive coding	Huffman coding
4x4	8x8	5x5
maximum variance of the transform coefficients	probabilituy concept	dictionary based approach
Laplacian	Guassian	Rayleigh
transform coding	predictive coding	Huffman coding
Daubachies	DWT	Haar
P	2P	P+1
An enlarged quantization interval around aero	a compressed quantization interval around aero	normal quantization steps around zero
adaptive arithmetic coding	provides high compression for binary images	provides high compression for color images
100	) 0001	) 1000
JBIG	MPEG	JPEG
JBIG	MPEG	JPEG
JBIG	MPEG	JPEG
JPEG	MPEG	PNG
JPEG	MPEG	PNG
sampling	quantization	framing
Pixel	Matrix	Frames

opt4	opt5	opt6	answer
Predictive coding			uniform quantizer
The transform coefficient			The difference between prediction value and the original value
The transform coefficient			The difference between prediction value and the original value
16			8
Statement 1 wrong and 2 true			a) Statement 1 and 2 are true
1			1
32			64
64			16
predictive coding			LZW coding
Wavelet transform			Wavelet transform
) lossy element which exploits the statistical redundancy			lossly element which exploits the psycho visual redundancy
assign uniform code words to more probable symbols			assign shorter code words to more probable symbols
1			1.7
poor coding redundancy			good spatial redundancy
Rd=1-CR			) Rd=1-(1/CR)
Frequency domain			Interpixel
0.78			0.62
Frequency domain			psycho visual
1:01			4:01:01
i(A)= -$\log_2$ p(A)			i(A)= -$\log_2$ p(A)
increases the compression ratio			) increases the noise immunity of the source encoder output
Source decoder			a) Source encoder
mpeg-10			mpeg-4
Hamming code			Huffman code
Hamming code			) Huffman code
Hamming code			LZW code
Hamming code			LZW code
perquisite of probability information			dictionary overflow

Hamming code	arithmetic code
) 01000001	) 01000000
black color is coded as 0 and white color is coded as 1	white color is skipped while coding
Huffman coding	Huffman coding
decreases distortion	increases compression ratio
0.99	0.18
constant area coding	contour tracing and coding
when we want to show haziness	there are so many colors in the picture
K-L Transform	Walsh Hadamard transform
arithmetic coding	Lossless predictive coding
exponential PDF	Guassian PDF
4 times greater than	less than
decreased subjective fidelity	accuracy of the reconstructed image
fn= 2a f’n-1	fn= a f’n-1
wavelet coding	transform coding
9x9	8x8
prediction concept	maximum variance of the transform coefficients
uniform	Rayleigh
wavelet coding	wavelet coding
symlets	Daubachies
P-1	P
Lolydmax quantizer around aero.	An enlarged quantization interval around aero
extended Huffman coding is used.	adaptive arithmetic coding
) 1001	) 0001
group 3 facsimile	JPEG
group 3 facsimile	MPEG
group 3 facsimile	JPEG
GIF	JPEG
GIF	MPEG
Both A and B	quantization
Coordinates	Frames

question	opt1	opt2
Image segmentation algorithms are based on ------ properties of the intensity value	reflectance	discontinuity
.-------- is a set of connected pixels that lie on the boundary between two regions.	line	point
The direction of the edge is ---- to the direction of gradient vector at that point	parallel	perpendicular
Identify the maskIdentify the mask. 0 1 2 -1 0 1 -2 -1 0	Horizontal line detection mask	vertical line detection mask
The magnitude of the gradient vector in an edge detection is calculated as	|Gx|+|Gy|	|Gx|-|Gy|
In laplacian of Gaussian operator, what is the purpose of laplacian ?	used to find the zero crossings in an image	for smoothening the image
Which is called Maxican Hat function?	Laplacian	Guassian
In threshold based image segmentation, if T depends only on f(x,y), then that method is called ---.	adaptive thresholding	local thresholding
Which image segmentation method uses seed points for image segmentation?	Region merging	region splitting
Which thresholding method produces minimum average segmentation error?	adaptive thresholding	local thresholding
In general the threshold values are determined ------.	) by analyzing the histogram of the image	based on the thickness of the edge
Which property of the pixels are not used in region based image segmentation?	gray level	connectivity or adjacency
Which segmentation approach is based on quadtree approach?	Region merging and splitting	gradient techniquesregion growing
. From the following which is represented using external characteristics of a segmented region?	color	smoothness
From the following which is represented using internal l characteristics of a segmented region?	color	smoothness
What are chain code and shape number?	polygonal approximation	boundary descriptions
What is signature representation?	polygonal approximation	boundary descriptions
.If the distance between two pixels is d , then what is the error in minimum perimeter polygonal approximation technique?	a) 2/d	a) SQRT(2)*d
Which boundary representation is invariant to translation?	signature	boundary segments
The magnitude of gradient vectors of an edge are as follows.Dx=10, .Dy=-10, then what is the magnitude of the resultant gradient vector?	10	0

Which polygonal approximation technique represents distance in terms of angles?	boundary segments	skeleton
How the convex deficiency D of a convex hull is calculated?	D=H+S	D=2H+S
Which boundary representation technique uses thinning algorithm?	boundary segments	skeleton
Meadial Axis Transformation is used in which boundary representation?	boundary segments	skeleton
In skeleton representation the contour point P and its neighborhood pixel values are as follows. 0 0 0 1 p1 0 1 0 1 If this is the case , what is T(P1)?	3	4
How the length of a boundary is calculated?	number of vertical components in the chain coded curve.	) number of horizontal components in the chain coded curve
.How the diameter of the a boundary is calculated ?	B= min(D(P_I,P_J))	) B= max(D(P_I,P_J))
What is eccentricity of a boundary?	The ratio of major axis to minor axis	The ratio of minor axis to major axis
Which is the chain code for the following boundary.	312	1230
Which is the chain code for the following boundary.	1223	1123
What is the difference code for the chain code 0321?	3333	3123
What is the difference code for the chain code 003221?	330303	3300
What is the shape number of the chain code 0321?	3133	3333
Which fourier descriptor determine global shape?	low frequency	High frequency
Which fourier descriptor determine fine details?	low frequency	High frequency
. Which is the translated boundary fourier description of atu?	) a(u)+D_{xy}d(u)	a(u)-• xy• (u)
Which is the scaled boundary fourier description of • s(k)?	aa(u)	) a-a(u

.In simple descriptor , the number of pixels in aregion is called -----.	length	area
The compactness of a region is defined as ------.	perimeter/area	) perimeter-area
Which defined as the study of properties of a figure?	simple descriptor	topology
The number of holes in a region is 4.If it is folded along its lengthwise, then what will be the number of holes?	4	3
The Euler number E is defined as ----.	E=C+H	E=C-H
If the number of components in a region is 4 and the number of connected region 1 then the Euler number E is --------.	-2	2
.A region containing a polygonal network has 7 vertices 11 edges ,2 edges,1 connected region and 3 holes, then what is the Euler number?	2	-2
The smooth and coarse ,texture information of a region is calculated by---- approach.	) structural	statistical
Regularly spaced parallel lines are described in ---- texture approach.	) structural	statistical
The skew ness of the histogram is -----.	first moment	second moment
Which is used to measure the relative flatness of the histogram?	first moment	second moment
What is the shape order n for a closed boundary?	even	odd
What is the closest rectangle for the shape order n=18?	9x2	3x6
The uniformity of the histogram in texture measurement is given by ------.	$\sum_{i=0}^{L-1} P-2(Zi)$	$\sum_{i=0}^{L-1} P(Zi)$
In fourier descriptors, how (x1,y1),(x2,y2),…(xk,yk) co ordinate pairs are represented?	s(k)= x(k)-jy(k)	s(k)= x(k)+jy(k)
.In fourier descriptors the fourier coefficients are denoted as------.	b(k)	a(u)
A boundary region has major axis dimension 4 mm and minor axis dimension is 2 mm , what is the eccentricity?	4	3
. A boundary region chain code contains 4 vertical components and 3 horizontal components, then What is the approximate length of the boundary?	7	5

How three level images are formed in segmentation?	By defining three threshold values	based on gradient operator outputs
Which of the following method is apply for digital signature in image processing?	Only Encryption	Only Decryption

opt3	opt4	opt5	opt6	answer
discontinuity and similarity	redundancy			discontinuity and similarity
edge	diagonal line			edge
tangent	same			perpendicular
)-45 degree line detection mask	point detection mask			)-45 degree line detection mask
|Gx|*|Gy|	|Gx|/|Gy|			|Gx|+|Gy|
used to find lines	used to find isolated points			used to find the zero crossings in an image
Laplacian of Guassian	Gradient of guassian			Laplacian of Guassian
optimum global thresholding	global thresholding			global thresholding
region growing	) thresholding			region growing
optimum global thresholding	global thresholding			local thresholding
based on the contrast of the image	) backgroung information.			) by analyzing the histogram of the image
discontinuity of pixels	discontinuity of pixels			connectivity or adjacency
region growing	thresholding			gradient techniquesregion growing
texture	shape			shape
texture	shape			texture
regional descriptors	1 D representation of a boundary			boundary descriptions
regional descriptors	1 D representation of a boundary			boundary descriptions
c) d/SQRT(2				a) SQRT(2)*d
	d-1			
skeleton	minimum perimeter			) boundary segments
20	5			20

minimum perimeter	signature	signature
D=H-S	D=2-(H+S)	D=H-S
minimum perimeter	signature	skeleton
minimum perimeter	signature	skeleton
2	1	3
number of diagonal components in the chain coded curve	) number of vertical components+ number of horizontal components+• 2 diagonal components)	) number of vertical components+ number of horizontal components+Ö2 diagonal components
B=SQRT(D(P_I,P_J))	B=(D(PI,PJ))distance between any two points along the boundary.	B= max(D(P_I,P_J))
difference between major axis to minor axis	addition of major axis length and minor axis length	The ratio of major axis to minor axis
2310	321	321
3221	122300	3221
3311	1122	3333
303303	3300221	303303
3311	1122	3333
both low and high frequency	center frequency component	low frequency
both low and high frequency	center frequency component	High frequency
a(u)+• xy	a(u)+• xy	a(u)+D_{xy}d(u)
) a/a(u)	) • +a(u)	• a(u

compactness		perimeter		area	
perimeter*area		) (perimeter)2*area		) (perimeter)2*area	
skeleton		minimum and maximum gray levels		topology	
) E=C+2H	2	) E=C*H	1	) E=C-H	2
	1		-3		-3
	-1		4		-2
spectral		polygonal approximation		statistical	
spectral		polygonal approximation		) structural	
third moment		fourth moment		third moment	
third moment		fourth moment		fourth moment	
	1	above 10		even	
4x3		3x6		3x6	
$\sum_{i=0}^{L-1} P / 2(Zi)$		$\sum_{i=0}^{L-1} P * P(Zi)$		$\sum_{i=0}^{L-1} P * P(Zi)$	
s(k)= 2*[x(k)+jy(k)]		) [x(k)+jy(k)]/2		) [x(k)+jy(k)]/2	
F(k)		) c(k)		a(u)	
	2		6		2
	6		12		7

based on gradient operator outputs and laplacian outputs with single threshold	based on laplacian operator outputs		based on gradient operator outputs and laplacian outputs with single threshold
Both Encryption and Decryption	None of the above		Both Encryption and Decryption